U.S. Coast Guard Research and Development Center
1082 Shennecossett Road, Groton, CT 06340-6096

Report No. CG-D-23-98

Finite Element Analysis of Barriers

FINAL REPORT
MARCH 1998

This document is available to the U.S. public through the
National Technical Information Service, Springfield, VA 22161

Prepared for:

U.S. Department of Transportation
United States Coast Guard
Systems (G-S)
Washington, DC 20593-0001

Technical Report Documentation Page

1. Report No. CG-D-23-98	2. Government Accession No.	3. Recipient's Catalog No.
4. Title and Subtitle Finite Element Analysis of Barriers		5. Report Date March 1998 6. Performing Organization Code Project No.3309.26 / UDI 138
7. Author(s) Jonathan R. Barnett, S.P. Hunt		8. Performing Organization Report No. R&DC 24/93
9. Performing Organization Name and Address Worcester Polytechnic Institute 100 Institute Road Worcester, MA 01608-0007	U.S. Coast Guard Research and Development Center 1082 Shennecossett Road Groton, CT 06340-6096	10. Work Unit No. (TRAIS) SHRD Report No. 79 11. Contract or Grant No. DTCG39-90-D-E38425, DO 0010
12. Sponsoring Agency Name and Address U.S. Department of Transportation United States Coast Guard Systems (G-S) Washington, DC 20593-0001		13. Type of Report and Period Covered Final Report 14. Sponsoring Agency Code Commandant (G-SEN-1) U.S. Coast Guard Headquarters Washington, DC 20593-0001

15. Supplementary Notes
The Coast Guard technical contact is Robert Richards (860-441-2760) of the U.S. Coast Guard Research and Development Center. The project officer at Coast Guard Headquarters (G-SEN-1) is CDR Dan Oliver.

16. Abstract

This project report discusses the development of a complete procedure for a finite element analysis of the failure of selected shipboard barriers under hostile fire exposures.

The work consisted of the analysis of three different barrier materials. It included the determination of temperature dependent thermal properties of the materials followed by the development of a finite element analysis protocol. The protocol was illustrated using the computer codes ANSYS and NASTRAN for the structural analysis and TASEF-2 and FIRES-T3 for the thermal analysis.

17. Key Words		18. Distribution Statement
finite element method composite fire test	Honeycomb barrier ISO fire	This document is available to the U.S. public through the National Technical Information Service, Springfield, VA 22161.

19. Security Classif. (of this report)	20. SECURITY CLASSIF. (of this page)	21. No. of Pages	22. Price
UNCLASSIFIED	UNCLASSIFIED		

Form DOT F 1700.7 (8/72) Reproduction of form and completed page is authorized

METRIC CONVERSION FACTORS

Approximate Conversions to Metric Measures

Symbol	When You Know	Multiply By	To Find	Symbol
		LENGTH		
in	inches	*2.5	centimeters	cm
ft	feet	30	centimeters	cm
yd	yards	0.9	meters	m
mi	miles	1.6	kilometers	km
		AREA		
in^2	square inches	6.5	square centimeters	cm^2
ft^2	square feet	0.09	square meters	m^2
yd^2	square yards	0.8	square meters	m^2
mi^2	square miles	2.6	square kilometers	km^2
	acres	0.4	hectares	ha
		MASS (WEIGHT)		
oz	ounces	28	grams	g
lb	pounds	0.45	kilograms	kg
	short tons (2000 lb)	0.9	tonnes	t
		VOLUME		
tsp	teaspoons	5	milliliters	ml
tbsp	tablespoons	15	milliliters	ml
fl oz	fluid ounces	30	milliliters	ml
c	cups	0.24	liters	l
pt	pints	0.47	liters	l
qt	quarts	0.95	liters	l
gal	gallons	3.8	liters	l
ft^3	cubic feet	0.03	cubic meters	m^3
yd^3	cubic yards	0.76	cubic meters	m^3
		TEMPERATURE (EXACT)		
°F	Fahrenheit temperature	5/9 (after subtracting 32)	Celsius temperature	°C

*1 in = 2.54 (exactly).

Approximate Conversions from Metric Measures

Symbol	When You Know	Multiply By	To Find	Symbol
		LENGTH		
mm	millimeters	0.04	inches	in
cm	centimeters	0.4	inches	in
m	meters	3.3	feet	ft
m	meters	1.1	yards	yd
km	kilometers	0.6	miles	mi
		AREA		
cm^2	square centimeters	0.16	square inches	in^2
m^2	square meters	1.2	square yards	yd^2
km^2	square kilometers	0.4	square miles	mi^2
ha	hectares (10,000 m^2)	2.5	acres	
		MASS (WEIGHT)		
g	grams	0.035	ounces	oz
kg	kilograms	2.2	pounds	lb
t	tonnes (1000 kg)	1.1	short tons	
		VOLUME		
ml	milliliters	0.03	fluid ounces	fl oz
l	liters	0.125	cups	c
l	liters	2.1	pints	pt
l	liters	1.06	quarts	qt
l	liters	0.26	gallons	gal
m^3	cubic meters	35	cubic feet	ft^3
m^3	cubic meters	1.3	cubic yards	yd^3
		TEMPERATURE (EXACT)		
°C	Celsius temperature	9/5 (then add 32)	Fahrenheit temperature	°F

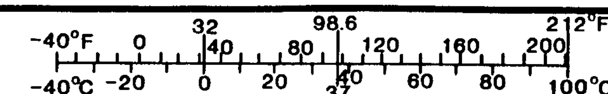

TABLE OF CONTENTS

TABLE OF CONTENTS
(continued)

Page

TABLE OF CONTENTS
(continued)

LIST OF FIGURES

LIST OF TABLES

LIST OF GRAPHS

List of Abbreviations and Symbols

Variables, Constants, and Greek Letters

a - h	Constants
a	Length; as measured from the left
A	Area; weighted area
b	Height; as measured from the right
c	Boundary surface
c_p	Heat capacity
E	Voltage; mass equivalent of fluid (water) or Young's Modulus
F	Airy stress function or Shape Factor
G	Rigidity modulus
ΔH	Relative change in enthalpy; Activation Energy
h	Convection coefficient
I	Current; Moment of Inertia
J	Jacobean coordinate transformation (equation 2-13)
K_o	Lattice constant
k	Thermal Resistance; Constant
L	Length
l	Length
M	Moment
m	Mass
m,n	Current number
N	Total number; normal reaction
n	Total (number of nodes)
o	Opening factor
Q	Heat flux; unit heat flux; power
P	Axial load; concentrated load
q_c	Unit heat flux
R	Ideal gas constant; Residual
RHS	Right hand side
S	Heat generation
T	Temperature
t	Time; Thickness
u,v,w	displacements in the x,y,z or X,Y,Z directions
V	Volume; valence
x,y,z	Spatial coordinates; element coordinates
X,Y,Z	Global coordinates
W	Weighting constant
α	Coefficient of thermal expansion
β	Non-linear convection power
γ	Angular strain
Δ	Change in; difference between
δ	Maximum deflection
ϵ	Emissivity; strain
θ	Weighting constant

κ	Thermal conductivity
λ	Eigenvalue multiplier
ν	Poisson's ratio
ρ	Density
σ	Stress
ϕ	Finite element shape function
$\tilde{\omega}$	Airy stress function

Subscripts

c	Critical
cr	Creep; critical
g	Gap
i,j	Node number
m	meter; melting
n	New; time increment; total number
O	Initial
o	Old
r	Reference
S	Surface
xx,yy,...	Acting on denoted plane
∞	Ambient

Superscripts

a	Applied; acceleration
A	Axial
B	Bending
c	Creep
cr	Critical
C	Constant; creep
e	Element
el	Element
E	Elastic
M,N	Nodes
nr	Restoring
nd	Node
o	Reference surface
P	Load state
pl	Plastic
pr	Pressure
Q	Trivial load
r	relaxation
S	Shear
T	Torsion
Th	Thermal
*	Non-dimensional

Operations

∇	Gradient: $\partial/\partial x\,\mathbf{i} + \partial/\partial y\,\mathbf{j} + \partial/\partial z\cdot\mathbf{k}$
∇^2	Divergence: $\partial^2/\partial x^2\,\mathbf{i} + \partial^2/\partial y^2\,\mathbf{j} + \partial^2/\partial z^2\cdot\mathbf{k}$
$D()/Dt$	Substantial derivative: $\partial()/\partial t + \nabla()\,\mathbf{u}$
∂^4	Divergence squared (quirk): $\partial^4/\partial x^4+\partial^4/\partial y^4+\partial^4/\partial z^4+2\cdot\partial^4/\partial x^2\partial y^2+2\cdot\partial^4/\partial x^2\partial z^2+2\cdot\partial^4/\partial y^2\partial z^2$
N_T	Thermal normal force: $\alpha E\int_{t/2} T(z)\,dz$
M_T	Thermal Moment: $\alpha E\int_{t/2} zT(z)\,dz$
D	Flexural Rigidity of a plate: $Et^3/12(1-\nu)$

Matrices

$\{a_T\}$	Acceleration
[B]	Geometric
[D]	Elastic Stiffness
[K]	Stiffness
[M]	Mass
[S]	Stress stiffness
$\{u\}$	Displacement
$\{\epsilon\}$	Strain
$\{\sigma\}$	Stress

Executive Summary

Introduction

This project report discusses the activities conducted as part of U.S. Coast Guard contract number DTCG39-87-D-E38E46, Delivery Order Number 0010. The main project goal as listed in Task A of the Work/Delivery Order was to:

> Lay out a complete procedure to develop a finite element analysis of the failure of selected barriers through the range of their capability. [3]

This goal was achieved in its entirely.

The original task statement subdivided the project into five specific subtasks:

1. Identify the small-scale test protocol and requirements to determine the temperature-dependent material properties that are needed for the finite element analysis.
2. Identify the restraint and other structural conditions to sue in the computer analysis to apply to the barriers and ship construction conditions.
3. Identify the appropriate finite element computer program and elements needed in the analysis.
4. Develop a test plan, conduct tests, and obtain the temperature dependent material properties necessary for the finite element analysis of the follow three (3) materials:

    a) Steel joiner bulkhead with thermal insulation.
    b) Nomex honeycomb core panel with plastic laminate surfaces.
    c) Nomex honeycomb core panel with stainless steel surfaces.

5. Develop a test program and a test plan to predict cracking and spalling potential.

The main project goal as listed in Task A of the Work/Delivery Order was completed successfully. There was an increase in the scope of work which replaced the act of developing a test plan as specified in subtask 5 with a preliminary finite element analysis of the barriers being investigated. This was necessary to achieve the project's goal. It became obvious as the research progressed, that it was essential to actually conduct computer analyses of the barriers being evaluated rather than just lay out a complete procedure. This was necessary to ensure that items two and three of the original task statement were complete and correct. Therefore, a new and more rigorous and time consuming task of conducting preliminary computer analyses of the barriers was added to the project's scope of work. Based on these analyses it was determined that it was premature to develop the test protocol specified in subtask 5 until additional computer studies of the barriers were completed. This is because a study of the results of the computer analyses indicated that there was a weak understanding of the failure mode of the barrier's being studied. The primary uncertainty is due to a lack of understanding of the structural support conditions of the barriers and the actual failure mechanisms. The uncertainty raised here must be resolved prior to the development of any test plan to evaluate cracking and spalling.

This report discusses these issues in detail, presents the results of actual testing of the barrier materials being evaluated as well as the results of finite element modeling of the thermal and structural performance of the barriers.

Technical Approach

The Delivery Order's objective was achieved by subdividing the problem into three components. These were:

1. To determine the temperature dependent material properties of the three barriers,
2. To evaluate the transient thermal gradients in the barriers when subjected to a fire, and
3. To perform a protocol thermo-elastic analysis of the barrier assemblies.

The temperature dependent material properties of the barriers which were of concern in this study were their thermal conductivity and their heat capacity. It was concluded that the thermal conductivity of the two honeycomb materials were identical and that the heat capacity of the steel honeycomb composite material was dominated by the steel. As a result, only four tests were required and only for the honeycomb material and the fiberglass insulation; two for the thermal conductivity and two for the heat capacity. The properties of the steel panel and that of an aluminum stiffening post used in the barrier assembly are well known and well documented in the literature. Thus no additional tests of the thermal properties for these items were necessary.

The temperature distribution in each of the panels was determined using two finite element heat transfer programs. The programs used were TASEF-2 [20] and FIRES-T3 [18]. Both programs were used for verification purposes. The fire boundary condition was assumed to follow a standard logarithmic fire curve [20]. In the computer analysis, the panels were modeled using the temperature dependent properties. The modeling continued until the aluminum stiffening post reached a temperature of about 2600 R (1444 K).

Lastly, the structural analysis was done using the finite element computer programs ANSYS [31], [32], [38], and NASTRAN [33], [34], [36], [37]. These programs are structural analysis codes capable of modeling materials with non-linear properties. The results of such an analysis is a time varying deflection and stress history of the barrier being evaluated. Eventually, this information is necessary to evaluate the quality of the model through comparisons with test data. Ultimately, this information will form the basis for a predictor of failure due to cracking and or buckling of the barrier in a fire environment.

The structural analysis was divided into two parts: one for the main surface of the barrier which was modeled as a plate and one for the supporting struts which were modeled as posts. The U.S. Coast Guard was unable to provide information on the structural properties of the plastic laminate barrier or the dimensions of the struts supporting the steel joiner. Thus, only the steel-honeycomb composite barrier was modeled. This did not affect the findings as the material modeled was the most challenging of the ones being analyzed. The barrier was modeled in such a way as to simulate the boundary constraints expected in-situ. This was done by constraining the axial displacements of the upper and lower portions of the posts by using a force-deflection constraint corresponding to that which would be expected due to the stiffness of the bounding deck. Rotations were allowed.

The plate was restrained against displacements on all four edges but allowed to rotate.

The post was found to be very dependent on the boundary conditions. The post buckled near the edges of the deck and tended to melt and warp near the center. It was also sensitive to rotation restrictions placed on the axes.

The plate was found to buckle very early in the fire. The result of early buckling is that the plate spent little time in the linear strain zone. Thus a large strain analysis was required to complete the model. This was an important component so that the methodology may be used for crack and spalling prediction.

Conclusions

The complete procedure for a finite element analysis of three types of barrier materials has been determined and presented in this report by means of an actual sample analysis.

As part of this Task, the original scope of work was expanded to include actual finite element analyses of shipboard barriers.

Future work should include an extension of this work to the prediction of barrier crack formation and prediction of material spalling. Once this is completed, a test plan should be developed to validate all of the finite element work done as part of this research.

Introduction

New materials are continually being developed to meet the needs and requirements of many applications. The behavior of these new materials is not fully understood, especially their response to high thermal loads as encountered in unexpected fires. In order to make fully informed decisions when implementing them, a reasonable assessment of the response to a fire must be undertaken.

Among the most difficult materials to predict the behavior of are composite materials. Composite materials are those that have two or more independent materials that are incorporated into one entity. These materials each retain their individual properties, but when combined, the separate materials interact with each other ultimately behaving as a single material with completely different properties. The motivation to explore composites is akin to the motivation to experiment with alloys. The new composite can have more desirable properties than any of its constituents alone. The desired properties include weight reduction, increased strength, lower production cost, tractability, superior fire resistance, and any combination or extension of the latter list.

When considering the applications of new materials, the materials response to fire should impact the final decision. The criteria that must be addressed when appraising a new materials response to a fire are how long will it retain its function and how susceptible is it to Tbar and Dbar failure (thermal hot spot and massive failure, respectively).

The response of composite materials is very complex and requires the assistance of a computer. The finite element method has proven worthy of solving a wide variety of complex structural problems [4,5] and is a natural selection to evaluate composite materials response to fire. It should be recognized that the computer is useful at estimating what to expect, but not at providing exact answers. By changing the input conditions and observing the impact on the solution, a degree of confidence can be achieved that is directly related to the confidence level of the input conditions. Also, the computer model should be compared and contrasted to actual fire tests.

In the future, computer models may replace the need for costly fire tests. If computer simulations can be run efficiently, accurately, and cheaply, they are certain to replace the need for fire tests. The tremendous advantage of a computer simulation is the ability to alter the fire load and boundary conditions to observe the effect on the solution. The alterations can all be made with a few commands. If a real fire test were performed, any change in the fire curve or boundary conditions would require another test.

This report attempted to verify computer predictions by comparison with a set of fire tests conducted in 1978. The tests were conducted with unrealistic boundary conditions and indicate a serious pitfall to the fire test method. These tests did serve to verify the model because the results were reproduced with the computer model when the boundary conditions of the fire tests were used.

A good computer model requires accurate material properties and an accurate assessment of the boundary conditions. The material properties may require additional tests, which may become the most costly part of the computer analysis. The boundary conditions are very important to correctly address, as will be shown in this report. Ultimately, the decision to employ computer models, either in conjunction with fire tests or as a replacement will depend on the success in reproducing the results of fire tests and the ease in which other fire and boundary conditions may be modelled.

Ultimately, a decision is to be made concerning the suitability of a material for a particular application. The response to a fire is just one component to this evaluation.

CHAPTER ONE
Determination of the Thermal Properties

1.0 Introduction

For the purpose of this report, three materials were analyzed: One fiberglass-steel joiner panel and two honeycomb panels. Two thermal properties, thermal conductivity ($\kappa(T)$) and heat capacity ($c_p(T)$) were determined for each material.

1.1 Material Description

1.1.1 Fiberglass-Steel Joiner Panel

This material will be referred to as material one. The sample used in the tests was manufactured by:

Claremont Company Inc.
174 State St.
P.O. Box 952
Meriden, CT 06450
203-238-2384

Claremont Company Inc. refers to this material in its literature as "Steel Joiner Bulkhead with Thermal Insulation" (Refer to Appendix A for names of additional manufacturers [6,7,8]). It consists of two 0.0625 in. (0.2588 cm) steel panels with 1 in. (2.54 cm) of fiberglass compressed between them. There is no adhesive between the steel and the fiberglass. The total thickness of the steel and fiberglass is 1.125 in. (2.8575 cm). The average density of the fiberglass is 5.079 lb/ft^3 (81.4 Kg.m^3) and the steel is 491.1 lb/ft^3 (7870 Kg/m^3). [9]

1.1.2 Plastic Nomex

This is material number two and the samples analyzed were manufactured by:

Hexcel Products Inc.
Two Stoney Hill Rd.
Bethel, CT 06801
203-798-8311

It is referred to by its manufacturer as "Plastic Laminate Nomex Honeycomb Core Panel". Appendix A lists additional manufacturers of this panel. [6,7,8] This material consists of a plastic front and rear panel glued to a honeycomb core (see Figure 1-1). Two fiberboard layers bonded together comprise the plastic faces. Each plastic face is 0.0625 in. (0.1588 cm) thick. The total thickness of the panel is 0.689 in (1.75 cm). The density is 13.35 lb/ft^3 (213.96 Kg/m^3). [9]

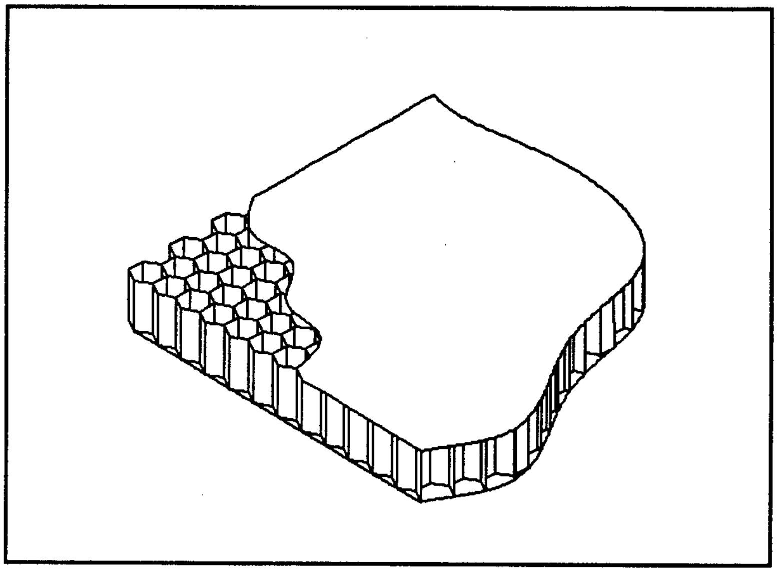

Figure 1-1 Honeycomb Material

1.1.3 Steel Laminate Honeycomb

This is referred to as material three. The panel in this report were made by Hexcel Products also, and is referred to by them as Steel Laminate Nomex Honeycomb Core Panel. The panel has steel plate front and rear surfaces glued to a core of honeycomb. The steel plates are 0.0625 in (0.1588 cm) thick and the total panel thickness is 0.689 in (1.75 cm).

The density is 92.35 lb/ft^3 (1480 Kg/m^3). [9]

1.2 Testing Procedure

The three materials were tested in accordance with ASTM test standards and C351-90 (thermal conductivity) and C177-85 (specific heat). The conductivity and heat capacity for the honeycomb materials were effective values. Effective values assume the material to be a pseudo-solid. The effective conductivity takes into account all the heat transfer mechanisms in the material: conduction, convection and radiation. The heat capacity value ignores the heat capacity of the internal air gap, and combines the capacity of the honeycombs and face materials. The conductivity and heat capacity are determined under steady state conditions. The impact of a transient thermal load on effective values is not known. The testing was conducted by Holometrix, Inc. between February 21, 1991 and February 26, 1991. Its report is listed in Appendix B.

1.3 Test Descriptions

1.3.1 ASTM C177-85

ASTM C177-85 is called "The Standard Test Method for Steady State Heat Flux Measurements and Thermal Transmission Properties by Means of the Guarded-Hot-Plate Apparatus". [10] The purpose of this test procedure is to determine the thermal conductivity of a sample by use of Fourier's Law ($Q/L=\kappa\cdot\Delta T$). It sets up a one dimensional heat flow in the sample with known surface temperatures. The temperature difference between the two surfaces is assumed small enough that conductivity is constant.

The test is conducted by placing a specimen between two parallel plates - a hot metered heater and a cold heater. The temperature imbalance induces a heat flow in the direction of the cold plate. Ideally, this energy flow is exactly equal to the power delivered to the hot heater. To realize this idealization primary guard heaters heated to the same temperature, are strategically placed around the metered heater in the same plane (refer to Figures 1-2a through 1-2c). This cuts down on two dimensional heat flow at the edges. The circular specimen is extended over the guards well beyond the metered heater. The entire system is surrounded by an insulation, such as diatomaceous earth. Tests run at temperatures much higher or lower than room temperature require an additional secondary guard heater that is placed in the insulation surrounding the apparatus. These guard heaters are maintained at the average temperature between the hot and cold heaters and act to minimize heat loss to the surroundings.

The procedure is monitored by thermocouples and volt meters. The thermocouple serve both to control the guard heaters and to collect the boundary condition data for the specimens. The voltmeter provides information to calculate the power delivered to the hot heater. Normally, all of the thermocouples are hooked up to a computer which controls the temperature of the heaters from that information.

The calculation of the conductivity (and resistivity) is straightforward. First:

$$Q=E\cdot I \tag{1-1}$$

E is the voltage drop across the hot heater circuit, I is the current and Q is the power delivered to the hot heater.

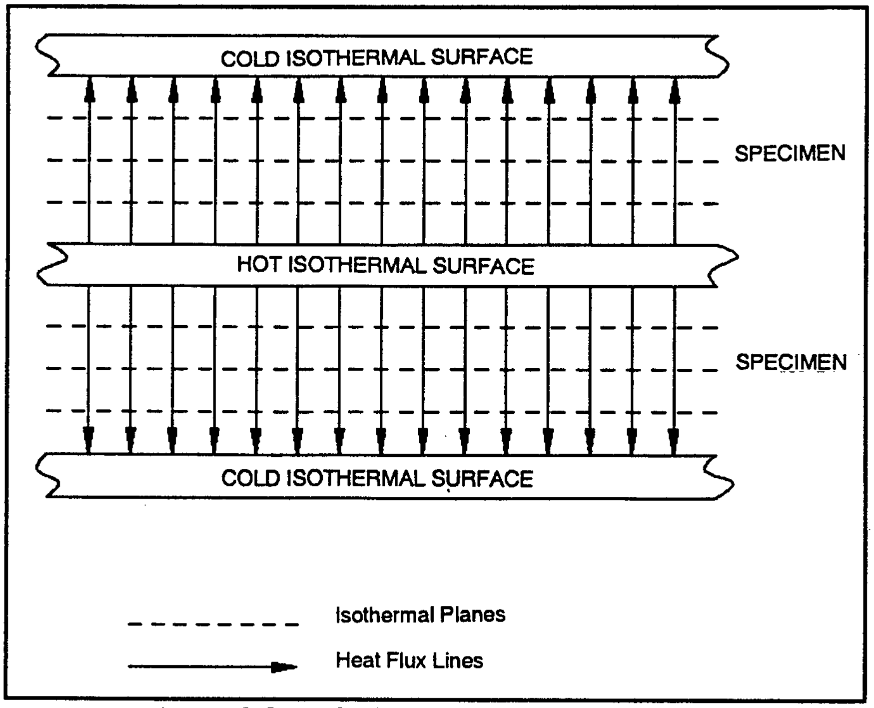

Figure 1-2a Ideal Heat Flow in ASTM C177

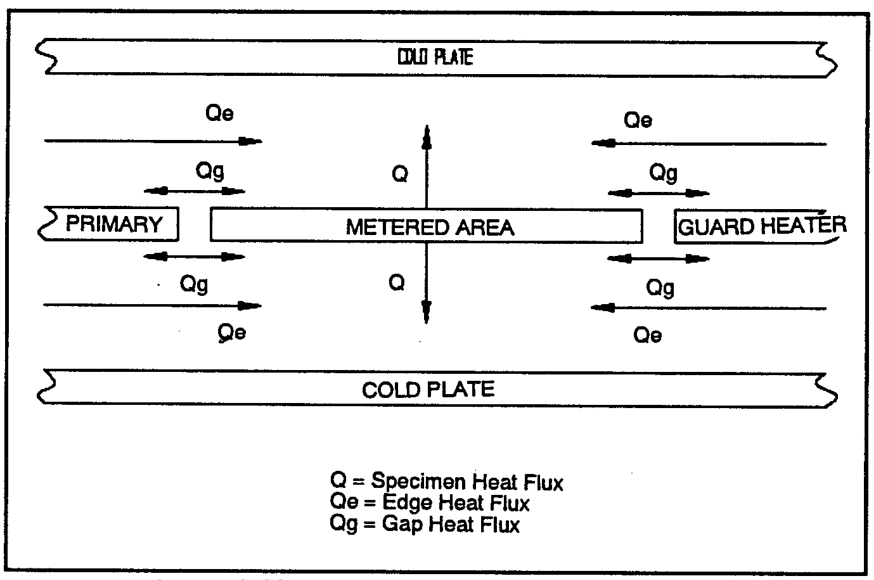

Figure 1-2b Sources of Error in ASTM C177

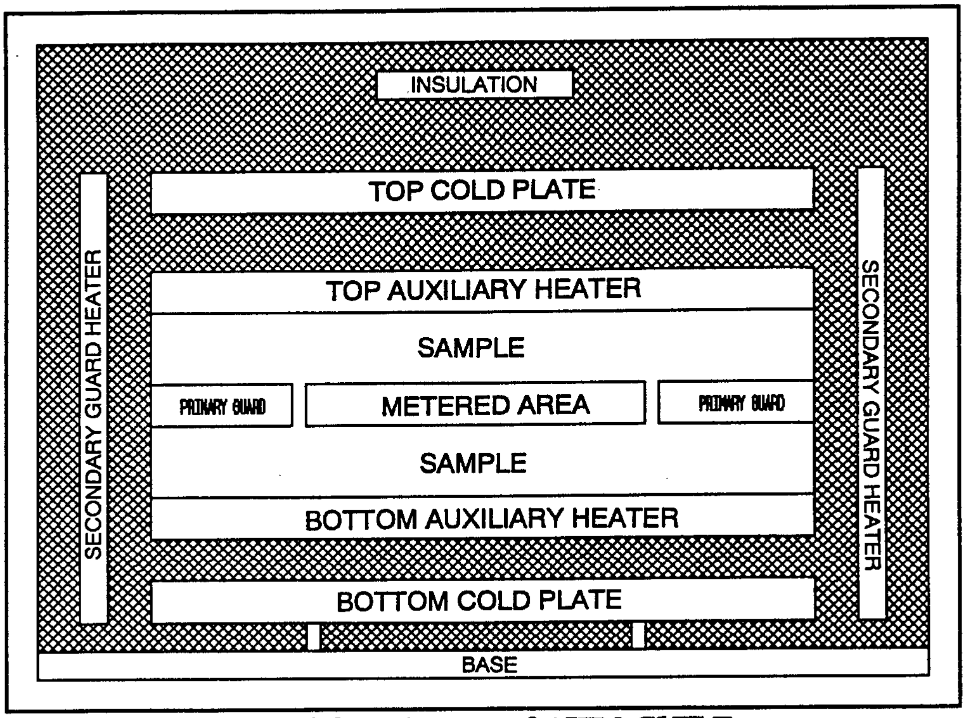

Figure 1-2c Diagram of ASTM C177 Test

The area of this heater is:

$$A=A_m+\frac{1}{2}A_g \qquad (1\text{-}2)$$

A_m is the actual area and A_g is the area of the gap between the heater and the primary guard. Fourier's Law can be rearranged to read:

$$\kappa=\frac{Q}{A}\cdot\frac{\Delta x}{\Delta T} \qquad (1\text{-}3)$$

with Δx the specimen thickness, Q/A the heat flow per unit area and ΔT the temperature difference between the hot and cold plates.

Actual tests are performed using two specimens, one above and one below the hot heater. The area is the area of both specimens plus the area of the gap ($2A_g$).

Four conditions account for the most pertinent deviations from the ideal setup:

1. Specimen inhomogeneities
2. The gap between the metered heater and the primary guard
3. Heat loss at the edges of the specimen
4. Systematic errors arising from instrument imperfection

The ASTM standard explains in some detail how to estimate the impact of these conditions on the results.

1.3.2 ASTM C351-90

ASTM C351-90 is called the "Standard Test Method for Mean Specific Heat of Thermal Insulation". [10] C351-90 determines the heat capacity (c_p) of a material by heating a specimen of known mass. The specimen is then dropped in a fluid bath of known temperature and heat capacity. The equilibrium temperature of the specimen and fluid is used to calculate the enthalpy, ΔH (energy/mass), and the heat capacity, c_p (energy/mass-temperature).

The testing apparatus consists of four components:

1. A heater for both the fluid bath and the specimen
2. A calorimeter containing the bath
3. Temperature sensors
4. A capsule for specimen

The calorimeter is required to be thermally isolated from the environment.

The apparatus is calibrated before each test with a copper sample. The calibration procedure determines the heat capacity of the calorimeter at the testing temperature.

Three steps are required to determine the heat capacity. First, to calibrate the apparatus, the calorimeter must be converted to the mass equivalent of fluid used in the test. This conversion accounts for the energy lost to the calorimeter during the experiment. This is accomplished by heating a copper specimen and then dropping it in the fluid bath. The thermal equilibrium equations are used to calculate the fluid mass equivalent.

$$\Delta H_{copper} = \Delta H_{bath} + \Delta H_{calorimeter} \tag{1-4}$$

or

$$E = \frac{(mc_p \Delta T)_{copper}}{(c_p \Delta T)_{bath}} - m_{bath} \tag{1-5}$$

E is the bath fluid mass equivalent, m is mass and c_p is heat capacity.

Next, the thermal capacity of the capsule $(mc_p)_{caps}$ that will contain the specimen is determined $(mc_p)_{caps}$. An empty capsule is heated and then dropped in the fluid bath before each experiment. Since:

$$\Delta H_{capsule} = \Delta H_{calorimeter} \tag{1-6}$$

the thermal capacity of the capsule is:

$$(mc_p)_{capsule} = \frac{(m_{bath}+E)\, c_{bath} \Delta T_{bath}}{\Delta T_{capsule}} \tag{1-7}$$

Last, a sample is inserted in the capsule and heated. After dropping the capsule in the calorimeter, and thermal equilibrium has been reached, the heat capacity of the specimen is:

$$(c_p)_{specimen} = \frac{\left\{\left[\frac{(m_{ba}+E) c_{ba} \Delta T_{ba}}{\Delta T_{specimen}}\right] - (mc_p)_{capsule}\right\}}{m_{specimen}} \tag{1-8}$$

The accuracy of ASTM C351-90 is +/- 10 percent.

Variations to this procedure include using a quadratic curve fit for the enthalpy. Holometrix used this method anticipating a non-linear temperature dependence.

1.4 Assumptions

Three assumptions were made at the initial meeting with Holometrix. [11] These were:

1. The conductivity of both of the honeycomb materials is the same because each involve the same internal heat transfer mechanisms - radiation and convection.

2. The heat capacity of the steel honeycomb is the same as that of the steel, corrected for the additional volume.

3. It is not necessary to test the fiberglass insulation with the steel attached. It is only necessary to use a composite in the calculations since the steel properties are well documented.

Thus, the number of tests required was four, two conductivity and two heat capacity tests.

1.5 The Test Results

1.5.1 Conductivity

The results of the thermal conductivity tests are given in Table 1-1 and 1-2. Table 1-3 shows the conductivity data for the stainless steel. [12,13] The units J/hr-cm-K are used in the heat transfer analysis in Chapter Two.

Table 1-1 Conductivity of Fiberglass

T °C	J/s-m-K	J/hr-cm-K	Btu/s-ft-R	T °F
31	0.0327	1.177	18.932	87.8
100	0.0401	1.444	23.216	212.0
200	0.0527	1.897	30.511	328.0
301	0.0720	2.592	41.685	573.8
402	0.0986	3.549	57.086	755.5
504	0.1320	4.752	76.422	939.2
604	0.4250	15.30	246.06	1119.2

Table 1-2 Conductivity of Honeycomb

T °C	J/s-m-K	J/hr-cm-K	Btu/s-ft-R	T °F
30.0	0.0755	2.718	43.712	87.8
101.0	0.0958	3.448	55.464	213.8
200.0	0.1390	5.004	80.475	392.0
302.0	0.1750	6.300	101.32	575.6
353.0	0.1980	7.138	114.63	667.4
404.0	0.1940	6.984	112.32	759.2

Table 1-3 Conductivity of Steel

T °C	J/s-m-K	J/hr-cm-K	Btu/s-cm-R	T °F
100.0	65.3	2347	37806.0	212.0
200.0	60.3	2172	34911.0	392.0
400.0	54.9	1976	31784.0	752.0
600.0	45.2	1627	26169.0	1112.0
800.0	36.4	1310	21074.0	1472.0

Graph 1-1 shows the conductivity versus temperature for the honeycomb panels, fiberglass and stainless steel. The conductivity data is normalized with the value of conductivity at 212 °F (100 °C):

$$\kappa^* = \frac{\kappa(T, {}^\circ F)}{\kappa(212^\circ F)} \qquad \textbf{(1-9)}$$

The temperature is normalized by:

$$T^* = \frac{(T - T_{REF})}{(T_O - T_{REF})} \qquad \textbf{(1-10)}$$

The initial temperature (T_0) taken as 529.69 R (298 K) and the reference temperature (T_{REF}) taken as 77 R (25 K).

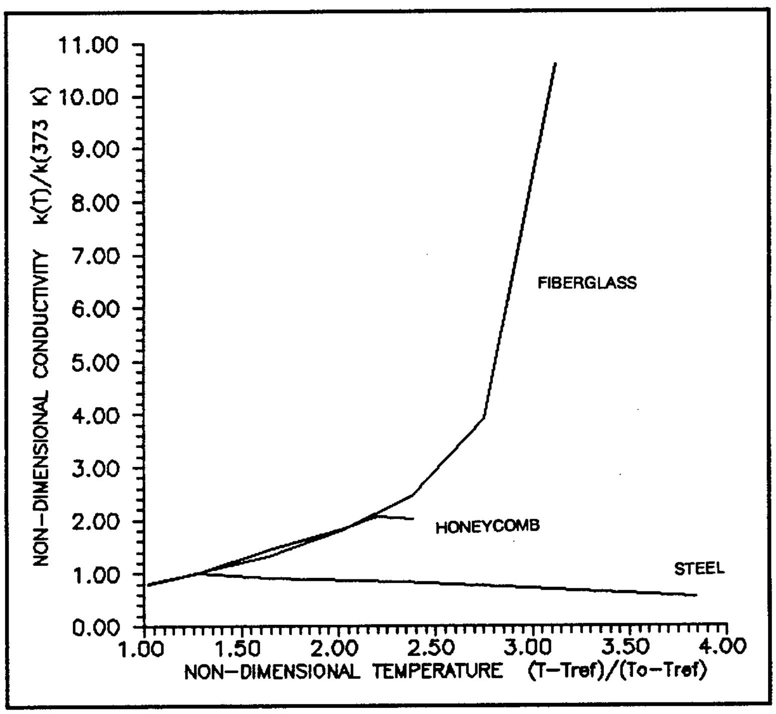

Graph 1-1 Conductivity vs Temperature

1.5.2 Specific Heat

The heat capacity for the fiberglass, plastic honeycomb and steel honeycomb materials are shown in Tables 1-4 through 1-6. Additionally, the heat capacity for stainless steel is shown in Table 1-7. [14]

Table 1-4 Specific Heat of Fiberglass

T °C	J/Kg-K	J/cm^3 - K	Btu/lb-R	T °F
25.0	812.0	0.07123	1818.2	77.0
50.0	833.0	0.07123	1865.9	122.0
100.0	875.0	0.07123	1960.0	212.0
150.0	917.0	0.07461	2054.0	302.0
200.0	955.0	0.07775	2139.2	392.0
300.0	1038.0	0.0845	2325.12	572.0
400.0	1122.0	0.09130	2513.2	752.0
500.0	1206.0	0.09820	2701.4	932.0
550.0	1248.0	0.10100	2795.5	1022.0

Table 1-5 Specific Heat of Plastic Honeycomb

T °C	J/Kg-K	J/cm^3-K	Btu/lb-R	T °F
0.0	901.0	0.2644	2018.2	32.0
101.0	901.0	0.2644	2018.2	213.8
151.0	1096.0	0.3214	2455.0	303.8
201.0	1016.0	0.2977	2275.8	393.8
304.0	1313.0	0.3846	2941.0	579.2
349.0	1189.0	0.3438	2663.4	660.2
401.0	1137.0	0.3330	2546.9	753.8

Table 1-6 Specific Heat of Steel Honeycomb

T °C	J/Kg-K	J/cm^3-K	Btu/lb-R	T °F
0.0	445.0	0.634	996.8	32.0
100.0	445.0	0.634	996.8	212.0
200.0	465.0	0.663	2042.6	392.0
300.0	504.0	0.720	1129.0	572.0
400.0	546.0	0.770	1223.0	752.0
500.0	547.0	0.780	1225.2	932.0
600.0	561.0	0.800	1256.6	1112.0
700.0	580.0	0.827	1299.2	1292.0

Table 1-7 Specific Heat of Steel

T °C	J/Kg-K	J/cm^3-K	Btu/lb-R	T °F
0.0	470.0	3.89	1052.8	32.0
100.0	482.0	3.89	1079.7	212.0
200.0	520.0	3.89	1164.8	392.0
400.0	595.0	4.195	1332.8	752.0
600.0	754.0	4.767	1689.0	1112.0
800.0	-----	5.364	------	1472.0

Because the plastic honeycomb material lost mass during the testing [9], Holometrix only reported the enthalpy for this material. This study required a calculation of the specific heat. The conversion of enthalpy (ΔH) to heat capacity (c_p) for the plastic honeycomb is:

$$c_p = \frac{\Delta H}{\Delta T} \tag{1-11}$$

where ΔT is the difference between the initial temperature and the equilibrium temperature of the sample and calorimeter.

The heat capacity of the steel honeycomb material is the heat capacity of the steel corrected for the additional volume. This correction is the ratio of steel honeycomb density to the density of stainless steel.

$$c_p = c_{p(steel)} \cdot \frac{\rho_{steel\text{-}honey}}{\rho_{steel}} \tag{1-12}$$

TASEF, a Swedish fire endurance model and one of the heat transfer programs used in Chapter Two of this report, requires either the capacitance or volume-enthalpy. The volume-enthalpy is the enthalpy multiplied by the density or:

$$\Delta H_V = \Delta H_m \cdot \rho \tag{1-13}$$

where ρ is the density of the material (mass/volume) and ΔH_v is the volume enthalpy. Similarly, the conversion of specific heat to capacitance is:

$$C = c_p \cdot \rho \tag{1-14}$$

Graph 1-2 shows the heat capacity for the three panels and steel versus temperature. As with the conductivity, both axes are normalized. The normalized heat capacity is:

$$c_p^* = \frac{c_p(T, {}^\circ F)}{c_p(212^\circ F)} \tag{1-15}$$

The temperature is normalized with:

$$T^* = \frac{(T - T_{REF})}{(T_O - T_{REF})} \tag{1-16}$$

with T_o taken as 529.69 R (298 K) and T_{REF} equal to 77 R (25 K).

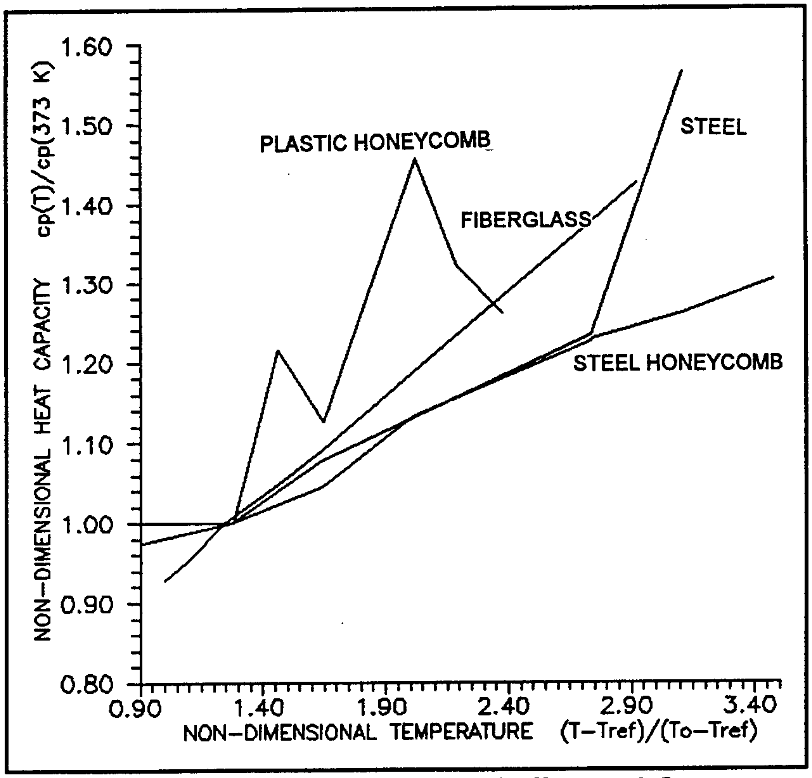

Graph 1-2 Specific Heat of All Materials

CHAPTER TWO
Heat Transfer Analysis of the Panels

2.0 Introduction

The purpose of this Chapter is to determine the time-temperature distribution in each of the three panels when subjected to a fire load. The fire temperature is assumed to follow a standard ISO logarithmic time-temperature curve: [15]

$$T(R) = T_o(R) + 621 \cdot \log(480 \cdot t(hr) + 1) \tag{2-1}$$

$$T(K) = T_o(K) + 345 \cdot \log(480 \cdot t(hr) + 1) \tag{2-2}$$

The temperature distribution is determined by using TASEF and FIRES-T3. Both computer programs use the finite element method to solve for the temperature field. Included in this section is a two dimensional heat transfer analysis of the steel-fiberglass panel that is supported by an aluminum stiffening post. The steel panel and aluminum post form the structural configuration analyzed in Part Three.

2.1 The Governing Heat Transfer Equation

Conservation of energy states that the total energy of a system and its surroundings does not change with time. The energy equation [16] summarizes the conservation of energy:

$$\rho c_p \cdot \frac{DT}{Dt} = \nabla \cdot q_c + S \tag{2-3}$$

The three parts of the equation, from left to right, are the change in energy of the system, the energy flux, either internal or external, and the energy that is generated within the system, as in combustion.

Convection within a solid is practically nonexistent; therefore, $DT/Dt = \partial T/\partial t$.

The internal heat flux vector per unit length, q_c, can be replaced with Fourier's heat conduction equation. [16,17]

$$q_c = \kappa \cdot \nabla T \qquad \kappa = \kappa(x, T) \tag{2-4}$$

where

$$\nabla \cdot T = i \cdot \frac{\partial T}{\partial x} + j \cdot \frac{\partial T}{\partial y} + k \cdot \frac{\partial T}{\partial z} \tag{2-5}$$

On the surface of a solid, the heat flux vector is the combination of the radiation and convection heat exchange equations. The surface heat flux vector is thus: [17,18]

$$q_c = hA\,(T_S - T_\infty)^{\beta} + \epsilon F A \sigma\,(T_S^4 - T_\infty^4) \tag{2-6}$$

If density, ϱ, heat capacity, c_p, heat generation, S, and conductivity, κ, are functions of temperature (time) and/or space a nonlinear heat transfer equation results. This equation is:

$$\rho\,(x,T)\, c_p(x,T) \cdot \frac{\partial T}{\partial t} = \nabla \cdot \kappa\,(x,T)\, \nabla T + S\,(x,T) \tag{2-7}$$

In this study, equation 2-7 is nonlinear and requires an iterative numerical solution method. Also, the spatial dependencies of the density, heat capacity, and conductivity are ignored.

2.2 Finite Elements Method of Solution

The finite element method (FEM) is a numerical technique to solve many different types of differential equations. The finite element method solves these equations by dividing a region into a finite number of sub-regions. These subregions are called elements. Each element has a specific number of nodes depending on the type of solution required. Figure 2-1 shows a subdivided region and Figure 2-2 shows a four node element.

The finite element method solves a differential equation at each node. In this part of the report, temperature is the unknown value. A nodal value is obtained by using the information from the surrounding nodes. This information is adjusted with shape functions that serve to assign weights to each of the surrounding nodes. The neighboring nodes are summed and averaged with the respective nodal weights. In this report, a linear-elliptical finite element solution is used. A linear-elliptical solution employs a linear shape function and assigns equal weights to all equidistant nodes. [17]

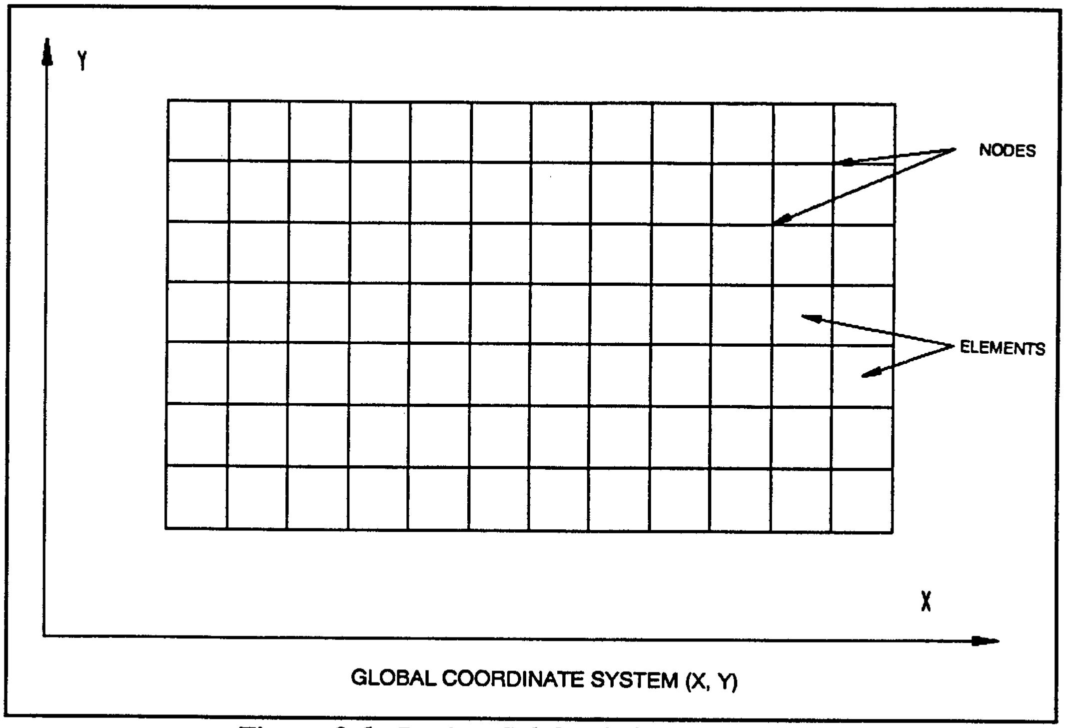

Figure 2-1 Region Subdivided into Elements

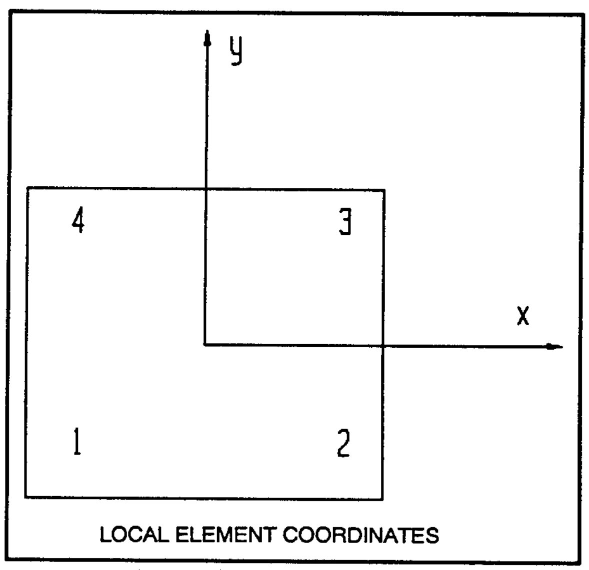

Figure 2-2 Single Element

2.2.1 Coordinate Systems and Shape Functions

For a four node element, each corner is a node. The coordinate system of the region is called the global coordinate system and is denoted with X,Y pairs. The individual elements use a local coordinate system, x,y, with the origin at the center of the element. The coordinates of the nodes in a four node element are (-1,-1), (-1,1), (1,1), and (1,-1), starting at the lower left and proceeding counterclockwise (refer to Figure 2-2).

The coordinates of any point in a two dimensional rectangular four node element are:

$$x=\sum_i \phi_i x_i \tag{2-8a}$$

$$y=\sum_i \phi_i y_i \tag{2-8b}$$

ϕ_i is the shape function of node i evaluated at x,y, and x_i,y_i are the local node coordinates of node i. The shape function can be regarded as a percent contribution of each node to the coordinate of the x,y location. For a four node square, the shape functions (numbered according to Figure 2-2) are: [17]

$$\phi_1=\frac{(1-x)(1-y)}{4} \qquad \phi_2=\frac{(1+x)(1-y)}{4}$$
$$\phi_3=\frac{(1+x)(1+y)}{4} \qquad \phi_4=\frac{(1-x)(1+y)}{4} \tag{2-9}$$

When the shape functions are evaluated at a node, three are zero and one is unity. An element is not restricted to four nodes or even straight lines. Other shape functions include quadratic functions for mapping curves, triangular shape functions, and three dimensional shape functions. For additional information, the reader is referred to [1,4,5,19] which provide a detailed documentation of finite element variations. For a non-linear heat transfer analysis the linear square elements work well. [17,18,20]

2.2.2 Steady State Heat Transfer Equation

The Galerkin FEM is used in this project. Galerkin FEM uses the same shape function that is used to map the geometry (equation 2-9) to solve for the unknowns at a node. The temperature at a node is then:

$$T=\sum_i \phi_i T_i \tag{2-10}$$

The governing equation is also spread out in the region with the same shape function. It is integrated over the area for two dimensional elements and global coordinates:

$$\iint [\phi_i (\nabla\cdot \kappa(T)\nabla T+S(T)]\, dA \tag{2-11}$$

To integrate this equation, it must be transformed to local coordinates:

$$\int_{-1}^{1}\int_{-1}^{1} \phi_i[\nabla\cdot k(T)\nabla T+S(T)]\, Jdxdy \tag{2-12}$$

J is the Jacobean coordinate transformation for two dimensions: [21]

$$J=\frac{\partial X}{\partial x}\cdot\frac{\partial Y}{\partial y}-\frac{\partial X}{\partial y}\cdot\frac{\partial Y}{\partial x} \tag{2-13}$$

Gaussian numerical integration is then used to evaluate equation 2-12. This method integrates a function with integration limits of -1 and 1: [17]

$$\int_{-1}^{1}\int_{-1}^{1} f(x,y)\, dx\; dy=\sum_i\sum_j W_i W_j\cdot f(x_i,y_j) \tag{2-14}$$

where x_i and y_j are the integration points and W_i and W_j are the weights at those locations. The number and location of the points depends on the degree of the polynomial integrated. For degrees less than four, two points are sufficient. [17] For two point gaussian integration, $x_1 = y_1 = 0.5774$, $x_2 = y_2 = -0.5774$, and the weights (W_i) are 1.0.

Since the second derivative of equation 2-10 would be equal to zero, the Divergence Theorem must be applied to reduce the order of equation 2-12: [17,21]

$$\int_{-1}^{1}\int_{-1}^{1} [(\nabla\phi_i\cdot \kappa(T)\nabla T+\phi_i S(T)]\, JdA - \int_s [\phi_i \kappa(T)\cdot\nabla T]\, Jds = 0 \tag{2-15}$$

The second integral term is a line integral which is only evaluated at a boundary.

Besides equation 2-10, two derivatives are required in equation 2-15. The derivatives are:

$$\frac{\partial T}{\partial x}=\sum_{i=1}^{n}\frac{\partial \phi_i}{\partial x}\cdot T_i \tag{2-16a}$$

$$\frac{\partial T}{\partial y}=\sum_{i=1}^{n}\frac{\partial \phi_i}{\partial y}\cdot T_i \tag{2-16b}$$

If the material properties are non-linear, additional derivatives will arise. Assuming a linear interpolation between a temperature-property table, the additional derivatives are:

$$\frac{\partial}{\partial T_j}(\kappa\cdot T) = \phi_j\cdot\kappa \tag{2-17a}$$

$$\frac{\partial}{\partial T_j}(c_p\cdot T) = \phi_j\cdot c_p \tag{2-17b}$$

$$\frac{\partial}{\partial T_j}(S\cdot T) = \phi_j\cdot S \tag{2-17c}$$

If non-linear material properties are used in equation 2-12, the unknown temperatures cannot be isolated. For a non-linear case, the Newton-Raphson method is used to solve equation 2-12. The Newton-Raphson technique begins with an initial guess at the temperature field, usually zero. Equation 2-12 is solved with this initial guess and yields a residual value:

$$\int_{-1}^{1}\int_{-1}^{1}[\nabla\phi_i\cdot\kappa(T)\nabla T+\phi_i S(T)]\ JdA - \int_{s}[\phi_i\kappa(T)\cdot\nabla T]\ Jds=R_i \tag{2-18}$$

The initial guess is then corrected:

$$\left(\frac{\partial R_i}{\partial T_j}\right)\cdot\Delta T=-R_i \tag{2-19}$$

The derivative of the residual, $\partial R_i/\partial T_j$, is found by taking the derivative of R. The additional derivatives encountered in this operation are:

$$\frac{\partial}{\partial T_j}\left(\frac{\partial T}{\partial x}\right)=\frac{\partial \phi_j}{\partial x} \qquad \frac{\partial}{\partial T_j}\left(\frac{\partial T}{\partial y}\right)=\frac{\partial \phi_j}{\partial y} \tag{2-20}$$

After solving for ΔT, the initial guess is corrected and the process is repeated until the correction term, ΔT, is smaller than a specified convergence value.

2.2.3 Unsteady State Heat Transfer Equation

If the heat transfer process is transient, time must be incorporated into equation 2-12. From equation 2-7:

$$[\rho(T)\,c_p(T)]\,\partial T = [\,\nabla\cdot\kappa(T)\nabla T+S(T)]\,\partial t \tag{2-21}$$

or

$$\int_{T_{old}}^{T_{new}} \rho(T)\,c_p(T)\,dT=\int_{t1}^{t2}[\,\nabla\cdot\kappa(T)\nabla T+S(T)]dt \tag{2-22}$$

The right integration can be assumed constant if the time step is small [17], so that:

$$\int_{T_{old}}^{T_{new}} [\rho(T)\,c_p(T)]\;dT = RHS\int_{t_1}^{t_2} dt \tag{2-23}$$

with:

$$RHS = \nabla\cdot\kappa(T)\nabla T+S(T) \tag{2-24}$$

After integrating equation 2-23, the RHS becomes:

$$\frac{\rho(T)\,c_p(T)\,(T_N-T_O)}{(t_2-t_1)} = RHS \tag{2-25}$$

There are three methods of evaluating the RHS term. These are explicitly (using the RHS from the previous solution), implicitly (using the RHS from the current iteration), and a combination of the both. The latter method is most stable:

$$RHS = \Theta\cdot RHS_O+(1-\Theta)\cdot RHS_N \tag{2-26}$$

The best results occur at Θ=0.42. [17]

The Galerkin method is used to solve for the temperature distribution:

$$\int_{-1}^{1}\int_{-1}^{1}\left[\frac{(\phi_i\rho(T)\,c_p(T)\,(T_N-T_O))}{\Delta t}-RHS\right]JdA = R \tag{2-27}$$

This is solved with the Newton-Raphson method described in Section 2.2.2. The only new derivatives are:

$$\frac{\partial}{\partial T_j}\left[\frac{(T_N-T_O)}{\Delta t}\right] = \frac{\Phi_j}{\Delta t} \tag{2-28}$$

$$\frac{\partial}{\partial T_j}(RHS) = \frac{\partial}{\partial T_j}\Phi_i\,(RHS_N)\,(1-\Theta) \tag{2-29}$$

The time increment must be small enough so that the routine will converge and RHS is approximately constant. The maximum time increment allowed for convergence is called the critical time step, t_c. Some finite element codes offer a dampening effect which chooses a $t<t_c$ by a specified fraction. The dampening effect is useful for rapidly changing parameters, such as temperature or material properties.

2.3 Description of the Heat Transfer Codes

Two heat transfer codes were used to solve the governing heat transfer equation (equation 2-7). Both heat transfer codes use the finite element method described in Section 2.2.

2.3.1 TASEF

TASEF is a two dimensional FEM program written in 1983 by Mats Paulsson. [20] It was developed at Lund Institute of Technology in Sweden. In addition to the main program are a preprocessor and a postprocessor. At the time of the writing of this report the post processor was not operational at WPI.

The preprocessor (TPRE) writes an input file to TASEF after the user has responded to each question. Because TASEF has an unusual input file format, the preprocessor is very useful.

TASEF uses four node square and three node triangular elements. The squares and triangles may be used separately or combined. The square elements in TASEF can only be orthogonal.

TASEF initializes the geometry of a region as rectangular. Further operations subtract areas, separate different materials, and sub-divide square elements into triangles.

Elements that are identical in size to adjacent ones may be automatically generated by TASEF. Element generation significantly reduces the size of the input file. The nodes of each element are numbered globally with an x,y coordinate. The positive x axis runs vertically down and the positive y runs right to left. The origin, (1,1) is located in the upper left hand corner. Figure 2-3 shows the nodal numbering system and coordinate system used by TASEF. TASEF uses the shape functions given in equation 2-9 for rectilinear elements and a linear triangular shape function for the triangular elements. [20,22]

Thermal conductivity and capacitance are entered in TASEF as temperature-property pairs. Only the conductivity, capacitance, and density may vary with temperature. Each material in a problem is numbered uniquely. The material identification number must match the material number given when defining the geometry.

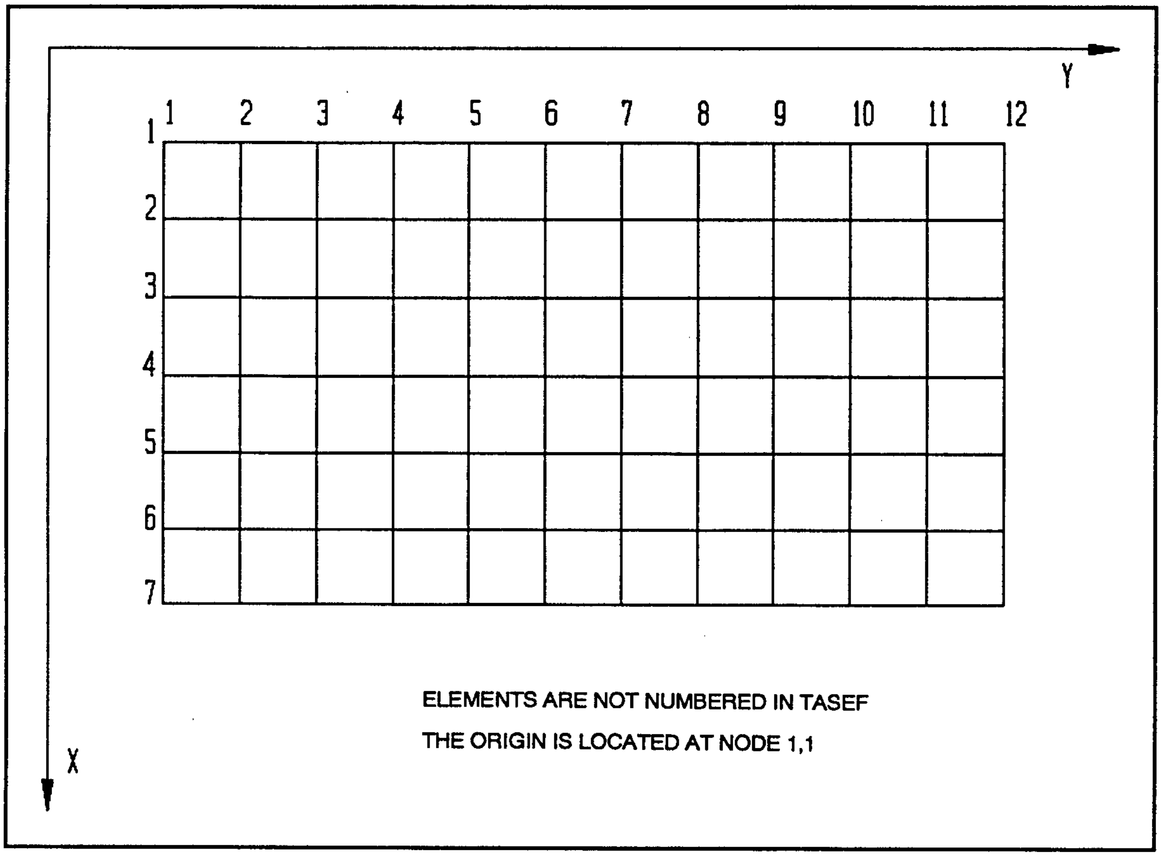

Figure 2-3 TASEF Nodal Coordinate System

TASEF allows for seven boundary conditions. These are:

1. Adiabatic - with zero heat flow across the boundary. The adiabatic boundary condition is the default for TASEF.

2. Prescribed temperature - the temperature on this boundary remains constant. This is useful for a fluid boundary.

3. Prescribed heat flow - this specifies the heat flow across a boundary.

4. Linear convective heat exchange - $hA(T_8 - T_\infty)$.

5. Non-linear convective heat exchange - $hA(T_8 - T_\infty)^\beta$.

6. Radiative heat exchange - $\sigma A \varepsilon F (T_8^4 - T_\infty^4)$.

7. Both 5 and 6 - $hA(T_8 - T_\infty)^\beta + \sigma A \varepsilon F (T_8^4 - T_\infty^4)$.

There are four options for defining the surrounding temperature:

1. Constant temperature.

2. Time/temperature pairs as with conductivity and heat capacitance. The intermediate values are linearly interpolated.

3. ISO standard fire - temperature values are given according to:

$$T = T_0 + 345 \cdot \log(480t+1) \qquad t \ hours$$

The duration of the fire is specified and at the end it declines according to:

$$\begin{array}{ll} 625 \ \frac{°C}{hr} & t_d < \frac{1}{2} \\ 250(2-t_d) \ \frac{°C}{hr} & \frac{1}{2} \le t_d \le 2 \\ 250 \ \frac{°C}{hr} & t_d > 2 \end{array}$$

with t_d the fire duration.

4. Natural fire - temperatures are calculated according to:

$$T_F - T_O = 1100 - 369.7e^{-0.617t_m} - 200e^{4.94t_m} - 539.9e^{23.2T_m}$$

$$t_m = \alpha t^2$$

$$\alpha = \frac{k_r}{k} \cdot \frac{o}{o_r}$$

'k' is the thermal resistance of the surface, o is an opening factor and the subscript r is an arbitrary reference value.

If heat is generated within the material, a heat flux or temperature-time values must be entered.

TASEF allows the user to assist with the numerical convergence of a problem. The user may alter the critical time step, increase the number of iterations TASEF performs in a time step or change the convergence criteria. The default values are adequate for many problems. Problem sets that do not converge with the default values require trial and error changes to the convergence controls. This report found it favorable to reduce the critical time step and increase the number of iterations. The smaller the critical time step, the longer the computer processing time. The amount of time a problem takes can be quite long for small critical time steps. Appendix C has the input files for TASEF that were used to determine the temperature distribution in the panels.

TPRE has the properties of four materials stored in the program code. The materials are stainless steel, concrete, and two mineral wool materials. If these materials are required, little research effort is needed to determine the nonlinear material properties. Care must be applied to units because the material properties are always given in J, Kg, m, s. TASEF can model internal voids. This feature requires the subtraction of a region inside a domain and specifying a radiation boundary condition on all surfaces in the void.

2.3.2 FIRES-T3

FIRES-T3 is a one, two, or three dimensional heat transfer FEM program written in 1977 by R. Iding, Z. Nizamuddin and B. Bresler. [18] There is no preprocessor for FIRES-T3. The input file arrangement is not difficult to interpret, so lack of a preprocessor is not a problem.

The elements FIRES-T3 uses are one dimensional lines, two dimensional quadrilaterals and triangles, and three dimensional hexahedrons and pentahedrons (five-faced volume elements). Figure 2-4 shows the elements available in FIRES-T3. The elements can be virtually any shape because the nodal coordinates are entered for each element. One dimensional elements require two node values, two dimensional elements require four; eight are required for three dimensions. For triangles and pentahedrons, some nodes must be entered with identical coordinates (refer to Figure 2-4 for the numbering sequence). Greater accuracy is achieved with shapes approximating squares, cubes, equilateral triangles and equilateral pentahedrons. [18]

FIRES-T3 can generate the nodal coordinates of identical neighboring elements, as could TASEF. This reduces both the time required to prepare a data file and the size of the file.

Unlike TASEF, the elements in FIRES-T3 must be individually numbered. The numbering for one dimensional elements proceeds from right to left. Two dimensional elements are numbered right to left, then the row is incremented and so on. The three dimensional elements are numbered like the two dimensional elements in a plane; then each plane is incremented. Elements are specified by identifying the nodes at the corners. It is important that the nodes are in the proper sequence when describing an element. The sequences for each element are (refer to Figure 2-4 for location of nodes):

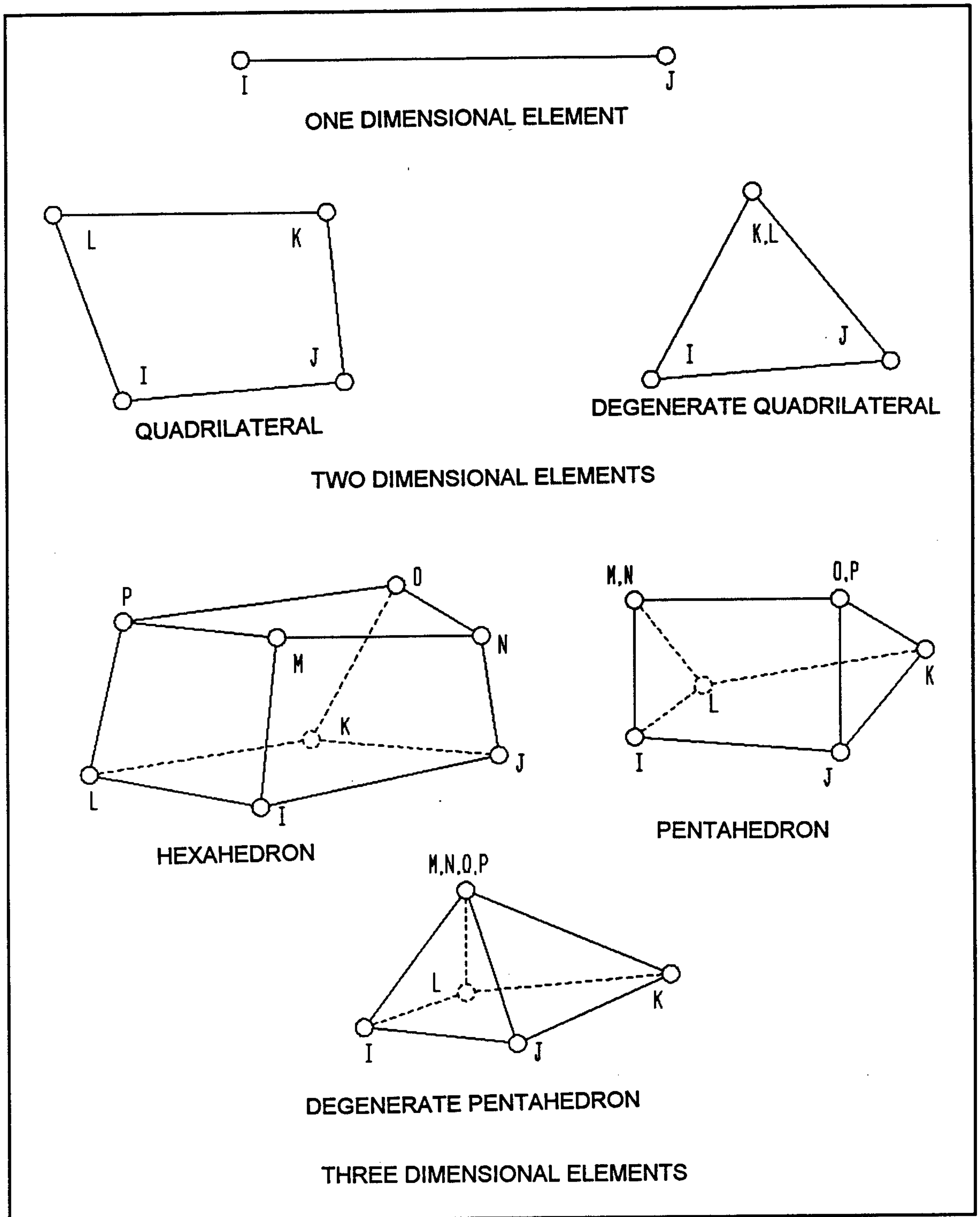

Figure 2-4 FIRES-T3 Elements

1. One dimensional elements: I,J
2. Two dimensional elements: I,J,K,L
3. Three dimensional elements: I,J,K,L,M,N,O,P

Each element requires a material identification number corresponding to a set of material properties. The material properties are entered in the same manner as they are for TASEF. Conductivity and heat capacity can be temperature dependant in FIRES-T3. FIRES-T3 cannot extrapolate outside the maximum and minimum values of the material properties.

The program allows seven boundary conditions:

1. Adiabatic.
2. Prescribed temperature.
3. Prescribed heat flow.
4. Linear convection ($\epsilon=0$, $\beta=1$).
5. Radiative (h=0) (includes flame emissivity/surface absorbtivity).
6. Non-linear convective.
7. Non-linear/linear convective and radiative.

The thermal load is specified as time-temperature pairs. There may be four different thermal load curves. Internal heat generation is specified as either a thermal flux or with time-temperature values.

FIRES-T3 allows the user to control convergence by dampening the critical time step and altering the error tolerance. The default values worked with all the models used in this report except for the steel-fiberglass model. For unstable models, the convergence controls must be changed by trial and error until FIRES-T3 converges.

2.4 Input for TASEF and FIRES-T3

2.4.1 Materials

Three materials and an aluminum post were analyzed with TASEF and FIRES-T3. The materials are identified as:

material 1 - steel/fiberglass
material 2 - plastic honeycomb
material 3 - steel honeycomb
post - aluminum H-post

Each of the three panel materials were analyzed individually. The post was modeled together with the steel-honeycomb material. Figure 2-5 shows the post-panel connection modeled. Appendix C contains both the TASEF and FIRES-T3 input files for all four models.

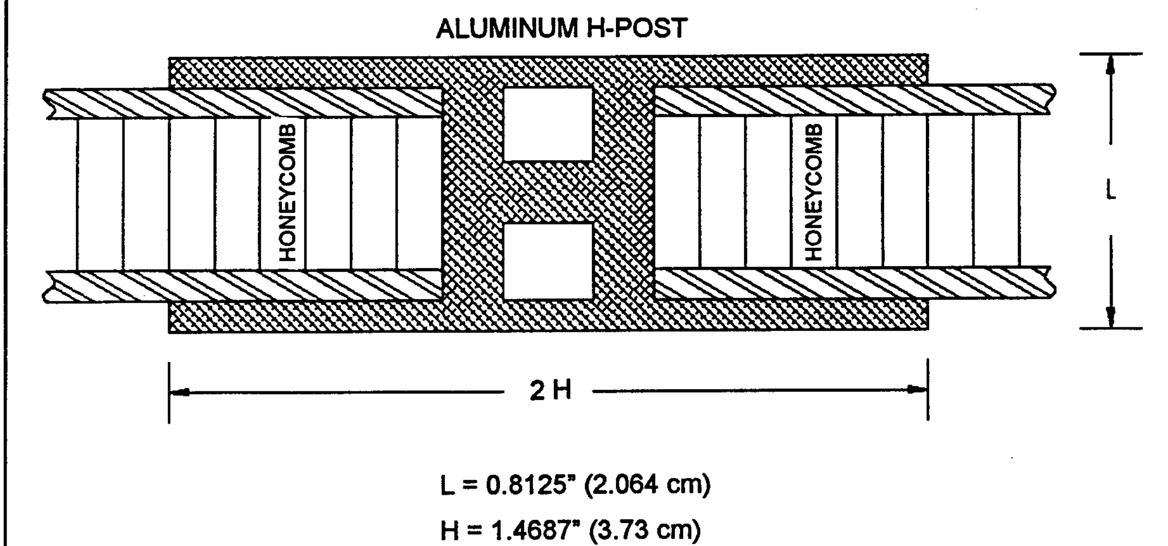

Figure 2-5 Panel-Post Connection Analyzed

2.4.2 Material Properties

The material properties for the panels are listed in Section 1-5. The material properties for the post are shown in Table 2-1. [12,14]

Table 2-1 Material Property for Aluminum

κ Btu/s-ft-R	κ J,s-m-K	c_p Btu/lb-R	c_p J/Kg-K	ρ lb/ft^3	ρ Kg/m^3
137000.	238.0	2063.0	920.93	169.5	2700.0

2.4.3 Boundary Conditions

Table 2-2 summarizes the boundary condition data for the exposed and unexposed sides of the panels and post.

Table 2-2 Boundary Conditions

Fire Boundary			
const. (units)	METRIC	ENGLISH	const. (units)
h (J/cm^2-K)	0.36	4410.0	h (Btu/in^2-R)
ϵ	0.6 (steel)	0.8 (plastic)	ϵ
ϵ_{flame}	1.0	1.0	ϵ_{flame}
β	1.33	1.33	β
F	1.0	1.0	F
$T-T_o$ (K)	345log(480t+1)	621log(480t+1)	$T-T_o$ R
σ (J/cm^2-hr-K^4)	0.204	14756	σ (Btu/in^2-h-R^4)
Air Boundary			
h (J/cm^2-K)	1.0	12251	h (Btu/in^2-R)
ϵ	0.0	0.0	ϵ
β	1.0	1.0	β
T (K)	298	536.4	T (R)

2.4.4 Mesh Geometry

Eight elements were used across the temperature gradient. Figures 2-6 and 2-7 show the mesh that was used for the panels and post.

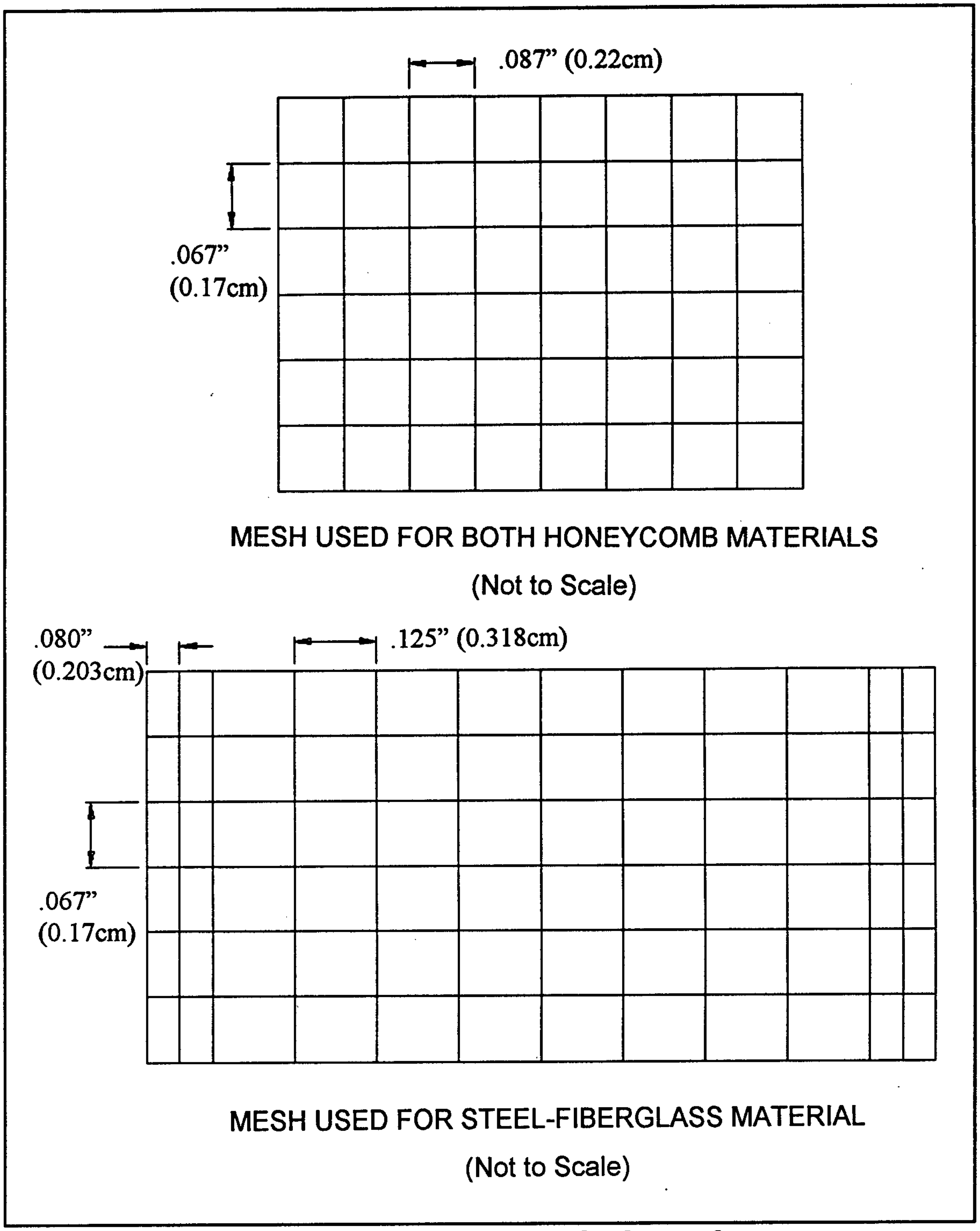

Figure 2-6 Meshed Regions for the Panels

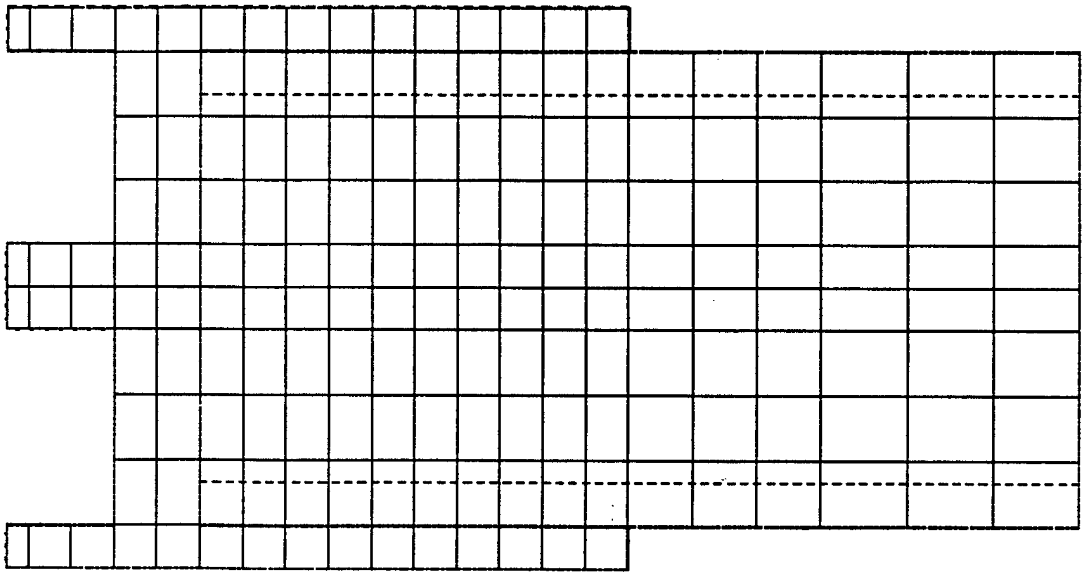

Figure 2-7 Meshed Region for Post-Panel

2.5 Results of the Heat Transfer Analysis

The temperature distributions which result from the ISO fire plot in Graph 2-1 are shown in Graphs 2-2 through 2-7 for each of the three panels at various times. The temperature and position are non-dimensional:

$$T^* = \frac{(T - T_R)}{(T_O - T_R)} \qquad \textbf{(2-30a)}$$

$$L^* = \frac{X}{L} \qquad \textbf{(2-30b)}$$

The reference temperature, T_R, was 77 R (25 K) and the initial temperature, T_O, was 537 R (298 K). The problem modeled was one dimensional. The one dimensional elements in FIRES-T3 were just as effective for modeling the panels. Two dimensions were chosen to give a better visual picture of the model.

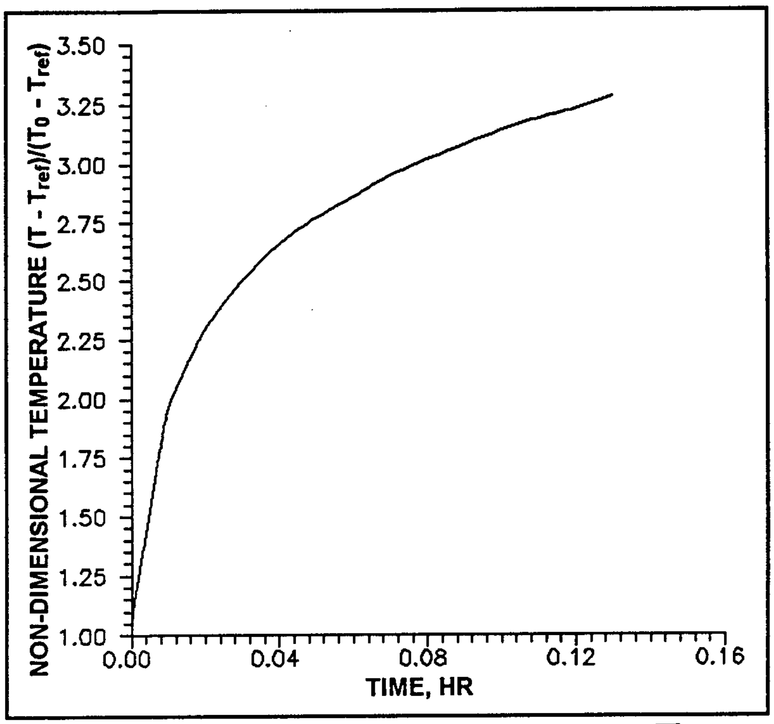

Graph 2-1 Plot of ISO Fire Temperature vs Time

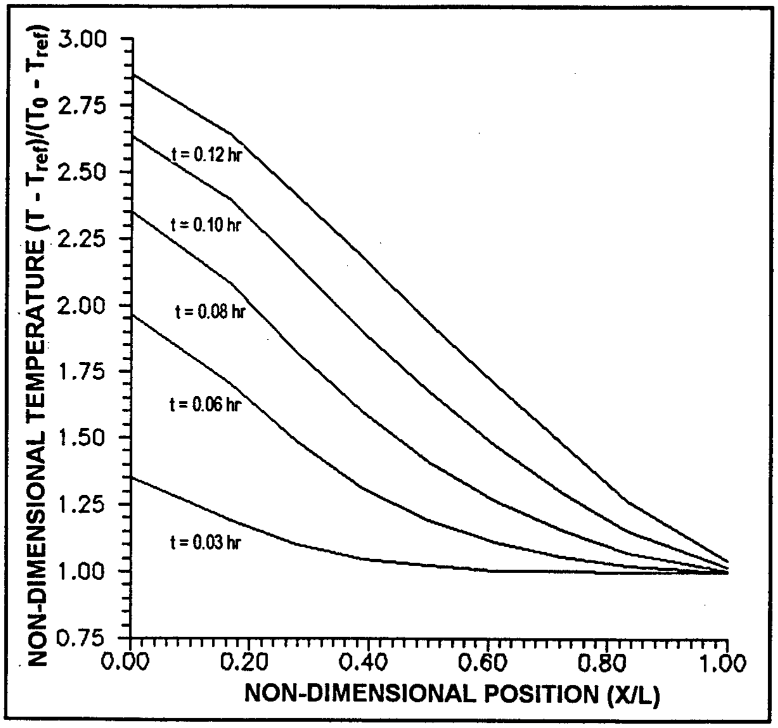

Graph 2-2 TASEF Results for Material One

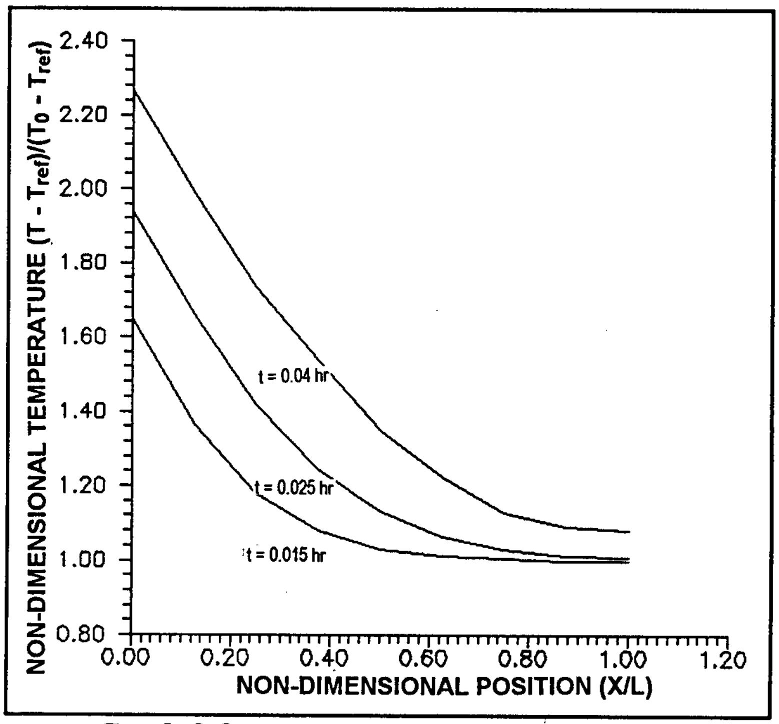

Graph 2-3 TASEF Results for Material Two

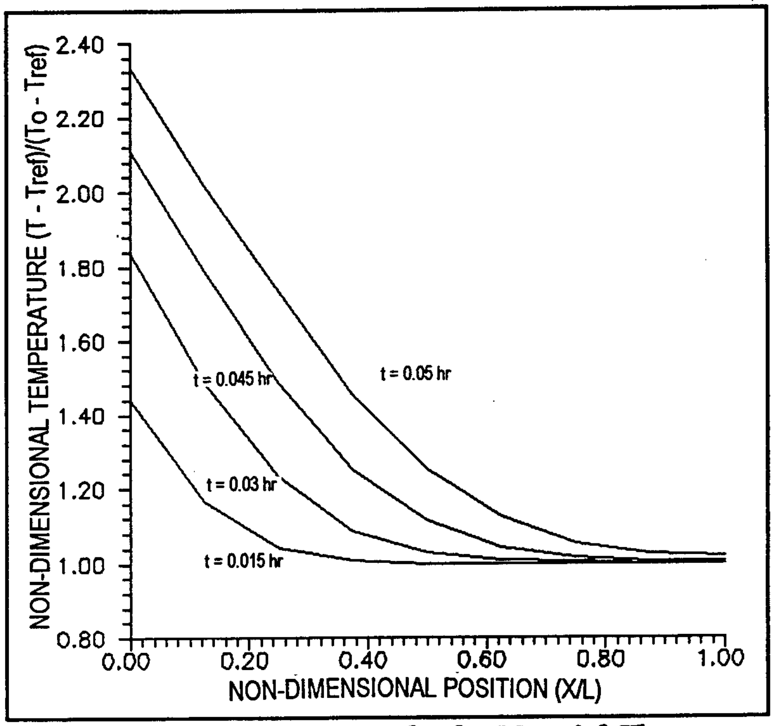

Graph 2-4 TASEF Results for Material Three

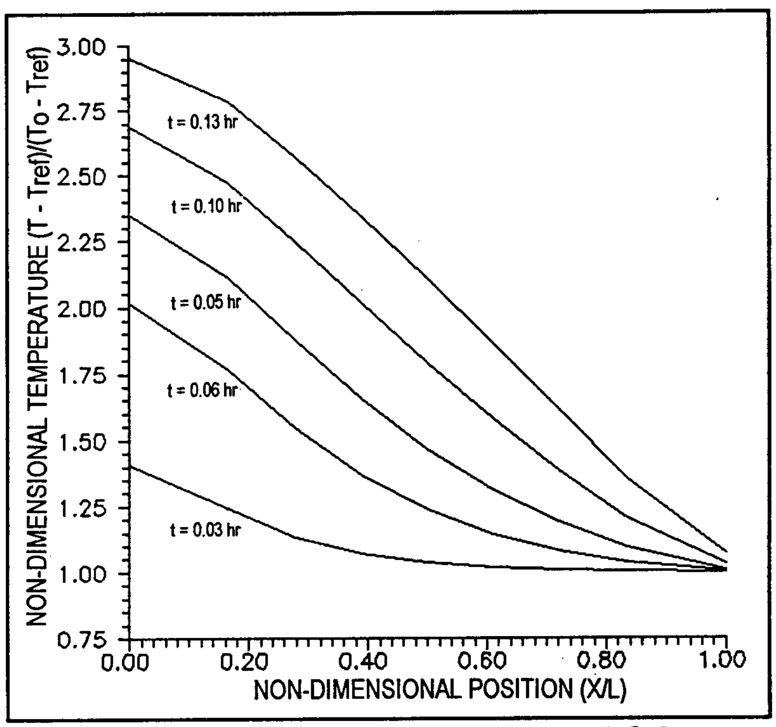

Graph 2-5 FIRES-T3 Results for Material One

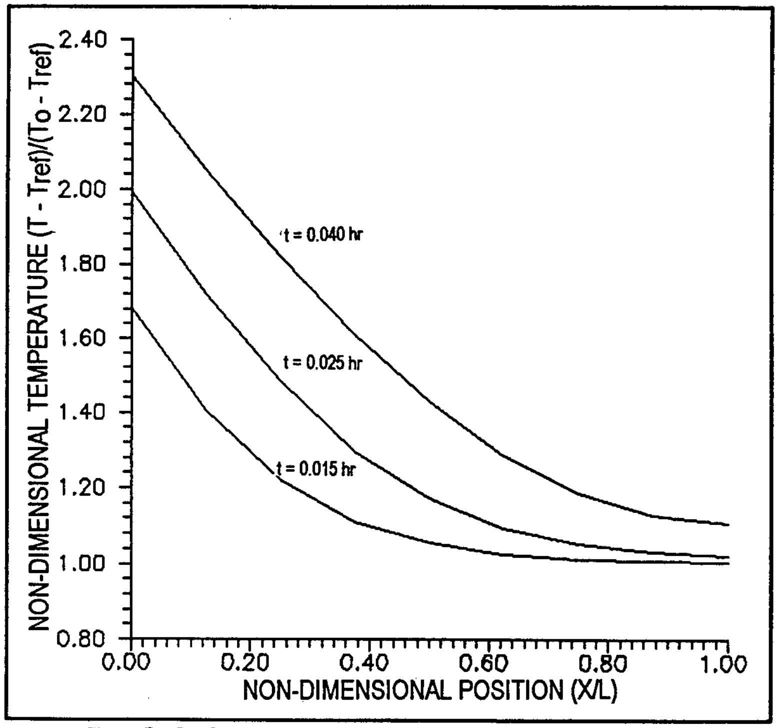

Graph 2-6 FIRES-T3 Results for Material Two

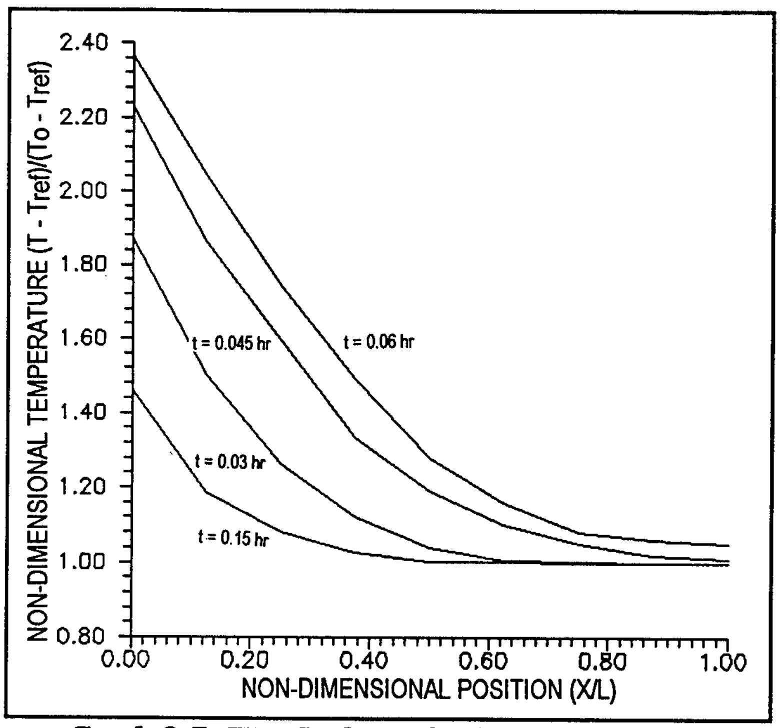

Graph 2-7 FIRES-T3 Results for Material Three

Figures 2-8a-c show the temperature distribution in the aluminum post and material three at several time steps. Both axes were non-dimensional as well as the temperature:

$$T^*=\frac{(T-T_{REF})}{T_O-T_{REF})} \qquad \textbf{(2-34a)}$$

$$L^*=\frac{x}{L} \qquad \textbf{(2-34b)}$$

$$H^*=\frac{y}{H} \qquad \textbf{(2-34c)}$$

The dimensions H and L are labeled in Figure 2-5. The reference temperature was (20 K), the initial temperature (283 K), the length 0.8125 in. (2.0638 cm), and the height 1.4687 in. (3.7306 cm).

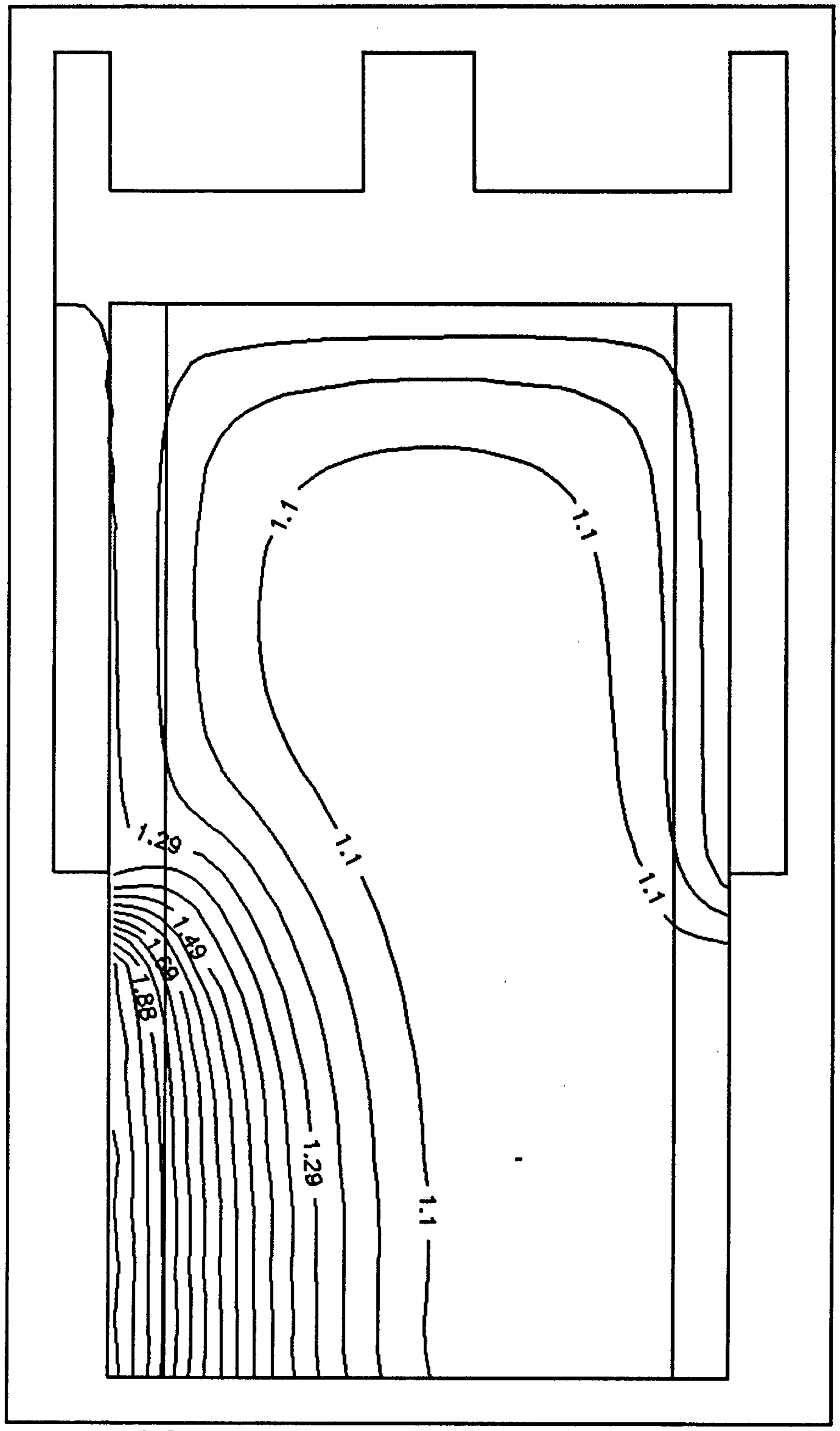

Figure 2-8a Temperature Field in Post-Panel (t=0.04 hr)

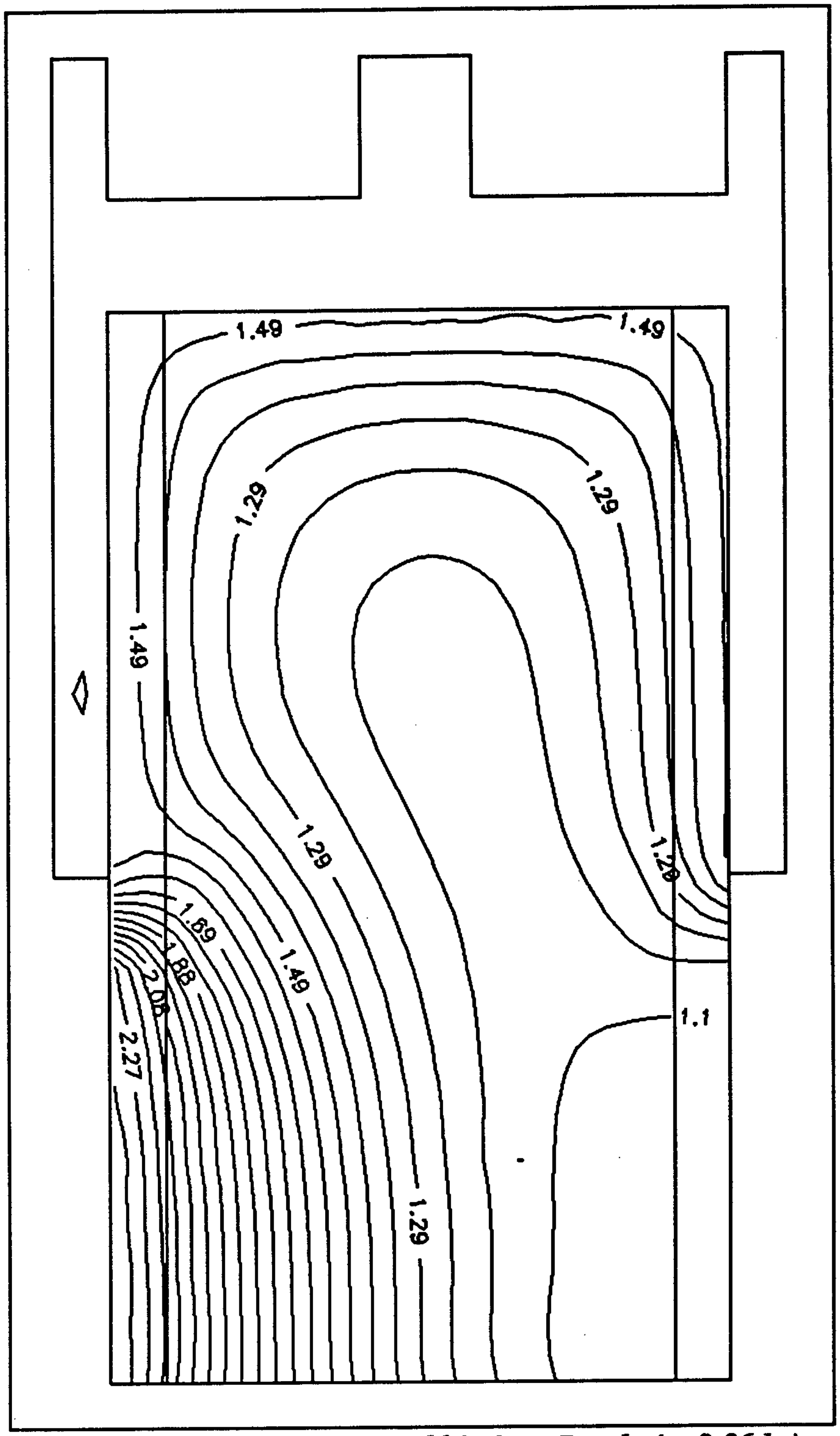

Figure 2-8b Temperature Field in Post-Panel (t=0.06 hr)

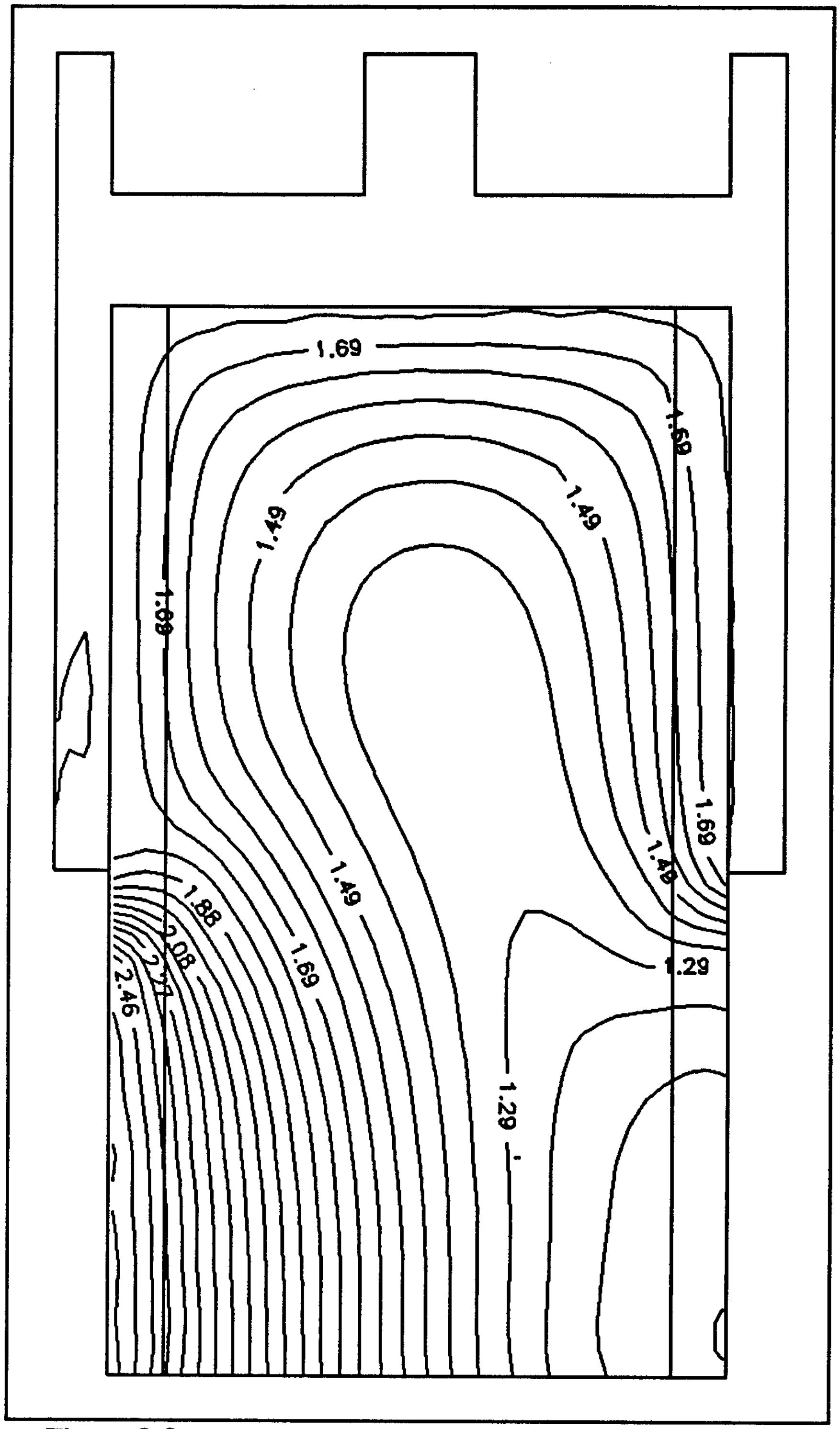

Figure 2-8c Temperature Field in Post-Panel (t=0.08 hr)

2.5.1 Panel Decomposition

Table 2-3 shows the decomposition time for the panels. The decomposition time was reported by Holometrix during the conductivity and heat capacity tests. This study required temperature distributions beyond the reported decomposition temperature for the thermo-elastic analysis in Chapter Three. For times greater than those in Table 2-3, the conductivity and heat capacity were assumed to be the final values determined by Holometrix.

Table 2-3 Time to Decomposition (seconds)

material one	432	468
material two	144	144
material three	216	216

2.5.2 Program Run Times

The amount of time for TASEF and FIRES-T3 to reach the decomposition load is shown for each material in Table 2-4.

Table 2-4 Computer Run Times (seconds)

	TASEF	FIREST3
material one	2688	10
material two	8	5
material three	8	5

TASEF took particularly long for material one because the critical time step was small and the number of iterations enormous. The steel faces were not lumped because a temperature gradient in the panels was required for a static analysis. If the steel faces were eliminated the run took only twenty-five seconds.

2.6 Comparison of TASEF and FIRES-T3

Graphs 2-8, 2-9, and 2-10 compare the results of TASEF and FIRES-T3 for the three materials. They display the deviation of FIRES-T3 from TASEF in percent.

$$\frac{FIRES\text{-}T3}{TASEF}\cdot 100 \qquad \textbf{(2-35)}$$

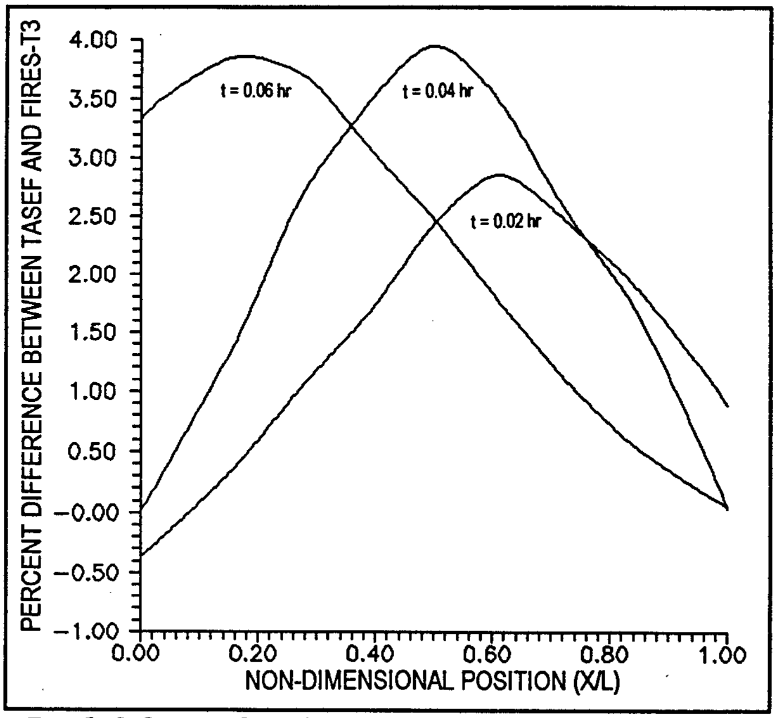

Graph 2-8 Results of TASEF and FIRES-T3 Compared

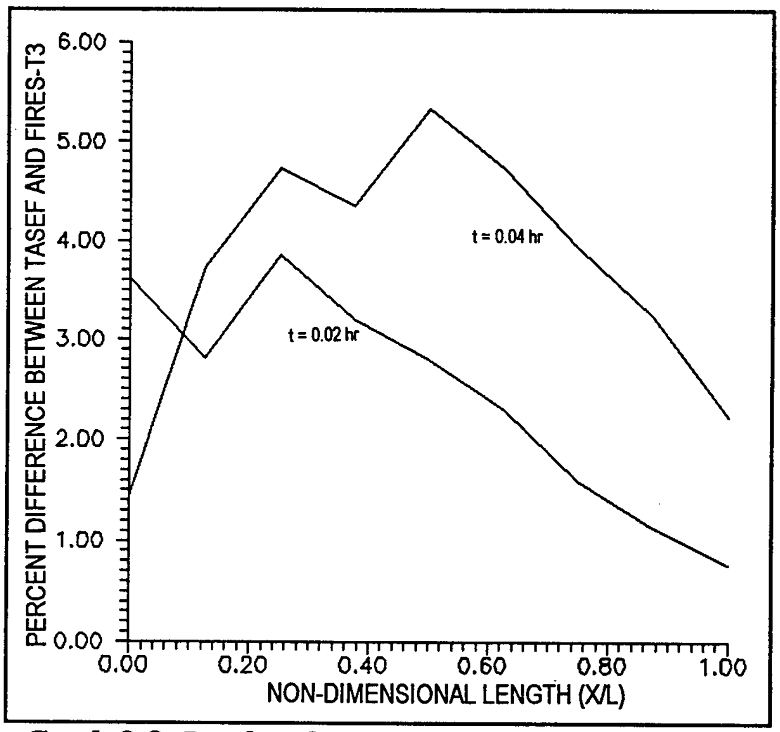

Graph 2-9 Results of TASEF and FIRES-T3 Compared

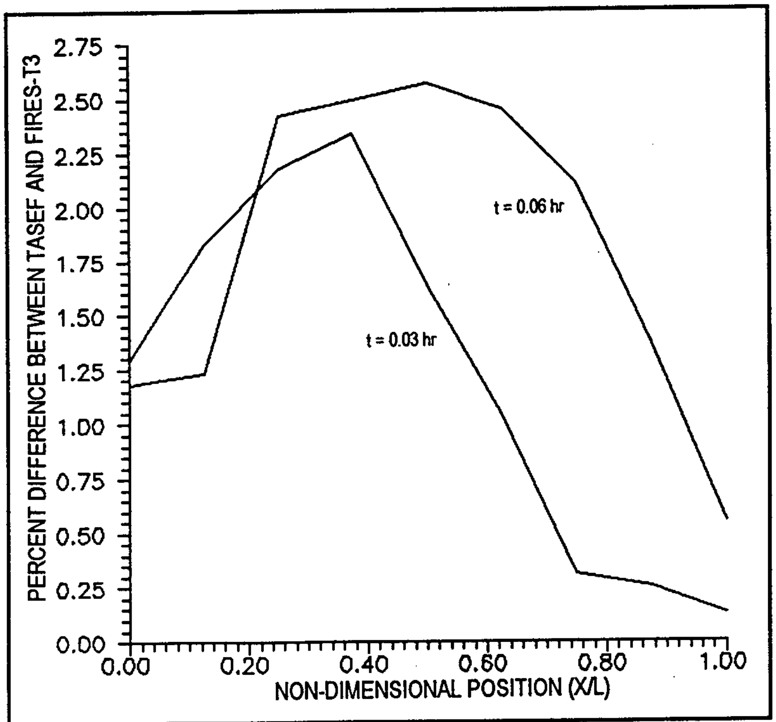

Graph 2-10 Results of TASEF and FIRES-T3 Compared

TASEF and FIRES-T3 differ by no more than five percent. Most of the temperatures are within three percent. The greatest deviations occur in the middle of the materials. The boundaries have almost zero difference. Thus, TASEF and FIRES-T3 report the same temperature distributions when set up correctly.

2.7 Model Verification

2.7.1 Mesh Convergence

The mesh used for the panels (Figures 2-6 and 2-7) was verified by altering the number of elements along the temperature gradient. The range was between two and sixteen. Graphs 2-11 through 2-14 show the convergence of the mesh for material three for both TASEF and FIRES-T3. Materials one and two had a similar mesh convergence. Eight elements along the temperature gradient were found sufficient to model the panels.

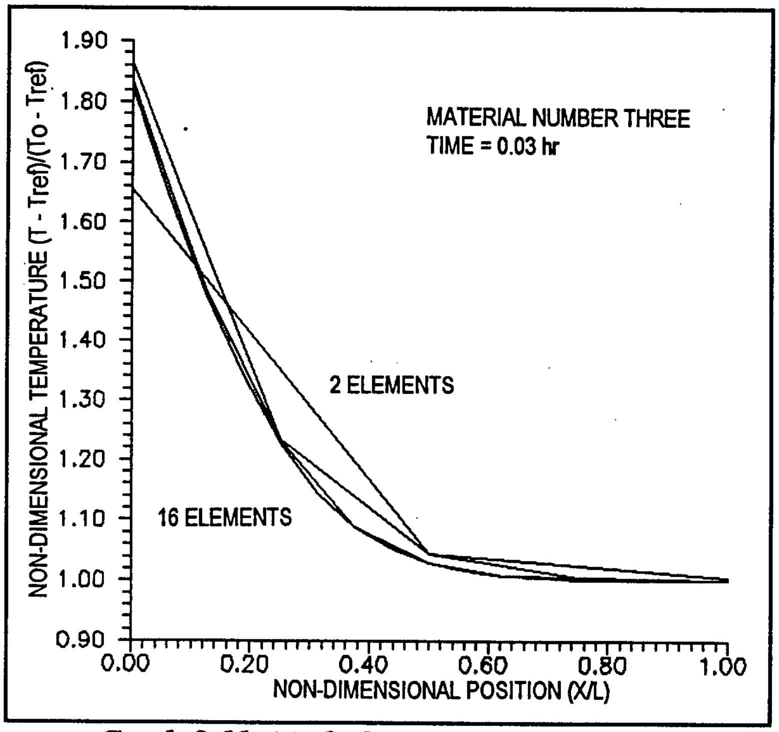

Graph 2-11 Mesh Convergence for TASEF

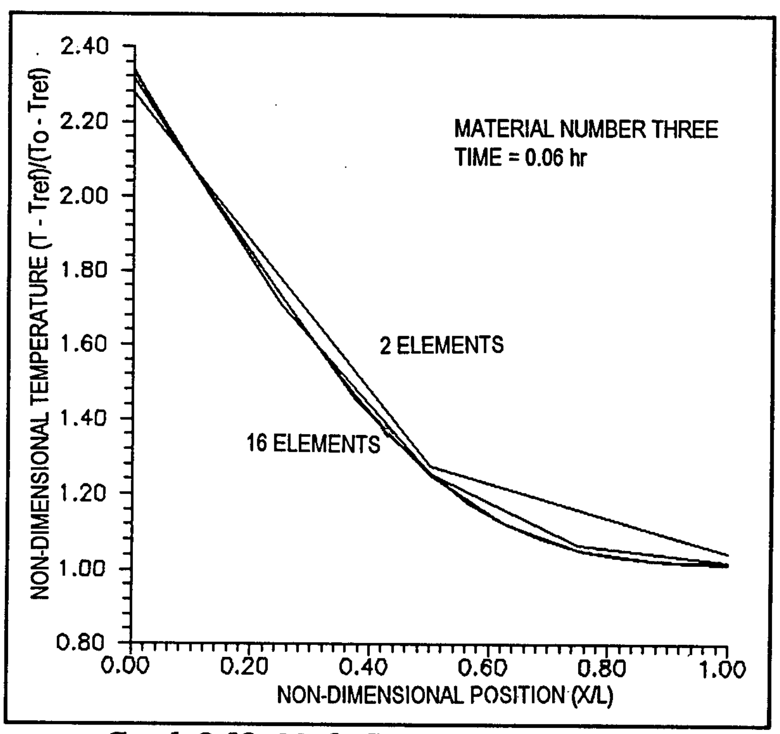

Graph 2-12 Mesh Convergence for TASEF

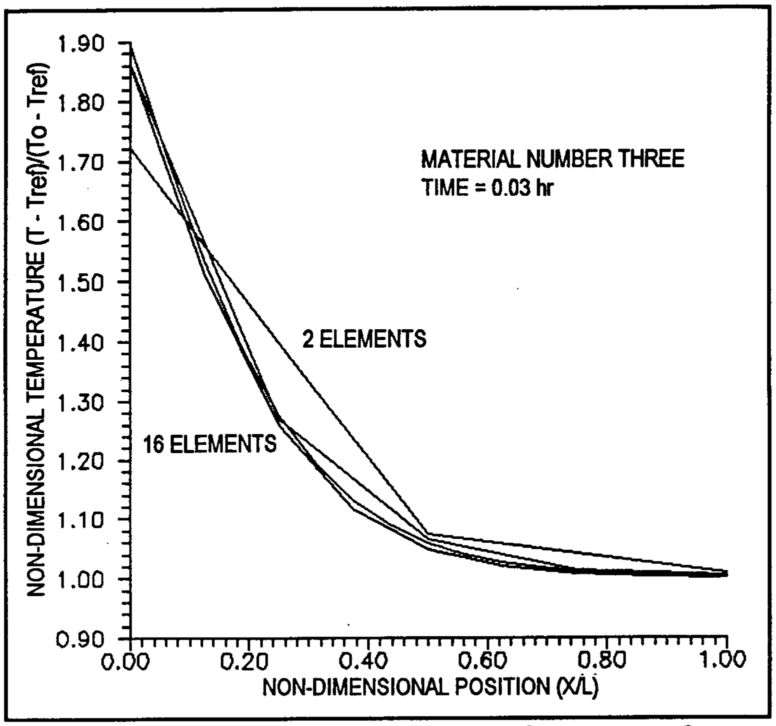

Graph 2-13 Mesh Convergence for FIRES-T3

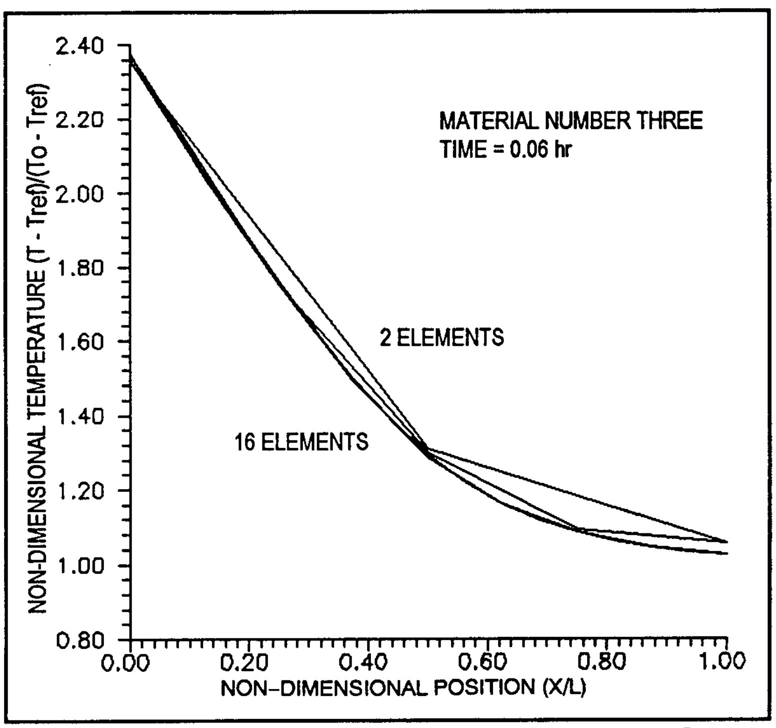

Graph 2-14 Mesh Convergence for FIRES-T3

2.7.2 The Convection Coefficient

The convection coefficient on the ambient side was next altered to examine its impact on the solution. When the convection coefficient on the unexposed side was quadrupled (to 4 J/cm^2 - K) in FIRES-T3, the surface temperatures on the exposed side were reduced by 3.6 - 5.4 R (2 - 3 K). When the convection coefficient was quadrupled in TASEF, the program became unstable, despite experimentation with the convergence criteria. This is perhaps due to violating the energy equation: [17]

$$Q_{\epsilon}=Q_{stored}+Q_{out} \tag{2-36}$$

Since the heat flux in and out and the amount of heat stored are specified with the convection coefficients and heat capacity respectively, care should be taken to ensure equation 2-36 is not violated. Since the convection coefficient has a minimal effect on the final solution when within the bounds of equation 2-36, the specific value selected is not a major concern. A value of about 1 J/hr-cm^2-K is advisable since it worked well in both TASEF and FIRES-T3.

2.7.3 Emissivity

The surface emissivity was altered to observe the effect on the solution. When the emissivity of the plastic honeycomb material was reduced from 0.8 to 0.6, the fire boundary temperature fell as much as 18 R (10 K). The internal temperatures were comparably lower. Therefore, the emissivity of the surface should be selected with care.

2.8 Summary of the Heat Transfer Analysis

This section briefly summarizes the advantages and disadvantages of TASEF and FIRES-T3 observed during use.

2.8.1 TASEF

The advantages of TASEF can be summarized:

1. Easy mesh generation.
2. Ability to handle many types of boundary conditions.
3. Preprocessor to assist in setting up the data file.
4. Capability to deal with internal voids.
5. Density, heat capacity, conductivity and heat generation can be temperature dependent.
6. The output is easy to follow.
7. The preprocessor has several materials stored in the code.

The disadvantages were:

1. Unable to utilize 1 and 3 dimensional elements.
2. Cannot use deformed elements.
3. Program tends to diverge with extreme values of ϱ, c_p, and k, requiring small critical times and many trials.
4. Several precalculations are required to combine the density and specific heat terms.
5. The preprocessor needs a lot of work, there are many problems with it.
6. The data file is difficult to set up without the preprocessor.

2.8.2 FIRES-T3

The advantages of FIRES-T3 are:

1. 1,2,3 dimensional elements can be used in any combination.
2. Can use deformed elements.
3. ϱ, c_p, and k can be temperature dependent.
4. Can handle several boundary conditions.
5. Accounts for flame emissivity, shape factor and surface absorbtivity.
6. The program is stable and quick.

The disadvantages noticed:

1. There is no preprocessor. The data file must be created directly.
2. It cannot deal with internal voids easily.
3. Elements and node values are more time consuming to input.
4. It does not have any built in material properties.
5. The fire and other boundary condition data must be entered for each time step, which means to properly model a fire curve a very long fire step list must be entered.

CHAPTER THREE
Thermo-Elastic Analysis

3.0 Objectives

There were three objectives to the thermo-elastic analysis. These were to find acceptable finite element software that can predict the response of the panels and post subject to a fire load, to run a protocol analysis, and to point out the portions of the analysis that require more information.

ANSYS and NASTRAN were selected for the thermo-elastic analysis because both were able to model materials at elevated temperatures under a variety of boundary conditions. The ability to model materials at elevated temperatures entails temperature-dependent material properties, stress dependent material properties, multiple thermal load steps, and creep. There were five steps to the protocol analysis. These were to make the necessary assumptions, determine the material properties, apply the boundary conditions, run the model, and, finally, to validate the model.

The assumptions and boundary conditions most influential to the final results are then pointed out.

3.1 Governing Equations for Thermo-Elasticity

3.1.1 Post Equations

A restrained post subject to a thermal load will exhibit three distinct behaviors. These behaviors are pre-buckling, buckling, and post-buckling. Each behavior has unique equations that describe the stress conditions and deflections.

3.1.1.1 Equations for a Pre-Buckled Beam

For a two-dimensional problem, T=T(x,y), where x is the vertical and y is the depth for a post (see Figure 3-1 for coordinate system). The equation T=T(x,y) implies plane strain, or: [23,24]

$$u=u(x,y) \quad \text{(3-1a)}$$

$$v=v(x,y) \quad \text{(3-1b)}$$

$$w=0 \quad \text{(3-1c)}$$

$$\sigma_{zz}=\sigma_{xz}=\sigma_{yz}=0 \quad \text{(3-1d)}$$

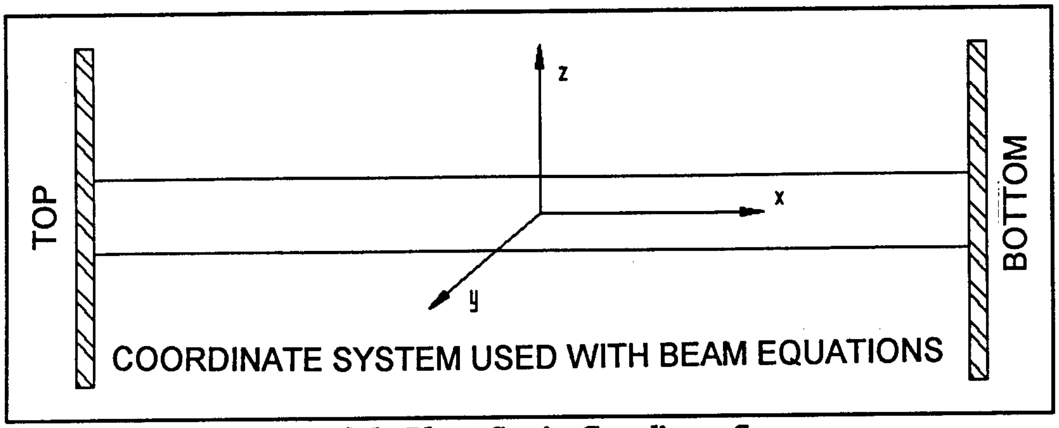

Figure 3-1 Plane Strain Coordinate System

There are eight unknowns: $u, v, \sigma_{xx}, \sigma_{yy}, \sigma_{xy}, \epsilon_{xx}, \epsilon_{yy}, \epsilon_{xy}$.
From basic mechanics of materials, the equations that relate the unknowns are:

$$\frac{\partial \sigma_{xx}}{\partial x}+\frac{\partial \sigma_{xy}}{\partial y}=0 \qquad (3\text{-}2)$$

$$\frac{\partial \sigma_{xy}}{\partial x}+\frac{\partial \sigma_{yy}}{\partial y}=0 \qquad (3\text{-}3)$$

$$\epsilon_{xx}=\frac{1}{E}(\sigma_{xx}-\nu\sigma_{yy})+\alpha T \qquad (3\text{-}4)$$

$$\epsilon_{yy}=\frac{1}{E}(\sigma_{yy}-\nu\sigma_{xy})+\alpha T \qquad (3\text{-}5)$$

$$\epsilon_{xy}=2G\sigma_{xy} \qquad (3\text{-}6)$$

$$\epsilon_{xx}=\frac{\partial u}{\partial x} \qquad (3\text{-}7)$$

$$\epsilon_{yy}=\frac{\partial v}{\partial y} \qquad (3\text{-}8)$$

$$\epsilon_{xy}=\frac{1}{2}\left(\frac{\partial u}{\partial x}+\frac{\partial v}{\partial y}\right) \qquad (3\text{-}9)$$

The stresses and strains in equations 3-2 through 3-9 can be rearranged to give the general displacement equations:

$$\frac{E}{2(1-\nu)}\frac{\partial}{\partial x}\left(\frac{\partial u}{\partial x}+\frac{\partial v}{\partial y}\right)+\frac{E}{2(1+\nu)}\nabla^2 u-\left(\frac{\alpha E}{1-\nu}\right)\frac{\partial T}{\partial x}+X=0 \qquad \textbf{(3-10)}$$

$$\frac{E}{2(1-\nu)}\frac{\partial}{\partial y}\left(\frac{\partial u}{\partial x}+\frac{\partial v}{\partial y}\right)+\frac{E}{2(1+\nu)}\nabla^2 v-\left(\frac{\alpha E}{1-\nu}\right)\frac{\partial T}{\partial y}=0 \qquad \textbf{(3-11)}$$

In these equations X is the body force due to gravity. From the equations of equilibrium [23,25], and using equations 3-2 through 3-9, the compatibility equation in terms of strain is:

$$\frac{\partial^2\epsilon_{xx}}{\partial y^2}+\frac{\partial^2\epsilon_{yy}}{\partial x^2}-\frac{2\partial^2\epsilon_{xy}}{\partial x\partial y}=0 \qquad \textbf{(3-12)}$$

and in terms of stress with gravity in the x direction:

$$\nabla^2(\sigma_{xx}+\sigma_{yy}\alpha ET)+(1+\nu)\left(\frac{\partial X}{\partial x}\right)=0 \qquad \textbf{(3-13)}$$

Commonly, a stress function is used to solve these equations. The Airy stress formulation assumes a stress function (φ) with the properties:

$$\frac{\partial^2\varphi}{\partial y^2}=\sigma_{xx} \qquad \textbf{(3-14a)}$$

$$-\frac{\partial^2\varphi}{\partial x\partial y}=\sigma_{xy} \qquad \textbf{(3-14b)}$$

$$\frac{\partial^2\varphi}{\partial x^2}=\sigma_{yy} \qquad \textbf{(3-14c)}$$

Substitution of 3-14a-c into 13 gives the two-dimensional thermo-elastic equation:

$$\nabla^4\varphi=-\alpha E\nabla^2 T \qquad (3\text{-}15a)$$

$$\nabla^4\varphi=\frac{\partial^4\varphi}{\partial x^4}+2\frac{\partial^4\varphi}{\partial x^2\partial y^2}+\frac{\partial^4\varphi}{\partial y^4} \qquad (3\text{-}15b)$$

Exact solutions to this equation are difficult and only exist for basic geometries and boundary conditions. Table 3-1 shows the stress functions for a rectangular beam with a general temperature distribution. [24] The far left column gives the form of the stress function solved divided by αE, namely φ, $\partial^2\varphi/\partial x\cdot\partial y$ and $\partial^2\varphi/\partial y^2$. Also, the stress function is broken up so that:

$$\varphi=\sum_{i=1}^{N}\varphi_i \qquad (3\text{-}16)$$

with the functions satisfying the following constraints and boundary conditions:

$$\frac{\partial^4\varphi_1}{\partial y^4}=-\alpha E\frac{\partial^2 T}{\partial y^2} \qquad (3\text{-}17a)$$

$$\frac{\partial^4\varphi_2}{\partial y^4}=-\alpha E\frac{\partial^2 T}{\partial x^2}-2\frac{\partial^4\varphi_1}{\partial x^2\partial y^2} \qquad (3\text{-}17b)$$

$$\frac{\partial^4\varphi_i}{\partial y^4}=-2\frac{\partial^4\varphi_{i-1}}{\partial x^2\partial y^2}-\frac{\partial^4\varphi_{i-2}}{\partial x^4} \qquad (3\text{-}17c)$$

$$\varphi=\frac{\partial\varphi}{\partial y}=0 \quad at\ y=\pm c \qquad (3\text{-}17d)$$

The tables go out to φ_3, which is reasonably accurate. [24] The deflections are then obtained by integrating the following equation:

$$E\frac{\partial u}{\partial x}=\sigma_{xx}-\nu\sigma_{yy}+\alpha ET \qquad (3\text{-}18a)$$

$$E\frac{\partial v}{\partial y}=\sigma_{yy}-\nu\sigma_{xx}+\alpha ET \qquad (3\text{-}18b)$$

using the stress functions found in the table. The equations are very long and will not be reproduced here. The reader is referred to [24, pp. 323-324] for these.

$\int \equiv \int_{-c}^{y} \qquad \oint \equiv \int_{-c}^{c}$ Stress Functions φ_i and the Corresponding Stresses for $i = 1, 2, 3.$ $(\sigma_{yy})_i = \dfrac{\partial^2 \varphi_i}{\partial x^2}$

i	1	2	3
$\dfrac{\varphi_i}{\alpha E}$	$-y\int T\,dy + \int Ty\,dy +$ $+\frac{c}{4}\left[1 + 2\left(\frac{y}{c}\right) + \left(\frac{y}{c}\right)^2\right]\oint T\,dy -$ $-\frac{1}{4}\left[2 + 3\left(\frac{y}{c}\right) - \left(\frac{y}{c}\right)^3\right]\oint Ty\,dy$	$\frac{\partial^2}{\partial x^2}\Big\{\frac{y^3}{6}\int T\,dy - \frac{y^2}{2}\int Ty\,dy + \frac{y}{2}\int Ty^2\,dy - \frac{1}{6}\int Ty^3\,dy -$ $-\frac{c^3}{24}\left[\left(\frac{y}{c}\right)^2 + 2\left(\frac{y}{c}\right)^3 + \left(\frac{y}{c}\right)^4\right]\oint T\,dy +$ $+\frac{c^2}{40}\left[4\left(\frac{y}{c}\right) + 10\left(\frac{y}{c}\right)^2 + 7\left(\frac{y}{c}\right)^3 - \left(\frac{y}{c}\right)^5\right]\oint Ty\,dy -$ $-\frac{c}{8}\left[1 + 2\left(\frac{y}{c}\right) + \left(\frac{y}{c}\right)^2\right]\oint Ty^2\,dy +$ $+\frac{1}{24}\left[2 + 3\left(\frac{y}{c}\right) - \left(\frac{y}{c}\right)^3\right]\oint Ty^3\,dy\Big\}$	$-\frac{\partial^4}{\partial x^4}\Big\{\frac{y^5}{120}\int T\,dy - \frac{y^4}{24}\int Ty\,dy + \frac{y^3}{12}\int Ty^2\,dy - \frac{y^2}{12}\int Ty^3\,dy + \frac{y}{24}\int Ty^4\,dy - \frac{1}{120}\int Ty^5\,d +$ $+c^5\left[\frac{1}{180} - \frac{1}{90}\left(\frac{y}{c}\right)^2 + \frac{1}{288}\left(\frac{y}{c}\right)^4 - \frac{1}{240}\left(\frac{y}{c}\right)^5 - \frac{1}{480}\left(\frac{y}{c}\right)^6\right]\oint T\,dy +$ $+c^4\left[-\frac{1}{1050}\left(\frac{y}{c}\right) + \frac{2}{175}\left(\frac{y}{c}\right)^3 + \frac{1}{48}\left(\frac{y}{c}\right)^4 + \frac{9}{800}\left(\frac{y}{c}\right)^5 - \frac{1}{1120}\left(\frac{y}{c}\right)^7\right]\oint Ty\,dy +$ $+c^3\left[-\frac{1}{48}\left(\frac{y}{c}\right)^2 - \frac{1}{24}\left(\frac{y}{c}\right)^3 - \frac{1}{48}\left(\frac{y}{c}\right)^4\right]\oint Ty^2\,dy +$ $+c^2\left[\frac{1}{60}\left(\frac{y}{c}\right) + \frac{1}{24}\left(\frac{y}{c}\right)^2 + \frac{7}{240}\left(\frac{y}{c}\right)^3 - \frac{1}{240}\left(\frac{y}{c}\right)^5\right]\oint Ty^3\,dy -$ $-\frac{c}{96}\left[1 + 2\left(\frac{y}{c}\right) + \left(\frac{y}{c}\right)^2\right]\oint Ty^4\,dy + \frac{1}{480}\left[2 + 3\left(\frac{y}{c}\right) - \left(\frac{y}{c}\right)^3\right]\oint Ty^5\,dy\Big\}$
$-\dfrac{(\sigma_{xy})_i}{\alpha E}$ $= \dfrac{1}{\alpha E}\dfrac{\partial^2 \varphi_i}{\partial x \partial y}$	$\frac{\partial}{\partial x}\Big\{-\int T\,dy +$ $+\frac{1}{2}\left[1 + \left(\frac{y}{c}\right)\right]\oint T\,dy -$ $-\frac{3}{4c}\left[1 - \left(\frac{y}{c}\right)^2\right]\oint Ty\,dy\Big\}$	$\frac{\partial^3}{\partial x^3}\Big\{\frac{y^2}{2}\int T\,dy - y\int Ty\,dy + \frac{1}{2}\int Ty^2\,dy -$ $-\frac{c^2}{12}\left[\left(\frac{y}{c}\right) + 3\left(\frac{y}{c}\right)^2 + 2\left(\frac{y}{c}\right)^3\right]\oint T\,dy +$ $+\frac{c}{40}\left[4 + 20\left(\frac{y}{c}\right) + 21\left(\frac{y}{c}\right)^2 - 5\left(\frac{y}{c}\right)^4\right]\oint Ty\,dy -$ $-\frac{1}{4}\left[1 + \left(\frac{y}{c}\right)\right]\oint Ty^2\,dy + \frac{1}{8}\left[1 - \left(\frac{y}{c}\right)^2\right]\oint Ty^3\,dy\Big\}$	$-\frac{\partial^5}{\partial x^5}\Big\{\frac{y^4}{24}\int T\,dy - \frac{y^3}{6}\int Ty\,dy + \frac{y^2}{4}\int Ty^2\,dy - \frac{y}{6}\int Ty^3\,dy + \frac{1}{24}\int Ty^4\,dy +$ $+c^4\left[-\frac{1}{45}\left(\frac{y}{c}\right) + \frac{1}{72}\left(\frac{y}{c}\right)^3 - \frac{1}{48}\left(\frac{y}{c}\right)^4 - \frac{1}{80}\left(\frac{y}{c}\right)^5\right]\oint T\,dy +$ $+c^3\left[-\frac{1}{1050} + \frac{6}{175}\left(\frac{y}{c}\right)^2 + \frac{1}{12}\left(\frac{y}{c}\right)^3 + \frac{9}{160}\left(\frac{y}{c}\right)^4 - \frac{1}{160}\left(\frac{y}{c}\right)^6\right]\oint Ty\,dy +$ $+c^2\left[-\frac{1}{24}\left(\frac{y}{c}\right) - \frac{1}{8}\left(\frac{y}{c}\right)^2 - \frac{1}{12}\left(\frac{y}{c}\right)^3\right]\oint Ty^2\,dy + c\left[\frac{1}{60} + \frac{1}{12}\left(\frac{y}{c}\right) + \frac{7}{80}\left(\frac{y}{c}\right)^2 -\right.$ $\left.-\frac{1}{48}\left(\frac{y}{c}\right)^4\right]\oint Ty^3\,dy - \frac{1}{48}\left[1 + \left(\frac{y}{c}\right)\right]\oint Ty^4\,dy + \frac{1}{160c}\left[1 - \left(\frac{y}{c}\right)^2\right]\oint Ty^5\,dy\Big\}$
$\dfrac{(\sigma_{xx})_i}{\alpha E}$ $= \dfrac{1}{\alpha E}\dfrac{\partial^2 \varphi_i}{\partial y^2}$	$-T + \frac{1}{2c}\oint T\,dy + \frac{3y}{2c^3}\oint Ty\,dy$	$\frac{\partial^2}{\partial x^2}\Big\{y\int T\,dy - \int Ty\,dy - \frac{c}{12}\left[1 + 6\left(\frac{y}{c}\right) +\right.$ $\left.+6\left(\frac{y}{c}\right)^2\right]\oint T\,dy + \frac{1}{20}\left[10 + 21\left(\frac{y}{c}\right) - 10\left(\frac{y}{c}\right)^3\right]\oint Ty\,dy -$ $-\frac{1}{4c}\oint Ty^2\,dy - \frac{y}{4c^3}\oint Ty^3\,dy\Big\}$	$-\frac{\partial^4}{\partial x^4}\Big\{\frac{y^3}{6}\int T\,dy - \frac{y^2}{2}\int Ty\,dy + \frac{y}{2}\int Ty^2\,dy - \frac{1}{6}\int Ty^3\,dy -$ $-c^3\left[\frac{1}{45} - \frac{1}{24}\left(\frac{y}{c}\right)^2 + \frac{1}{12}\left(\frac{y}{c}\right)^3 + \frac{1}{16}\left(\frac{y}{c}\right)^4\right]\oint T\,dy + c^2\left[\frac{12}{175}\left(\frac{y}{c}\right) + \frac{1}{4}\left(\frac{y}{c}\right)^2 +\right.$ $\left.+\frac{9}{40}\left(\frac{y}{c}\right)^3 - \frac{3}{80}\left(\frac{y}{c}\right)^5\right]\oint Ty\,dy - c\left[\frac{1}{24} + \frac{1}{4}\left(\frac{y}{c}\right) + \frac{1}{4}\left(\frac{y}{c}\right)^2\right]\oint Ty^2\,dy +$ $+\left[\frac{1}{12} + \frac{7}{40}\left(\frac{y}{c}\right) - \frac{1}{12}\left(\frac{y}{c}\right)^3\right]\oint Ty^3\,dy - \frac{1}{48c}\oint Ty^4\,dy - \frac{1}{80c^2}\left(\frac{y}{c}\right)\oint Ty^5\,dy\Big\}$

Table 3–1. Stress Functions

3.1.1.2 Buckling Equations of a Column

The differential equation that predicts the buckling load for a column is: [26]

$$\frac{d^2y}{dx^2}+k^2y=k^2\delta \tag{3-19}$$

where $k = (P/EI)^{0.5}$ and δ equals the maximum y deflection. The solution to this for a beam with built in edges, all material properties constant, and mode 1 buckling is: [26,27]

$$P_{cr}=\frac{4\pi^2EI}{l^2} \tag{3-20}$$

Although this could not be directly applied to the post modeled in this report, it served to verify the eigenvalue buckling prediction method used by ANSYS. The eigenvalue method is used for more complicated buckling problems, those that involve irregular geometries and non-linear material properties (refer to Section 3.2.8).

3.1.1.3 Post-Buckling Post Equations

The model is terminated when the post buckles. These equations are thus not required in this analysis but can be found in [24,26].

3.1.2 The Equations for Plates

The governing equations that describe a thermally excited plate also have three distinct behaviors: pre-buckling, buckling, and post buckling. A restrained plate subject to a thermal load has equations similar to those of a plate compressed on all sides. The thermal plate equations are derived from the compressed plate equations. [24]

3.1.2.1 Pre-Buckling Restrained Plate Equations

Four assumptions are applied to a pre-buckled plate. These are: [28]

1. Kirchoff's Hypothesis - all the lines perpendicular to the middle surface remain normal in the deformed surface.

2. The deflections are small compared to the thickness of the plate.

3. The thickness is small compared to the other dimensions.

4. The plate is isotropic and homogeneous.

Assumptions 1-4 imply that: [24,28,29]

$$\epsilon_{zz}=\gamma_{xz}=\gamma_{yz}=0 \tag{3-21}$$

where z is the depth (refer to Fig 3-2). Using the middle surface as a reference (superscript o), the displacements are:

$$u=u^{o}-z\frac{\partial w^{o}}{\partial x} \tag{3-22a}$$

$$v=v^{o}-z\frac{\partial w^{o}}{\partial y} \tag{3-22b}$$

$$w=w^{o} \tag{3-22c}$$

the strains:

$$\epsilon_{xx}=\frac{\partial u^{o}}{\partial x}-z\frac{\partial^2 w}{\partial x^2} \tag{3-23a}$$

$$\epsilon_{yy}=\frac{\partial v^{o}}{\partial y}-z\frac{\partial^2 w}{\partial y^2} \tag{3-23b}$$

$$\gamma_{xy}=\frac{\partial u^{o}}{\partial x}+\frac{\partial v^{o}}{\partial y}-2\cdot z\frac{\partial^2 w}{\partial x\partial y} \tag{3-23c}$$

the stresses:

$$\sigma_{xx}=\frac{E}{1-\nu^2}(\epsilon_{xx}+\nu\epsilon_{yy})-\frac{E}{1-\nu}\alpha T \tag{3-24a}$$

$$\sigma_{yy}=\frac{E}{1-\nu^2}(\nu\epsilon_{xx}+\epsilon_{yy})-\frac{E}{1-\nu}\alpha T \tag{3-24b}$$

$$\sigma_{xy}=\frac{E}{2\,(1+\nu)}\gamma_{xy} \tag{3-24c}$$

and the resultant forces and moments are:

$$N_x = \frac{Et}{1-\nu^2}\left(\frac{\partial u}{\partial x} + \nu \frac{\partial v}{\partial y}\right) - \frac{N_T}{1-\nu} \tag{3-25a}$$

$$N_y = \frac{Et}{1-\nu^2}\left(\frac{\partial v}{\partial y} + \nu \frac{\partial u}{\partial x}\right) - \frac{N_T}{1-\nu} \tag{3-25b}$$

$$N_{xy} = \frac{Et}{2(1+\nu)}\left(\frac{\partial u}{\partial x} + \frac{\partial v}{\partial y}\right) \tag{3-25c}$$

$$M_x = -D\left(\frac{\partial^2 w}{\partial x^2} + \nu \frac{\partial^2 w}{\partial y^2}\right) - \frac{M_T}{(1-\nu)} \tag{3-25d}$$

$$M_y = -D\left(\frac{\partial^2 w}{\partial y^2} + \nu \frac{\partial^2 w}{\partial x^2}\right) - \frac{M_T}{(1-\nu)} \tag{3-25e}$$

$$M_{xy} = (1-\nu) D \frac{\partial^2 w}{\partial x \partial y} \tag{3-25f}$$

N_T and M_T are the thermal normal force and thermal moment respectively. If the strains are eliminated from equations 3-23a-c using equations 3-25a-f, the stress becomes:

$$\sigma_{xx} = \frac{1}{1-\nu}\left(-\alpha ET + \frac{1}{t}[(1-\nu)N_x + N_T] + 12\frac{z}{t^3}[(1-\nu)M_x + M_T]\right) \tag{3-26a}$$

$$\sigma_{yy} = \frac{1}{1-\nu}\left(-\alpha ET + \frac{1}{t}[(1-\nu)N_y + N_T] + 12\frac{z}{t^3}[(1-\nu)M_y + M_T]\right) \tag{3-26b}$$

$$\sigma_{xy} = \frac{1}{t}N_{xy} - 12\frac{z}{t^3}M_{xy} \tag{3-26c}$$

The equilibrium equations for a plate with no body forces are:

$$\frac{\partial N_x}{\partial x} + \frac{\partial N_{xy}}{\partial y} = 0 \qquad \frac{\partial N_{xy}}{\partial x} + \frac{\partial N_y}{\partial y} = 0 \tag{3-27}$$

Introducing the Airy stress function and combining equations 3-23 through 3-26, the general plate equation arises. This equation in terms of stress is:

$$\nabla^4 F = -\nabla^2 N_T \tag{3-28}$$

where F is the stress function. Equation 3-28 can also be expressed in terms of displacements:

$$D\nabla^4 w = P - \frac{1}{1-\nu}\nabla^2 M_T \tag{3-29}$$

where P is applied force and the M_T group is the contribution to the deflection from the thermal moment. The out-of-plane deflection (w) is not affected by the net temperature increase, only the gradient in the z direction.

The solution of equation 3-29 for a simply supported plate with temperature variation in the z direction only is:

$$w = \frac{16 M_T}{(1-\nu) D\pi^4} \sum_{m=1,3,5}^{\infty} \sum_{n=1,3,5}^{\infty} \frac{1}{mn\left[\left(\frac{m^2}{a^2}\right)^2 + \left(\frac{n^2}{b^2}\right)^2\right]} \sin\left(\frac{m\pi x}{a}\right) \sin\left(\frac{m\pi y}{b}\right) \tag{3-30}$$

For solutions to other geometries and conditions refer to [24,28].

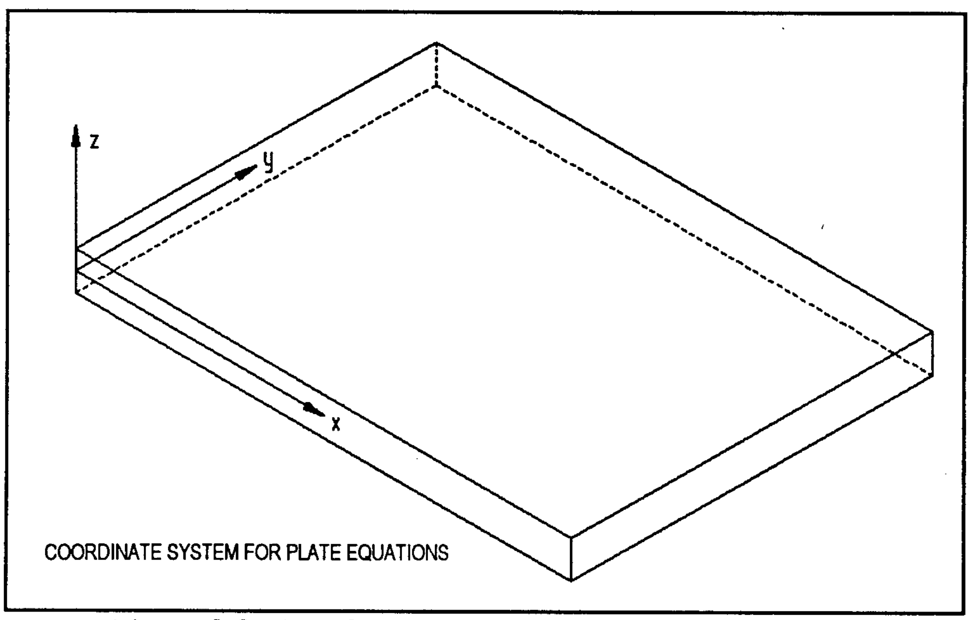

Figure 3-2 Coordinate System Used for Plate Equations

3.1.2.2 Buckling Prediction in Plates

Under continued heating, a thin, restrained plate will become unstable with respect to the z plane due to the compressive normal forces acting on the curvature. Consequently, the plate buckles and converts the compressive stress into permanent strain. Plates will buckle even under free space conditions due to the thermal moment. [24]

If the effects of in-plane stresses acting on the curvature are added to equation 3-29, the resulting equation is:

$$D\nabla^4 w = P - \frac{1}{1-\nu}\nabla^2 M_T + N_x\frac{\partial^2 w}{\partial x^2} + N_y\frac{\partial^2 w}{\partial y^2} + 2N_{xv}\frac{\partial^2 w}{\partial x \partial y} \tag{3-31}$$

where the last three terms are the moment caused by the curvature.

The solution to equation 3-31 for a fully restrained plate in terms of the thermal normal stress is:

$$N_{Tcr} = (1-\nu)\left(1+\frac{a^2}{b^2}\right)\frac{\pi^2 D}{a^2} \tag{3-32}$$

Equation 3-32 served to verify the eigenvalue buckling method used by ANSYS.

3.1.2.3 Post Buckling Plate Behavior

Experience has shown that after buckling the behavior of plates is quite different from that of compressed struts. The critical load for a strut can be considered the ultimate load but a thin plate can carry a much larger load than the critical load at which buckling begins. [24]

It is thus worthwhile to model the behavior of a plate after it has buckled. Large strain behavior cannot be ignored with post-buckling behavior. Assumptions 1 and 2 in Section 3.1.2.1 must be modified to account for large strain. The equations for large strain are: [24,29,30]

$$\epsilon_{xx} = \frac{\partial u}{\partial x} + \frac{1}{2}\left(\frac{\partial w}{\partial x}\right)^2 \tag{3-33a}$$

$$\epsilon_{yy} = \frac{\partial v}{\partial y} + \frac{1}{2}\left(\frac{\partial w}{\partial y}\right)^2 \tag{3-33b}$$

$$\gamma_{xy} = 2\epsilon_{xy} = \frac{\partial u}{\partial y} + \frac{\partial v}{\partial x} + \frac{\partial w}{\partial x}\cdot\frac{\partial y}{\partial y} \tag{3-33c}$$

Using equations 33a-c and using the stress-strain and constitutive equations of Section 3.1.2.1, the post-buckled plate equation are found to be: [24]

$$\frac{\partial^2 \epsilon_{xx}}{\partial y^2}+\frac{\partial^2 \epsilon_{yy}}{\partial x^2}-2\frac{\partial^2 \epsilon_{xy}}{\partial x \partial y}=\left(\frac{\partial^2 w}{\partial x \partial y}\right)^2-\frac{\partial^2 w}{\partial x^2}\frac{\partial^2 w}{\partial y^2} \tag{3-34}$$

If the Airy stress function (F) is used, equation 34 becomes:

$$\nabla^4 F=-\nabla^2 N_T+Et\left[\left(\frac{\partial^2 w}{\partial x \partial y}\right)^2-\frac{\partial^2 w}{\partial x^2}\cdot\frac{\partial^2 w}{\partial y^2}\right] \tag{3-35}$$

Analytical solutions to equations 34 and 35 are nonexistent except for a few very simple problems [24]. ANSYS and NASTRAN both currently do not have this large strain ability.

Although not incorporated into this report, the equations in this section provide a base for which to alter NASTRAN to handle large strain behavior of plates.

3.2 The Finite Element Formulation of ANSYS and NASTRAN

ANSYS and NASTRAN both use the finite elements method to solve the stress-strain and constitutive equations described in 3.1.1.1 and 3.1.2.1. ANSYS was selected to model the post and NASTRAN for the plate. The reasons for the respective finite element code selection are discussed in a later section.

The formulation for ANSYS and NASTRAN are nearly identical but use different notation. To avoid confusion, only ANSYS will be explained here.

3.2.1 The Equilibrium Equation

For each element in a model, ANSYS solves the following equilibrium equation: [31]

$$([K]+[S])\{u\}=\{F^a\}+\{F^r\} \tag{3-36}$$

where:

$[K]$ = total stiffness matrix $\Sigma_N [K_e]$
$[S]$ = stress stiffness matrix (see element descriptions)
$\{u\}$ = nodal displacement vector
N = number of elements
$[K_e]$ = element stiffness matrix, specific for each element type
$\{F^r\}$ = relaxation load vector
$\{F^a\}$ = applied load vector

And:

$$\{F_a\}=\{F^{nd}\}-[M]\{a_T\}+\sum_{m=1}^{N}\left(\{F_e^{Th}\}+\{F_e^{Pl}\}\right) \tag{3-37}$$

With:

$\{F^{nd}\}$ = applied forces at nodes
$[M]$ = mass matrix = Σ_N $[M_e]$
$[M_e]$ = element mass matrix, also specific for each element
$\{a_T\}$ = acceleration vector
$\{F_e^{The}\}$ = element thermal load
$\{F_e^{Pl}\}$ = element pressure load

The thermal component (F_e^{Th}) of the applied forces is solved in increments. Thus,

$$\{F_e^{Th}\}=\iiint\left([B]^T[D]\{\Delta\epsilon_n^{Th}\}\right)dV \tag{3-38a}$$

$$\{\Delta\epsilon_n^{Th}\}=\{\alpha_n\}(T_n-T_{ref})-\{\alpha_{n-1}\}(T_{n-1}-T_{ref}) \tag{3-38b}$$

Equation 3-38a just subtracts the previous thermal load from the current for the increment within the time step. The integration is done using Gaussian integration, as explained in Section 2.2. The [B] and [D] matrices are the elasticity and geometric matrices. Both [B] and [D] are explained in the next two sections.

If the stiffness matrix [K] is nonlinear then the Newton-Raphson method must be used to solve equation 3-36 for {u}. Non-linear behavior includes temperature and time dependent and stress dependent material properties. The Newton-Raphson solution method for elasticity is:

$$[K_n]\{\Delta u\}=[F^a]-\{F_n^{nr}\} \tag{3-39}$$

where:

$[K_n]$ = Jacobean tangent matrix, which given initial guess $\{u_i\}$, is the tangent of equation 3-36 at that point
$[F_n^{nr}]$ = the restoring force (see section 3.2.5)

The general form of the Newton-Raphson equation is:

$$[K_{m,n}]\{\Delta u_n\}=\{F_m^a\}-\{u_{m,n}^{nr}\} \tag{3-40}$$

with m indicating the load step and n indicating the iteration within a load step.

3.2.2 Stress-Strain Relations Used by ANSYS and NASTRAN

The stress is related to the strain via the relation:

$$\{\sigma\}=[D]\ (\{\epsilon\}-\{\epsilon^{Th}\}-\{\epsilon^{C}\}) \tag{3-41}$$

$\{\epsilon\}$ is the total strain matrix and [D] is the elasticity matrix. The elasticity matrix is an n by n matrix for each node where n is the total number of degrees of freedom per element. For isotropic materials, [D] is just the elasticity modulus (E) and rigidity modulus (G) evaluated at the corresponding stress and temperature value on the stress-strain curves.

The total strain matrix has four components:

$$\{\epsilon\}=\{\epsilon^{E}\}+\{\epsilon^{C}\}+\{\epsilon^{Th}\}+\{\epsilon^{pl}\} \tag{3-42}$$

Equation 3-42 divides the strain into four components: elastic (E), creep (C), thermal (Th) and plastic (pl). In this model, the plastic strain is not used. For a complete description of the stress-strain matrices and their derivation using the principle of virtual work, the reader is referred to [31, chapter 2.0].

3.2.3 Beam Element Geometric Properties

The two-dimensional plastic beam element, selected to model the aluminum H-post, uses two shape functions. The shape function for the length of an element (vertical axis) is linear, and the shape function for the depth is cubic. [31,32]

$$u=C_1+C_2x \tag{3-43a}$$

$$v=C_3+C_4x+C_5x^2+C_6x^3 \tag{3-43b}$$

ANSYS uses five integration points along the depth of an element and three along the length. If the element has an irregular cross section, ANSYS uses a weighted area method to solve for the unknowns along the depth (refer to Figure 3-3). The weighted area method is necessary because it is impractical to specify the cross section and integrate over the area of the specified cross section. Instead, the area is assigned a weight at each integration point along the depth. The weighted areas are used in the integration. The weighted areas are determined with the following equations:

$$A=2(0.0625A(-50)+0.2893A(-30))+0.2963A(0) \tag{3-44a}$$

$$I_{zz}=2(0.015625(A-50)+0.0260417A(-30))h^2 \tag{3-44b}$$

The centerline of the beam referred to as zero and the outer surfaces are (-50) and (+50) (refer to Figure 3-3). ANSYS uses the integration points (-50), (-30), (0), (30) and (50).

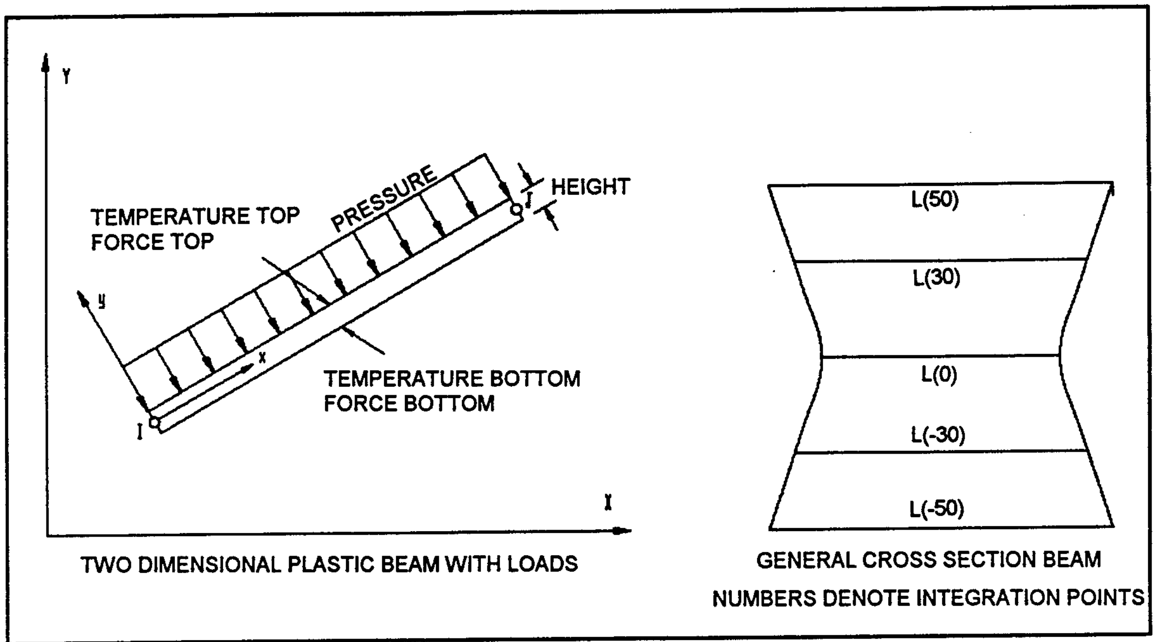

Figure 3-3 Details of the ANSYS Beam Element

3.2.4 Beam Element Matrices

There are four major matrices required to solve the H-post model. These are the elastic stiffness matrix [D], the mass matrix [M], stress stiffness matrix [S], and the stiffness matrix [K].

Both the [D] and [M] matrices that were described earlier apply to this element. They are displayed in [31, Chapters 2.0 and 2.1].

The [S] matrix is necessary for an eigenvalue buckling analysis. The derivation of the [S] matrix is given in [31]. The form of the stress stiffness matrix for the beam element is:

$$[S] = \frac{F}{L}\begin{Bmatrix} 0 & 0 & 0 & 0 & 0 & 0 \\ 0 & \frac{6}{5} & \frac{L}{10} & 0 & -\frac{6}{5} & \frac{L}{10} \\ 0 & \frac{L}{10} & 2\frac{L^2}{15} & 0 & -\frac{L}{10} & -\frac{L^2}{30} \\ 0 & 0 & 0 & 0 & 0 & 0 \\ 0 & -\frac{6}{5} & -\frac{L}{10} & 0 & \frac{6}{5} & -\frac{L}{10} \\ 0 & \frac{L}{10} & -\frac{L^2}{30} & 0 & -\frac{L}{10} & 2\frac{L^2}{15} \end{Bmatrix} \qquad \textbf{(3-45)}$$

The stiffness matrix [K] for the beam has four components:

$$[K] = [K^B] + [K^S] + [K^A] + [K^T] \tag{3-46}$$

where the superscripts denote the bending, shear, axial and torsional contributions, respectively. In this report, the shear and torsional effects are ignored.

The bending contribution is given as:

$$[K^B] = \iiint_V \{B_x^B\}[D]\, I_{zz} \{B_x^B\} dV \tag{3-47}$$

and the [B] matrix is:

$$\{B_x^B\} = \frac{1}{L^2} \begin{Bmatrix} 12\frac{x}{L}-6 \\ 6x-4L \\ -\left(12\frac{x}{L}-6\right) \\ 6x-2L \end{Bmatrix} \tag{3-48}$$

The axial contribution is similar:

$$[K^A] = \iiint_V \{B^A\}[D]\{B^A\} dV \tag{3-49}$$

and the [B] matrix is:

$$\{B^A\} = \begin{Bmatrix} \frac{1}{L} \\ -\frac{1}{L} \end{Bmatrix} \tag{3-50}$$

3.2.5 The Restoring Force Vectors for Newton-Raphson

The restoring force vector (F^{nr}) is the force required to give the displacement {u} so that equation 3-36 is satisfied. The restoring force is used in the Newton-Raphson method to make corrections to the displacement vector. When $\{F^{nr}\}$ is equal to the applied force, $[F^a]$, then a solution is reached. There are four components to the restoring force vector: bending, axial, shear, and torsional. The shear and torsional are not used in this report.

The bending restoring force vector is:

$$\{F_B^{nr}\} = \iiint_V \{B_x^B\}[D]\{\epsilon^{el}\} dV \tag{3-51}$$

The axial restoring force vector is:

$$\{F_A^{nr}\}=\iiint_V \{B^A\}[D]\{\epsilon^{el}\}dV \tag{3-52}$$

Equations 3-47, 3-49, 3-51, and 3-52 are evaluated in the same manner as equation 3-38.

3.2.6 Large Deflection and Creep

Large deflection is modeled in ANSYS with periodic updates in the position in the stiffness matrix. For a brief description of this feature, refer to Chapter 3.0 in [31].

Creep is modeled by increments in ANSYS. The number of increments per load step is chosen by the user. Both primary and secondary creep equations are available in ANSYS and a general creep equation is available in NASTRAN. The equations are discussed in the ANSYS and NASTRAN input sections.

3.2.7 Properties of the Plate Element

The element in ANSYS is identical to that in NASTRAN except a nonlinear temperature gradient may be specified in NASTRAN (see Figure 3-4). Refer to [31, chapter 2.93], [33], and [34] for a summary of the plate element properties. The shape functions and matrices are far too large to be reproduced here but are analogous to the beam's.

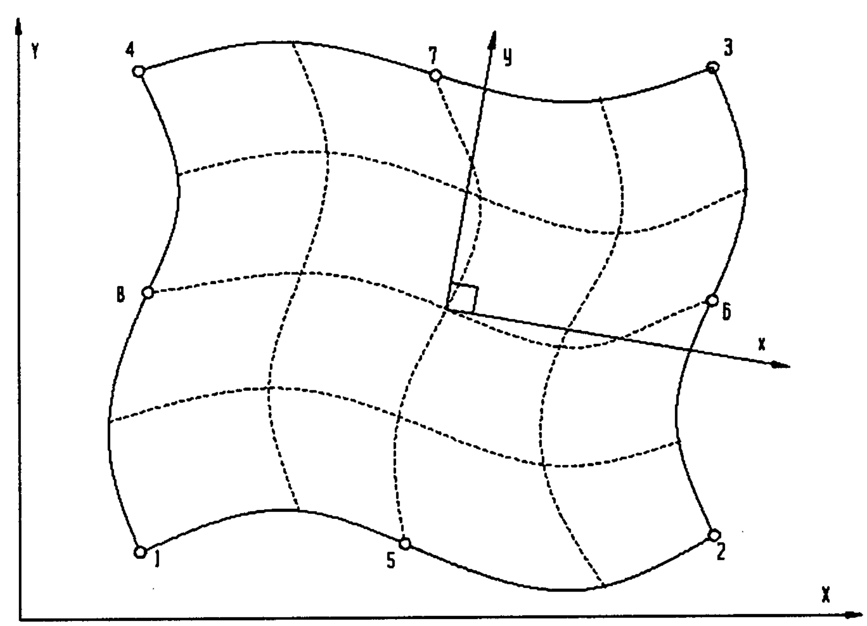

DASHED LINES DENOTE CONSTANT x OR y
NUMBERS DENOTE NODE SEQUENCE

Figure 3-4 Details of the NASTRAN Plate Element

3.2.8 Eigenvalue Buckling Prediction

The eigenvalue buckling prediction uses the equation: [32,35]

$$\left([K_P^{NM}]+\lambda\,[S_{PQ}^{NM}]\right)\{du^M\}=dF^N \tag{3-53}$$

N and M are nodes and P and Q are load states. If $\{P^n\}$ is the static load vector, and $[K_P]$ is the stuffiness matrix of the initial loading condition, then after an incremental load $\{Q^n\}$, the new stuffiness matrix becomes:

$$[K_Q]=[K_P]+\Delta\,[S_{PQ}] \tag{3-54}$$

where the last term is the change in stiffness due to the load Q. If Q is a specified load, then a multiplier is needed to extract a buckling load. This is lambda. Because buckling occurs without an additional load, dF in equation 3-53 is taken as zero. The eigenvalue equation is:

$$\left(K_P^{NM}+\lambda\Delta K_{PQ}^{NM}\right)du^M=0 \tag{3-55}$$

with each lambda value extracted being equal to one buckling mode. The one with the lowest stress state is the mode that the column will buckle.

3.3 Description of the Finite Element Codes Used

ANSYS and NASTRAN were both selected to model the structural response of the stiffening post and panel. They were chosen because both could model materials at elevated temperatures. ANSYS and NASTRAN have similar abilities. There were advantages and disadvantages with each that led to implementing ANSYS to analyze the post and NASTRAN for the panel.

3.3.1 ANSYS

ANSYS is a finite element software package written by Swanson Analysis Systems. [32] The edition used in this report was version 4.4a, which came out in 1989. This version is capable of the following finite element solutions: static, thermal, transient structural,transient thermal, dynamic structural loading, large deflection, stress stiffening, buckling prediction, nonlinear material properties, plasticity, creep, swelling, modal, and harmonic static. Version 4.5, capable of large strain modeling, will be out in 1992.

The element library of ANSYS is quite extensive, with linear and bi-linear one-, two-, and three-dimensional elements. Among the two-dimensional elements are the elastic beam and plastic membrane, which were the most useful to this project. There are also a number of special case elements which consist of force-deflection constraints, spring elements, mass, radiation, and pipe elements.

ANSYS is divided into three phases: pre-processor, solution, and post-processor. The pre-processor is a mesh generator that can specify material properties and place boundary conditions. The analysis type and certain finite element solution controls, such as convergence criteria and the output writing frequency, are included in this phase. In the solution phase ANSYS solves the model created in the pre-processor. This phase takes up the most CPU time. The post-processor graphically displays the results of the solution phase. It has an excellent graphics capacity but it is difficult to obtain good hard copies. It is suggested that an alternate software such as ARIES be used to observe and present the results.

Two problems were encountered with ANSYS. First, it was not effective at predicting the thermal behavior of a thin plate restrained at the sides before and after buckling. This is likely due to the inability of accurately describing the temperature gradient through the thickness. It only permitted a linear gradient between the front and rear surfaces. Second, ANSYS has no ability to model the post-buckling portions of a plate analysis because it does not have large strain equations.

3.3.2 NASTRAN

NASTRAN is a general purpose finite element software package created by MacNeal-Schwendler Corporation. The edition used in this report was version 66a. [36]

Version 66a can model all of the problems that ANSYS can, except for swelling and pipe flow. However, NASTRAN has a programming language called DMAP that enables the user to control the matrix operations performed by NASTRAN. DMAP allows virtually any problem to be modeled with NASTRAN. [36,37]

NASTRAN has only twelve elements available to the user. A couple of outdated elements from older versions of NASTRAN are compatible with version 66a. [38] Each of the twelve elements in NASTRAN has a broad range of applicability, unlike ANSYS. The eight node quadrilateral was the element used in the plate analysis because it was able to model creep and to approximate a temperature gradient across the depth (see Figure 3-4).

NASTRAN is subdivided into five parts called decks. [36,37] They are the NASTRAN Deck, the File Management Deck, the Executive Control Deck, the Case Control Deck and Bulk Data. The deck commands must be entered in the order listed above. In addition to NASTRAN is a pre-processor, called MSGMESH. MSGMESH is separate software and must be called by NASTRAN. The NASTRAN Deck includes commands that set the computer type, call MSGMESH, activate/deactivate certain commands, and specify memory allocation sizes. This Deck is optional and is often not used.

The File Management Deck is used to search for, delete, rename, move, and retrieve logical files created by NASTRAN in earlier runs. The logical files are the files that NASTRAN creates to store geometry, stiffness matrices and so on. The default NASTRAN setting is to delete the logical files upon completion of an analysis. The File Management Deck is also optional.

The Executive Control Deck is the first deck required by NASTRAN. It has two functions: to control the solution and to read and compile the DMAP statements. The solution is controlled by specifying the type of problem (such as static or heat transfer) and by specifying what information is written to the output file (*filename*`.f06`).

The Bulk Data section contains all the geometric, material, boundary condition, and load data. It also contains parameter settings. There is no required order to the data, including the load steps. All of the bulk data entries except the parameters have an identifying number that corresponds either to another bulk data card or to a case control card. All of the bulk data cards can be traced to a case control card. The parameters that are set include automatic constraints and nonlinear time steps.

There were three undesirable attributes encountered with NASTRAN. First, the software is extremely user unfriendly. There are ten manuals and nine handbooks. The information in the manuals is redundant in some portions and lacking in other sections. The revision of the theoretical handbook that was available was written in 1972 and has information corresponding to outdated elements and routines. There are five manuals explaining the DMAP programming language and the specifics of the NASTRAN matrices. Unfortunately, the DMAP manuals provided with version 66a were for version 64. Version 64 required activity in the File Management Deck in order to operate the DMAP language. Version 66 did away with DMAP operations in the File Management Deck [34,37]. The replacement procedure was not found.

Second, NASTRAN has a limited number of creep equations. The small number of equations to work with required an effort to fit experimental creep curves to the equations provided. Ultimately, the curve fitting was approximate at best.

Finally, NASTRAN has limited ability to view the results. There is a post-processor, but it was not operational at the time of the report. The results had to be viewed using other software packages. Among the software packages that could interpret the NASTRAN results are ARIES, SURFER and PATRAN.

3.4 Problem Setup

3.4.1 The Structural Configuration

The structure that was analyzed in this section is shown in Figures 3-5 and 3-6. [39,40] The post serves to stiffen the barrier and to support the panels. The panels can be any of the three materials analyzed in Chapters 1 and 2, but only the steel-honeycomb panel was modeled in this section.

Two boundary conditions were considered. One was an attempt to recreate the conditions of the fire tests of the plastic-honeycomb panel and aluminum post. These tests were conducted August 8, 1978 and August 9, 1978. The tests are the same as those mentioned in Chapter 2 and are listed in Appendix D. For these tests, the posts were allowed to expand vertically. The results from this test served to confirm the predictions of the ANSYS post analysis. They were not applicable to the panel because the material modelled was different from that used in the test.

The second boundary condition considered was a restrained post. The restrained post corresponds to actual construction conditions [40]. The posts were allowed some axial displacement that was equal to the product of the stiffness of the bounding decks and the developed reaction force.

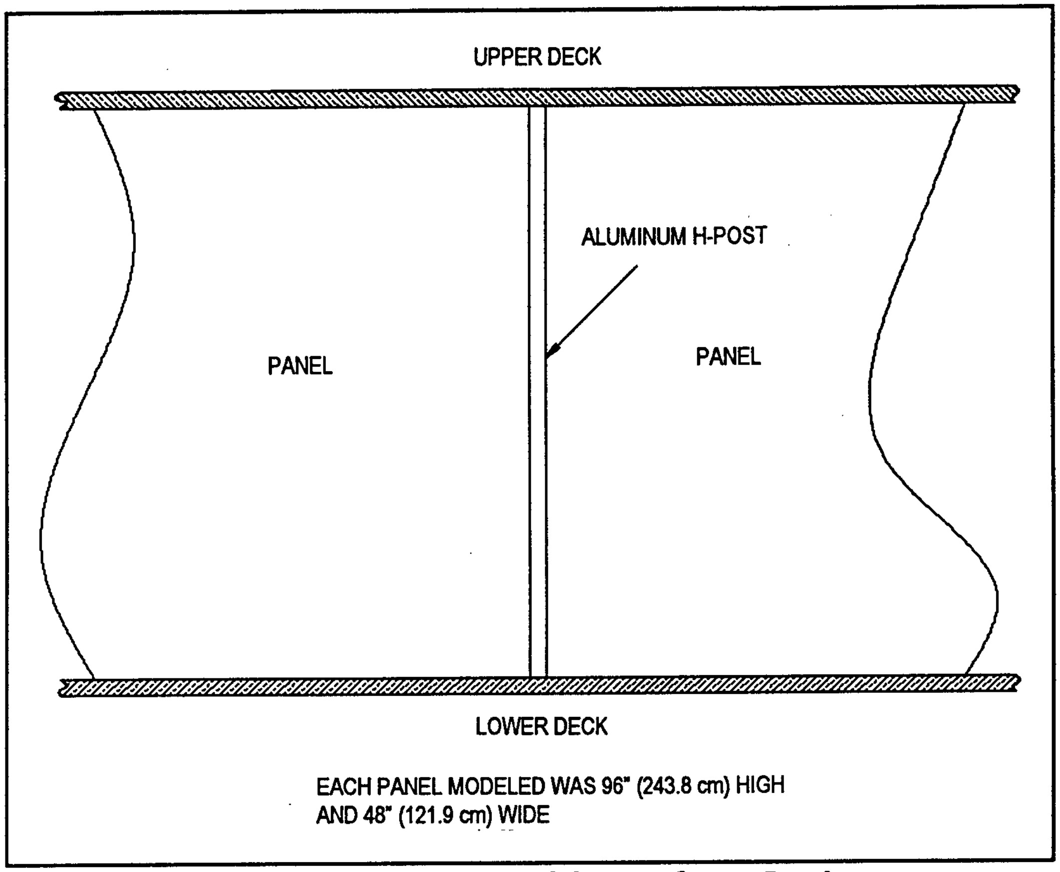

Figure 3-5 Dimensions of the Panel-Post Barrier

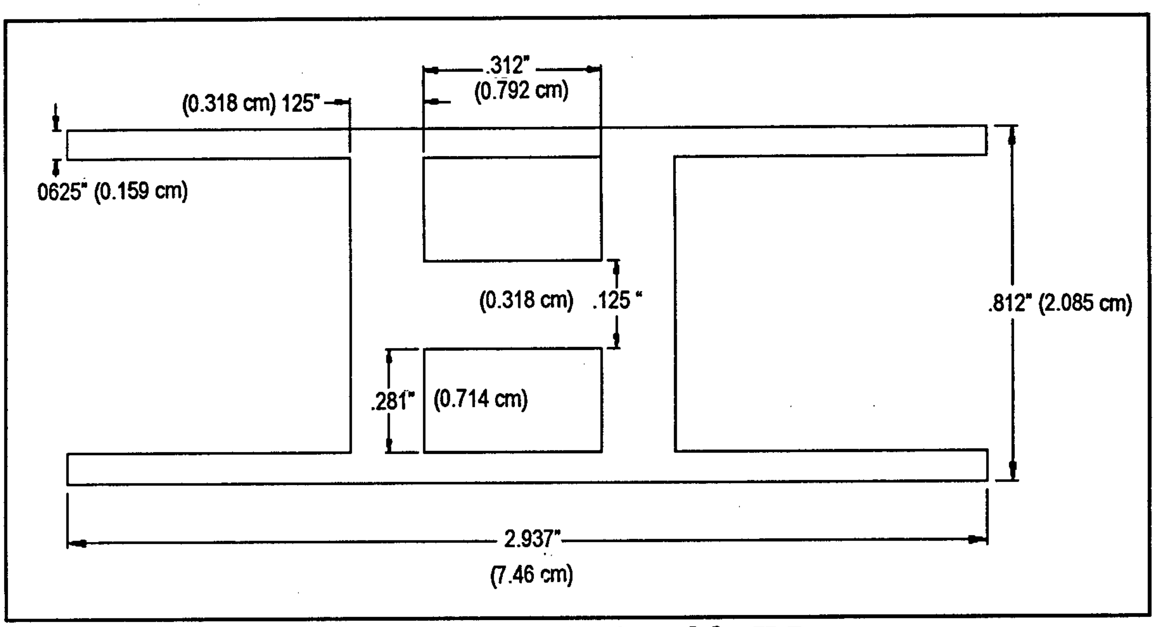

Figure 3-6 Cross Section of the H-Post

3.4.2 Problem Approach

The approach taken in this report was to separate the panel and post analyses. This reduces the complexity of the problem and allows different software to be used to predict the behavior. Since all the posts, except for perhaps the corner posts, have panels on each side exerting equal and opposite forces, the forces exerted by the panels cancel. An error that arises from this approach is the failure to account for the increased stress stiffening due to the compression.

Only the steel-honeycomb material was structurally analyzed with the aluminum H-post. The lack of structural material data for the plastic-honeycomb material and a lack of post dimensions for the steel joiner bulkhead precluded their inclusion.

3.4.3 Assumptions

There were four assumptions necessary to model the panel-post configuration.

First, the steel-honeycomb panel was assumed to be a thin plate. Evidence from Holometrix indicates the glue softens early, which essentially frees the outer face from the rest of the panel.

Next, the stress concentrations that arise at the panel-post connections (pins) were ignored. The stress concentrations will in reality allow some lateral deflection in the plates due to tearing. Due to a lack of data on the exact diameters, spacings and compositions of the connections, the expected force-deflection boundary condition of the plate was omitted.

Third, the barrier was assumed to have failed when or if the post buckled. If the post did not buckle, failure was assumed when the program diverged because of extensive creep.

Finally, when or if the post buckled, it was assumed that it buckled with sufficient force so that the effect of the plate was negligible.

3.5 Structural Analysis of the Post

3.5.1 Material and Geometric Properties

The H-post was assumed to be pure aluminum. The required material properties for aluminum were the density (ρ), coefficient of thermal expansion ($\alpha(T)$) and the nonlinear stress strain curves and the creep rate ($\epsilon(t,T,\epsilon,\sigma)$. Table 3-2 presents the values of ρ [13], α [13] and E [41] for selected temperatures. Graph 3-1 shows the stress strain curves for aluminum.

Table 3-2 Material Properties for Aluminum

	ENGLISH UNITS			SI UNITS			
T,°F	ρ,sg/in³	α,in/in	E, psi	ρ,Kg/cm³	α,cm/cm	E, MPa	T, °C
29.0	2.5e-4	2.3e-5		2.2e-4	5.8e-5		-1.67
70.0	2.5e-4		10e6	2.2e-4		68940	21.1
200.0	2.5e-4		9.52e6	2.2e-4		65630	93.3
260.0	2.5e-3	1.5e-5		2.2e-4	3.8e-5		126.7
400.0	2.5e-3		9.1e6	2.2e-4		62735	204.4
440.0	2.5e-3	3.6e-5		2.2e-4	9.4e-5		226.7
600.0	2.5e-3		8.43e6	2.2e-4		58116	315.6
620.0	2.5e-3	3.2e-5		2.2e-4	8.1e-5		326.7
800.0	2.5e-3	2.9e-5	7.63e6	2.2e-4	7.4e-5	52601	426.7
980.0	2.5e-3	3.2e-5		2.2e-4	8.1e-5		526.7
1100.	2.5e-3		6.8e6	2.2e-4		46879	593.3

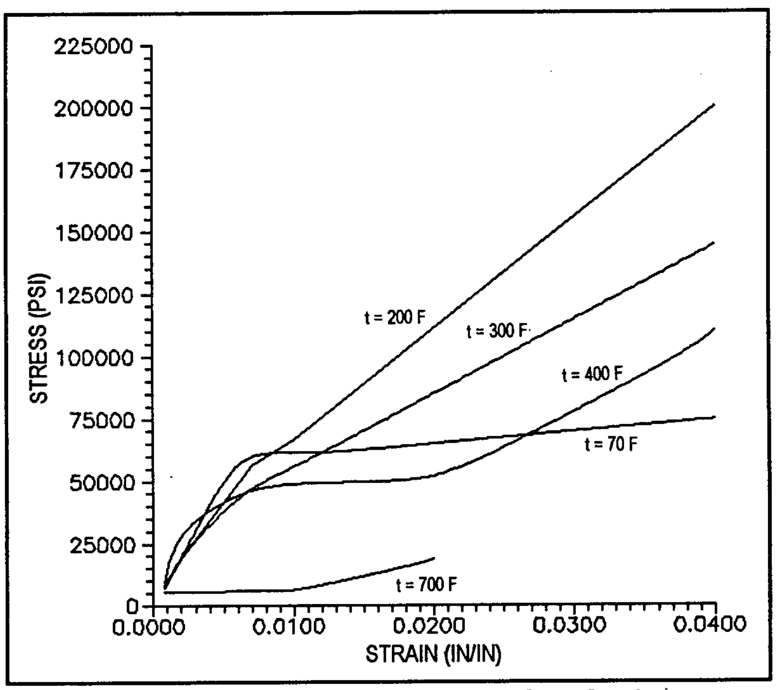

Graph 3-1 Stress-Strain Curves for Aluminum

ANSYS provides a number of equations to model creep. There are two kinds of creep considered: primary and secondary. Primary creep is creep that occurs at a decreasing rate and secondary creep is approximately constant. [2,42] Tertiary creep arises from the increased stress from a decreased cross section. Figure 3-7 shows an ideal creep curve. [2] The most versatile primary and secondary creep equations provided by ANSYS are shown in Table 3-3. [32]

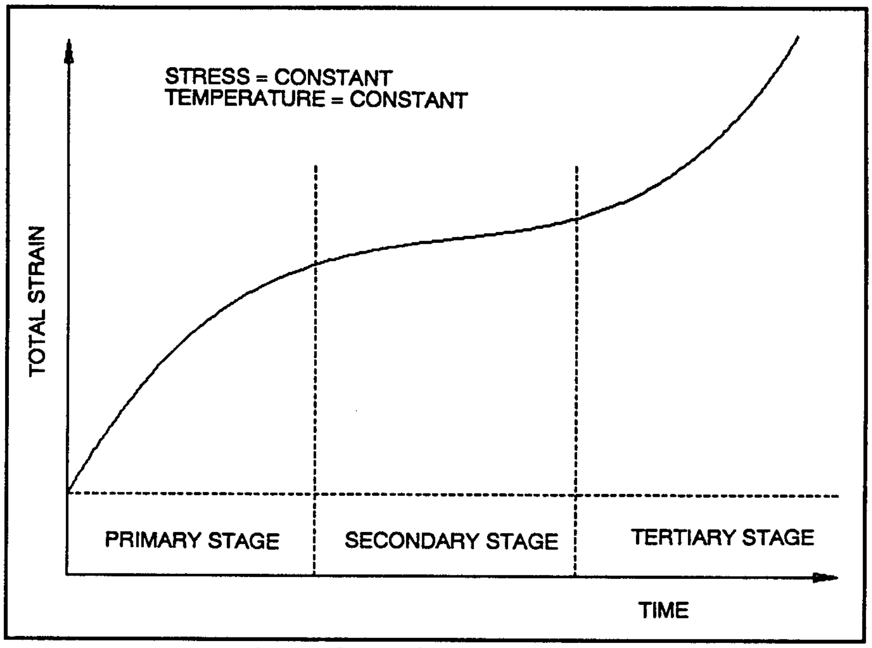

Figure 3-7 Ideal Creep Curve

Table 3-3 ANSYS Creep Equations

	Primary Creep	Secondary Creep
Equation One	$\frac{\Delta\epsilon_{cr}}{\Delta t}=C_1\sigma^{C_2}\epsilon^{C_3}e^{-\frac{C_4}{T}}$	$\frac{\Delta\epsilon_{cr}}{\Delta t}=C_7 e^{\frac{\sigma}{C_8}}e^{-\frac{C_{10}}{T}}$
Equation Two	$\frac{\Delta\epsilon_{cr}}{\Delta t}=C_1\sigma^{C_2}t^{C_3}e^{-\frac{C_4}{T}}$	$\frac{\Delta\epsilon_{cr}}{\Delta t}=C_7\sigma^{C_8}e^{-\frac{C_{10}}{T}}$
Equation Three	$\frac{\Delta\epsilon_{cr}}{\Delta t}=C_1\sigma^{C_2}re^{-rt}$ $r=C_5\sigma^{C_3}e^{-\frac{C_4}{T}}$	

Graph 3-2 shows the actual creep curves for aluminum as a function of temperature and stress [43]. Some curve fitting was required to describe the creep curves by one or more of the ANSYS creep equations. The most obvious equation to try first was the second secondary creep one, because the creep curves are only functions of temperature and stress. GRAPHER was used to determine the approximate stress dependence. The resulting stress exponent was then used as C_8. Next, points on the extreme curves were used to determine the remaining two constants. The resulting creep equation was:

$$\frac{\Delta\epsilon_{cr}}{\Delta t}=0.1962\cdot\sigma^{4.207}e^{\frac{-31091.7}{T}} \tag{3-56}$$

Graph 3-2 displays the actual creep curves overlaid with the curves predicted by equation 3-56. There is some error near the fringes; however, it is acceptably small. Also, note that the units of equation 3-56 and Graph 3-2 are in psi, R, and in/in. For conversion to SI the method must be repeated for the SI units.

Three geometric properties were required for the post: the height, area, and moment of inertia about the z axis. The height and area were determined to be 0.8125 in. (2.064 cm) and 0.3984 in^2 (1.012 cm^2) respectively. The moment of inertia was calculated to be 0.0387 in^4 (1.611 cm^4).

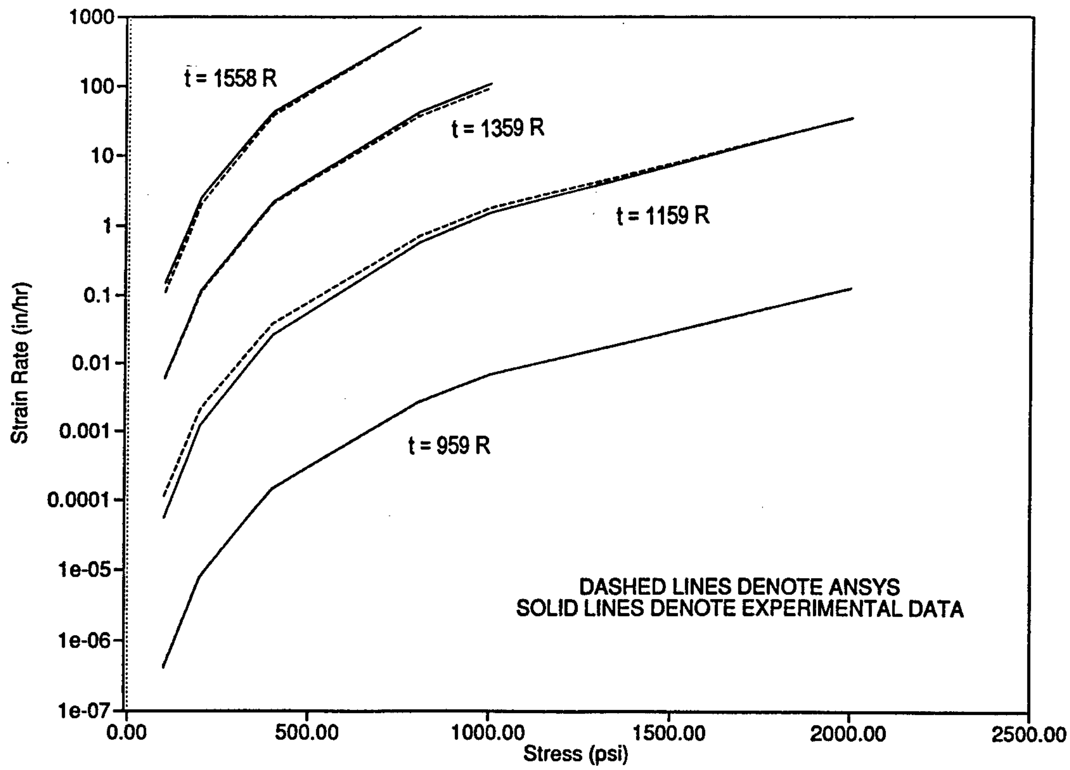

Graph 3-2 Creep Curves for Aluminum

3.5.2 Boundary Conditions

Two boundary conditions were used. The first allowed vertical expansion in the axial direction. The base was restrained from translational displacement, but permitted to rotate. The upper portion was allowed all degrees of freedom except left and right displacement. See Figure 3-8 for a diagram of the boundary conditions.

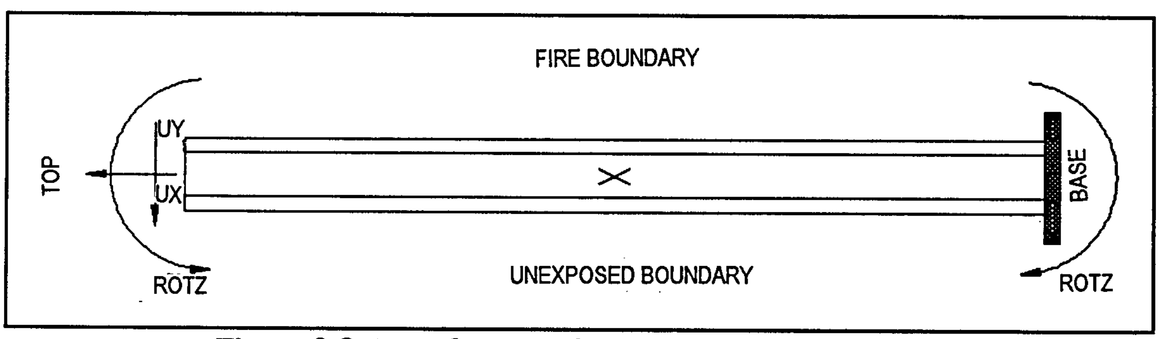

Figure 3-8 Boundary Conditions for Unrestrained Post

The second set of boundary conditions used a force-deflection constraint for the axial displacement. The force-deflection was assumed to be equal to the stiffness of the bounding decks. The equation for the deflection of a plate with a concentrated load is [23]:

$$w(x,y)=\frac{4P}{\pi^4 Dab}\sum_{m=1}^{\infty}\sum_{n=1}^{\infty}\frac{\sin\frac{m\pi\xi}{a}\sin\frac{n\pi\eta}{b}}{\left(\frac{m^2}{a^2}+\frac{n^2}{b^2}\right)^2}\sin\frac{m\pi x}{a}\sin\frac{n\pi y}{b} \qquad \textbf{(3-57)}$$

ξ and η are the position of the load, x and y are the location of the deflection and a and b are the length of the x and y sides, respectively (see Figure 3-9). The deflection of the post is at the point of contact with the plate. Thus, $x=\xi$ and $y=\eta$. This report assumed a 96 in. by 96 in. by 0.25 in (243.8 by 243.8 by 0.635 cm) deck above and below the post. Equation 3-57 can be reduced to:

$$w=K\cdot P \qquad \textbf{(3-58)}$$

for a single position. P is the reaction force at the deck post interface. A small FORTRAN program was written to solve for K at any desired position (refer to Appendix E for a listing of all FORTRAN codes). Table 3-4 shows the value of K at the positions shown in Figure 3-10.

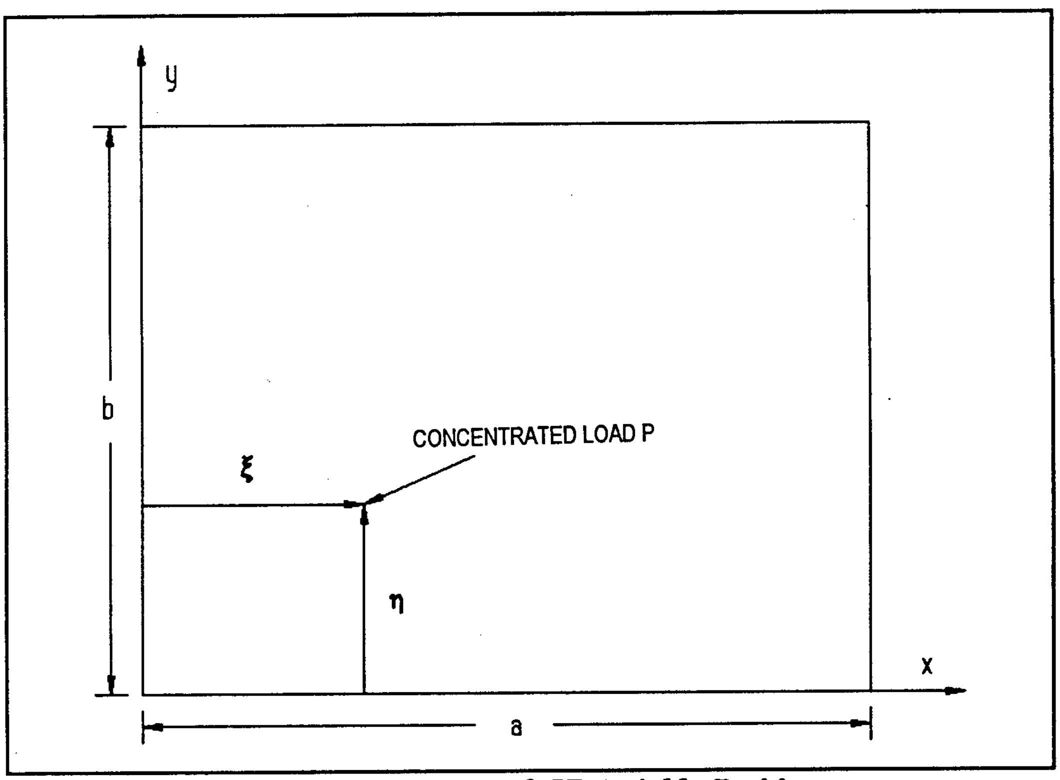

Figure 3-9 Equation 3-57 Variable Positions

Table 3-4 Deck Stiffness Values

position	A	B	C	D	E	F
K value	0.0	.0000506	.0001827	.000345	.0004756	.000525

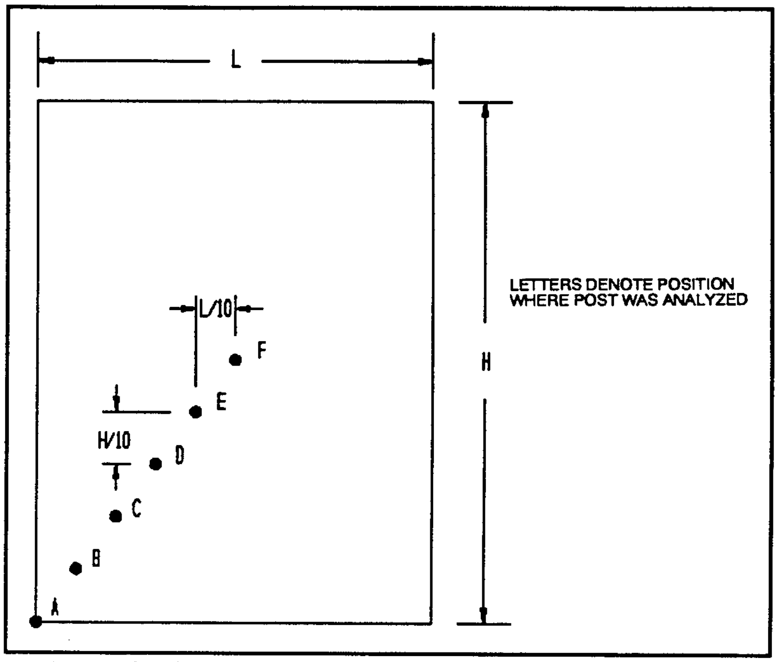

Figure 3-10 Boundary Conditions for Restrained Post

All rotations were allowed for the post, although there was no observed effect when the y and z rotations were restricted.

3.5.3 Thermal Load

The post was subject to an ISO fire as presented in Graph 2-1. The time-temperature distribution that was determined with TASEF and FIRES-T3 was used in the structural analysis. The average face temperatures were used. These are shown in Graph 3-3.

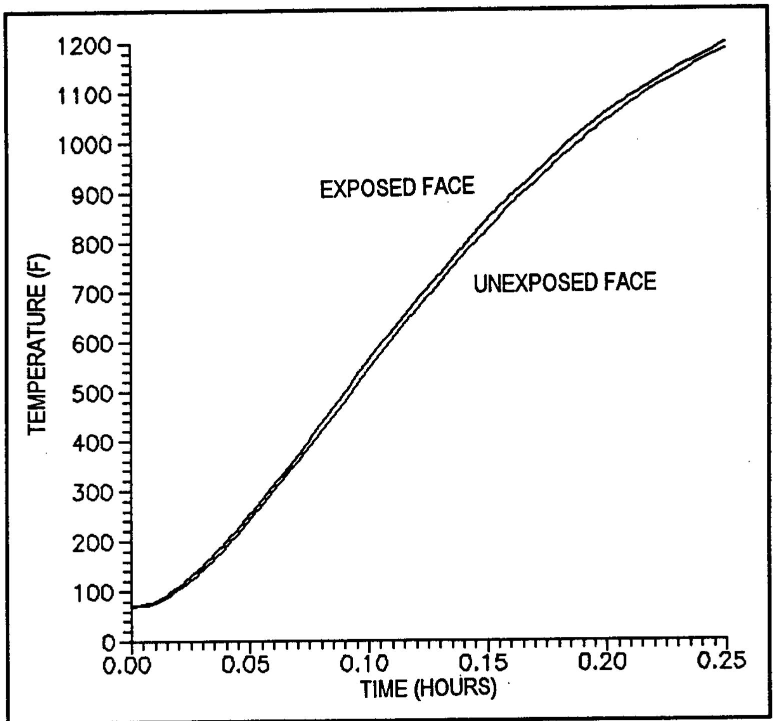

Graph 3-3 Time-Temperature Distribution in Post

3.5.4 The Solution Method

There were three separate solution runs. First, the unrestrained post was run, incrementing the time and temperature until creep diverged. Second, the restrained post for the five positions along the bounding plate were run in a similar fashion to the unrestrained post. No consideration for buckling was made. The third solution was for buckling. Since ANSYS considers a buckling solution a termination point, a UNIX program was written that repeatedly called ANSYS and incremented the time-temperature load. The results of the restrained post and the buckling prediction were compared for several positions along a deck and when the two results were equal, buckling was assumed. All three batch input files are listed in Appendix F.

3.5.5 UNIX Program

The purpose of the UNIX program was to call ANSYS, solve a static unit load, recall ANSYS, solve the eigenvalue buckling load, write the output, and then increment the load. It is as follows:

```
ansys.e < load1 > stat1.out
ansys.e < buckle > buck1.out
rm file* filestat* fort*
              :
              :
ansys.e < loadn > statn.out
ansys.e < buckle > buckn.out
rm file* filestat* fort*
```

ansys.e is the local command to call ANSYS. The *loadn* files had the appropriate time-temperature loads. The *load* file also instructed ANSYS to read another file that had the geometry, unit static load, and boundary conditions. The *buckle* file contained the instructions for ANSYS to run the eigenvalue buckling procedure on the last load iteration.

3.5.6 ANSYS Input Files

Due to the similarity of the static post input files, only the restrained post is thoroughly discussed.

The first group of commands defined the type of analysis.

```
/prep7
/title,RESTRAINED POST POSITION F
kan,0
kay,6,1 $kay,8,1 $kay,9,0
krf,2
```

/prep7 enters the standard preprocessor. The *kan* command requests a static analysis and the kay commands are switches for special static functions. *kay,6* is large deflection, *kay,8* is stress stiffening, and *kay,9* requests the full Newton-Raphson method. The *krf* command instructs ANSYS to write the reaction forces in the output.

The next group of commands defined the elements and geometric properties:

```
et,1,23,,,,,,3    $et,2,39
r,1,0.8125,0.9712,0.5461,0.0003
r,2,0.0518,100,0.259,500,0.518,1000
rmor,1.36,2000,2.72,4000,4.44,8000
rmor,5.18,10000
```

The plastic beam that was used to model the post is number 23 in the element library and the force deflection constraint is element number 2. The key-option (3) for *et,1* specifies an element with a general cross sectional area. The first set of geometric properties (*r,1*) are the beam depth, and the weighted areas A(50), A(30), and A(0), respectively. The second set (*r,2* and *rmor*) are the force-deflection values. Refer to Figure 3-3 in Section 3.2.3.

The material properties were next entered:

```
mp,dens,1,0.0002543
mpte,1,29,119,260,440,620,800
mpda,alpx,1,1,2.326e-5,2.105e-5,1.5e-5,3.6e-5,3.2e-5,2.9e-5
mpte,7,980   $mpda,alpx,1,7,3.2e-5
mpte,1,70,200,300,400,500
mpda,ex,1,1,10e6,9.524e6,9.091e6,8.333e-5
mpte,6,600,700,800,1000
mpda,ex,1,6,8.243e6,7.931e6,7.343e6,7.065e6
mpte,11,1100
mpda,ex,1,11,6.798e6 $mpte
knl,1
nlta,1,1 $nlsi,48
nl,1,1,0.0
nl,1,7,0.1962,4.207,0,31091.7,0,1.0
nl,1,13,-2,0.00075,0.002,0.007,0.01,0.04
nl,1,19,70.0,7500,20000,60000,61333,74667
nl,1,25,200,7143,19048,56667,66667,200000
nl,1,31,300,7143,19048,47058,55888,144117
nl,1,37,400,6818,18181,46346,52115,109807
nl,1,43,700,5298,5488,5744,6250,18750
```

The *knl* command is a switch that activates the nonlinear property table (*nl*), *nlsi* indicates 48 nonlinear (*nl*) entries and *nlta* labels the table and specifies the beginning number. The first 12 *nl* entries define the creep. Since only a secondary creep equation was used, the first six entries are 0. The last value on the secondary creep input (1.0) specifies the equation. The next row contains the strain values that the subsequent stresses are evaluated at on the stress-strain curve. Five entries per curve are allowed. The additional term with the stresses is the temperature of the stress-strain curve.

The geometry was next defined:

```
n,1  $n,45,96  $fill
n,100,0.0  $n,200,96.0
type,1  $real,1  $mat,1
e,1,2  $egen,44,1,1
type,2  $real,2
e,100,1  $e,45,200
```

The post is divided into 45 structural elements. The force-deflection elements have no length. [32]

The boundary conditions were set with:

```
d,1,uy,,,,,rotz
d,23,ux
d,45,uy,,,,,rotz
d,100,ux,0,,,,uy,rotz
d,200,ux,0,,,,uy,rotz
```

The displacement restriction at node 23 was because of symmetry. Also, the ends of the force-displacement elements (nodes 100 and 200) were completely fixed.

Two commands control the convergence and the number of iterations that were performed per load step:

```
cnvr,0.25,0.25,0.25
iter,400,400     OR     iter,-400,400
```

The command *cnvr* lists the convergence criterion for the plasticity, creep, and large deflection. These are the ratios of the current value to a prescribed criterion. For creep, this ratio is:

$$\textit{convergence criteria} > \frac{\Delta\epsilon_{cr}}{\epsilon_{el}} \tag{3-59}$$

Equation 3-59 states that the creep strain must be less than the product of the convergence criteria and the elastic strain. The maximum ratio of creep strain to elastic strain allowed by ANSYS is 0.25. The *iter* command has two forms. The first instructs ANSYS to go through 400 iterations per load step and print the results of only the 400th iteration. The second form allows ANSYS to skip iterations on load steps that are very stable. If the problem begins to diverge, ANSYS may use up to 400 iterations per load step. The second form was much quicker but diverged at a lower load step because it caught the diverging problem too late. For the full set of load steps on the restrained post, the first form diverged at the last on the last load step (26), but took about ten hours of computer time on a mainframe computer. The second form diverged at the 13th load step and only took five minutes. The results of the first 10 load steps were nearly identical.

Last, the load steps were specified and the solution executed:

```
ktem,-1  $tref,70  $tuni,70  $toff,459.67
time,0.0
acel,,384
$lwri
te,all,80.6,77.0  $time,0.01  $lwri
te,all,109.4,104.0  $time,0.02  $lwri
afwr  $fini
/inp,27  $fini
```

ktem activates the thermal loads. *tref* is the reference temperature that all material properties are evaluated at and *tuni* is the initial temperature. The creep equations required a Rankine temperature scale, so the offset (*toff*) converts Fahrenheit to Rankine. The acceleration of gravity was set with the *acel* command, in/s^2. The temperature loads were input with the *te* command, front first, then rear. *lwri* writes the load step and *afwr* wraps up the pre-processor session. A solution is executed with */inp,file27,dat* (also */inp,27*). *file27.dat* contains all the loads, and the geometry is stored on *file3.dat*. *file12.dat* contains the results of the analysis.

The unit load was applied to the top of the post in the static solution preceding the buckling prediction:

```
f,45,fz,-1.0
```

The displacement constraints are removed from this node because the buckling analysis constrains this node.

The buckling routine was activated with:

```
/buc,3,1,0,0,0,1
iter,1,1,1
end
fini
/eof
```

The arguments on the */buc* command are the master degrees of freedom, the maximum eigenvalue extraction mode, and the iteration method. The master degrees of freedom are the significant displacements that occur in the necessary static analysis at each node. The maximum number of degrees of freedom per node for a two-dimensional beam element are three: ux, uy, and uz. If the master degrees of freedom specified on the */buc* command are less than the actual amount, then ANSYS automatically calculates it.

3.5.7 Theoretical Checks

ANSYS was compared to exact analytical equations for three cases: a simply supported beam with a concentrated load, a thermally excited beam in free space, and a column buckling problem. The three theoretical checks were done to verify that the element geometric properties were correct, that ANSYS could reasonably model out of plane thermal deflection, and that the eigenvalue buckling prediction method was applicable to a general cross section column.

The deflection of a simply supported beam with constant material properties is: [22]

$$v(x) = \frac{P}{6EIl}\left(-b(l^2-b^2)x + bx^3 - l\langle x-a\rangle^3\right) \qquad \textbf{(3-60)}$$

The function $<x-a>$ is evaluated only when $x > a$ (refer to Figure 3-11).

A 96 in. (243.8 cm) simply supported beam with identical geometric properties as the post was used. A 28 lb (124.5 N) force was applied at x=85.1 in. (216.1 cm), as shown in Figure 3-11. Equation 3-60 was solved with a Fortran program (refer to appendix D) for the same locations as the nodes in the 45 node ANSYS model. Graph 3-4 shows excellent correlation between the results of the loading condition for equation 3-60 and ANSYS. Thus, the geometric properties were correctly calculated.

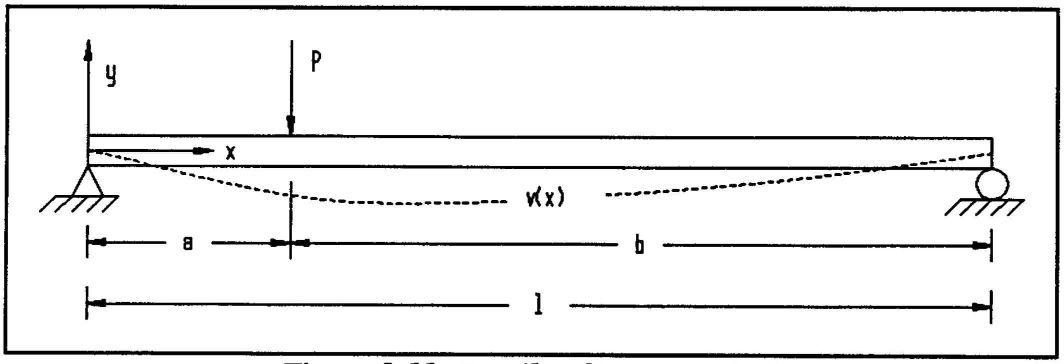

Figure 3-11 Details of Equation 3-60

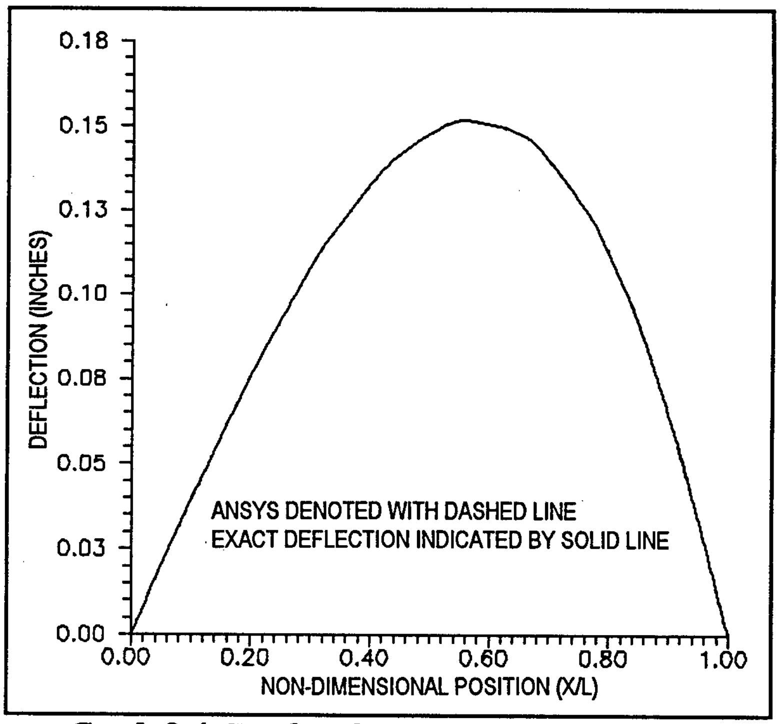

Graph 3-4 Results of ANSYS and Equation 3-60

The deflection of a rectangular beam in free space with a temperature gradient in the depth only is (refer to Figure 3-1, z and y coordinates interchanged): [24]

$$u(x) = \frac{x}{E}\left\{\frac{(bN_T)}{A} + \frac{z}{I}(bM_T)\right\} \quad \textbf{(3-61a)}$$

$$w(x) = -\frac{(bM_T)}{2EI}x^2 - \frac{\nu}{E}\left\{\frac{(bN_T)}{A}z + \frac{z^2}{2I}(bM_T)\right\} + \alpha\left(\frac{1+\nu}{E}\right)\int_0^z T dz \quad \textbf{(3-61b)}$$

The coordinate system used by equations 3-61a and 3-61b is at the exact center of the beam. Another Fortran program was written to solve equations 3-61a-b (listed in Appendix E). They were solved using a 2 in. by 4 in. beam (5.08 cm by 10.16 cm) cross section rectangular beam 96 in. (243.84 cm) in length. Table 3-5 shows the required constants and input for equations 3-61a-b. The results of ANSYS for both the x and w deflections correlated well with the equations indicating ANSYS correctly predicts thermal deflections for beams (Graphs 3-5 and 3-6).

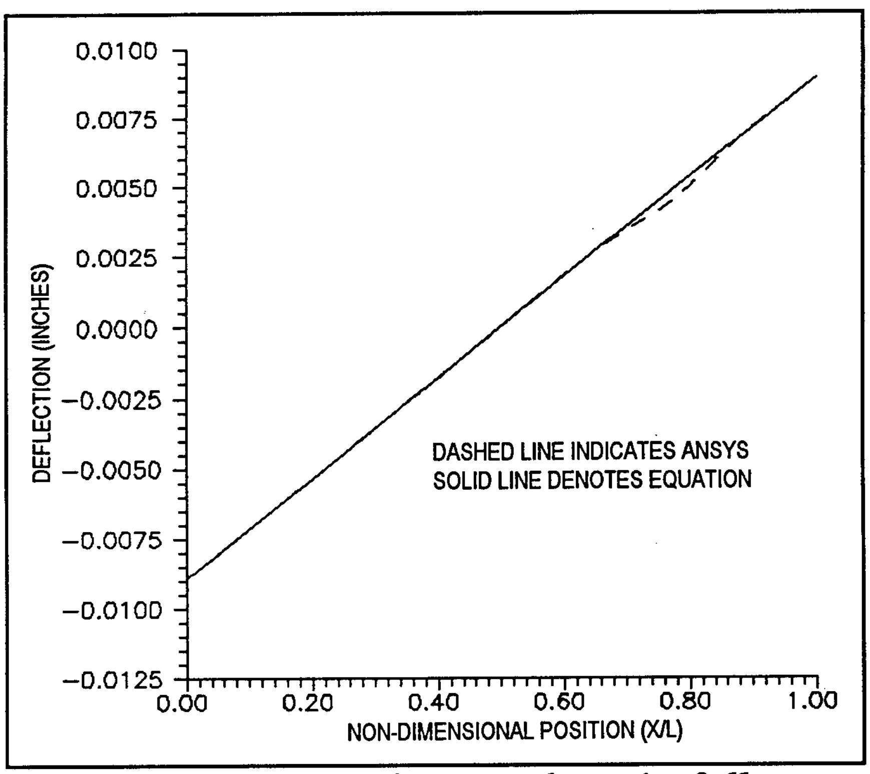

Graph 3-5 Results of ANSYS and Equation 3-61a

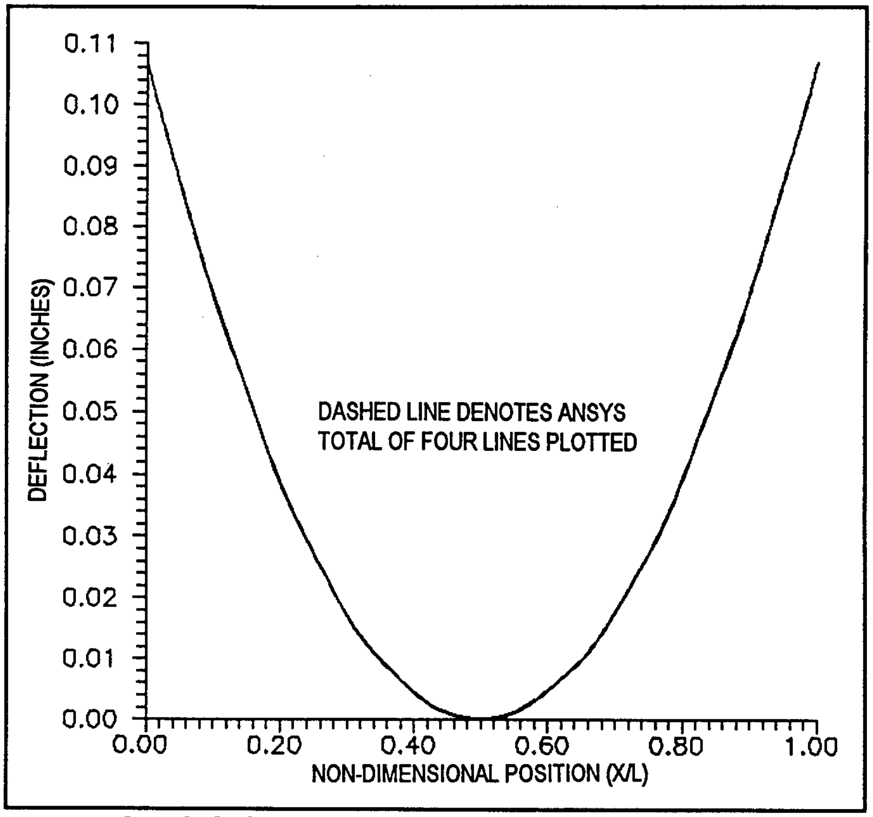

Graph 3-6 Result of ANSYS and Equation 3-61b

Table 3-5 Properties and Thermal Loads for Free Space Thermal Deflection

parameter	E psi	I in^4	T top °F	T bot °F	Length	Area	height
value	10e6	10.667	70.0	86.0	96.0	8.0	4.0

Last, the eigenvalue buckling prediction was verified using equation 3-20 and the aluminum H-post. Table 3-6 compares the results of ANSYS and equation 3-20 for the buckling reaction required at room temperature and all properties constant.

TABLE 3-6 ANSYS vs EXACT THEORY FOR BUCKLING

$P = 4\pi^2 EI/l^3$	ANSYS
1657.78	1662.5999

3.5.8 Results of ANSYS

The results of the unrestrained post are displayed in Graph 3-7. The out of plane (z) deflection vs time is plotted in inches for several time steps. The unrestrained post diverged at load step 25 corresponding to a time of about fifteen minutes. The results were consistent with the observations made during the fire tests conducted in 1978 which indicated severe deformation and the initiation of melting at about twelve to fifteen minutes. [39]

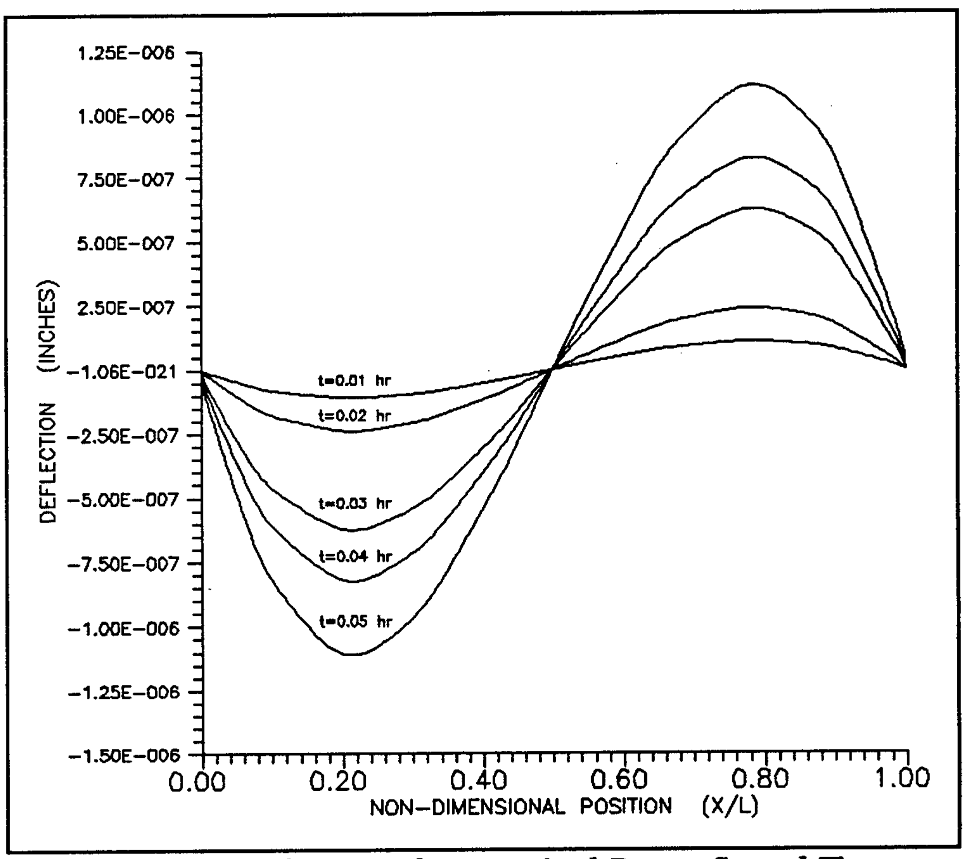

Graph 3-7 Deflections of Unrestrained Post at Several Times

The results of the restrained post analysis are shown in the next set of graphs. Graph 3-8 shows the reaction force developed in the post for the various positions. The required buckling force is also plotted on Graph 3-8. Intersection of the required buckling force with the developed reaction force indicates that buckling occurred. Posts near to the edge of the deck (refer to Figure 3-9) tended to buckle early and those near the center tended to behave like the fire tests. Graph 3-9 shows the deflection at various times for the post at position F. Other positions are directly analogous.

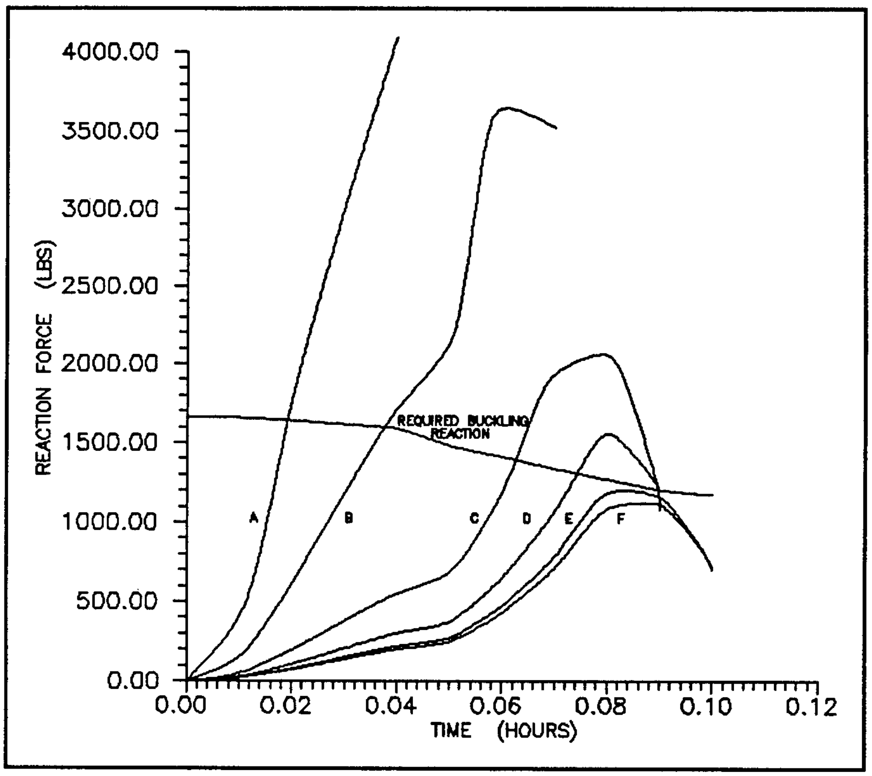

Graph 3-8 Buckling Potential for H-Post

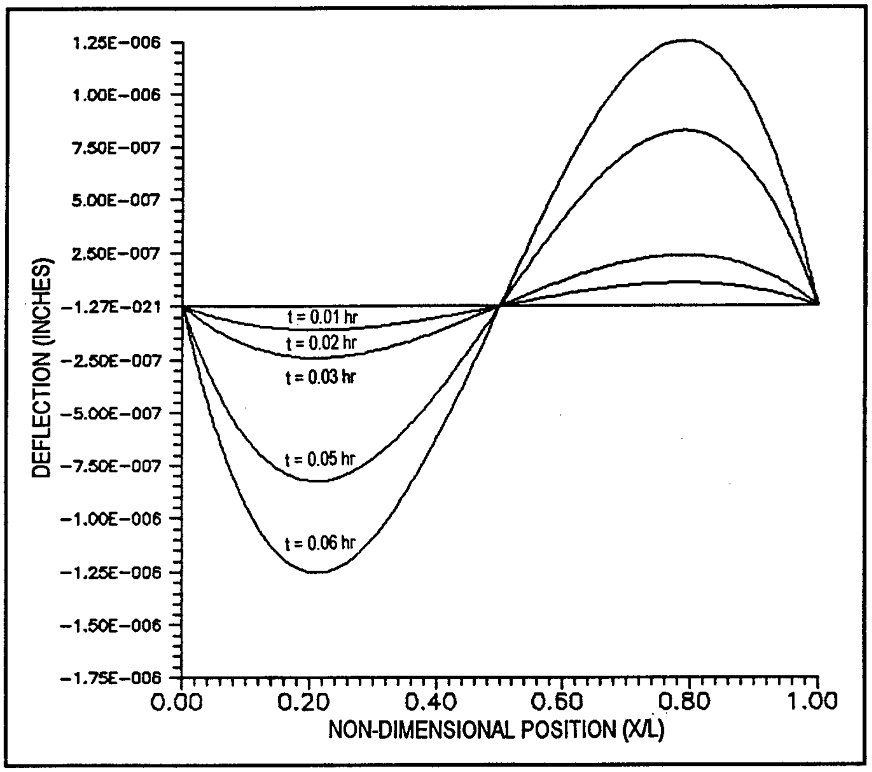

Graph 3-9 Deflection of Restrained Post at Position F

3.6 Structural Analysis of the Plate

3.6.1 Material and Geometric Properties

The plate was assumed to be a typical stainless steel. The required material properties were the modulus of elasticity (E(T)), the thermal expansion coefficient (α(T)), the density (ρ), and creep (ϵ(T,t,σ)). The former three properties are listed in Table 3-7. [13,45]

Table 3-7 Material Properties of the Plate

	English Units			Metric Units			
T °F	E psi	α in/in	ρ sl/in³	E Mpa	α cm/cm	ρ kg/cm³	T °C
70	29.5e6	6.5e-6	0.0088	203373	11.7e-6	0.0077	21.11
200	28.9e6	6.5e-6	0.0088	199237	11.7e-6	0.0077	93.33
400	27.9e6	6.9e-6	0.0088	192343	12.4e-6	0.0077	204.4
600	24.5e6		0.0088	168903		0.0077	315.6
800	23.8e6	7.6e-6	0.0088	164077	13.7e-6	0.0077	426.7
1000	17.4e6		0.0088	119956		0.0077	537.8
1200	11.2e6		0.0088	77212		0.0077	648.9
1300		8.6e-6	0.0088		15.5e-6	0.0077	704.4

The creep equations in NASTRAN are summarized in Table 3-8. [36]

Table 3-8 NASTRAN Creep Equations

Equation 1	$\epsilon_c = a\sigma^b\left[1-e^{-c\sigma^d t}\right]+f(\sinh(g\sigma))^h$
Equation 2	$\epsilon_c = ae^{b\sigma}\left[1-e^{c\sigma^d}\right]+fe^{g\sigma}$
Equation 3	$\epsilon_c = a\sigma^b t^d$

The constants a-h in the creep equations are constants that must be determined by a curve fitting method from actual experimental data. All the creep equations are corrected for temperature changes with:

$$\frac{\epsilon_c}{\epsilon_{c\,(o)}} = \left(e^{\frac{-\Delta H}{RT_o}}\right)\left(\frac{T_o}{T}-1\right) \tag{3-63}$$

The creep equations and the temperature correction are consistent with experimental empirical relations found in creep texts [42,44] as well as the temperature correction equation. For the steel used in the model, the creep is in ANSYS format and English units: [45]

$$\epsilon_c=4.3706e-8\cdot\sigma^{2.7333}t^{-0.66667}e^{\left(-\frac{23333}{T}\right)}t \qquad \textbf{(3-64a)}$$

$$\epsilon_c=0.026\cdot\sigma^{4.7}e^{\left(-\frac{70000}{T}\right)}t \qquad \textbf{(3-64b)}$$

Equations 3-64a-b are the primary and secondary creep, respectively. When the worst conditions expected, σ=5000psi, T=900°F, and t=0.09 hrs, were inserted in equations 3-64a-b, it was found that secondary creep contributed less than 2 percent to the total creep. Thus, ignoring the secondary creep, the primary creep was remarkably similar to NASTRAN creep equation three shown in Table 3-8. The constants b and d in equation three were thus taken as those in equation 3-56. The NASTRAN constant a was determined by using an initial temperature of 637 R (298 K) to eliminate the temperature term.

The temperature correction was estimated by noting that:

$$\Delta H=R\cdot T_m(K_o+V) \qquad \textbf{(3-65)}$$

For iron, the lattice constant (K_o) is 14 (BCC lattice) and the valence (V) is 8. [46] The melting temperature for stainless steel is about 1768 °F (1050°C). The ideal gas constant (R) is 1.1 cal/mole-R (1.98 J/mole-K). This gives an activation energy (ΔH) of 42.786 kcal/mole (267.7 KJ/mole). The temperature correction was checked with equation 3-65 and found to be off by a factor of ten for higher temperatures. This was compensated for by reducing the first NASTRAN constant (a) by a factor of ten.

3.6.2 Boundary Conditions

All translational displacements were restrained at the plate boundaries. Rotations were allowed since the panes were connected with pins. It was suspected, however, that a force-displacement boundary condition would arise due to the stress concentrations at the pins which would result in tearing the plate.

3.6.3 Thermal Loads

The temperature gradient in the steel plate was determine in Chapter 2. They are shown in Table 3-9.

TABLE 3-9 Temperature Distribution in Plate

	English Units			Metric Units		
time, hrs	t=0.0 in	t=0.0313 in	t=0.0625 in	t=0.0 cm	t=0.0794 cm	t=0.1588cm
0.0	77.0	77.0	77.0	25.0	25.0	25.0
0.005	90.41	90.356	90.338	32.45	32.42	32.41
0.010	114.26	114.188	114.17	45.70	45.66	45.65
0.015	146.39	146.282	146.246	63.55	63.49	63.47
0.020	185.054	184.928	184.874	85.03	84.96	84.93
0.025	229.118	228.956	228.902	109.51	109.42	109.39
0.030	277.754	277.574	27.502	136.53	136.43	136.39
0.035	327.902	327.722	327.65	164.39	164.29	164.25
0.040	379.436	379.238	379.148	193.02	192.91	192.86
0.045	431.474	431.348	431.258	221.93	221.86	221.81
0.050	482.162	481.946	481.838	250.09	249.97	249.91
0.055	530.582	530.348	530.258	276.99	276.86	276.81
0.060	576.608	576.374	576.266	302.56	302.43	302.37
0.065	621.122	620.888	620.78	327.29	327.16	327.10
0.070	663.404	663.152	663.044	350.78	350.64	350.58
0.075	703.418	703.184	743.076	373.01	372.88	372.87
0.080	777.074	776.84	776.714	413.93	413.80	413.73
0.085	811.508	811.274	811.148	433.06	432.93	432.86
0.090	844.682	844.43	844.322	451.49	451.35	451.29
0.095	876.682	876.236	876.11	469.15	469.02	468.95
0.100	906.746	906.494	906.386	485.97	485.83	485.77
0.105	935.438	935.204	935.078	501.91	501.78	501.71
0.110	963.464	963.23	963.104	517.48	517.35	517.28

3.6.4 Solution Method

NASTRAN allowed a non-linear temperature gradient to be specified for a plate element; thus, NASTRAN was selected for the pre-buckling and post-buckling analyses. ANSYS was used to estimate the buckling stresses in the plate.

First, the plate was modeled with no consideration for buckling. Next, ANSYS was used to determine buckling reaction forces at each time-temperature load. The intersection on the developed and required reaction forces indicated buckling had occurred. Finally, the deflections of the buckled plate were inserted into NASTRAN and the time-temperature loads continued. The rotations were arbitrarily set to zero because the moments were at least six orders of magnitude lower than the principal stresses. A UNIX program was written to continually call ANSYS and increment the load files during the buckling prediction analysis.

3.6.5 UNIX Program

The UNIX program for the plate is identical in format to the UNIX program used for the post (see Section 3.5.5). The differences were the file names and the number of loads. The plate was expected to buckle early; thus, only 11 load steps were created.

3.6.6 NASTRAN and ANSYS Input Files

The NASTRAN and File Management Decks were not used in the plate model. The executive control deck used was succinct:

```
ID    MSC,D2460
TIME 200
SOL 24
CEND
```

The ID command is just an identification code for the run, used if a restart is required or if file operations should be required. It is analogous to the program statement in FORTRAN. The maximum computational time was set at 200 minutes, and SOL 24 specifies a static solution.

The general case control deck was as follows:

```
TITLE = 48in X 96 in steel plate
SUBTITLE = includes creep and nonlinear material properties
     ECHO = NONE
     SPC = 51
     DISPLACEMENT = ALL
     ELFORCE = ALL
     STRESSES = ALL
```

Besides specifying the title and the subtitle, all the displacement vectors, element forces, and element stresses were requested in the output file (*filename*`.f06`). The specific instructions for each load in the Case Control Deck were:

```
SUBCASE 1
        LABEL = LOAD ONE
        TEMP(LOAD) = 800
        NLPARM = 909
SUBCASE 2
        LABEL = LOAD TWO
        TEMP(LOAD) = 802
        NLPARM = 910
```

which continued to load step 24. The TEMP(LOAD) and NLPARM command direct NASTRAN to Bulk Data entries for the thermal load and time step, respectively.

The Bulk Data cards are sensitive to column field. There are two field formats available, a sixteen and an eight character field. Compatible software such as ARIES uses the sixteen character field because the numbers are written in double precision. The eight character field was found to be adequate for this model. NASTRAN is also sensitive to real and integer input. It will prematurely terminate a model if a real number and an integer are switched.

The material properties were entered as:

```
BEGIN BULK
$
MAT1    31      29.5E6          0.28    0.0088  6.5E-6  70.0
MATT1   31      66                              68
MATS    31      79      NLELAST                         2.0E7
```

BEGIN BULK is the required command to initiate the Bulk Data card section. MAT1 specifies the room temperature material properties E, nu, rho, and α. The reference temperature was 70°F (21.11°C). The material identification number was 31 and corresponded to an element card. The last two commands directed NASTRAN to the nonlinear material tables, for E(T) (table card 66), α(T) (table card 68) and E(σ,T) (table card 79). The NLELAST argument on the stress-strain table call card indicates that the table is non-linear elastic.

The tables called by the above cards are:

TABLEM1 66							
70.0	29.5E6	200.0	28.9E6	400.0	27.9E6	600.0	24.5E6
800.0	23.8E6	1000.0	17.4E6	1200.0	11.2E6	ENDT	
TABLEM1 68							
70.0	6.5E-6	200.0	6.5E-6	400.0	69.E-6	800.0	7.6E-6
1300.0	8.6E-6	ENDT					
TABLEST 79							
70.0	600	200.0	602	400.0	604	600.0	606
800.0	608	1000.0	1200.0	612	ENDT		
TABLES1 600							
0.0	0.0	0.001	29500.0	0.002	44000.0	0.005	42000.0
0.010	42400	0.015	47500.0	0.0183	46000.0	ENDT	
TABLES1 602							
0.0	0.0	0.001	28900.0	0.002	40600.0	0.005	40000.0
0.010	40500.0	0.001	44000.0	0.0183	46000.0	ENDT	
TABLES1 604							
0.0	0.0	0.001	27900.0	0.002	39000.0	0.005	39300.0
0.010	43500.0	0.015	50100.0	0.0183	52300.0	ENDT	
TABLES1 606							
0.0	0.0	0.001	24500.0	0.002	29800.0	0.005	36300.0
0.010	43000.0	0.015	49300.0	0.0183	52000.0	ENDT	
TABLES1 608							
0.0	0.0	0.001	23800.0	0.002	25300.0	0.005	33400.0
0.010	40000.0	0.015	43100.0	0.0183	45000.0	ENDT	
TABLES1 610							
0.0	0.0	0.001	17400.0	0.002	24000.0	0.005	29600.0
0.010	31200.0	0.015	33300.0	0.0183	34700.0	ENDT	
TABLES1 612							
0.0	0.0	0.001	11200.0	0.002	14800.0	0.005	16700.0
0.010	16900.0	0.015	17300.0	0.0183	17500.0	ENDT	

TABLEM1 contains both E and α versus temperature. The TABLEST command controls the stress strain tables by assigning a temperature to a table. TABLES1 has the strain-stress pairs used by NASTRAN.

Creep was specified with:

CREEP	31	70.0	CRLAW	1.3e-32	
	300	3.23E-26			-0.667

PARAM,TABS,459.69

NLPARM	909	10	0.0005
NLPARM	910	10	0.0005
NLPARM	911	10	0.0005

The reference temperature for the creep was 70°F (21.11°C) and was converted to Rankine with the PARAM command. Note that there is no format for a PARAM command. The CRLAW argument specifies that one of the NASTRAN creep equation is to be used. The 300 on the creep command is the code for the desired creep equation. The NLPARM command set the number of iterations per time step and the amount per iteration. Ten 0.0005 hr iterations were requested per load step for a total time of 0.005 hr. Each load step could have a different number of iterations.

Next, the geometry was entered:

```
GRID      1       0   0.0        0.0  0.1
GRID      2       0   4.0        0.0  0.1
GRID      3       0   8.0        0.0  0.0
GRID      4       0   12.0       0.0  0.0
$
$GRID     NODE    #   COORDSYS   X    Y    Z
$

CQUAD8    1       21  1          3    23   21   2    15   +CQUAD1
+CQUAD1   22      14
CQUAD8    2       21  3          5    25   23   4    16   +CQUAD2
+CQUAD2   24      15
CQUAD8    3       21  5          7    27   26   6    17   +CQUAD3
+CQUAD3   26      16
$
PSHELL    21      31  0.0625     31
$
```

The boundary conditions were specified via:

```
$
PARAM           AUTOSPC         YES
$
SPC             51              1               123
SPC             51              2               123
SPC             51              3               123
SPC             51              4               123
END DATA
```

The parameter requested that a nodal displacement or rotation less than 10e-16 be automatically constrained. The SPC command set the boundary conditions. Transnational displacement ux, uy, and uz are set with 1, 2, and 3, respectively. The rotations are set with 4, 5, and 6. A fully restrained node would thus have an SPC argument of 123456. END DATA ended the Bulk Data section. The entire input file is listed in Appendix F.

The ANSYS input file follows directly from the ones used with the post. For the plate analysis, a quarter section was used due to symmetry. Appendix F also contains this file.

The elements and geometry were defined with:

```
n,1,0,0,0.1
n,13,24,0,0.1  $fill
n,14,0,6,0.1
n,20,24,6,0.1  $fill
ngen,9,20,1,20,1,0,12  $ndel,174,180
et,1,93
type,1  $real,1  $mat,1
e,1,3,23,21,2,15,22,14
e,3,5,25,23,4,16,24,15
e,5,7,27,25,6,17,26,16
e,7,9,29,27,8,18,28,17
e,9,11,31,29,10,19,30,18
e,11,13,33,31,12,20,32,19
egen,8,20,1,6,1
```

There were 36 elements total, six horizontal and six vertical. The element selected was an eight node thin membrane shell capable of all the non-linear properties.

The load and boundary conditions for the plate were:

```
nsel,x,0.0
d,all,uy  $d,all,uz  $d,all,ux  $nall
nsel,y,0.0
d,all,uy  $d,all,uz  $d,all,ux  $nall
f,20,fx,-1.0,,160,20
f,33,fx,-1.0,,173,20
f,162,fy,-1.0,,173,1
tref,77  $tuni,77  $time,0.005
te,all,90.41,90.41,90.41,90.41,90.356,90.356
temo,90.356,90.356
```

There was a load of 1.0 on the upper and right boundaries at each node (refer to Figure 3-12). The translational displacements on the lower and left boundaries were constrained. The buckling analysis automatically set a zero displacement along the unrestrained boundaries. The *nsel* command served to activate only the nodes meeting the argument conditions (in this case an x or y coordinate of 0.0). The rest of the nodes were ignored by ANSYS until an *nall* command was hit. The *te* command specified the front and rear surface temperatures of the plate at the four corner nodes.

The ANSYS buckling file was identical to the one used by the post:

```
/buckle,3,1,,,,1
iter,1,1,1
end
fini
/eof
```

After buckling had occurred, the out-of-plane displacements for each node were inserted into a NASTRAN file. The buckling action was assumed to relieve all the stresses; thus, the stresses were all set to zero. The in-plane displacements were also set to zero because they were all in excess of six orders of magnitude less than the out-of-plane displacements. The NASTRAN model was then continued with the post-buckling displacements.

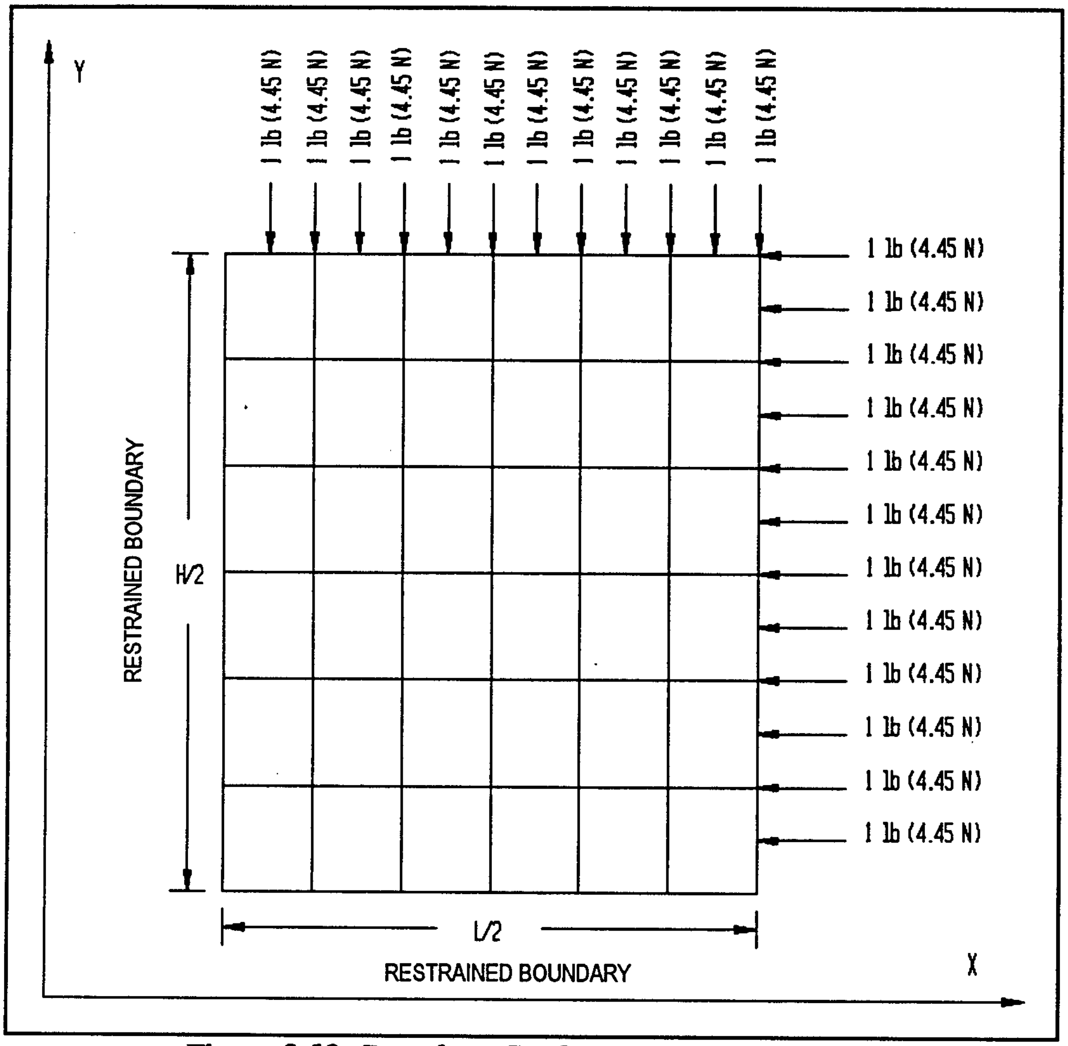

Figure 3-12 Boundary Conditions Buckling Analysis

3.6.7 Theoretical Checks

The NASTRAN and ANSYS models were compared to analytical solutions for two cases. These were a simply supported plate with a concentrated load and the buckling reaction required for a restrained plate. They served to verify the element selection and the ANSYS buckling prediction, respectively.

Graph 3-10 shows the results of NASTRAN and equation 3-57 for a 96 in. (243.8 cm) by 48 in. (121.8 cm) by 0.125 in. (0.318 cm) plate with a ten pound force applied at (24,12) in. ((61,30.5) cm). The results correlated perfectly, indicating that the elements were adequate and the mesh was refined sufficiently.

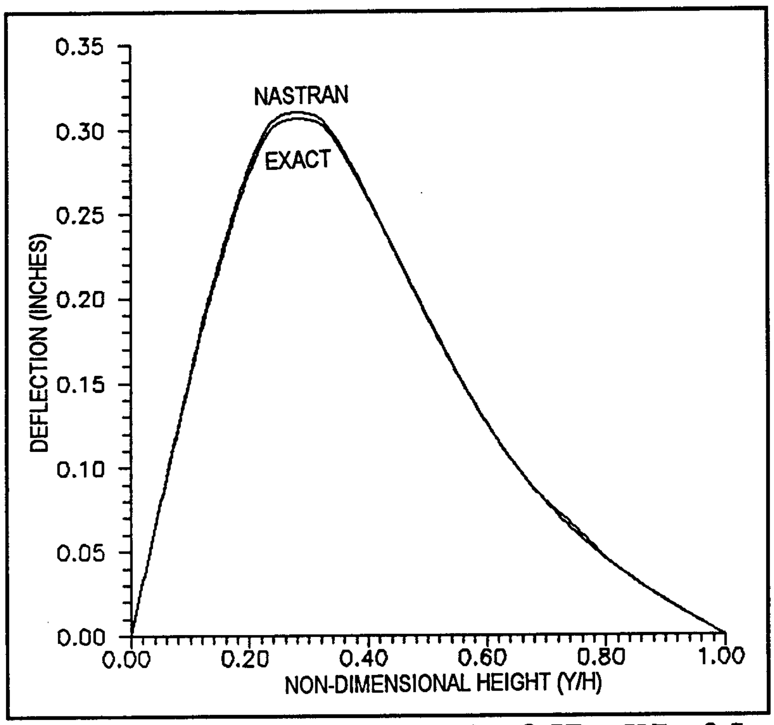

Graph 3-10 NASTRAN vs Equation 3-57 at X/L=0.5

The ANSYS buckling prediction for the plate was checked using equation 3-32:

$$N_{T_{cr}} = (1-\nu)\left(1+\frac{a^2}{b^2}\right)\frac{\pi^2 D}{a^2} \qquad \textbf{(3-32)}$$

The steel plate with room temperature properties was used. The plate stiffness (D) was 670.7, and equation 3-32 yielded a critical thermal normal stress of 2.514. The critical temperature rise was then determined by solving for temperature in the plate normal stress equation: [24]

$$N_T=\alpha E\int_{-t/2}^{t/2} T(z)\,dz \tag{3-66}$$

A constant temperature was used in equation 3-66, so that:

$$T(z)=\Delta T \tag{3-67a}$$

$$\int_{-t/2}^{t/2} T(z)=\Delta T\cdot t \tag{3-67b}$$

where t is the plate thickness. For the plate used in this model, a critical temperature rise was estimated to be 0.21 R (0.116 K). NASTRAN was then used to predict the developed reaction force with 0.21 R (0.116 K) temperature rise. The results are shown in Table 3-10. There was a larger error than expected, perhaps due to the complexity of a plate problem.

Table 3-10 ANSYS vs Equation for Plate Buckling

Equation 3-66	48.3
ANSYS	70.84

3.6.8 Results of ANSYS and NASTRAN

The results of the pre-buckling and buckling analysis are shown in Graph 3-11. Buckling occurs at the intersection of the buckling reaction and developed reaction forces. The plate buckled before the first load step as can be seen in Graph 3-11. The buckling deflections of the first load step were however used in the post-buckling analysis. This was not surprising because the assumptions reduced the panel to a very thin and independent steel plate.

NASTRAN gave the reaction force at each node in component form. The shorter edge was selected for the calculations. Although there was a higher stress in the vertical direction, the length was smaller. Since the material was homogenous, the same critical reactions occur on both axes (ignoring gravity). NASTRAN determines the forces at each corner node in each element. Thus, the total reaction is:

$$R=\sum_{i=1}^{N}(F_1+F_3)_i \tag{3-68}$$

where N is the number of elements on the lower bounding surface and 1 and 3 denote local nodes 1 and 3.

The ANSYS model was a quarter section with unit loads applied at each node across the upper surface. The buckling reaction from ANSYS was thus:

$$R_B = BF \cdot \left[\left(2 \sum_{i=1}^{N} i \right) - 1 \right] \tag{3-69}$$

BF is the buckling factor and the 2 arises because the section is one-half the total plate.

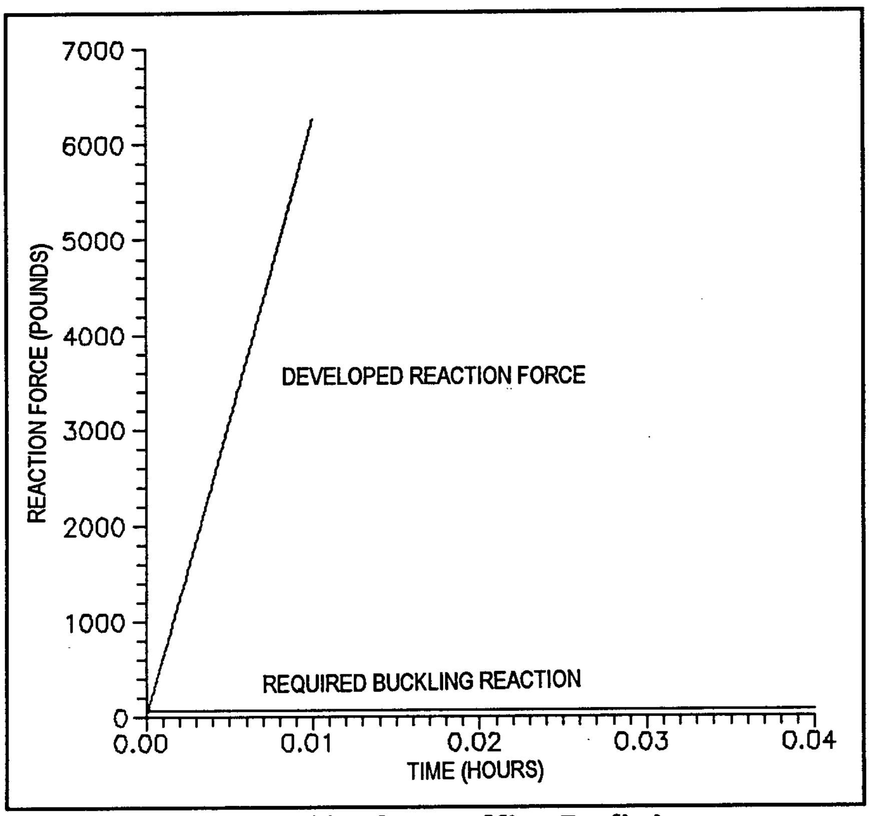

Graph 3-11 Plate Buckling Prediction

Figure 3-13 shows the displacement of the panel at time 0.005, just before buckling has occurred. Figure 3-14 shows the plate at time=0.005 hr, just after buckling. Figure 3-15 shows the post-buckled displacements of the plate at time 0.03 hr. Figures 3-13 through 3-15 are in English units (in.). Graph 3-12 shows the stresses at the center of the plate after buckling for several time steps. It is the stress values that will be of most assistance in determining the integrity of the plate for a fracture/crack analysis.

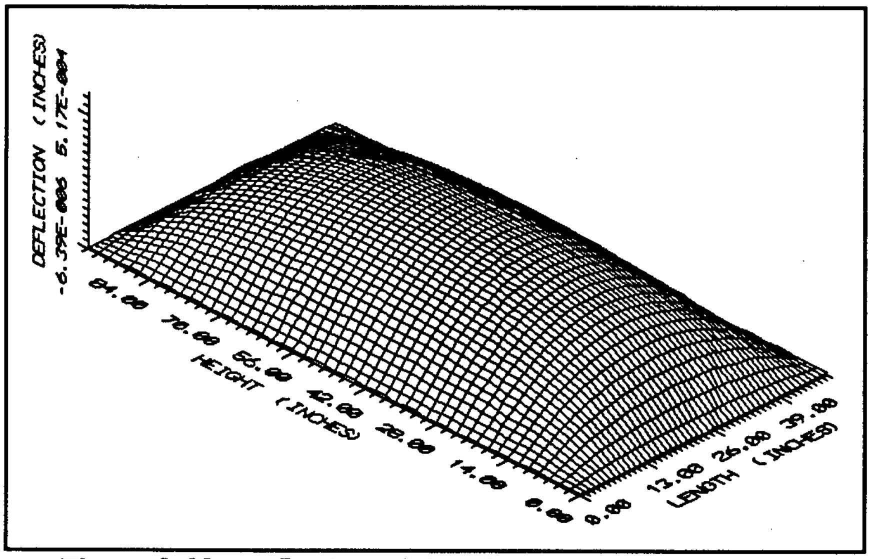

Figure 3-13 Deflection of the Plate Just Before Buckling

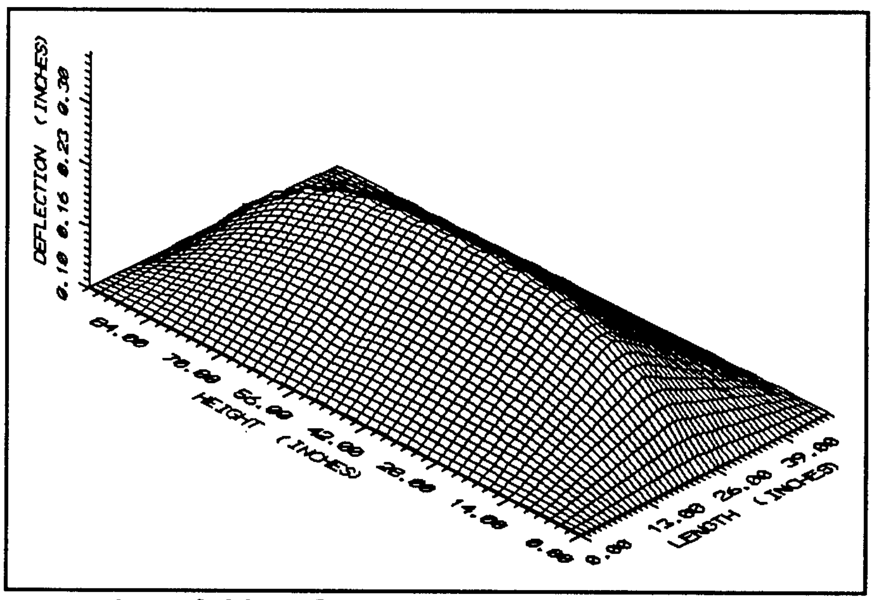

Figure 3-14 Deflection of Plate Just After Buckling

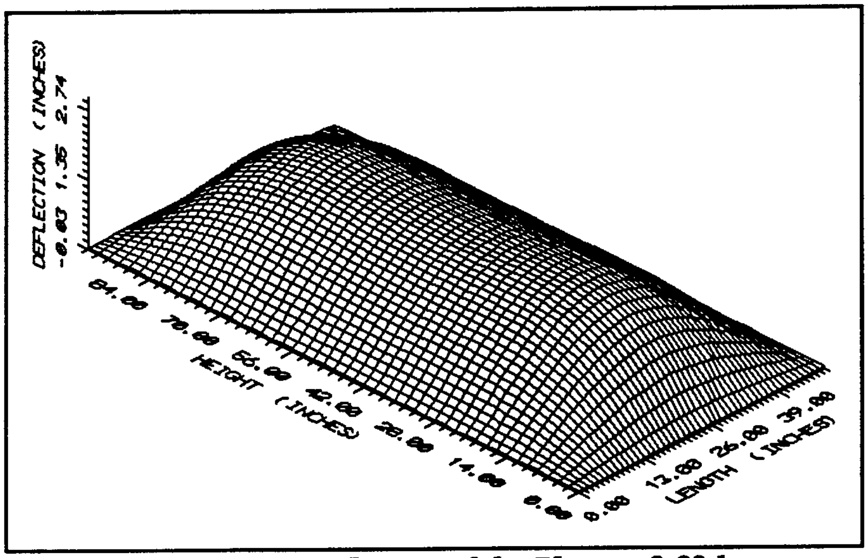

Figure 3-15 Deflection of the Plate at 0.03 hr

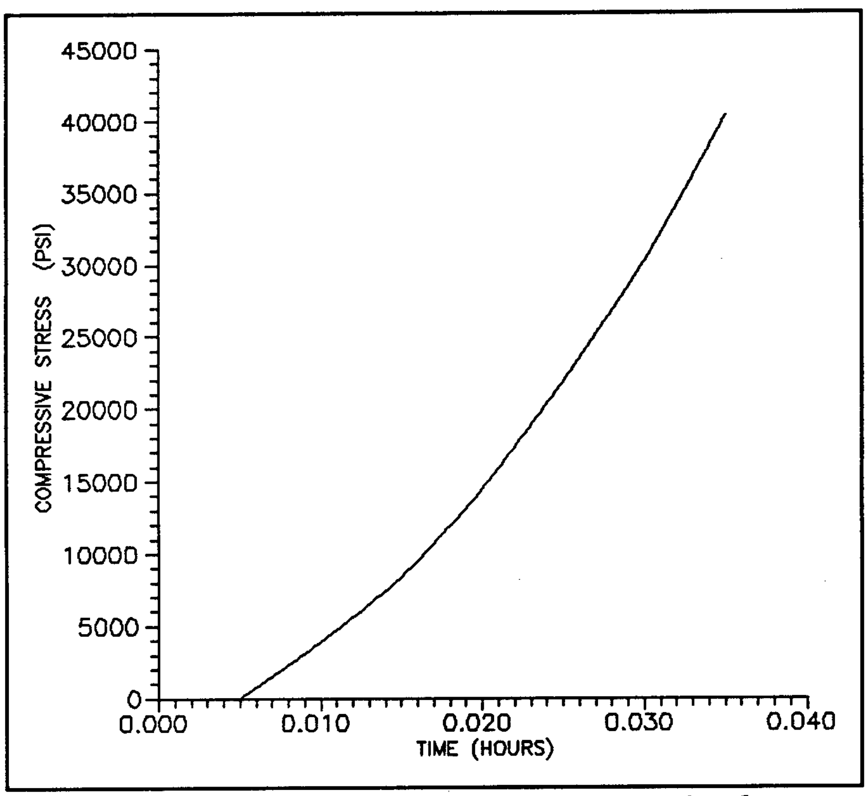

Graph 3-12 Maximum Compressive Stresses in Plate

3.7 Conclusions of the Structural Analysis

3.7.1 Interpretation of Results

It is apparent that the position of the post is important in determining the failure mode and length of time to failure. This is an important consideration when considering the entire barrier, because the panels may or may not fail before the post. Also, it was shown that the panel as modeled buckles before the first 45 seconds of the fire load. The early buckling indicates a need for using the large-strain equations to model the post for meaningful results. The post was analyzed for the complete range of possible boundary conditions, from fully restrained to completely free. It was shown that the failure mode of the post is different for each extreme. Thus, the exact local boundary conditions are critical in predicting the method of failure for the post.

It is also apparent that the restraint conditions of the barrier must be adequately assessed. It is clear that the plate buckles much earlier in this model than would actually occur in the construction conditions. The reason the plate buckles too soon is because it was fully restrained at the boundaries. The actual construction will allow some displacement, which will significantly alter the predicted buckling time. For example, if there was 0.1 in. (0.254 cm) gap at the connections, the plate could be heated to a temperature of 392 °F (300 °C) with no increase in compressive stress. Further, when the plate develops compressive stress due to the restraint, the stress concentrations at the pin connections will cause greater deformation in the vicinity of the pin. The increased deformation will reduce the overall compressive stress in the plate, thereby extending the pre-buckled phase. Thus, it is very important to accurately address the local boundary conditions.

3.7.2 Error and Uncertainty

The objective of the structural analysis in this report was only to estimate the feasibility of using finite element structural software to predict the mode and time of failure for the barrier under consideration. For a more accurate analysis, the following sources of error in this report must be addressed:

1. The exact composition and non-linear material properties of the aluminum post, the stainless steel, and the plastic laminate (the honeycombs and fiberglass carry zero load).

2. The exact position and dimensions of the bounding surfaces of the post for an accurate force-deflection constraint.

3. The behavior of the panel at the panel-post connection. This may involve a separate finite element analysis of the pin region to determine the force deflection constraint to be allowed for the plates.

4. The behavior of the glue under moderate thermal loads. There will also have to be a force deflection boundary condition along the surface connected to the glue, based on how much freedom is given to the plate at specified temperatures, and ending with complete dissociation at some temperature-stress pair.

5. The amount of rotation permitted the post and panels due to the wielded and pinned connections respectively. The rotation of the post will alter dramatically the buckling stresses (in fact, rotation restrictions will increase them).

6. The non-linear strain must be addressed for any crack growth models to be run. This can be either using DMAP in NASTRAN, using version 4.5 of ANSYS or an entirely different software with that potential.

3.7.3 Future Work

Future work, the last objective of this report, is to estimate the cracking potential of the panels in the barrier. There are two very different materials under consideration: the steel and plastic laminate.

The steel is quite readily modeled further in ANSYS for cracking potential, development and growth. By using the stresses from the post-buckling analysis, cracks can be predicted using the ANSYS crack elements. The material properties required for this analysis will include the yield strength and plastic deformation curves. [47]

The plastic panel, which has spalling potential as well as cracking, will have to be tested to determine under what stresses it cracks and what combination of shear and normal stresses cause spalling. The panel may be evaluated for cracking with ANSYS, and both the post-buckling output and crack output will have to be examined for the shear and normal stresses that result in spalling. NASTRAN can be programmed to detect these, however there is no crack analysis in NASTRAN. Thus, a combination of ANSYS and NASTRAN may be effective for estimating the cracking potential of the panels. Other software the author is unaware of may combine all of the above.

Glossary

Beam Element: An element having three degrees of freedom and an approximated cross section. Only the length is exactly specified.

Boundary Condition: An imposed displacement, force, rotation, and/or moment at a location on a system that the governing equation(s) must adhere.

Buckling: A sudden and large deflection indicating a breakdown of internal bending resistance.

Composite: Two or more component materials that retain their individual properties and act collectively to form a material with completely different characteristics.

Divergence: The failure of a computer program to mathematically converge on a solution to a governing equation.

Element: A single component of a subdivided region used in a finite element analysis. An element is the fictitious boundary connecting **nodes**. Nodes are the locations where the finite element method determines a solution to a governing equation.

Finite Element Method: A numerical method that solves differential equations by assuming a simple function (linear or quadratic, for instance) for small regions. The regions are connected in a domain that describes the geometry of the problem. The regions are called elements.

Honeycomb: A campsite material consisting of a two faces glued to hexagonal tubes and form a material aesthetically resembling the natural honeycombs of wasps.

Mesh: The sub-divided region consisting of elements and nodes. The more refined a mesh, the better the results of a finite element analysis.

Non-linear: Any property or boundary condition that can not be approximated as a linear connection between two points. A non-linear property is usually approximated by using linear interpolations between many points.

Plate Element: An element with six degrees of freedom and two dimensions exactly specified. The thickness is approximated as a linear interpolation between the bounding nodes.

Stiffening Post: A post that carries no structural load besides itself and a barrier, and serves to increase the rigidity of a barrier.

Tbar and Dbar Failure: Hot spot (flame passage) and massive failure (collapse) respectively.

Thermo-elasticity: The analysis of the structural response (deflections, stresses, and strains) of a solid structure subject to a thermal load.

References

[1] Rao, S.S. 1982. The Finite Element Method in Engineering. New York, New York: Pergamon Press.

[2] Boyle, J.T., and J. Spence. 1983. Stress Analysis for Creep. Boston, MA: Butterworths.

[3] Department of Transportation, United States Coast Guard, 1987(?) "Statement of Work: Delivery Order NO. 10, Finite Element Analysis of Barriers, Contract DTCG39-87-D-E38E46". New London, CT: USCG.

[4] Taylor, R.L., and O.C. Zienkiewicz. 1989. The Finite Element Method. Fourth Ed. Vol. 1, Basic Formulation and Linear Problems. London, UK: McGraw Hill Book Company.

[5] Oden, J. Tinsley and Grahan F. Carey. 1984. Finite Elements. Vol. 5, Special Problems in Solid Mechanics. Englewood, NJ: Prentice-Hall, Inc.

[6] Thomas Register of American Manufacturers and Thomas Register Catalog File. 1988. Products & Services. Paints: elastomeric thru Pumps: boat. New York, NY: Thomas Publishing Company.

[7] Thomas Register of American Manufacturers and Thomas Register Catalog File. 1988. Company Profiles: A thru M. New York, NY: Thomas Publishing Company.

[8] Thomas Register of American Manufacturers and Thomas Register Catalog File. 1988. Company Profiles: N thru Z. New York, NY: Thomas Publishing Company.

[9] Desjarlais, A. O. 1991. The Apparent Thermal Conductivity, Thermal Resistance, and Specific Heat of Two Specimens of Thermal Insulation Materials. Holometrix Report Number WCP-1. Cambridge, MA: Holometrix, Inc.

[10] American Society of Testing Materials. 1990. Annual Book of ASTM Standards . Vol 4.06, Thermal Insulation; Environmental Acoustics. Philadelphia, PA: ASTM.

[11] Desjarlais, A. 1991. Meeting, 17 January. Holometrix, Inc. Cambridge, MA.

[12] Toulouhian, Y.S., R.W. Powell, C.Y. Ho, and P.G. Klemens, eds. 1970. Thermo Physical Properties of Matter. Vol. 1, Thermal Conductivity of Metallic Elements and Alloys. Washington, D.C.: IFI/Plenum.

[13] Brandy, ed. 1983. Smithells Metals Refer Butterworths.

[14] Toulouhian, Y.S., R.W. Powell, C.Y. Ho, and P.G. Klemens, eds. 1970. Thermo Physical Properties of Matter. Vol. 4, Specific Heat of the Metallic Elements and Alloys. Washington, D.C.: IFI/Plenum.

[15] O'Brien, Kevin Michael. 1985. "Thermal Conductivity Calculation Using Experimental Furnace Data and Finite Difference/Finite Element Unsteady State Heat Transfer Program". Masters Thesis. Worcester Polytechnic Institute, Worcester, MA.

[16] Yang, K. 1987. Handbook of Single Phase Convective Heat Transfer. Chap. in Natural Convection in Enclosures. New York, NY: Wiley & Sons, Inc.

[17] Alexandrou, A. 1991. 10 January through 15 May. Class Notes. ME526, Worcester Polytechnic Institute. Worcester, MA.

[18] Iding, R., B. Bresler, and Z. Mizamuddin. 1977. FIRES-T3, A Computer Program for Fire Response of Structures, Thermal. Berkeley, CA: University of California-Berkeley.

[19] Chandrupatla, Tirupathi R. and Ashok D. Belegundu. 1991. Introduction to Finite Elements in Engineering. Englewood Cliffs, NJ: Prentice Hall.

[20] Mats, Paulsson. 1983. TASEF. Lund, Sweden: Lund Institute of Technology.

[21] Hurley, J. 1987. Calculus. Belmont, CA: Wadsworth Publishing Company.

[22] Grandin, H. 1986. Fundamentals of the Finite Element Method. New York, NY: MacMillan Publishing Company.

[23] Volterra, Enricho and J.H. Gaines. 1971. Advanced Strength of Materials. Englewood, NJ: Prentice-Hall, Inc.

[24] Boley, B.A., and J.H. Weiner. 1960. Theory of Thermal Stresses. New York, NY: John Wiley & Sons.

[25] Boresi, Arthur and Omar M. Sidebottom. 1985. Advanced Mechanics of Materials. Fourth ed. New York, NY: John Wiley & Sons, Inc.

[26] Timoshenko, S. 1936. Theory of Elastic Stability. New York, NY: McGraw-Hill Book Company.

[27] Oberg, Erik, Franklin D. Jones, and Holbrook L. Horton. 1984. Machinery's Handbook. Twenty-Third ed. New York, NY: Industrial Press.

[28] Hetarski, R., ed. 1986. Thermal Stresses I. Amsterdam, Netherlands: North-Holland.

[29] Timoshenko, S. 1940. Theory of Plates and Shells. New York, NY: McGraw-Hill Book Company.

[30] Burgreen, D. 1971. Elements of Thermal Stresses. Jamaica, NY: C.P. Press.

[31] Swanson Analysis Systems, Inc. 1987. ANSYS Theoretical Manual. Houston, PA: Swanson Analysis Systems, Inc.

[32] DeSalvo, Gabriel J. and Robert W. Gorman. 1989. ANSYS Engineering Analysis System Users Manual for ANSYS Revision 4.4. Vol 1. Houston, PA: Swanson Analysis Systems, Inc.

[33] MacNeal, Richard H., ed. 1972. The NASTRAN Theoretical Manual (Level 15.5). Los Angeles, CA: The MacNeal-Schwendler Corporation.

[34] The MacNeal-Schwendler Corporation. 1989. MSC/NASTRAN Users Manual. Vol. 2. Los Angeles, CA: The MacNeal-Schwendler Corporation.

[35] Hibbitt, Karlsson & Sorensen, Inc. 1989. ABAQUS Theory Manual for Version 4.8. Palo Alto, CA: Hibbitt, Karlsson & Sorensen, Inc.

[36] The MacNeal-Schwendler Corporation. 1989. MSC/NASTRAN Users Manual. Vol. 1. Los Angeles, CA: The MacNeal-Schwendler Corporation.

[37] Joseph, Jerrard A, ed. 1991. Application Manual MSC/NASTRAN Version 66a. vol I. Los Angeles, CA: The MacNeal-Schwendler Corporation.

[38] Swanson Analysis Systems, Inc. 1989. ANSYS Demonstration Examples Manual. Houston, PA: Swanson Analysis Systems, Inc.

[39] Beitel, Jesse J. 1979. "Fire Tests of Bulkhead Materials". SwRI Project No. 03-5347. San Antonio, TX: Gibbs and Cox, Inc.

[40] United States Coast Guard. 1986. Blueprints, USCG Plan # 905 WNEC-621-011. New London, CT: USCG.

[41] Van Horn, K.R., ed. 1967. Aluminum. Vol 1, Properties, Physical Metallurgy and Phase Diagrams. Metals Park: American Society for Metals.

[42] Kraus, Harry. 1980. Creep Analysis. New York, NY: Wiley Inter-Science Publications.

[43] Hertzberg, Richard. 1989. Deformation and Fracture Mechanics of Engineering Materials. Third ed. New York, NY: John Wiley & Sons, Inc.

[44] Kennedy, A.J. 1963. Process of Creep and Fatigue in Metals. New York, NY. John Wiley & Sons, Inc.

[45] Chandran, Anand. 1990. Determination of β-Factors. Major Qualifying Project, Worcester Polytechnic Institute, Worcester, MA.

[46] Brady, James E. and Gerard E. Humiston. 1975. General Chemical Principles and Structure. New York, NY: John Wiley & Sons, Inc.

[47] Solecki, J.S. 1989. Fracture Mechanics: A Revision 4.4 Tutorial. Houston, PA: Swanson Analysis Systems, Inc.

APPENDIX A

PARTIAL LISTING OF COMPANIES MANUFACTURING STEEL JOINER AND HONEYCOMB PANELS

The following companies manufacture ship bulkhead panels. The bulkhead panels include both the steel joiner and honeycomb products.

1. Pacific Marine Systems Corp.
   1135 Kirkwall Road
   Azusa, CA

2. M.C. Gill, Inc.
   4056-T Easy Street
   El Monte, CA 91731
   818-443-6094

3. Unicel Corporation (Honeycomb only)
   1520 Industrial Avenue
   Dept. TR
   Escondido, CA 92025
   619-741-3912

4. Astech
   P.O. Box 11030-T
   Santa Ana, CA

5. Best Manufacturing Co.
   1202-T North Park Avenue
   Montrose, CO

6. Arjay Industries, Inc.
   2020 Wild Acre Road
   Largo, FL

7. McDermott, Inc.
   P.O. Box 60035
   1010-T Common Street
   New Orleans, LA

8. Plasicore Inc.
   3022 88th Avenue
   Zeeland, MI 49464
   616-772-1220

9. Dallas Corp. Todco Division
   2330 Fairground Road East
   Marion, OH 43302
   614-383-6376

10. Advanced Structures Corp.
    235-T West Industry Court
    Deer Park, NY

11. Orville Products, Inc.
    P.O. Drawer 902-T
    Orville, OH

12. Emron, Corp.
    20650 Enterprise Avenue
    Brookfield, WI 53005
    414-784-5395

The following companies can be contacted for information regarding the steel-fiberglass panels. The product name may vary from one company to another.

1. Plascore Inc.
   3022 88th Avenue
   Zeeland, Mi 49464
   616-772-1220

2. Baron, Inc.
   1835 Briarwood Road
   Atlanta, GA

3. Baltek Corp.
   10 Fairway Court
   P.O. Box 195-T
   Northvale, NJ 07647
   201-67-1400

4. MBI Metal Building Interior Products Co.
   5309 Hamilton Avenue At E.53 Rd. St.
   Cleveland, OH 44114-3909
   216-431-6400

5. South & Sons Panels, Inc.
   142 Industrial Drive
   Franklin, OH 45005
   513-756-3544

6. Laminated Panel Products Inc.
   5220-T Rear Facility
   Mills Industrial Parkway
   North Ridgeville, OH

7. CID Associates, Inc.
   P.O. Box 445, Dept 6
   Oakmont, PA 15139
   412-828-2130

8. Bally Engineered Structures, Inc.
   P.O. Box 98
   Bally, PA 19503
   800-242-2559

9. W.A. Brown, Inc.
   Dept T, P.O. Box 1408
   Salisbury, NC 28145-1408
   800-438-2316

10. Palladino Brothers
    Palbro Products Division Tri-County
    71-73 Robinson Street
    Pottstown, PA

The last group of companies can be contacted regarding honeycomb panels.

1. Hexcel Structural Products Division
   11711-13 Dublin Boulevarde
   Dublin, CA 94566
   415-828-4200

2. Northfield Corp.
   Unit of Plastic Fabrication Technologies
   36 Kenosia Avenue
   Danbury, CT 06810
   203-792-5110

3. Cardinal Industries, Inc.
   P.O. Box G
   24 West 351 Army Trail Road
   Bloomingdale, IL

4. TAS Building Systems, Inc.
   2540 Main Street
   Dept. T
   Chula Vista, CA 92011

5. Baltek Corp.
   10 Fairway Court
   P.O. Box 195-T
   Northvale, NJ 07647
   201-767-1400

6. Limco Mfg. Corp.
   1 Garvies Point Road
   Glen Cove, NY 11542
   516-671-7400

Appendix B Holometrix Report

Appendix B lists the entire report prepared by Holometrix, Incorporated, February, 1991. The results of the two thermal conductivity tests and two heat capacity tests are at the end of the report.

HOLOMETRIX, INC.

Report on

THE APPARENT THERMAL CONDUCTIVITY, THERMAL RESISTANCE, AND
SPECIFIC HEAT OF TWO SPECIMENS OF
THERMAL INSULATION MATERIALS

Prepared for:

Worcester Polytechnic Institute
Center for Firesafety Studies
100 Institute Road
Worcester, MA 01609

Holometrix Report Number WCP-1

Work Performed under Purchase Order No. 52838

Submitted by: [signature]
A. O. Desjarlais
Manager
Thermal Insulation Evaluation
Thermophysics Laboratory

February 1991

HOLOMETRIX, INC.

Report on

THE APPARENT THERMAL CONDUCTIVITY, THERMAL RESISTANCE, AND SPECIFIC HEAT OF TWO SPECIMENS OF THERMAL INSULATION MATERIALS

Holometrix, Inc. was contracted by Worcester Polytechnic Institute to measure two specimens of thermal insulation materials for apparent thermal conductivity, thermal resistance, and specific heat over the approximate temperature range of 24 to 600°C (75 to 1100°F) or until decomposition occurred. The specimens were identified as a fiberglass blanket and a honeycomb.

The specimens were analyzed for apparent thermal conductivity in accordance with ASTM C 177-85, "Steady-State Heat Flux Measurements and Thermal Transmission Properties by Means of the Guarded Hot Plate Apparatus." Two samples of each specimen approximately dimensioned 200 mm (8 inches) in diameter were prepared. The fiberglass blanket was to be tested at a thickness of 25.4 mm (1.00 inches) while the honeycomb was evaluated at the as-received thickness of 17.5 mm (0.69 inches). The average test densities of the test samples were 81.4 and 293 kg m^{-3} (5.08 and 18.3 lbs ft^{-3}) respectively.

The specific heat was determined using a high temperature copper drop calorimeter following the procedure of ASTM C 351-90, "Mean Specific Heat of Thermal Insulation." A sample container approximately dimensioned 25 mm (1 inch) in diameter by 76 mm (3 inches) long was used to house the maximum weight of each specimen.

Only enthalpy data is presented for the honeycomb material. Weight changes of 1, 3, 13, and 6 percent were noted after testing at 200, 300, 350, and 400°C (390, 570, 660, and 750°F) respectively. The changes occurring in the material preclude the meaningful calculation of specific heat.

Experimental Procedure for Testing by C 177-85

Each specimen was evaluated in accordance with ASTM C 177-85, "Steady-State Heat Flux Measurements and Thermal Transmission Properties by Means of the Guarded Hot Plate Apparatus", utilizing a Holometrix Model TCFGM guarded hot plate instrument. A schematic diagram of the test facility is shown in Figure 1. Two samples were sandwiched between a heating unit, which consisted of a central metering section and an annular guard section. This composite stack was mounted between two cooling units and surrounded with an environmental heater unit, a fluid-cooled shroud, and edge insulation. The metering section of the heating unit consisted of a metering area heater and metering area surface plates, while the guard section comprised a single guard heater and guard surface plates. The cooling units consisted of a cooling plate, a cooling unit heater, and a cooling surface plate. All surface plates were fabricated of 10 mm (0.38 inch) thick stainless steel, were smoothly finished to conform to a true plane to within 0.025 percent, and were treated to have a total hemispherical emittance of 0.82 at 24°C (75°F).

The heating unit was fabricated by sandwiching a two element mica heater unit between two thin sheets of ceramic fiber paper and two surface plates. The overall geometry of the heating unit was 200 mm (8 inches) in diameter, with the metering area being the central 100 mm (4 inch) round section. The unit was bolted together at four points, one being in the metering section. The two sections of the heater unit were separated by a 3 mm (0.125 inch) gap around the perimeter of the metering section. The area of the gap represented 3.3 percent of the total metering section area. The area of the metering section was determined by measurements to the centers of the gap. A 16 junction

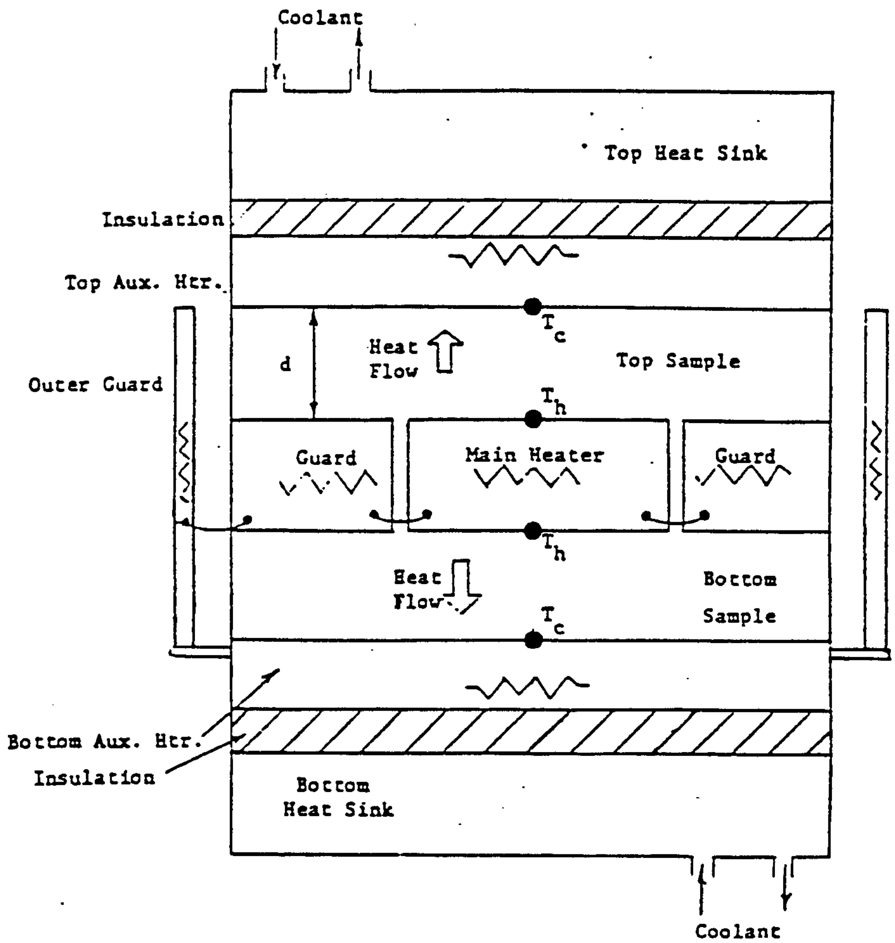

Figure 1

SCHEMATIC OF GUARDED HOT PLATE THERMAL CONDUCTIVITY INSTRUMENT differential thermopile was installed between the mica heating unit and the ceramic fiber sheets such that alternate junctions were in the metering and guard sections respectively and close to the annular gap between the sections. This thermopile was fabricated of 32 gauge Type K Chromel/Alumel wire. The sensitivity of this thermopile was approximately 0.33 mV $\cdot C^{-1}$ (0.18 mV $\cdot F^{-1}$) at 24°C (75°F).

The metering area heater was connected to a Lambda Model LK 342 FM DC Power Supply. A 0.001 Ω precision resistor was connected in series with the heater and the voltage drop across this resistor (0.001 times the amperage) was monitored. The voltage drop across the metering area heater was determined using a high resistance voltage divider connected in parallel with the heater. The three resistors used in the power measurement circuit were routinely checked against a precision resistor traceable to NIST. The output of the differential thermopile was connected to a differential temperature controller which supplied power to the guard heater such that the thermopile output was minimized. The voltage drops, current, and thermopile output were metered with a Newport Model 2400 A/S Digital Millivolt Meter, having a range of ±0 to 39.999 mV. The resolution of the meter is 1 microvolt with a maximum error of 0.01 percent of the output and ±2 microvolts over an eight hour period.

The cooling units consisted of a 10 mm (0.38 inch) thick copper plate which had a series of interconnected 6 mm (0.25 inch) diameter copper tubes soldered to the plate and foamed in place with a spray urethane foam, a mica electric resistance heater unit, and a surface plate. The plates and heater were similar in cross-section to the heating unit. The tubing was connected to a temperature controlled circulating chiller unit and a control thermocouple was attached to the underside of the surface plate and connected to a temperature controller. Temperature control at the surface plates was accomplished by operating the circulating chiller continuously and reheating with the electrical resistance heaters.

The environmental heating unit consisted of a sheathed electric resistance cable heater sandwiched between two tightly fitting passivated stainless steel rings 300 mm (12 inches) in diameter by 100 mm (4 inches) high. The electric resistance heater was connected to a temperature controller. The environmental heating unit and a 430 mm (17 inch) diameter by 610 mm (24 inch) high shroud were placed concentrically around the test stack.

The temperature of the environmental heating unit was controlled and monitored by thermocouples attached to its inner surface. The interspaces between the test stack, environmental heating unit, and shroud were filled with a diatomaceous silica loose-fill insulation material.

Temperature measurements were performed by utilizing Type K Chromel/Alumel thermocouples calibrated to the special limits of error specified in ASTM E 230-83, "Temperature-Electromotive Force (EMF) Tables for Standardized Thermocouples". All thermocouple sensors were fabricated with No. 30AWG wire. The thermocouples were fixed to the surface plates by cementing them into 1.6 mm (0.062 inch) square grooves that had been machine cut into all the surface plates. A total of four thermocouples were cemented into each working surface; two in the metering section and two in the guard section. The temperature sensors were referenced to an Acromag Model 320 Electronic Ice Reference and their output measured with a Newport 2400 A/S Digital Millivolt meter. The setpoint accuracy for the reference is $\pm 0.5^\circ C$ ($\pm 0.9^\circ F$) with a $0.1^\circ C$ ($0.2^\circ F$) stability over an eight hour period.

In operation, a steady temperature equilibrium was established in the test system. The temperatures of the cooling surface plates were set to their required levels. The required temperature difference across each sample was maintained by the adjustment of the power to the metering area heater. If no specific temperature difference was requested, a $40^\circ C$ ($75^\circ F$) difference was used. The temperature of the environmental heating unit was controlled to the mean sample temperature level. The differential output was checked and adjusted such that the thermopile output was maintained between $\pm$ 0.01 mV. At equilibrium, established after ensuring that during five regular sets of data taken 1200 seconds apart, the apparent thermal conductivity did not change by more than 1 percent and that there was no consistent drift, the power to the metering area heater was measured with the precision resistor network and the temperatures of the working surfaces were evaluated from thermocouple readings.

The apparent thermal conductivity was calculated from

$$\lambda = \frac{q \, \Delta x}{A \, \Delta T} ,$$

and the thermal resistance was calculated from

$$R = \frac{A \, \Delta T}{q} ,$$

where λ = apparent thermal conductivity, $Wm^{-1}K^{-1}$ (Btu-in $hr^{-1}ft^{-2}F^{-1}$);

q = power dissipation in the metering heater, W (Btu hr^{-1});

Δx = total thickness of both test specimens, m (inches);

A = the metering surface area taken twice, m^2 (ft^2);

ΔT = the total temperature difference across both specimens, °C (°F);and

R = thermal resistance, $m^2K\ W^{-1}$ (hr ft^2FBtu^{-1}).

The results for the specimens tested are shown in the following tables.

The instrument performance was verified using the National Institute of Standards and Technology Standard Reference Material 1450b. The calibration specimen is a high density fibrous glass material, 25.4 mm (1.00 inches) thick, having a thermal resistance of approximately 0.803 m^2KW^{-1} (4.56 Btu^{-1} hr ft^2F) at 24°C (75°F). The tests were certified on 21 May 1982. The overall uncertainty of the thermal resistance of the standard is estimated by NIST to be 2 percent. The instrumentation is verified after any repair or modification.

Experimental Procedure for Testing by C 351-90

The specific heat was determined using a high temperature copper drop calorimeter following the procedure of ASTM C 351-90 as modified for high temperature use and using the procedure of ASTM D 2766-83 for the data analysis. The basic procedure is to bring the sample to a constant, uniform temperature and then to drop it into a receiver at room temperature. The temperature rise of the receiver is then a measure of the heat loss from the sample, and if the calorimeter has been calibrated with a reference sample the specific heat can be determined. The copper drop calorimeter uses a copper receiver with a mass of about 100 lb for thermal stability. It is highly isolated from the environment by several layers of thermal insulation.

The test specimen was instrumented with a type K (Chromel/Alumel) thermocouple and supported in a three-zone temperature controlled furnace. The sample was allowed to come to equilibrium at the selected temperature. This required a time of 1 to 2 hr, during which regular temperature readings were taken. The temperature of the copper receiver was also recorded during this time. When equilibrium was reached, the thermocouple leads to the sample were cut and the support wire was melted with an electrical pulse to quickly drop the sample into the receiver. Radiation shields were quickly opened and then closed after the drop to reduce any radiative or convective transfer of heat between the furnace and receiver or to the environment.

The temperature of the receiver was measured before and after the drop using a differential thermopile. The temperature of the receiver was measured until it reached a maximum and then decreased towards the temperature of the environment.

The adiabatic exchange of heat from the sample to the receiver does not change the total enthalpy of the system:

$$(\Delta H)_r = (\Delta H)_s$$

where H is the enthalpy and the subscripts r and s refer to the receiver and sample respectively. This equation can also be expressed as

$$(mc_p)_r \; (T_f - T_i) = (mc_p)_s \; (T_0 - T_f)$$

where

m = mass,
c_p = specific heat at constant pressure,
T_f = final temperature of the receiver plus sample,
T_i = initial temperature of the receiver, and
T_0 = initial temperature of the sample.

Prior to the sample drops, the calorimeter was calibrated by dropping an alumina or copper reference specimen over the temperature range in which the calorimeter was to be used. The measured temperature changes, the known specific heat integrated over the temperature, and the above equation were used to determine $(mc_p)_r$. The enthalpy change, ΔH, during the sample drops can then be found from

$$\Delta H = (mc_p)_r \; (T_f - T_i)$$

This change in enthalpy for different drop temperatures was fit to a two parameter curve to give the enthalpy as a function of temperature

$$\Delta H(T) = A\ (T - T_f) + B\ (T - T_f)^2$$

This form insures that $\Delta H(T_f) = 0$. The specific heat is derived by differentiation of the equation with respect to the temperature

$$c_p = \frac{d(\Delta H)}{dT}$$

$$= A + 2B\ (T - T_f)$$

The test results are summarized in Tables 2 and 3.

HOLOMETRIX, INC.

TABLE 1

THE APPARENT THERMAL CONDUCTIVITY AND THERMAL RESISTANCE OF TWO SPECIMENS OF THERMAL INSULATION MATERIALS

Specimen	Test Thickness		Test Density		Mean Temperature		Apparent Thermal Conductivity		Thermal Resistanc
	mm	inches	Kg/m^3	lbs/ft^3	C	F	W/m K	Btu-in/hr ft^2 F	hr ft^2 F/Btu
Fiberglass	25.4	1.00	81.4	5.08	31	87	0.0327	0.226	4.4
					100	213	0.0401	0.278	3.5
					200	391	0.0527	0.366	2.7
					301	573	0.0720	0.499	2.0
					402	756	0.0986	0.683	1.4
					504	939	0.132	0.916	1.0
					604	1120	0.425	2.95	0.3
Honeycomb	17.5	0.69	293	18.3	30	87	0.0755	0.523	1.3
					101	213	0.0958	0.664	1.0
					200	392	0.139	0.967	0.7
					302	576	0.175	1.21	0.5
					353	668	0.198	1.37	0.5
					404	759	0.194	1.34	0.5

Notes:

1. Severe shrinkage of the fiberglass specimen was noted upon disassembly of the experiment. Diameter of sample was approximately 50% of original value and thickness was approximately 75% of original value.

2. Experiments on the honeycomb material at 350 and 400C never satisfied equilibrium requirements, suggesting that the specimen was degrading during testing at these temperature levels.

TABLE 2

THE ENTHALPY OF TWO SPECIMENS OF THERMAL INSULATION MATERIALS

Specimen	Temperature, C			Temperature, F			Enthalpy	
	Drop	Bath	Mean	Drop	Bath	Mean	J/gm	Btu/lb
Fiberglass	114.0	22.5	68.3	237.2	72.5	154.9	74.2	31.9
	201.5	22.8	112.2	394.7	73.0	233.9	159.6	68.6
	301.2	24.5	162.9	574.2	76.1	325.1	257.4	110.7
	400.3	26.5	213.4	752.5	79.7	416.1	362.6	155.9
	501.4	26.0	263.7	934.5	78.8	506.7	475.0	204.2
	551.0	25.9	288.5	1023.8	78.6	551.2	542.7	233.3
Honeycomb	101.2	23.5	62.4	214.2	74.3	144.2	91.1	39.2
	150.6	24.2	87.4	303.1	75.6	189.3	165.1	71.0
	200.9	23.4	112.2	393.6	74.1	233.9	204.1	87.7
	304.2	25.2	164.7	579.6	77.4	328.5	398.9	171.5
	349.0	25.6	187.3	660.2	78.1	369.1	372.0	159.9
	401.2	25.8	213.5	754.2	78.4	416.3	455.2	195.7

Appendix C Input Files for TASEF and FIRES-T3

The input that were used in TASEF and FIRES-T3 for the heat transfer analysis of the three panels and the panel-post assembly are listed in this appendix. Refer to [18,20] for an explanation of the syntax. The files set up the geometry, specify the material properties, place the boundary conditions, and set the load.

```
$$$$$$$$$$$$$$$$$$$$$$$$$$$$$$$$$$$$$$$$$$$$$$$$$$$$$$$$$$$$$$$$
$$                                                            $$
$$      This is the input file to TASEF for material one      $$
$$                                                            $$
$$$$$$$$$$$$$$$$$$$$$$$$$$$$$$$$$$$$$$$$$$$$$$$$$$$$$$$$$$$$$$$$
$$
$$

NO
T  T  0.
in111
F   1.0000    2.8560    1.0000    2.8560    3    5   11    0
F   0.        0.        1.0000    0.1580
F   0.        2.6980    1.0000    2.8560
    0.1667    0.3333    0.5000    0.6667    0.8333
    0.0790    0.1580    0.4755    0.7930    1.1105    1.4280   1.7455   2.06
    2.3805    2.6980    2.7770
  0
mat1
F    7    7    0    1.000
0.2000E+02  0.1177E+01  0.1000E+03  0.1444E+01  0.2000E+03  0.1897E+01
0.3010E+03  0.2592E+01  0.4020E+03  0.3549E+01  0.5040E+03  0.4752E+01
0.6040E+03  0.1530E+02
0.2000E+02  0.1425E+01  0.1000E+03  0.7123E+01  0.2000E+03  0.1555E+02
0.3000E+03  0.2535E+02  0.4000E+03  0.3652E+02  0.5000E+03  0.4910E+02
0.5500E+03  0.5555E+02
mat2
F    5    6    0    1.000
0.1000E+03  0.2347E+04  0.2000E+03  0.2171E+04  0.4000E+03  0.1976E+04
0.6000E+03  0.1627E+04  0.8000E+03  0.1310E+04
0.0000E+00  0.0000E+00  0.2000E+03  0.7780E+03  0.4000E+03  0.1678E+04
0.6000E+03  0.2729E+04  0.7000E+03  0.3337E+04  0.8000E+03  0.4291E+04
mat3
F    5    6    0    1.000
0.1000E+03  0.2347E+04  0.2000E+03  0.2171E+04  0.4000E+03  0.1976E+04
0.6000E+03  0.1627E+04  0.8000E+03  0.1310E+04
0.0000E+00  0.0000E+00  0.2000E+03  0.7780E+03  0.4000E+03  0.1678E+04
0.6000E+03  0.2729E+04  0.7000E+03  0.3337E+04  0.8000E+03  0.4291E+04
   25.00     25.00    2.04E-08   273.150
  2
  1    7     0.600     0.360     1.330
  1   14   27   40   53   66   79
  2    7     0.        1.000     1.000
 13   26   39   52   65   78   91
  2
T    1
F    2
  0
  0
NO VOIDS
 25         0.120     0.120     0.400     80000      1
 0.         0.005     0.010     0.015     0.020     0.025     0.030   0.035
 0.040      0.045     0.050     0.055     0.060     0.065     0.070   0.075
 0.080      0.085     0.090     0.095     0.100     0.105     0.110   0.115
 0.120
ISO834
0.120
```

```
$$$$$$$$$$$$$$$$$$$$$$$$$$$$$$$$$$$$$$$$$$$$$$$$$$$$$$$$$$$$
$$                                                        $$
$$     This is the TASEF input file for material two      $$
$$                                                        $$
$$$$$$$$$$$$$$$$$$$$$$$$$$$$$$$$$$$$$$$$$$$$$$$$$$$$$$$$$$$$
$$
$$

 NO
 T  T  0.
input222
F   1.0000    1.7500    1.0000    1.7500    1    5    7    0
    0.1667    0.3333    0.5000    0.6667    0.8333
    0.2188    0.4375    0.6563    0.8750    1.0938    1.3125    1.5313
  0
mat222
F    7    8    0    1.000
0.2000E+02  0.2720E+01  0.1010E+03  0.3450E+01  0.2000E+03  0.5000E+01
0.3020E+03  0.6300E+01  0.3530E+03  0.7140E+01  0.4040E+03  0.6980E+01
0.1500E+04  0.6980E+01
0.2000E+02  0.5328E+01  0.1010E+03  0.2691E+02  0.1510E+03  0.4853E+02
0.2010E+03  0.5984E+02  0.3040E+03  0.1169E+03  0.3490E+03  0.1200E+03
0.4010E+03  0.1335E+03  0.1401E+04  0.4699E+03
   25.00     25.00   0.204E-07   273.150
  2
  1    7     0.800      0.360      1.330
  1   10    19   28   37   46   55
  2    7     0.         .0750      1.000
  9   18    27   36   45   54   63
  2
T    1
F    2
  0
  0
NO VOIDS
 30          0.230      0.001      0.250    6000       1
 0.          0.005      0.010      0.015    0.020      0.025    0.030    0.035
 0.040       0.045      0.050      0.055    0.060      0.070    0.080    0.090
 0.100       0.110      0.120      0.130    0.140      0.150    0.160    0.170
 0.180       0.190      0.200      0.210    0.220      0.023
ISO834
   0.230
```

```
$$$$$$$$$$$$$$$$$$$$$$$$$$$$$$$$$$$$$$$$$$$$$$$$$$$$$$$$$$$$$$
$$                                                          $$
$$      This is the TASEF input file for material three     $$
$$                                                          $$
$$$$$$$$$$$$$$$$$$$$$$$$$$$$$$$$$$$$$$$$$$$$$$$$$$$$$$$$$$$$$$
$$
$$

NO
 T  T  0.
input333
F    1.0000     1.7500     1.0000     1.7500     1     5     7     0
     0.1667     0.3333     0.5000     0.6667     0.8333
     0.2188     0.4375     0.6563     0.8750     1.0938     1.3125     1.5313
  0
mat333
F    6     8     0      1.000
0.2500E+02  0.2718E+01  0.1010E+03  0.3448E+01  0.2000E+03  0.5004E+01
0.3020E+03  0.6300E+01  0.3530E+03  0.7138E+01  0.4040E+03  0.6984E+01
0.2000E+02  0.1299E+02  0.1000E+03  0.6497E+02  0.2000E+03  0.1436E+03
0.3000E+03  0.1990E+03  0.4000E+03  0.3080E+03  0.5000E+03  0.3900E+03
0.6000E+03  0.4800E+03  0.7000E+03  0.5789E+03
   25.00       25.00    0.204E-07    273.150
  2
  1     7      0.600       0.360       1.330
  1    10    19    28    37    46    55
  2     7      0.          1.000       1.000
  9    18    27    36    45    54    63
  2
T     1
F     2
  0
  0
NO VOIDS
 13          0.060       0.060       0.600    1000       1
   0.        0.005       0.010       0.015    0.020      0.025      0.030     0.035
   0.040     0.045       0.050       0.055    0.060
ISO834
   0.060
```

```
$$$$$$$$$$$$$$$$$$$$$$$$$$$$$$$$$$$$$$$$$$$$$$$$$$$$$$$$$$$$
$$                                                        $$
$$      This is the TASEF input file for the post         $$
$$                 and material three                     $$
$$                                                        $$
$$$$$$$$$$$$$$$$$$$$$$$$$$$$$$$$$$$$$$$$$$$$$$$$$$$$$$$$$$$$
$$
$$

NO
 T  T  0.
in222.11
F   3.7312     2.0638     3.7312     2.0638     11    19     9     0
F   0.         0.         0.3969     0.1588
T   0.         0.1588     0.3969     0.8731
F   0.         0.8731     0.3969     1.1906
T   0.         1.1906     0.3969     1.9050
F   0.         1.9050     0.3969     2.0638
F   0.3969     0.         0.7144     2.0638
F   0.7144     0.         2.3019     0.1588
F   0.7144     1.9050     2.3019     2.0638
T   2.3019     0.         3.7312     0.1588
T   2.3019     1.9050     3.7312     2.0638
    0.0794     0.2381     0.3969     0.5556     0.7144     0.8731   1.0319     1.19
    1.3494     1.5081     1.6669     1.8256     1.9844     2.1431   2.3019     2.54
    2.7787     3.0962     3.4137
    0.1588     0.3969     0.6350     0.8731     1.0318     1.1906   1.4287     1.66
    1.9050
  0
m1
F     7    8     0      1.000
0.2000E+02  0.2720E+01  0.1010E+03  0.3450E+01  0.2000E+03  0.5000E+01
0.3020E+03  0.6300E+01  0.3530E+03  0.7140E+01  0.4040E+03  0.6980E+01
0.1501E+04  0.6980E+01
0.2000E+02  0.1299E+02  0.1000E+03  0.6497E+02  0.2000E+03  0.1436E+03
0.3000E+03  0.1990E+03  0.4000E+03  0.3080E+03  0.5000E+03  0.3900E+03
0.6000E+03  0.4800E+03  0.7000E+03  0.5789E+03
m2
T     2    2     0      1.000
-.3000E+03  0.8568E+04  0.3000E+04  0.8568E+04
-.3000E+03  -.7454E+03  0.3000E+04  0.7454E+04
m2
T     2    2     0      1.000
-.3000E+03  0.8568E+04  0.3000E+04  0.8568E+04
-.3000E+03  -.7454E+03  0.3000E+04  0.7454E+04
m2
 T     2    2     0      1.000
-.3000E+03  0.8568E+04  0.3000E+04  0.8568E+04
-.3000E+03  -.7454E+03  0.3000E+04  0.7454E+04
m2
T     2    2     0      1.000
-.3000E+03  0.8568E+04  0.3000E+04  0.8568E+04
-.3000E+03  -.7454E+03  0.3000E+04  0.7454E+04
m2
T     2    2     0      1.000
-.3000E+03  0.8568E+04  0.3000E+04  0.8568E+04
-.3000E+03  -.7454E+03  0.3000E+04  0.7454E+04
m2
T     2    2     0      1.000
-.3000E+03  0.8568E+04  0.3000E+04  0.8568E+04
-.3000E+03  -.7454E+03  0.3000E+04  0.7454E+04
```

```
  20.00      20.00   0.204E-07   273.150
  5
  1   13      0.700       0.         2.000
  2   13   24   35   36   37   38   27   16    5    4    3    2
  2   13      0.700       0.         2.000
  7   18   29   40   41   42   43   32   21   10    9    8    7
  3   17      0.700       0.360      1.330
  1   12   23   34   45   56   67   78   89  100  111  122  133  144  155
166  167
  4    6      0.600       0.360      1.330
167  178  189  200  211  222
  5   22      0.          0.0100     1.000
 11   22   33   44   55   66   77   88   99  110  121  132  143  154  165
176  175  186  197  208  219  230
  3
T    3
T    4
F    5
  0
  0
VOID
   2
F  F     1     0     0     0
F  F     2     0     0     0
 26           0.250      0.250      0.800   375000      1
   0.         0.010      0.020      0.030   0.040       0.050    0.060    0.070
   0.080      0.090      0.100      0.110   0.120       0.130    0.140    0.150
   0.160      0.170      0.180      0.190   0.200       0.210    0.220    0.230
   0.240      0.250
ISO834
   0.250
```

```
$$$$$$$$$$$$$$$$$$$$$$$$$$$$$$$$$$$$$$$$$$$$$$$$$$$$$$$$$$$$$$$$$$
$$                                                              $$
$$    This is the FIRES-T3 input file for material one         $$
$$                                                              $$
$$$$$$$$$$$$$$$$$$$$$$$$$$$$$$$$$$$$$$$$$$$$$$$$$$$$$$$$$$$$$$$$$$
$$
$$

NODES,91,0
    1         0.          0.
    3    .158000     .000000
   11    2.69800     .000000
   13    2.85600     .000000
   14    .000000     .166667
   16    .158000     .166667
   24    2.69800     .166667
   26    2.85600     .166667
   27    .000000     .333333
   29    .158000     .333333
   37    2.69800     .333333
   39    2.85600     .333333
   40    .000000     .500000
   42    .158000     .500000
   50    2.69800     .500000
   52    2.85600     .500000
   53    .000000     .666667
   55    .158000     .666667
   63    2.69800     .666667
   65    2.85600     .666667
   66    .000000     .833333
   68    .158000     .833333
   76    2.69800     .833333
   78    2.85600     .833333
   79    .000000     1.00000
   81    .158000     1.00000
   89    2.69800     1.00000
   91    2.85600     1.00000
ELEMENTS,0,72,0
    1     1     2    15    14     2          1.0
    3     3     4    17    16     1          1.0
   11    11    12    25    24     2          1.0
   12    12    13    26    25     2          1.0
   13    14    15    28    27     2          1.0
   15    16    17    30    29     1          1.0
   23    24    25    38    37     2          1.0
   24    25    26    39    38     2          1.0
   25    27    28    41    40     2          1.0
   27    29    30    43    42     1          1.0
   35    37    38    51    50     2          1.0
   36    38    39    52    51     2          1.0
   37    40    41    54    53     2          1.0
   39    42    43    56    55     1          1.0
   47    50    51    64    63     2          1.0
   48    51    52    65    64     2          1.0
   49    53    54    67    66     2          1.0
   51    55    56    69    68     1          1.0
   59    63    64    77    76     2          1.0
   60    64    65    78    77     2          1.0
   61    66    67    80    79     2          1.0
   63    68    69    82    81     1          1.0
   71    76    77    90    89     2          1.0
```

```
   72    77    78    91    90     2         1.0
MATERIALS,2
    7     9     0
      20.0    1.1770       100.0     1.4440      200.0     1.8970      301.0
2.5920
     402.0    3.5490       504.0     4.7520      604.0     15.300
      20.0     812.0        50.0      833.0      100.0     875.00      150.0
 917.0
     200.0     955.0       300.0     1038.0      400.0    1122.00      500.0
1206.0
     550.0    1248.0
   8.14E-5
    5     5     0
     000.0    2347.0       200.      2171.0      400.0    1976.00      600.0
1627.0
     800.0    1310.0
     0.000     470.0       100.0     482.00      200.0    520.000      400.0
 745.0
     600.0     754.0
   7.86E-3
FIRE,0,12,0,2
NONLINEAR
   2.04E-8     273.0
      .360      1.33         1.0        0.6        1.0        0.6
      1.00      1.00         0.0        0.9        0.9        0.9
SURFACE,0,12,0
    1    14     1     1     1    14    27     1     1    13    27    40     1     1
25
   40    53     1     1    37    53    66     1     1    49    66    79     1     1
61
   13    26     2     2    12    26    39     2     2    24    39    52     2     2
36
   52    65     2     2    48    65    78     2     2    60    78    91     2     2
72
EXOTHERMIC,0,0,0,0
CONVERGENCE
 6000       .050        -.6
STEP       0      0.0      25.0
STEP       1     .005         208.400       25.0                        1
STEP       2     .005         288.400       25.0                        1
STEP       3     .005         340.300       25.0                        1
STEP       4     .005         378.700       25.0                        1
STEP       5     .005         409.300       25.0                        1
STEP       6     .005         437.400       25.0                        1
STEP       7     .005         456.400       25.0                        1
STEP       8     .005         475.300       25.0                        1
STEP       9     .005         492.200       25.0                        1
STEP      10     .005         507.300       25.0                        1
STEP      11     .005         521.000       25.0                        1
STEP      12     .005         533.000       25.0                        1
STEP      13     .005         545.200       25.0                        1
STEP      14     .005         556.000       25.0                        1
STEP      15     .005         566.000       25.0                        1
STEP      16     .005         575.400       25.0                        1
STEP      17     .005         584.000       25.0                        1
STEP      18     .005         592.700       25.0                        1
STEP      19     .005         600.500       25.0                        1
STEP      20     .005         608.100       25.0                        1
STEP      21     .005         615.200       25.0                        1
STEP      22     .005         622.000       25.0                        1
STEP      23     .005         628.700       25.0                        1
STEP      24     .005         634.900       25.0                        1
```

STEP	25	.005	640.900	25.0	1
STEP	26	.005	646.700	25.0	1
STEP	27	.005	653.300	25.0	1
STEP	28	-1.			

```
$$$$$$$$$$$$$$$$$$$$$$$$$$$$$$$$$$$$$$$$$$$$$$$$$$$$$$$$$$$$
$$                                                        $$
$$      This is the FIRES-T3 input file for material      $$
$$                        two                             $$
$$                                                        $$
$$$$$$$$$$$$$$$$$$$$$$$$$$$$$$$$$$$$$$$$$$$$$$$$$$$$$$$$$$$$
$$
$$

NODES,63,0
    1       0.          0.
    9   1.75000         0.
   10   .000000    .166667
   18   1.75000    .166667
   19   .000000    .333333
   27   1.75000    .333333
   28   .000000    .500000
   36   1.75000    .500000
   37   .000000    .666667
   45   1.75000    .666667
   46   .000000    .833333
   54   1.75000    .833333
   55   .000000    1.00000
   63   1.75000    1.00000
ELEMENTS,0,48,0
    1    1    2   11   10    1       1.0
    8    8    9   18   17    1       1.0
    9   10   11   20   19    1       1.0
   16   17   18   27   26    1       1.0
   17   19   20   29   28    1       1.0
   24   26   27   36   35    1       1.0
   25   28   29   38   37    1       1.0
   32   35   36   45   44    1       1.0
   33   37   38   47   46    1       1.0
   40   44   45   54   53    1       1.0
   41   46   47   56   55    1       1.0
   48   53   54   63   62    1       1.0
MATERIALS,1
    6    7    0
     20.0      2.718      101.0      3.448      200.0      5.004      302.0
  6.30
    353.0      7.138      404.0      6.984
      0.0      901.0      101.0      901.0      151.0     1096.0      201.0
1016.0
    304.0     1313.0      349.0     1189.0      401.0     1137.0
  0.293E-3
FIRE,0,12,0,2
NONLINEAR
   2.04E-8     273.0
      .36      1.33        1.0        0.8        1.0        0.8
     1.00      1.00        0.0        0.9        0.9        0.9
SURFACE,0,12,0
    1   10    1    1    1   10   19    1    1    9   19   28    1    1
17
   28   37    1    1   25   37   46    1    1   33   46   55    1    1
41
    9   18    2    2    8   18   27    2    2   16   27   36    2    2
24
   36   45    2    2   32   45   54    2    2   40   54   63    2    2
48
EXOTHERMIC,0,0,0,0
```

```
CONVERGENCE
   15        .005        -.1
STEP      0        0.0        25.0
STEP      1        .005         208.400        25.0                        1
STEP      2        .005         288.400        25.0                        1
STEP      3        .005         340.300        25.0                        1
STEP      4        .005         378.700        25.0                        1
STEP      5        .005         409.300        25.0                        1
STEP      6        .005         437.400        25.0                        1
STEP      7        .005         456.300        25.0                        1
STEP      8        .005         475.300        25.0                        1
STEP      9    -1.
```

```
$$$$$$$$$$$$$$$$$$$$$$$$$$$$$$$$$$$$$$$$$$$$$$$$$$$$$$$$$$$$
$$                                                        $$
$$      This is the FIRES-T3 input file for material      $$
$$                        three                           $$
$$                                                        $$
$$$$$$$$$$$$$$$$$$$$$$$$$$$$$$$$$$$$$$$$$$$$$$$$$$$$$$$$$$$$
$$
$$

NODES,63,0
    1        0.          0.
    9   1.75000          0.
   10   .000000    .166667
   18   1.75000    .166667
   19   .000000    .333333
   27   1.75000    .333333
   28   .000000    .500000
   36   1.75000    .500000
   37   .000000    .666667
   45   1.75000    .666667
   46   .000000    .833333
   54   1.75000    .833333
   55   .000000    1.00000
   63   1.75000    1.00000
ELEMENTS,0,48,0
    1    1    2   11   10    1       1.0
    8    8    9   18   17    1       1.0
    9   10   11   20   19    1       1.0
   16   17   18   27   26    1       1.0
   17   19   20   29   28    1       1.0
   24   26   27   36   35    1       1.0
   25   28   29   38   37    1       1.0
   32   35   36   45   44    1       1.0
   33   37   38   47   46    1       1.0
   40   44   45   54   53    1       1.0
   41   46   47   56   55    1       1.0
   48   53   54   63   62    1       1.0
MATERIALS,1
    7    9    0
     20.0      2.718      101.0      3.448      200.0      5.004      302.0
  6.30
    353.0      7.138      504.0      6.984     1500.0      6.984
      0.0      445.0      100.0      445.0      200.0      465.0      300.0
 504.0
    400.0      546.0      500.0      547.0      600.0      561.0      700.0
 580.0
   1500.0      580.0
  1.426E-3
FIRE,0,12,0,2
NONLINEAR
   2.04E-8     273.0
       .36      1.33        1.0        0.6        1.0        0.6
      5.00      1.00        0.0        0.9        0.9        0.9
SURFACE,0,12,0
    1   10    1    1    1   10   19    1    1    9   19   28    1    1
17
   28   37    1    1   25   37   46    1    1   33   46   55    1    1
41
    9   18    2    2    8   18   27    2    2   16   27   36    2    2
24
   36   45    2    2   32   45   54    2    2   40   54   63    2    2
```

```
48
EXOTHERMIC,0,0,0,0
CONVERGENCE
 2000      .005      -.6
STEP     0        0.0      25.0
STEP     1       .005        208.400       25.0                      1
STEP     2       .005        288.400       25.0                      1
STEP     3       .005        340.300       25.0                      1
STEP     4       .005        378.700       25.0                      1
STEP     5       .005        409.300       25.0                      1
STEP     6       .005        437.400       25.0                      1
STEP     7       .010        475.300       25.0                      1
STEP     8       .010        507.300       25.0                      1
STEP     9       .005        521.000       25.0                      1
STEP    10       .005        533.000       25.0                      1
STEP    11       .010        556.000       25.0                      1
STEP    12       .010        575.000       25.0                      1
STEP    13       .010        593.000       25.0                      1
STEP    14       .010        608.000       25.0                      1
STEP    15       .010        622.000       25.0                      1
STEP    16       .010        635.000       25.0                      1
STEP    17       .010        647.000       25.0                      1
STEP    18       .010        658.000       25.0                      1
STEP    19       .010        668.000       25.0                      1
STEP    20       .010        677.000       25.0                      1
STEP    21       .010        686.000       25.0                      1
STEP    22       .010        695.000       25.0                      1
STEP    23       .010        703.000       25.0                      1
STEP    24       .010        710.000       25.0                      1
STEP    25       .010        718.000       25.0                      1
STEP    26       .010        725.000       25.0                      1
STEP    27       .010        733.000       25.0                      1
STEP    28    -1.
```

```
$$$$$$$$$$$$$$$$$$$$$$$$$$$$$$$$$$$$$$$$$$$$$$$$$$$$$$$$$$$$
$$                                                        $$
$$        This is the FIRES-T3 input file for the         $$
$$                post and material three                 $$
$$                                                        $$
$$$$$$$$$$$$$$$$$$$$$$$$$$$$$$$$$$$$$$$$$$$$$$$$$$$$$$$$$$$$
$$
$$

NODES,209,0
     1   0.15880   0.00000
     4   0.87310   0.00000
     6   1.19060   0.00000
     9   1.90500   0.00000
    10   0.15880   0.31750
    13   0.87310   0.31750
    15   1.19060   0.31750
    18   1.90500   0.31750
    19   0.15880   0.63500
    22   0.87310   0.63500
    24   1.19060   0.63500
    27   1.90500   0.63500
    28   0.15880   0.95250
    31   0.87310   0.95250
    33   1.19060   0.95250
    36   1.90500   0.95250
    37   0.15880   1.19060
    40   0.87310   1.19060
    42   1.19060   1.19060
    45   1.90500   1.19060
    46   0.00000   1.42880
    47   0.15880   1.42880
    50   0.87310   1.42880
    52   1.19060   1.42880
    55   1.90500   1.42880
    56   2.06380   1.42880
    57   0.00000   1.58750
    58   0.15880   1.58750
    61   0.87310   1.58750
    63   1.19060   1.58750
    66   1.90500   1.58750
    67   2.06380   1.58750
    68   0.00000   1.74630
    69   0.15880   1.74630
    72   0.87310   1.74630
    74   1.19060   1.74630
    77   1.90500   1.74630
    78   2.06380   1.74630
    79   0.00000   1.90500
    80   0.15880   1.90500
    83   0.87310   1.90500
    85   1.19060   1.90500
    88   1.90500   1.90500
    89   2.06380   1.90500
    90   0.00000   2.06380
    91   0.15880   2.06380
    94   0.87310   2.06380
    96   1.19060   2.06380
    99   1.90500   2.06380
   100   2.06380   2.06380
   101   0.00000   2.22250
```

102	0.15880	2.22250
105	0.87310	2.22250
107	1.19060	2.22250
110	1.90500	2.22250
111	2.06380	2.22250
112	0.00000	2.38130
113	0.15880	2.38130
116	0.87310	2.38130
118	1.19060	2.38130
121	1.90500	2.38130
122	2.06380	2.38130
123	0.00000	2.54000
124	0.15880	2.54000
127	0.87310	2.54000
129	1.19060	2.54000
132	1.90500	2.54000
133	2.06380	2.54000
134	0.00000	2.69880
135	0.15880	2.69880
138	0.87310	2.69880
140	1.19060	2.69880
143	1.90500	2.69880
144	2.06380	2.69880
145	0.00000	2.85750
146	0.15880	2.85750
149	0.87310	2.85750
151	1.19060	2.85750
154	1.90500	2.85750
155	2.06380	2.85750
156	0.00000	3.01630
157	0.15880	3.01630
160	0.87310	3.01630
162	1.19060	3.01630
165	1.90500	3.01630
166	2.06380	3.01630
167	0.00000	3.17500
168	0.15880	3.17500
171	0.87310	3.17500
173	1.19060	3.17500
176	1.90500	3.17500
177	2.06380	3.17500
178	0.00000	3.33380
179	0.15880	3.33380
182	0.87310	3.33380
184	1.19060	3.33380
187	1.90500	3.33380
188	2.06380	3.33380
189	0.00000	3.49250
190	0.15880	3.49250
191	0.87310	3.49250
193	1.19060	3.49250
194	1.90500	3.49250
195	2.06380	3.49250
196	0.00000	3.65130
197	0.15880	3.65130
198	0.87310	3.65130
200	1.19060	3.65130
201	1.90500	3.65130
202	2.06380	3.65130
203	0.00000	3.93060
204	0.15880	3.93060
205	0.87310	3.93060

```
   207    1.19060     3.93060
   208    1.90500     3.93060
   209    2.06380     3.93060
ELEMENTS,0,172,0
     1     1     2    11    10     1          1.0
     8     8     9    18    17     1          1.0
     9    10    11    20    19     1          1.0
    16    17    18    27    26     1          1.0
    17    19    20    29    28     1          1.0
    24    26    27    36    35     1          1.0
    25    28    29    38    37     1          1.0
    32    35    36    45    44     1          1.0
    33    37    38    48    47     1          1.0
    40    44    45    55    54     1          1.0
    41    46    47    58    57     2          1.0
    42    47    48    59    58     1          1.0
    49    54    55    66    65     1          1.0
    50    55    56    67    66     2          1.0
    51    57    58    69    68     2          1.0
    52    58    59    70    69     1          1.0
    59    65    66    77    76     1          1.0
    60    66    67    78    77     2          1.0
    61    68    69    80    79     2          1.0
    62    69    70    81    80     1          1.0
    69    76    77    88    87     1          1.0
    70    77    78    89    88     2          1.0
    71    79    80    91    90     2          1.0
    72    80    81    92    91     1          1.0
    79    87    88    99    98     1          1.0
    80    88    89   100    99     2          1.0
    81    90    91   102   101     2          1.0
    82    91    92   103   102     1          1.0
    89    98    99   110   109     1          1.0
    90    99   100   111   110     2          1.0
    91   101   102   113   112     2          1.0
    92   102   103   114   113     1          1.0
    99   109   110   121   120     1          1.0
   100   110   111   122   121     2          1.0
   101   112   113   124   123     2          1.0
   102   113   114   125   124     1          1.0
   109   120   121   132   131     1          1.0
   110   121   122   133   132     2          1.0
   111   123   124   135   134     2          1.0
   112   124   125   136   135     1          1.0
   119   131   132   143   142     1          1.0
   120   132   133   144   143     2          1.0
   121   134   135   146   145     2          1.0
   122   135   136   147   146     1          1.0
   129   142   143   154   153     1          1.0
   130   143   144   155   154     2          1.0
   131   145   146   157   156     2          1.0
   132   146   147   158   157     1          1.0
   139   153   154   165   164     1          1.0
   140   154   155   166   165     2          1.0
   141   156   157   168   167     2          1.0
   142   157   158   169   168     2          1.0
   149   164   165   176   175     2          1.0
   150   165   166   177   176     2          1.0
   151   167   168   179   178     2          1.0
   152   168   169   180   179     2          1.0
   159   175   176   187   186     2          1.0
   160   176   177   188   187     2          1.0
```

```
  161   178   179   190   189     2          1.0
  162   182   183   192   191     2          1.0
  163   183   184   193   192     2          1.0
  164   187   188   195   194     2          1.0
  165   189   190   197   196     2          1.0
  166   191   192   199   198     2          1.0
  167   192   193   200   199     2          1.0
  168   194   195   202   201     2          1.0
  169   196   197   204   203     2          1.0
  170   198   199   206   205     2          1.0
  171   199   200   207   206     2          1.0
  172   201   202   209   208     2          1.0
MATERIALS,2
    7     8     0
     20.0      2.718      101.0      3.448      200.0      5.004      302.0
  6.30
    353.0      7.138      504.0      6.984      800.0      6.984
      0.0      445.0      100.0      445.0      200.0      465.0      300.0
 504.0
    400.0      546.0      500.0      547.0      600.0      561.0      700.0
 580.0
  1.426E-3
    0     0     0
     8568
    920.92
    2.7E-3
FIRE,0,42,0,2
NONLINEAR
   2.04E-8     273.0
       .36      1.33        1.0        0.7        1.0        0.7
     1.00       1.00        0.0        0.9        0.9        0.9
SURFACE,0,42,0
    1    10     1     1     1    10    19     1     1     9    19    28     1     1
17
   28    37     1     1    25    37    47     1     1    33    47    46     1     1
41
   46    57     1     1    41    57    68     1     1    51    68    79     1     1
61
   79    90     1     1    71    90   101     1     1    81   101   112     1     1
91
  112   123     1     1   101   123   134     1     1   111   134   145     1     1
121
  145   156     1     1   131   156   167     1     1   141   167   178     1     1
151
  178   189     1     1   161   189   196     1     1   165   196   203     1     1
169
    9    18     2     2     8    18    27     2     2    16    27    36     2     2
24
   36    45     2     2    32    45    55     2     2    40    55    56     2     2
50
   56    67     2     2    50    67    78     2     2    60    78    89     2     2
70
   89   100     2     2    80   100   111     2     2    90   111   122     2     2
100
  122   133     2     2   110   133   144     2     2   120   144   155     2     2
130
  155   166     2     2   140   166   177     2     2   150   177   188     2     2
160
  188   195     2     2   164   195   202     2     2   168   202   209     2     2
172
EXOTHERMIC,0,0,0,0
CONVERGENCE
```

```
  950       .005       -.6
STEP     0        0.0       20.0
STEP     1        .005          203.400       20.0                                1
STEP     2        .005          283.400       20.0                                1
STEP     3        .005          337.300       20.0                                1
STEP     4        .005          373.700       20.0                                1
STEP     5        .005          404.300       20.0                                1
STEP     6        .005          432.400       20.0                                1
STEP     7        .010          470.300       20.0                                1
STEP     8        .010          502.300       20.0                                1
STEP     9        .005          517.000       20.0                                1
STEP    10        .005          529.000       20.0                                1
STEP    11        .010          551.000       20.0                                1
STEP    12        .010          570.000       20.0                                1
STEP    13        .010          589.000       20.0                                1
STEP    14        .010          603.000       20.0                                1
STEP    15        .010          617.000       20.0                                1
STEP    16        .010          630.000       20.0                                1
STEP    17        .010          642.000       20.0                                1
STEP    18        .010          653.000       20.0                                1
STEP    19        .010          663.000       20.0                                1
STEP    20        .010          672.000       20.0                                1
STEP    21        .010          681.000       20.0                                1
STEP    22        .010          690.000       20.0                                1
STEP    23        .010          798.000       20.0                                1
STEP    24        .010          705.000       20.0                                1
STEP    25        .010          713.000       20.0                                1
STEP    26        .010          720.000       20.0                                1
STEP    27        .010          728.000       20.0                                1
STEP    28     -1.
```

Appendix D Fire Tests

This Appendix contains the important portions of the fire tests performed on the plastic-honeycomb panel and the aluminum post. The tests attempted to produce an E119 fire curve. The E119 fire curve is analagous to the ISO fire curve.

FIRE TESTS OF VARIOUS BULKHEAD MATERIALS

by

Jesse J. Beitel

FINAL REPORT

SwRI Project No. 03-5347

for

Gibbs and Cox, Incorporated
2341 Jefferson Davis Highway
Arlington, Virginia 22202

July 1979

Approved by:

G. E. Hartzell, Ph.D.
Dirarector, Department of
Fire Technology

[illegible]

TABLE OF CONTENTS

No hose stream test was performed since these evaluations were for fire endurance only.

Documentation of the ASTM E-119 evaluations was provided by 35mm color slides and 16mm color film taken at various times throughout the test period.

B. Test Materials

Three bulkhead systems were evaluated for fire endurance. The bulkhead system used in each of the evaluations is described below:

Test No. 1: Two panels, each 3.8 ft wide x 7.2 ft long x 0.625 in. thick. Panels consisted of GRP skins with phenolic resin with NOMEX honeycomb cores (1/4-in. cells), and manufactured by Hexcel Corporation. Panels were identified as HRH78/HX225. An aluminum H post assembly was used to join the panels together lengthwise. Steel boundary channel was placed around the perimeter of the joined panels. Aluminum pop rivets (3/16-in. diameter, solid core) were used for all fastening work.

Test No. 2: Two panels, each 4.0 ft wide x 8.0 ft long x 0.625 in. thick. Panels consisted of GRP skins with phenolic resin with NOMEX honeycomb cores (1/4-in. cells) and manufactured by Ciba-Geigy Company. Panels were identified as Firelam-Type D3. A phenolic H post assembly was used to join the panels together lengthwise. The H post consisted of 1/8-in. cell honeycomb core, foam-filled with fiberglass skin. Steel boundary channel was placed around the perimeter of the joined panels. Aluminum pop rivets (3/16-in. diameter, solid core) were used for all fastening work.

Test No. 3: Two panels, each 4.0 ft wide x 8.0 ft long x 0.625-in. thick. Panels consisted of GRP skins with phenolic resin with NOMEX honeycomb cores (1/4-in. cells) phenolic foam-filled and manufactured by Ciba-Geigy Company. Panels were identified as Firelam-Type D3-F. A phenolic H post assembly was used to join the panels together lengthwise. The H post consisted of 1/8-in. cell honeycomb core, foam-filled with fiberglass skin. Steel boundary channel was placed around the perimeter of the joined panels. Aluminum pop rivets (3/16-in. diameter, solid core) were used for all fastening work.

The test specimens were constructed as per details shown in Figures 7 and 8.

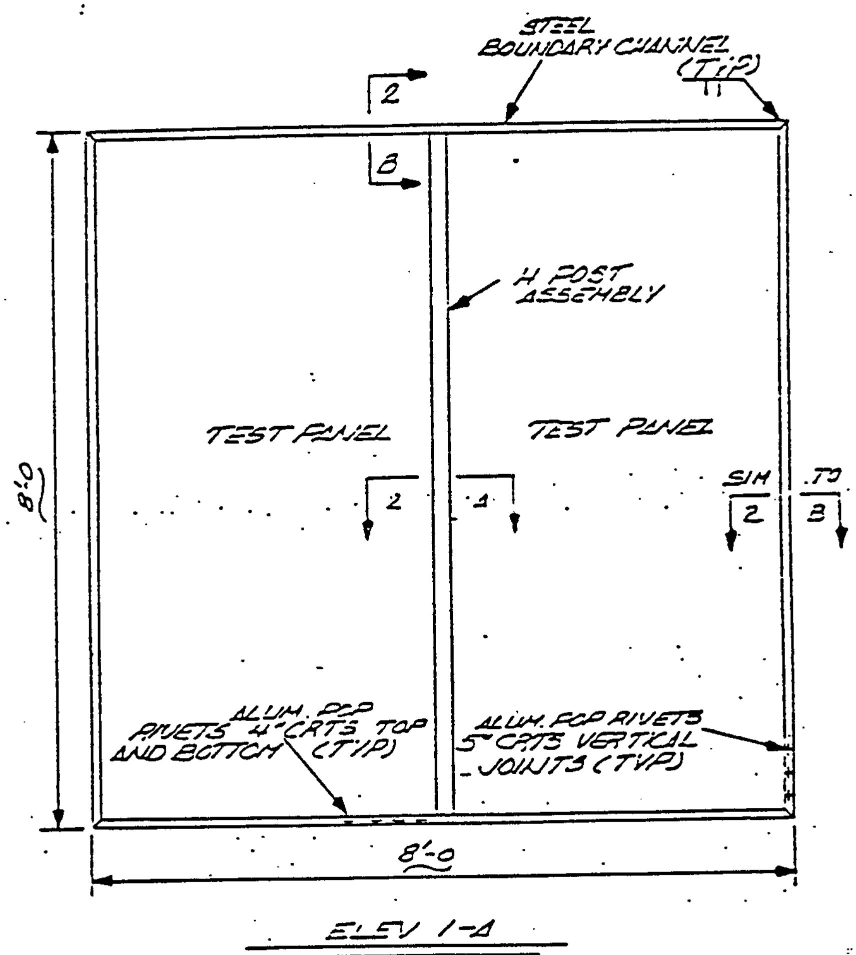

FIGURE 7. CONSTRUCTION DETAILS

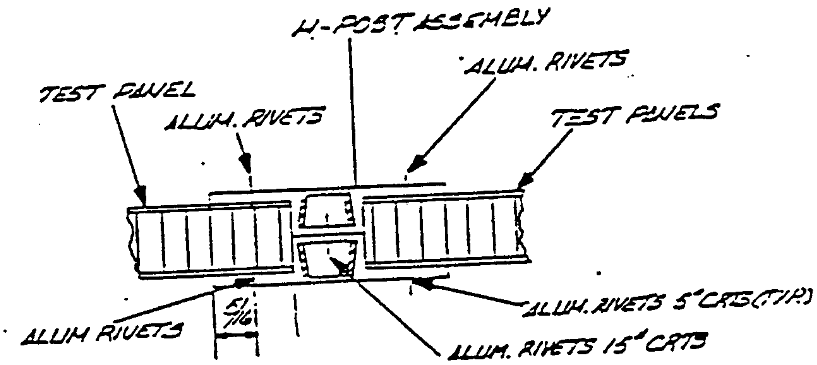

SECTION 2-A

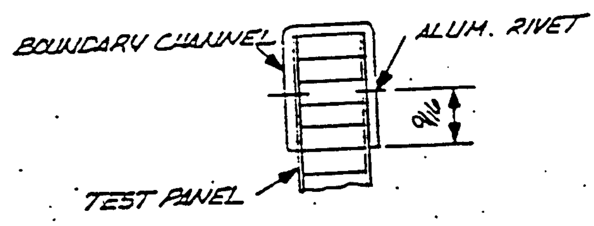

SECTION 2-B

FIGURE 8. CONSTRUCTION DETAILS

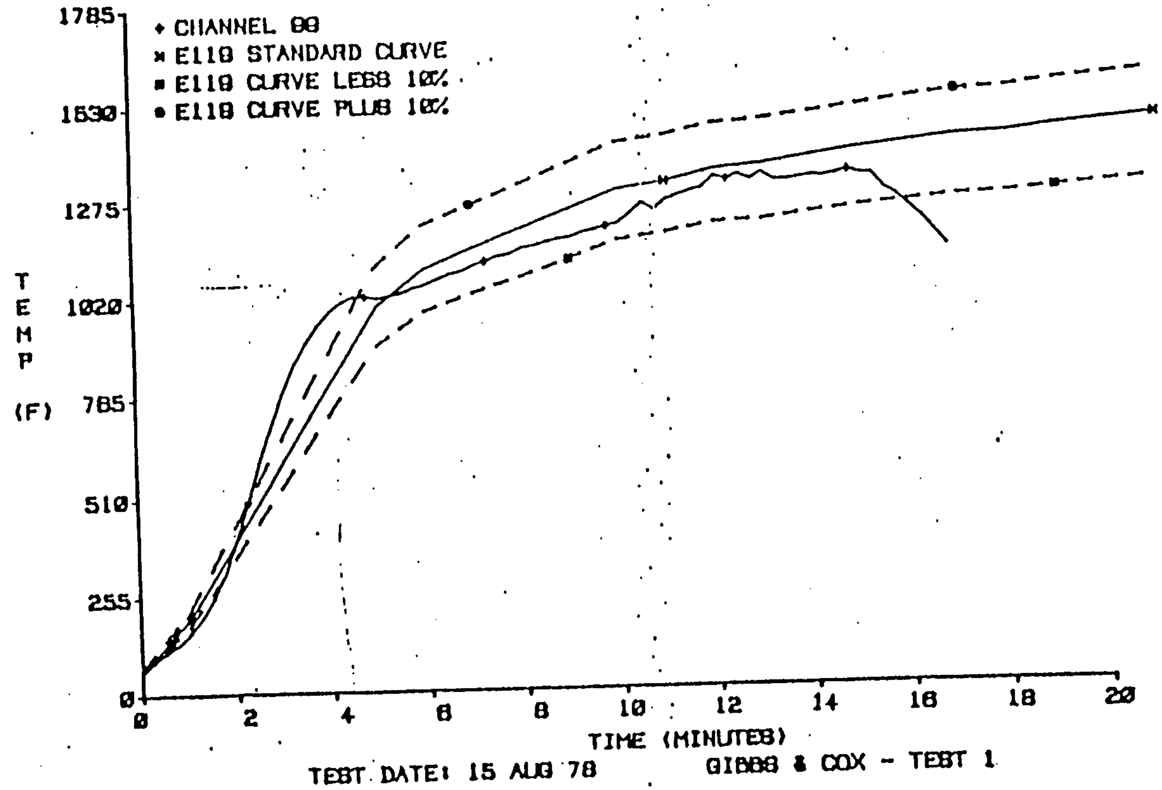

FIGURE 9. FURNACE TEMPERATURE - TEST 1

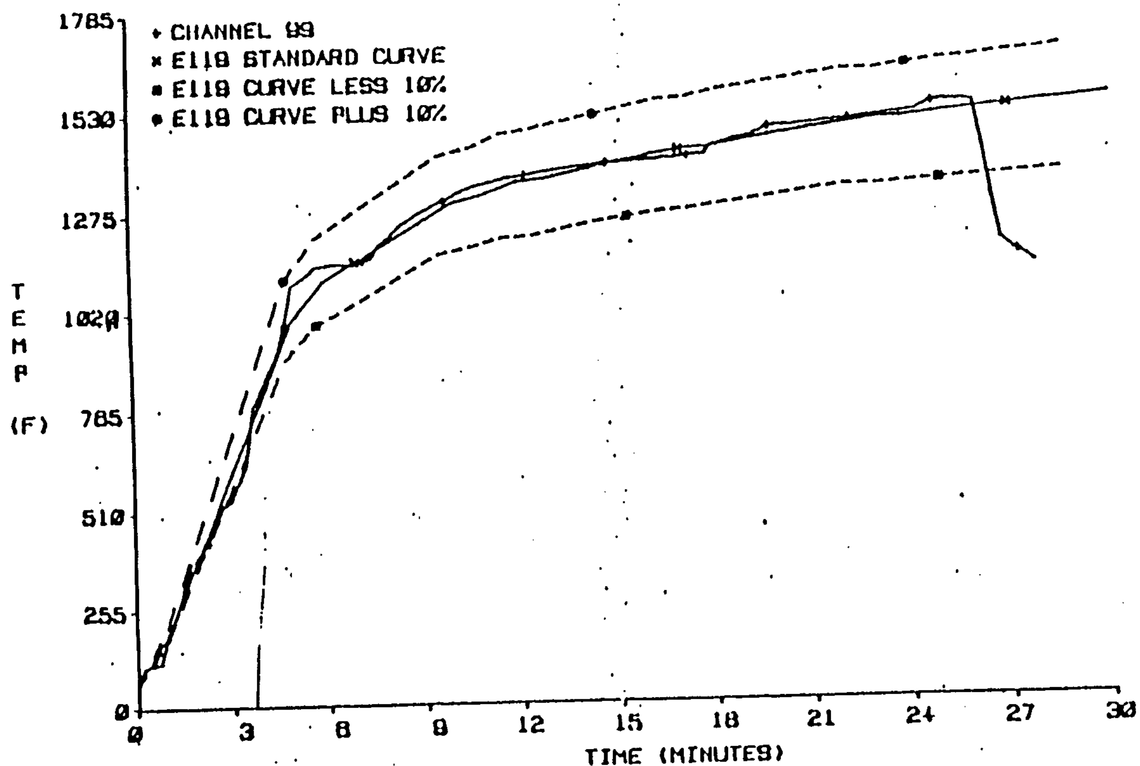

TEST DATE: 15 AUG 78 GIBBS & COX - TEST 2

FIGURE 10. FURNACE TEMPERATURE - TEST 2

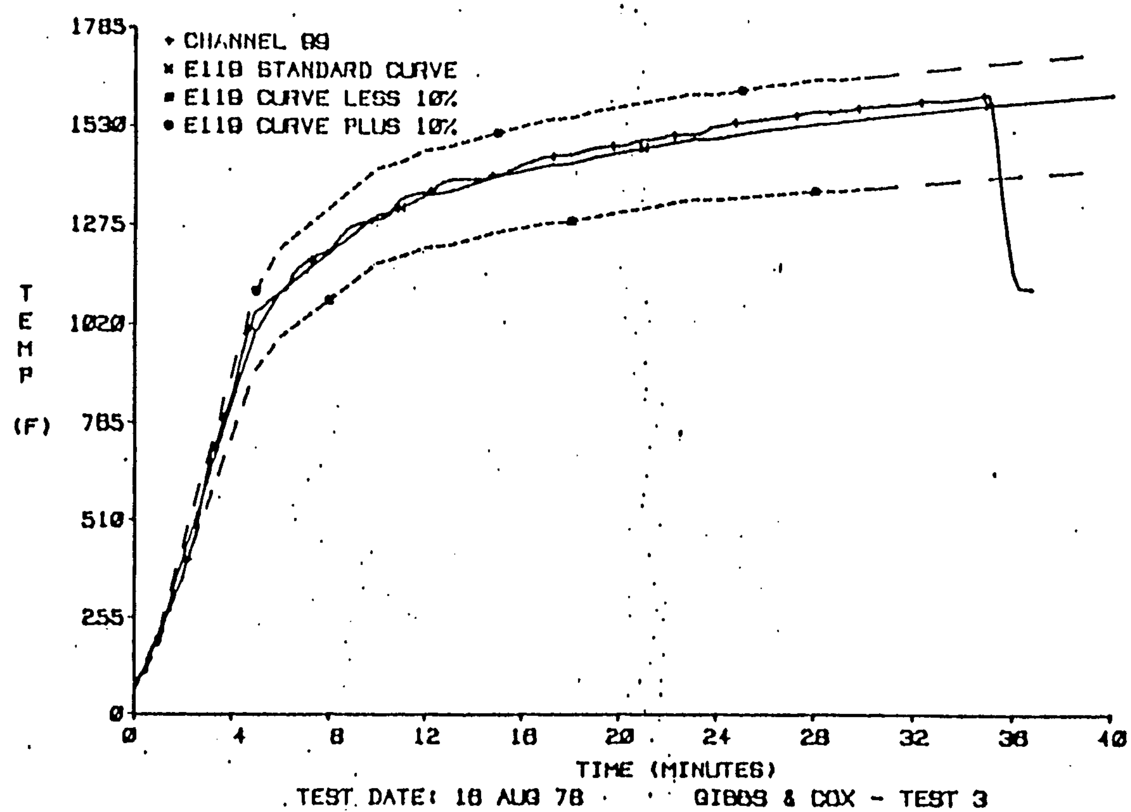

FIGURE 11. FURNACE TEMPERATURE - TEST 3

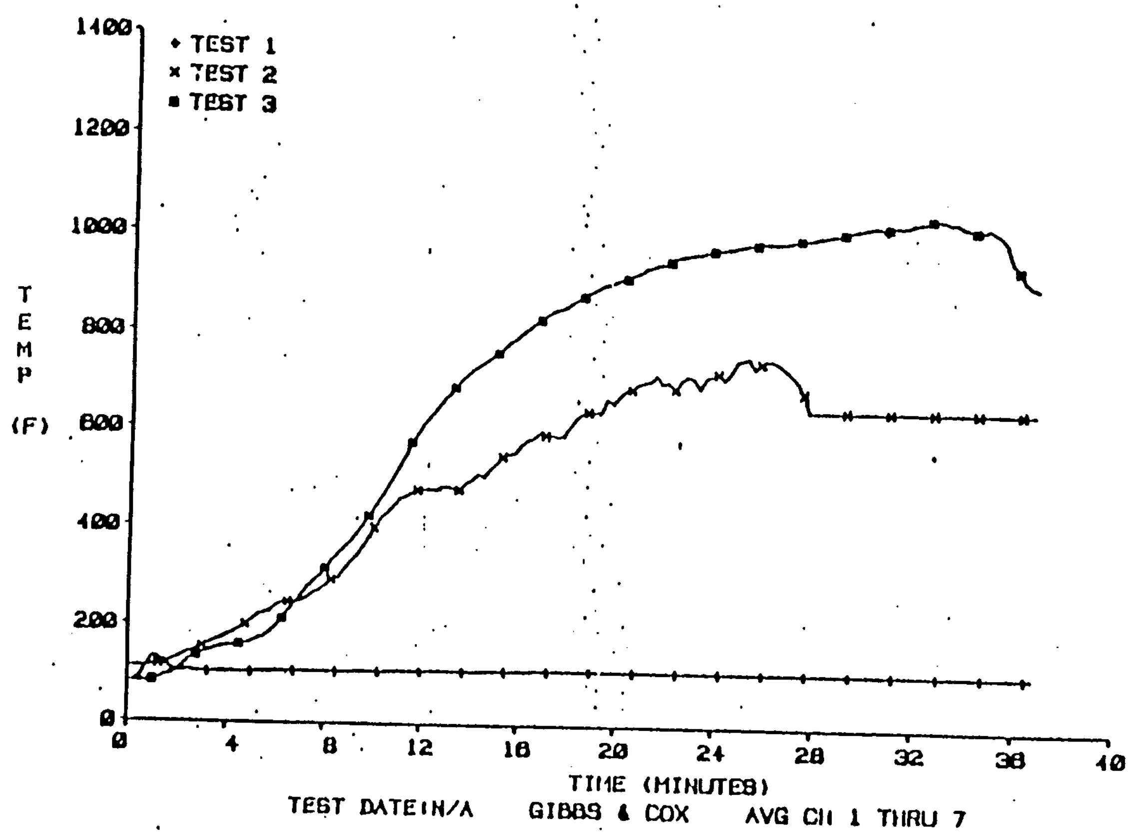

FIGURE 12. TEMPERATURES OF UNEXPOSED SIDE

Test No. 1 - GRP/NOMEX Core - Hexcel Corporation

TIME (Min:Sec)	OBSERVATION
0:00	Ignition of burners
0:29	Smoke begins to emerge through the H post to the unexposed side
1:04	The amount of smoke is increasing
1:17	Thermocouples begin to fall off the unexposed side
1:27	Discoloration of the right panel
1:45	Intermittant flaming on the right side
1:53	The panels begin to bubble (delaminate)
2:14	Flames emerge from around the H post
2:28	Intermittant flaming around the H post
2:48	The panels have warped
3:11	Flames continue on the unexposed side
3:27	Flames on the unexposed side have stopped. There is some burning on the exposed side of the bottom of the panels
5:03	The aluminum H post begins to melt (lower portion)
7:00	The lower 4 ft of the aluminum H post has melted and an opening between the panels is created
8:00	The panels continue to discolor and delaminate
16:00	End of Test

Test No. 2 - GRP/NOMEX Core - Ciba-Geigy Company

TIME (Min:Sec)	OBSERVATION
0:00	Ignition of burners
0:22	Popping sounds from the exposed side
1:38	The panels begin to warp
1:51	Slight smoke is emerging from around the H post
3:15	Smoke continues to emerge from around the H post
4:33	The left panel begins to discolor in the area of the H post
5:23	The panels begin to delaminate
6:36	The left side of the left panel begins to discolor
7:56	Discoloration of the right panel in the area of the H post
8:39	The panels have pulled away from the H post (rivets have melted)
10:36	Intermittant flaming in the area of the H post
12:31	Delamination and discoloration of the panels continues
13:05	The panels continue to warp
17:15	Smoke production has stopped
26:10	End of Test

Test No. 2 - GRP/NOMEX Core - Ciba-Geigy Company

TIME (Min:Sec)	OBSERVATION
0:00	Ignition of burners
0:22	Popping sounds from the exposed side
1:38	The panels begin to warp
1:51	Slight smoke is emerging from around the H post
3:15	Smoke continues to emerge from around the H post
4:55	The left panel begins to discolor in the area of the H post
5:25	The panels begin to delaminate
6:36	The left side of the left panel begins to discolor
7:56	Discoloration of the right panel in the area of the H post
8:29	The panels have pulled away from the H post (rivets have melted)
10:36	Intermittant flaming in the area of the H post
12:31	Delamination and discoloration of the panels continues
13:05	The panels continue to warp
17:15	Smoke production has stopped
26:10	End of Test

Test No. 3 - GRP/NOMEX Core - Phenolic Foam-filled - Ciba-Geigy Company

TIME (Min:Sec)	OBSERVATION
0:00	Ignition of burners
0:22	Delamination of the exposed side begins
1:07	Smoke begins to emerge from around the edges of the panels
1:23	Smoke begins to emerge from around the H post
2:49	The amount of smoke produced has increased
3:06	The amount of smoke produced has decreased now
3:15	The left panel begins to discolor in the area of the H post
4:30	The panels are warping
5:52	The panels begin to delaminate on the exposed side in the area of the H post
8:35	Delamination and discoloration of the panels continues
10:05	The top boundary channel has partially broken loose from the panels
10:13	Slight separation of the left panel from the H post
10:46	The amount of smoke produced has decreased
17:32	The panels have changed color from yellow to black
23:05	Delamination of the panels continues
27:06	A slight flame is emerging from the middle of the H post
30:43	The panels have separated from the H post (middle 3 ft)
35:00	End of Test

Appendix E Fortran Programs Used to Solve Mechanics Equations

This Appendix contains all the Fortran programs written to solve the various equations needed to verify the structural finite element codes. They are very specific.

```
      program k factor

dddddddddddddddddddddddddddddddddddddddddddddddddddddddddddd
d                                                          d
d     this program computes the 'K' constant for the       d
d     stiffeness of an arbitrary dimensioned rectangular   d
d     plate according to equation 3-57.                    d
d                                                          d
dddddddddddddddddddddddddddddddddddddddddddddddddddddddddddd

      implicit real*8 (a-h, o-z)

d     initialize variables

      top = 0.0
      bot=0.0
      ans = 0.0
      p = 0.0
      sq = 0.0
      anst = 0.0

d     specify constants

      v = 0.28
      e = 30.0e6
      pi = acos(-1.0)

d     input data

      write(*,*) 'enter plate thickness (t)'
      read(*,*) t
      write(*,*) 'enter plate length (x)'
      read(*,*) x
      write(*,*) 'enter plate height (y)'
      read(*,*) y
      write(*,*) 'enter x coordinate of post (xi)'
      read(*,*) xi
      write(*,*) 'enter y coordinate of post {eta)'
      read(*,*) eta
      write(*,*) 'enter E'
      read(*,*) e
      write(*,*) 'enter accuracy (i)'
      read(*,*) i

d     constant calculations

      d = (e*(t**3))/(12*(1-v**2))
      out = (4)/((pi**4)*d*x*y)

d     main summation loop
```

```
      do 20, m=1,i

      do 25, n=1,i

      sq = sin((m*pi*xi)/x)*sin((n*pi*eta)/y)
      top = sq**2

      bot = ((m**2)/(x**2) + (n**2)/(y**2))**(-2)

      anst = top*bot
      ans = ans + anst

      top = 0.0
      bot = 0.0
      anst = 0.0
      sq = 0.0

 25   continue
 20   continue

      ans = ans * out
      write(*,*) ans

      stop
      end
```

```
      program solve deflections

dddddddddddddddddddddddddddddddddddddddddddddddddddddddddddd
d                                                          d
d     This program calculates the deflection of a beam     d
d     subject to a concentrated load (equation 3-30)       d
d                                                          d
dddddddddddddddddddddddddddddddddddddddddddddddddddddddddddd

      implicit real*8 (a-h,o-z)
      dimension defl(200)

d      initialize variables

       e=0.0
       apl=0.0
       enr = 0.0
       p = 0.0
       tran = 0.0
       a = 0.0
       b = 0.0
       aa = 0.0
       bb = 0.0
       cc = 0.0
       x = 0.0
       const = 0.0
       poi = 0.0
       xinc = 0.0

       do 69, j = 1,200
       defl(j) = 0.0
 69    continue

d      start input section

       write(*,*) 'input E'
       read(*,*) e

       write(*,*) 'input aplied node'
       read(*,*) apl

       write(*,*) 'input I'
       read(*,*) enr

       write(*,*) 'input number of nodes'
       read(*,*) poi

       write(*,*) 'input l'
       read(*,*) tran

       write(*,*) 'input p'
```

```
      read(*,*) p

d     initial calculations

      const = p/(6*e*enr*tran)

      xinc = tran/(poi-1)

      a = (tran/(poi-1))*(apl-1)

      b = tran - a

d     start main program

      do 169, i = 1,poi

      aa = (tran**2 - b**2)*-1.0*b*x
      bb = b*x**3

      if(x.gt.a) then
         cc = tran*(x-a)**3
      else
         cc = 0.0
      end if

      defl(i) = const*(aa+bb-cc)

      x = x + xinc

      aa = 0.0
      bb=0.0
      cc=0.0

 169  continue

      do 269, i = 1,poi
      write(*,*) 'node = ',i,'deflection = ',defl(i)

 269  continue

      stop
      end
```

```
      program thermal eqn

dddddddddddddddddddddddddddddddddddddddddddddddddddddd
dd                                                    dd
dd    This program calculates the x and y             dd
dd    deflections of a rectangular beam in            dd
dd    free space with a thermal gradient ion the      dd
dd    z direction.  (equation 3-61a and 3-61b)        dd
dd                                                    dd
dddddddddddddddddddddddddddddddddddddddddddddddddddddd

      implicit real*8 (a-h,l-z)

      dimension defl(1200)
      dimension xdis(1200)

d     set initial conditions

      mt=0.0
      nt=0.0
      e=10.0e6
      v=0.3
      x=0.0
      alpha=2.326e-5
      b=2.0
      aa = 0.0
      bb = 0.0
      cc = 0.0
      nodes = 0.0
      z = 0.0
      xinc = 0.0
      const = 0.0

      do j=1,1200
         defl(j)=0.0
         xdis(j)=0.0
      end do

d     begin initial input

      write(*,*) ' input Mt'
      read(*,*) mt
      write(*,*) ' input Nt'
      read(*,*) nt
      write(*,*) ' input number of nodes'
      read(*,*) nodes
      write(*,*)' input z'
      read(*,*) z
      write(*,*) ' input length'
      read(*,*) length
      write(*,*) 'input I'
```

```
      read(*,*) enrt
      write(*,*) 'input area'
      read(*,*) area

d     begin initial calculations

      xinc = (length)/(nodes-1)

      corr1 = (z**2)*b*mt/(2*enrt)
      corr2 = b*nt*z/area

      corr1 = corr1 * v/e
      corr2 = corr2 * v/e
      const = b*mt/(2*e*enrt)

      x = -1*(length/2)

d     begin main loop

      do 69, i = 1,nodes

         defl(i) = -const*(x**2) - corr2 - corr1
         x = x + xinc

 69   continue

      do 169, i = 1,nodes

      write(*,*) 'node =',i,'deflection = ',defl(i)

 169  continue

      write(*,*)
      write(*,*)

      write(*,*) '========  x disp  ==================='

      grepa=0.0
      grepb=0.0

      grepa = (b*nt)/(e*area)
      grepb = (z*b*mt)/(e*enrt)

      x = (-1.0)*(length)/(2)

      do 269, k = 1,nodes

         xdis(k) = x*grepa + x*grepb
         x = x + xinc

 269  continue
```

```
k = 0.0

do k = 1,nodes

   write(*,*) 'node = ',k,'displacement = ',xdis(k)
end do

stop
end
```

```
      program force
      implicit real*8 (a-h,o-z)

dddddddddddddddddddddddddddddddddddddddddddddddddddddddd
d                                                      d
d     This program calculates the deflection of a plate d
d     at the line x/L = 0.5  (L=24 here) according to   d
d     equation  3-57                                    d
d                                                      d
dddddddddddddddddddddddddddddddddddddddddddddddddddddddd

      dimension disp(173)

      write(*,*) 'input x'
      read(*,*) x
      write(*,*) 'input y'
      read(*,*) y
      write(*,*) 'input x coord of force'
      read(*,*) ex
      write(*,*) 'input y coord of force'
      read(*,*) ey
      write(*,*) 'input force'
      read(*,*) p

d      calculate constant shit

       d = (30.0e6*0.0625**3)/(12*0.91)
       const = 4*p/((3.14159**4)*d*x*y)

d        first loop

       xx = 24.0
       yy = -6.0
       node = -3

       do k = 1,17,1

       yy = yy + 6.0
       node = node + 10

       do i = 1,100,1
       em = i

       do j = 1,100,1
       en = j

       bot = ((em**2/x**2) + (en**2/y**2))**-2
       top = (sin((em*3.14159*ex)/x))*(sin((en*3.14159*ey)/y))
       rgt = (sin((em*3.13159*xx)/x))*(sin((en*3.13159*yy)/y))

       summ = rgt*top*bot*const
```

```
disp(node) = disp(node) + summ


end do
end do

summ = 0.0
top = 0.0
rgt = 0.0
bot = 0.0

write(*,*) 'displacement of node',node,'is',disp(node)

end do

stop
end
```

Appendix F Input files for ANSYS and NASTRAN

Appendix F lists all the major input files used for ANSYS and NASTRAN. Also included are the unix programs written for the buckling analyses. The files appear in the order they were encountered in Chapter 3.

```
$$$$$$$$$$$$$$$$$$$$$$$$$$$$$$$$$$$$$$$$$$$$$$$$$$$$$$$$$$$$
$$                                                        $$
$$        Restrained Post input File for ANSYS            $$
$$                    Position F                          $$
$$                                                        $$
$$$$$$$$$$$$$$$$$$$$$$$$$$$$$$$$$$$$$$$$$$$$$$$$$$$$$$$$$$$$
$$
$$
/prep7
/title,RESTRAINED POST: POSITION F
et,1,23,,,,,,3 $et,2,39
knl,1 $toff,450.67
nltab,1,1
nl,1,1,0.0,5.6415,-0.80082,62400,0,0.0
nl,1,7,0.1962,4.207,0,31091.7,0,1.0
nl,1,13,-2,0.00075,0.002,0.007,0.01,0.04
nl,1,19,70.0,7500,20000,60000,61333,74667
nl,1,25,200,7143,19048,56667,66667,200000
nl,1,31,300,7143,19048,47058,55888,144117
nl,1,37,400,6818,18181,46346,52115,109807
nl,1,43,700,5298,5488,5744,6250,18750
mp,dens,1,0.00025443 $acel,384
mpte,1,29,119,260,440,620,800
mpda,alpx,1,1,2.326e-5,2.105e-5,1.5e-5,3.6e-5,3.2e-5,2.9e-5
mpte,7,980 $mpda,alpx,1,7,3.2e-5
mpte,1,70,200,300,400,500
mpda,ex,1,1,10e6,9.524e6,9.524e6,9.091e6,8.333e6
mpte,6,600,700,800,900,1000
mpda,ex,1,6,8.243e6,7.931e6,7.63e6,7.343e6,7.065e6
mpte,11,1100
mpda,ex,1,11,6.798e6 $mpte
r,1,0.8125,0.9712,0.5461,0.0003,12e6
r,2,0.02641,100,0.1321,500,0.2641,1000
rmor,0.5282,2000,1.0564,4000,2.1128,8000
rmor,2..641,10000
n,1 $n,45,6 $fill
n,100,0.0 $n,200,96.0
e,1,2 $egen,44,1,1
type,2 $real,2
e,100,1 $e,200,45 $krf,2
d,1,uy $d,1,rotz
/com,d,23,ux $d,23,rotz
d,45,uy $d,45,rotz
d,100,ux,0,,,,uy,rotz
d,200,ux,0,,,,uy,rotz
cnvr,0.25,0.25,0.25 $iter,-400,400
ktem,-1,0,0 $tref,70 $tuni,70 $time,0.0 $lwri
te,all,80.6,77.0 $time,0.01 $lwri
te,all,109.4,104.0 $time,0.02 $lwri
te,all,150.8,141.8 $time,0.03 $lwri
te,all,199.4,188.6 $time,0.04 $lwri
te,all,253.4,242.6 $time,0.05 $lwri
```

```
te,all,311,300.2 $time,0.06 $lwri
te,all,368.6,357.8 $time,0.07 $lwri
te,all,435.2,419.0 $time,0.08 $lwri
te,all,498.2,480.2 $time,0.09 $lwri
te,all,564.8,545.0 $time,0.10 $lwri
te,all,622.4,606.2 $time,0.11 $lwri
te,all,681.8,663.8 $time,0.12 $lwri
te,all,735.8,717.8 $time,0.13 $lwri
te,all,791.6,775.4 $time,0.14 $lwri
te,all,847.4,824.0 $time,0.15 $lwri
te,all,894.2,877.6 $time,0.16 $lwri
te,all,935.6,919.4 $time,0.17 $lwri
te,all,980.6,964.4 $time,0.18 $lwri
te,all,1022,1004   $time,0.19 $lwri
te,all,1058.,1041.8 $time,0.20 $lwri
te,all,1090.4,1076. $time,0.21 $lwri
te,all,1119.2,1108.4 $time,0.23 $lwri
te,all,1148,1133.6 $time,0.24 $lwri
te,all,1171.4,1162.4 $time,0.25 $lwri
te,all,1198.4,1184.0 $time,0.26 $lwri
afwr $fini
$/inp,27 $fini
```

```
$$$$$$$$$$$$$$$$$$$$$$$$$$$$$$$$$$$$$$$$$$$$$$$$$$$$$$$$$$$
$$                                                        $$
$$        Input file for ANSYS Solving the                $$
$$               Unrestrained Post                        $$
$$                                                        $$
$$$$$$$$$$$$$$$$$$$$$$$$$$$$$$$$$$$$$$$$$$$$$$$$$$$$$$$$$$$
$$
$$
/prep7
/title,UNRESTRAINED POST
et,1,23,,,,,,3 $et,2,39
knl,1 $toff,450.67
nltab,1,1
nl,1,1,0.0,5.6415,-0.80082,62400,0,0.0
nl,1,7,0.1962,4.207,0,31091.7,0,1.0
nl,1,13,-2,0.00075,0.002,0.007,0.01,0.04
nl,1,19,70.0,7500,20000,60000,61333,74667
nl,1,25,200,7143,19048,56667,66667,200000
nl,1,31,300,7143,19048,47058,55888,144117
nl,1,37,400,6818,18181,46346,52115,109807
nl,1,43,700,5298,5488,5744,6250,18750
mp,dens,1,0.00025443 $acel,384
mpte,1,29,119,260,440,620,800
mpda,alpx,1,1,2.326e-5,2.105e-5,1.5e-5,3.6e-5,3.2e-5,2.9e-5
mpte,7,980 $mpda,alpx,1,7,3.2e-5
mpte,1,70,200,300,400,500
mpda,ex,1,1,10e6,9.524e6,9.524e6,9.091e6,8.333e6
mpte,6,600,700,800,900,1000
mpda,ex,1,6,8.243e6,7.064e6,7.63e6,7.343e6,7.065e6
mpte,11,1100
mpda,ex,1,11,6.798e6 $mpte
r,1,0.8125,0.9712,0.5461,0.0003,12e6
r,2,0.01827,100,0.0914,500,0.1827,1000
rmor,0.3654,2000,0.7308,4000,1.4616,8000
rmor,1.827,10000
n,1 $n,45,96 $fill
n,100,0.0 $n,200,96.0
e,1,2 $egen,44,1,1
type,2 $real,2
e,100,1 $e,200,45 $krf,2
d,1,uy,,,,,rotz
d,45,uy,,,,,rotz
d,100,ux,0,,,,uy,rotz
d,200,ux,0,,,,uy,rotz
cnvr,0.25,0.25,0.25 $iter,-400,400
ktem,-1,0,0 $tref,70 $tuni,70 $time,0.0 $lwri
te,all,80.6,77.0 $time,0.01 $lwri
te,all,109.4,104.0 $time,0.02 $lwri
te,all,150.8,141.8 $time,0.03 $lwri
te,all,199.4,188.6 $time,0.04 $lwri
te,all,253.4,242.6 $time,0.05 $lwri
te,all,311,300.2 $time,0.06 $lwri
```

```
te,all,368.6,357.8 $time,0.07 $lwri
te,all,435.2,419.0 $time,0.08 $lwri
te,all,498.2,480.2 $time,0.09 $lwri
te,all,564.8,545.0 $time,0.10 $lwri
te,all,622.4,606.2 $time,0.11 $lwri
te,all,681.8,663.8 $time,0.12 $lwri
te,all,735.8,717.8 $time,0.13 $lwri
te,all,791.6,775.4 $time,0.14 $lwri
te,all,847.4,824.0 $time,0.15 $lwri
te,all,894.2,877.6 $time,0.16 $lwri
te,all,935.6,919.4 $time,0.17 $lwri
te,all,980.6,964.4 $time,0.18 $lwri
te,all,1022,1004   $time,0.19 $lwri
te,all,1058.,1041.8 $time,0.20 $lwri
te,all,1090.4,1076. $time,0.21 $lwri
te,all,1119.2,1108.4 $time,0.23 $lwri
te,all,1148,1133.6 $time,0.24 $lwri
te,all,1171.4,1162.4 $time,0.25 $lwri
te,all,1198.4,1184.0 $time,0.26 $lwri
afwr $fini
$/inp,27 $fini
```

```
$$$$$$$$$$$$$$$$$$$$$$$$$$$$$$$$$$$$$$$$$$$$$$$$$$$$$$$$$$$$
$$                                                        $$
$$      Unix program controlling the loads used in        $$
$$            the post buckling analysis                  $$
$$                                                        $$
$$$$$$$$$$$$$$$$$$$$$$$$$$$$$$$$$$$$$$$$$$$$$$$$$$$$$$$$$$$$
$$
$$
ansys.e < load1 > post1
ansys.e < buckle > postbk1
rm -f file* fort*
ansys.e < load2 > post2
ansys.e < buckle > postbk2
rm -f file* fort*
ansys.e < load3 > post3
ansys.e < buckle > postbk3
rm -f file* fort*
ansys.e < load4 > post4
ansys.e < buckle > postbk4
rm -f file* fort*
ansys.e < load5 > post5
ansys.e < buckle > postbk5
rm -f file* fort*
ansys.e < load6 > post6
ansys.e < buckle > postbk6
rm -f file* fort*
ansys.e < load7 > post7
ansys.e < buckle > postbk7
rm -f file* fort*
ansys.e < load8 > post8
ansys.e < buckle > postbk8
rm -f file* fort*
ansys.e < load9 > post9
ansys.e < buckle > postbk9
rm -f file* fort*
ansys.e < load10 > post10
ansys.e < buckle > postbk10
rm -f file* fort*
ansys.e < load11 > post11
ansys.e < buckle > postbk11
rm -f file* fort*
ansys.e < load12 > post12
ansys.e < buckle > postbk12
rm -f file* fort*
nsys.e < load13 > post13
ansys.e < buckle > postbk13
rm -f file* fort*
ansys.e < load14 > post14
ansys.e < buckle > postbk14
rm -f file* fort*
ansys.e < load15 > post15
ansys.e < buckle > postbk15
```

```
rm -f file* fort*
ansys.e < load16 > post16
ansys.e < buckle > postbk16
rm -f file* fort*
ansys.e < load17 > post18
ansys.e < buckle > postbk18
rm -f file* fort*
ansys.e < load18 > post19
ansys.e < buckle > postbk18
rm -f file* fort*
ansys.e < load19 > post20
ansys.e < buckle > postbk20
rm -f file* fort*
ansys.e < load20 > post21
ansys.e < buckle > postbk20
rm -f file* fort*
ansys.e < load21 > post22
ansys.e < buckle > postbk22
rm -f file* fort*
ansys.e < load22 > post23
ansys.e < buckle > postbk22
rm -f file* fort*
ansys.e < load23 > post23
ansys.e < buckle > postbk23
rm -f file* fort*
ansys.e < load24 > post24
ansys.e < buckle > postbk24
rm -f file* fort*
ansys.e < load25 > post25
ansys.e < buckle > postbk25
rm -f file* fort*
ansys.e < load26 > post26
ansys.e < buckle > postbk26
rm -f file* fort* *~
ls
$$$$$$$$$$$$$$$$$$$$$$$$$$$$$$$$$$$$$$$$$$$$$$$$$$$$$$$$$$$$
```

```
$$$$$$$$$$$$$$$$$$$$$$$$$$$$$$$$$$$$$$$$$$$$$$$$$$$$$$$$$$$$$$
$$                                                          $$
$$      Loads and times used for the post buckling          $$
$$      prediction in ANSYS.  Files are merged.             $$
$$                                                          $$
$$$$$$$$$$$$$$$$$$$$$$$$$$$$$$$$$$$$$$$$$$$$$$$$$$$$$$$$$$$$$$
$$
$$
$$  Load no. 1
/prep7
/inp,std20
tref,70 $tuni,70 $time,0.0
lwri $afwr $fini
/inp,27
fini $/eof
$$ Load no. 2
/prep7
/inp,std20
tref,78.8 $tuni,78.8 $time,0.01
lwri $afwr $fini
/inp,27
fini $/eof
$$ Load no. 3
/prep7
/inp,std20
tref,106.7 $tuni,106.7 $time,0.02
lwri $afwr $fini
/inp,27
fini $/eof
$$ Load no. 4
/prep7
/inp,std20
tref,146.3 $tuni,146.3 $time,0.03
lwri $afwr $fini
/inp,27
fini $/eof
$$ Load no. 5
/prep7
/inp,std20
tref,194.0 $tuni,194.0 $time,0.04
lwri $afwr $fini
/inp,27
fini $/eof
$$ Load no. 6
/prep7
/inp,std20
tref,248.0 $tuni,248.0 $time,0.05
lwri $afwr $fini
/inp,27
fini $/eof
$$ Load no. 7
```

```
/prep7
/inp,std20
tref,305.6 $tuni,305.6 $time,0.06
lwri $afwr $fini
/inp,27
fini $/eof
$$ Load no. 8
/prep7
/inp,std20
tref,368.2 $tuni,368.2 $time,0.07
lwri $afwr $fini
/inp,27
fini $/eof
$$ Load no. 9
/prep7
/inp,std20
tref,427.1 $tuni,427.1 $time,0.08
lwri $afwr $fini
/inp,27
fini $/eof
$$ Load no. 10
/prep7
/inp,std20
tref,489.2 $tuni,489.2 $time,0.09
lwri $afwr $fini
/inp,27
fini $/eof
$$ Load no. 11
/prep7
/inp,std20
tref,554.9 $tuni,554.9 $time,0.10
lwri $afwr $fini
/inp,27
fini $/eof
$$ Load no. 12
/prep7
/inp,std20
tref,614.3 $tuni,614.3 $time,0.11
lwri $afwr $fini
/inp,27
fini $/eof
$$ Load no. 13
/prep7
/inp,std20
tref,672.8 $tuni,672.8 $time,0.12
lwri $afwr $fini
/inp,27
fini $/eof
$$ Load no. 14
/prep7
/inp,std20
tref,726.8 $tuni,726.8 $time,0.13
```

```
lwri $afwr $fini
/inp,27
fini $/eof
$$ Load no. 15
/prep7
/inp,std20
tref,835.7 $tuni,835.7 $time,0.15
lwri $afwr $fini
/inp,27
fini $/eof
$$ Load no. 16
/prep7
/inp,std20
tref,835.7 $tuni,835.7 $time,0.15
lwri $afwr $fini
/inp,27
fini $/eof
$$ Load no. 17
/prep7
/inp,std20
tref,885.9 $tuni,885.9 $time,0.16
lwri $afwr $fini
/inp,27
fini $/eof
$$ Load no. 18
/prep7
/inp,std20
tref,927.5 $tuni,927.5 $time,0.17
lwri $afwr $fini
/inp,27
fini $/eof
$$ Load no. 19
/prep7
/inp,std20
tref,973.0 $tuni,973.0 $time,0.18
lwri $afwr $fini
/inp,27
fini $/eof
$$ Load no. 20
/prep7
/inp,std20
tref,1013.0 $tuni,1013.0 $time,0.19
lwri $afwr $fini
/inp,27
fini $/eof
$$ Load no. 21
/prep7
/inp,std20
tref,1049.9 $tuni,1049.0 $time,0.20
lwri $afwr $fini
/inp,27
fini $/eof
```

```
$$ Load no. 22
/prep7
/inp,std20
tref,1083.2 $tuni,1083.2 $time,0.21
lwri $afwr $fini
/inp,27
fini $/eof
$$ Load no. 23
/prep7
/inp,std20
tref,1113.8 $tuni,113.8 $time,0.22
lwri $afwr $fini
/inp,27
fini $/eof
$$ Load no. 24
/prep7
/inp,std20
tref,1140.8 $tuni,1140.8 $time,0.23
lwri $afwr $fini
/inp,27
fini $/eof
$$ Load no. 25
/prep7
/inp,std20
tref,1166.9 $tuni,1166.9 $time,0.24
lwri $afwr $fini
/inp,27
fini $/eof
$$ Load no. 26
/prep7
/inp,std20
tref,1191.2 $tuni,1192.1 $time,0.25
lwri $afwr $fini
/inp,27
fini $/eof
$$$$$$$$$$$$$$$$$$$$$$$$$$$$$$$$$$$$$$$$$$$$$$$$$$$$$$$$
```

```
$$$$$$$$$$$$$$$$$$$$$$$$$$$$$$$$$$$$$$$$$$$$$$$$$$$$
$$      Geometry file used with ANSYS buckling   $$
$$       prediction used on post                 $$
$$                                               $$
$$$$$$$$$$$$$$$$$$$$$$$$$$$$$$$$$$$$$$$$$$$$$$$$$$$$
$$
$$
/title,test
et,1,23,,,,,,3
knl,1
toff,459.67
nltab,1,1
nl,1,1,0,0,0,0,0,0
nl,1,7,.1962,4.207,0,31091.7,0,1.0
nl,1,13,-2,0.00075,0.002,0.007,0.01,0.04
nl,1,19,70.0,7500,20000,60000,61333,74667
nl,1,25,200,7143,19048,56667,66667,200000
nl,1,31,300,7143,19048,47058,55888,144117
nl,1,37,400,6818,18181,46346,52115,109807
nl,1,43,700,5298,5488,5744,6250,18750
mp,dens,1,0.00024335
mpte,1,29.03,119.03,260.33,440.33,620.33,800.33
mpda,alpx,1,1,2.326e-5,2.105e-5,1.5e-5,3.6e-5,3.2e-5,2.9e-5
mpte,7,800
mpda,alpx,1,7,3.2e-5
mpte,1,70,200,300,400,500
mpda,ex,1,1,10e6,9.524e6,9.524e6,9.09067e6,8.333e6
mpte,6,600,700,800,900,1000
mpda,ex,1,6,8.243e6,7.931e6,7.63e6,7.343e6,7.065e6
mpte,11,1100
mpda,ex,1,11,6.798e6
r,1,0.8125,0.9712,0.5461,0.0003,12e6
n,1 $n,45,96 $fill
type,1 $mat,1 $real,1
e,1,2
egen,44,1,1
iter,1,1,1
krf,2
d,1,uy,,,,,rotz,ux
d,45,uy,,,,,rotz
f,45,fx,-1.0
cnvr,,,.25
iter,-120,40
ktem,-1,0,0
$$$$$$$$$$$$$$$$$$$$$$$$$$$$$$$$$$$$$$$$$$$$$$$$$$$$
```

```
$$$$$$$$$$$$$$$$$$$$$$$$$$$$$$$$$$$$$$$
$$    Buckling program used by       $$
$$    ANSYS for post                 $$
$$                                   $$
$$$$$$$$$$$$$$$$$$$$$$$$$$$$$$$$$$$$$$$
$$
$$
/buckle,15,1,,,,1
iter,1,1,1
end
fini
/eof
$$$$$$$$$$$$$$$$$$$$$$$$$$$$$$$$$$$$$$$
```

```
$$$$$$$$$$$$$$$$$$$$$$$$$$$$$$$$$$$$$$$$$$$$$$$$$$$$$$$$$$$$$$$$
$$                                                            $$
$$       NASTRAN input file for prebuckled plate              $$
$$                                                            $$
$$$$$$$$$$$$$$$$$$$$$$$$$$$$$$$$$$$$$$$$$$$$$$$$$$$$$$$$$$$$$$$$
$$
$$
$DBDIR
ID    MSC, D2460
$ID MSC, D2460 $ BASIC STATICS, MG 14 JUN 79
TIME 200
SOL 24
CEND
$
$          CASE
$
TITLE=DEMENSTRATION OF A FOUR ELEMENT PLATE
SUBTITLE=STATIC ANALYSIS WITH TWO LOADING CONDITIONS
        ECHO = NONE
        SPC =  51
        DISPLACEMENT = ALL
        ELFORCE = ALL
        STRESSES=ALL
SUBCASE 1
        LABEL = MODEL, LOAD ONE
        TEMP(LOAD) = 800
        NLPARM = 909
        SUBCASE 2
        LABEL = LOAD TWO
        TEMP(LOAD) = 802
        NLPARM = 910
SUBCASE 3
        LABEL = LOAD THREE, TIME AT 0.015
        TEMP(LOAD) = 804
        NLPARM = 911
SUBCASE 4
        LABEL = LOAD FOUR, TIME AT 0.02
        TEMP(LOAD) = 806
        NLPARM = 912
SUBCASE 5
        LABEL = LOAD FIVE, TIME AT 0.025
        TEMP(LOAD) = 808
        NLPARM = 913
SUBCASE 6
        LABEL = LOAD SIX, TIME AT 0.03
        TEMP(LOAD) = 810
        NLPARM = 914
SUBCASE 7
        LABEL = LOAD SEVEN, TIME AT 0.035
        TEMP(LOAD) = 812
        NLPARM = 915
```

```
SUBCASE 8
        LABEL = LOAD EIGHT, TIME AT 0.04
        NLPARM = 916
        TEMP(LOAD) = 814
SUBCASE 9
        LABEL = LOAD NINE, TIME AT 0.045
        TEMP(LOAD) = 816
        NLPARM = 917
SUBCASE 10
        LABEL = LOAD TEN, TIME AT 0.05
        TEMP(LOAD) = 818
        NLPARM = 918
SUBCASE 11
        LABEL = LOAD ELEVEN, TIME AT 0.055
        TEMP(LOAD) = 820
        NLPARM = 919
SUBCASE 12
        LABEL = LOAD TWELVE, TIME AT 0.06
        TEMP(LOAD) = 822
        NLPARM = 920
SUBCASE 13
        LABEL = LOAD THIRTEEN, TIME AT 0.065
        TEMP(LOAD) = 824
        NLPARM = 921
SUBCASE 14
        LABEL = LOAD FOURTEEN, TIME AT 0.07
        TEMP(LOAD) = 826
        NLPARM = 922
SUBCASE 15
        LABEL = LOAD FIFTEEN, TIME AT 0.075
        TEMP(LOAD) = 828
        NLPARM = 923
SUBCASE 16
        LABEL = LOAD SIXTEEN, TIME AT 0.08
        TEMP(LOAD) = 830
        NLPARM = 924
SUBCASE 17
        LABEL = LOAD SEVENTEEN, TIME AT 0.085
        TEMP(LOAD) = 832
        NLPARM = 925
SUBCASE 18
        LABEL = LOAD EIGHTEEN, TIME AT 0.09
        TEMP(LOAD) = 834
        NLPARM = 926
SUBCASE 19
        LABEL = LOAD NINETEEN, TIME AT 0.095
        TEMP(LOAD) = 836
        NLPARM = 927
SUBCASE 20
        LABEL = LOAD TWENTY, TIME AT 0.1
        TEMP(LOAD) = 838
        NLPARM = 928
```

```
SUBCASE 21
        LABEL = LOAD TWENTY-ONE, TIME AT 0.105
        TEMP(LOAD) = 840
        NLPARM = 929
SUBCASE 22
        LABEL = LOAD TWENTY TWO, TIME AT 0.11
        TEMP(LOAD) = 842
        NLPARM = 930
SUBCASE 23
        LABEL = LOAD TWENTY THREE, TIME AT 0.115
        TEMP(LOAD) = 844
        NLPARM = 931
SUBCASE 24
        LABEL = LOAD TWENTY FOUR, TIME AT 0.12
        TEMP(LOAD) = 846
        NLPARM = 932
BEGIN BULK
$
$    ACTUAL MODEL -- GRID POINTS
$
GRID    1       0       0.0     0.0     0.1
GRID    2       0       4.0     0.0     0.1
GRID    3       0       8.0     0.0     0.1
GRID    4       0       12.0    0.0     0.1
GRID    5       0       16.0    0.0     0.1
GRID    6       0       20.0    0.0     0.1
GRID    7       0       24.0    0.0     0.1
GRID    8       0       28.0    0.0     0.1
GRID    9       0       32.0    0.0     0.1
GRID    10      0       36.0    0.0     0.1
GRID    11      0       40.0    0.0     0.1
GRID    12      0       44.0    0.0     0.1
GRID    13      0       48.0    0.0     0.1
GRID    14      0       0.0     6.0     0.1
GRID    15      0       8.0     6.0     0.1
GRID    16      0       16.0    6.0     0.1
GRID    17      0       24.0    6.0     0.1
GRID    18      0       32.0    6.0     0.1
GRID    19      0       40.0    6.0     0.1
GRID    20      0       48.0    6.0     0.1
GRID    21      0       0.0     12.0    0.1
GRID    22      0       4.0     12.0    0.1
GRID    23      0       8.0     12.0    0.1
GRID    24      0       12.0    12.0    0.1
GRID    25      0       16.0    12.0    0.1
GRID    26      0       20.0    12.0    0.1
GRID    27      0       24.0    12.0    0.1
GRID    28      0       28.0    12.0    0.1
GRID    29      0       32.0    12.0    0.1
GRID    30      0       36.0    12.0    0.1
GRID    31      0       40.0    12.0    0.1
GRID    32      0       44.0    12.0    0.1
```

GRID	33	0	48.0	12.0	0.1
GRID	34	0	0.0	18.0	0.1
GRID	35	0	8.0	18.0	0.1
GRID	36	0	16.0	18.0	0.1
GRID	37	0	24.0	18.0	0.1
GRID	38	0	32.0	18.0	0.1
GRID	39	0	40.0	18.0	0.1
GRID	40	0	48.0	18.0	0.1
GRID	41	0	0.0	24.0	0.1
GRID	42	0	4.0	24.0	0.1
GRID	43	0	8.0	24.0	0.1
GRID	44	0	12.0	24.0	0.1
GRID	45	0	16.0	24.0	0.1
GRID	46	0	20.0	24.0	0.1
GRID	47	0	24.0	24.0	0.1
GRID	48	0	28.0	24.0	0.1
GRID	49	0	32.0	24.0	0.1
GRID	50	0	36.0	24.0	0.1
GRID	51	0	40.0	24.0	0.1
GRID	52	0	44.0	24.0	0.1
GRID	53	0	48.0	24.0	0.1
GRID	54	0	0.0	30.0	0.1
GRID	55	0	8.0	30.0	0.1
GRID	56	0	16.0	30.0	0.1
GRID	57	0	24.0	30.0	0.1
GRID	58	0	32.0	30.0	0.1
GRID	59	0	40.0	30.0	0.1
GRID	60	0	48.0	30.0	0.1
GRID	61	0	0.0	36.0	0.1
GRID	62	0	4.0	36.0	0.1
GRID	63	0	8.0	36.0	0.1
GRID	64	0	12.0	36.0	0.1
GRID	65	0	16.0	36.0	0.1
GRID	66	0	20.0	36.0	0.1
GRID	67	0	24.0	36.0	0.1
GRID	68	0	28.0	36.0	0.1
GRID	69	0	32.0	36.0	0.1
GRID	70	0	36.0	36.0	0.1
GRID	71	0	40.0	36.0	0.1
GRID	72	0	44.0	36.0	0.1
GRID	73	0	48.0	36.0	0.1
GRID	74	0	0.0	42.0	0.1
GRID	75	0	8.0	42.0	0.1
GRID	76	0	16.0	42.0	0.1
GRID	77	0	24.0	42.0	0.1
GRID	78	0	32.0	42.0	0.1
GRID	79	0	40.0	42.0	0.1
GRID	80	0	48.0	42.0	0.1
GRID	81	0	0.0	48.0	0.1
GRID	82	0	4.0	48.0	0.1
GRID	83	0	8.0	48.0	0.1
GRID	84	0	12.0	48.0	0.1

GRID	85	0	16.0	48.0	0.1
GRID	86	0	20.0	48.0	0.1
GRID	87	0	24.0	48.0	0.1
GRID	88	0	28.0	48.0	0.1
GRID	89	0	32.0	48.0	0.1
GRID	90	0	36.0	48.0	0.1
GRID	91	0	40.0	48.0	0.1
GRID	92	0	44.0	48.0	0.1
GRID	93	0	48.0	48.0	0.1
GRID	94	0	0.0	54.0	0.1
GRID	95	0	8.0	54.0	0.1
GRID	96	0	16.0	54.0	0.1
GRID	97	0	24.0	54.0	0.1
GRID	98	0	32.0	54.0	0.1
GRID	99	0	40.0	54.0	0.1
GRID	100	0	48.0	54.0	0.1
GRID	101	0	0.0	60.0	0.1
GRID	102	0	4.0	60.0	0.1
GRID	103	0	8.0	60.0	0.1
GRID	104	0	12.0	60.0	0.1
GRID	105	0	16.0	60.0	0.1
GRID	106	0	20.0	60.0	0.1
GRID	107	0	24.0	60.0	0.1
GRID	108	0	28.0	60.0	0.1
GRID	109	0	32.0	60.0	0.1
GRID	110	0	36.0	60.0	0.1
GRID	111	0	40.0	60.0	0.1
GRID	112	0	44.0	60.0	0.1
GRID	113	0	48.0	60.0	0.1
GRID	114	0	0.0	66.0	0.1
GRID	115	0	8.0	66.0	0.1
GRID	116	0	16.0	66.0	0.1
GRID	117	0	24.0	66.0	0.1
GRID	118	0	32.0	66.0	0.1
GRID	119	0	40.0	66.0	0.1
GRID	120	0	48.0	66.0	0.1
GRID	121	0	0.0	72.0	0.1
GRID	122	0	4.0	72.0	0.1
GRID	123	0	8.0	72.0	0.1
GRID	124	0	12.0	72.0	0.1
GRID	125	0	16.0	72.0	0.1
GRID	126	0	20.0	72.0	0.1
GRID	127	0	24.0	72.0	0.1
GRID	128	0	28.0	72.0	0.1
GRID	129	0	32.0	72.0	0.1
GRID	130	0	36.0	72.0	0.1
GRID	131	0	40.0	72.0	0.1
GRID	132	0	44.0	72.0	0.1
GRID	133	0	48.0	72.0	0.1
GRID	134	0	0.0	78.0	0.1
GRID	135	0	8.0	78.0	0.1
GRID	136	0	16.0	78.0	0.1

```
GRID     137     0      24.0    78.0    0.1
GRID     138     0      32.0    78.0    0.1
GRID     139     0      40.0    78.0    0.1
GRID     140     0      48.0    78.0    0.1
GRID     141     0      0.0     84.0    0.1
GRID     142     0      4.0     84.0    0.1
GRID     143     0      8.0     84.0    0.1
GRID     144     0      12.0    84.0    0.1
GRID     145     0      16.0    84.0    0.1
GRID     146     0      20.0    84.0    0.1
GRID     147     0      24.0    84.0    0.1
GRID     148     0      28.0    84.0    0.1
GRID     149     0      32.0    84.0    0.1
GRID     150     0      36.0    84.0    0.1
GRID     151     0      40.0    84.0    0.1
GRID     152     0      44.0    84.0    0.1
GRID     153     0      48.0    84.0    0.1
GRID     154     0      0.0     90.0    0.1
GRID     155     0      8.0     90.0    0.1
GRID     156     0      16.0    90.0    0.1
GRID     157     0      24.0    90.0    0.1
GRID     158     0      32.0    90.0    0.1
GRID     159     0      40.0    90.0    0.1
GRID     160     0      48.0    90.0    0.1
GRID     161     0      0.0     96.0    0.1
GRID     162     0      4.0     96.0    0.1
GRID     163     0      8.0     96.0    0.1
GRID     164     0      12.0    96.0    0.1
GRID     165     0      16.0    96.0    0.1
GRID     166     0      20.0    96.0    0.1
GRID     167     0      24.0    96.0    0.1
GRID     168     0      28.0    96.0    0.1
GRID     169     0      32.0    96.0    0.1
GRID     170     0      36.0    96.0    0.1
GRID     171     0      40.0    96.0    0.1
GRID     172     0      44.0    96.0    0.1
GRID     173     0      48.0    96.0    0.1
$
$  ACTUAL MODEL  -  -  ELEMENTS
$
CQUAD8 1    21   1    3    23   21   2    15   +CQUAD1
+CQUAD1 22  14
CQUAD8 2    21   3    5    25   23   4    16   +CQUAD2
+CQUAD2 24  15
CQUAD8 3    21   5    7    27   25   6    17   +CQUAD3
+CQUAD3 26  6
CQUAD8 4    21   7    9    29   27   8    18   +CQUAD4
+CQUAD4 28  17
CQUAD8 5    21   9    11   31   29   10   19   +CQUAD5
+CQUAD5 30  18
CQUAD8 6    21   11   13   33   31   12   20   +CQUAD6
+CQUAD6 32  19
CQUAD8 7    21   21   23   43   41   22   35   +CQUAD7
+CQUAD7 42  34
CQUAD8 8    21   23   25   45   43   24   36   +CQUAD8
```

+CQUAD8 44	35							
CQUAD8 9	21	25	27	47	45	26	37	+CQUAD9
+CQUAD9 46	36							
CQUAD8 10	21	27	29	49	47	28	38	+CQUD10
+CQUD10 48	37							
CQUAD8 11	21	29	31	51	49	30	39	+CQUD11
+CQUD11 50	38							
CQUAD8 12	21	31	33	53	51	32	40	+CQUD12
+CQUD12 52	39							
CQUAD8 13	21	41	43	63	61	42	55	+CQUD13
+CQUD13 62	54							
CQUAD8 14	21	43	45	65	63	44	56	+CQUD14
+CQUD14 64	55							
CQUAD8 15	21	45	47	67	65	46	57	+CQUD15
+CQUD15 66	56							
CQUAD8 16	21	47	49	69	67	48	58	+CQUD16
+CQUD16 68	57							
CQUAD8 17	21	49	51	71	69	50	59	+CQUD17
+CQUD17 70	58							
CQUAD8 18	21	51	53	73	71	52	60	+CQUD18
+CQUD18 72	59							
CQUAD8 19	21	61	63	83	81	62	75	+CQUD19
+CQUD19 82	74							
CQUAD8 20	21	63	65	85	83	64	76	+CQUD20
+CQUD20 84	75							
CQUAD8 21	21	65	67	87	85	66	77	+CQUD21
+CQUD21 86	76							
CQUAD8 22	21	67	69	89	87	68	78	+CQUD22
+CQUD22 88	77							
CQUAD8 23	21	69	71	91	89	70	79	+CQUD23
+CQUD23 90	78							
CQUAD8 24	21	71	73	93	91	72	80	+CQUD24
+CQUD24 92	79							
CQUAD8 25	21	81	83	103	101	82	95	+CQUD25
+CQUD25 102	94							
CQUAD8 26	21	83	85	105	103	84	96	+CQUD26
+CQUD26 104	95							
CQUAD8 27	21	85	87	107	105	86	97	+CQUD27
+CQUD27 106	96							
CQUAD8 28	21	87	89	109	107	88	98	+CQUD28
+CQUD28 108	97							
CQUAD8 29	21	89	91	111	109	90	99	+CQUD29
+CQUD29 110	98							
CQUAD8 30	21	91	93	113	111	92	100	+CQUD30
+CQUD30 112	99							
CQUAD8 31	21	101	103	123	121	102	115	+CQUD31
+CQUD31 122	114							
CQUAD8 32	21	103	105	125	123	104	116	+CQUD32
+CQUD32 124	115							
CQUAD8 33	21	105	107	127	125	106	117	+CQUD33
+CQUD33 126	116							
CQUAD8 34	21	107	109	129	127	108	118	+CQUD34
+CQUD34 128	117							
CQUAD8 35	21	109	111	131	129	110	119	+CQUD35
+CQUD35 130	118							
CQUAD8 36	21	111	113	133	131	112	120	+CQUD36
+CQUD36 132	119							
CQUAD8 37	21	121	123	143	141	122	135	+CQUD37
+CQUD37 142	134							
CQUAD8 38	21	123	125	145	143	124	136	+CQUD38
+CQUD38 144	135							
CQUAD8 39	21	125	127	147	145	126	137	+CQUD39
+CQUD39 146	136							
CQUAD8 40	21	127	129	149	147	128	138	+CQUD40
+CQUD40 148	137							
CQUAD8 41	21	129	131	151	149	130	139	+CQUD41
+CQUD41 150	138							

```
CQUAD8 42      21     131    133    153    151    132    140    +CQUD42
+CQUD42 152    139
CQUAD8 43      21     141    143    163    161    142    155    +CQUD43
+CQUD43 162    154
CQUAD8 44      21     143    145    165    163    144    156    +CQUD44
+CQUD44 164    155
CQUAD8 45      21     145    147    167    165    146    157    +CQUD45
+CQUD45 166    156
CQUAD8 46      21     147    149    169    167    148    158    +CQUD46
+CQUD46 168    157
CQUAD8 47      21     149    151    171    169    150    159    +CQUD47
+CQUD47 170    158
CQUAD8 48      21     151    153    173    171    152    160    +CQUD48
+CQUD48 172    159
$
$    MATERIAL PROPERTY DEFINITION
$
PARAM,TABS,459.69
MAT1   31    29.5E6       0.28   0.00025 6.5E-6 70.0
MATT1  31    66                  68
MATS1  31    79     NLELAST                       2.0e7
TABLEM1 66
    70.0   29.5E6  200.0   28.9e6  400.0   27.9e6  600.0   24.5e6
    800.0  23.8E6  1000.0  17.4E6  1200.0  11.2E6  ENDT
TABLEM1 68
    70.0   6.5e-6  200.0   6.5e-6  400.0   6.9e-6  800.0   7.6e-6
    1300.0 8.6e-6   ENDT
TABLEST 79
    70.0   600    200.0  602    400.0  604    600.0  606
    800.0  608    1000.0 610    1200.0 612    ENDT
TABLES1 600
    0.0    0.0    0.001  29500.0 0.002  44000.0 0.005  42000.0
    0.010  42400.0 0.015  47500.0 0.0183  51500.0 ENDT
TABLES1 602
    0.0    0.0    0.001  28900.0 0.002  40600.0 0.005  40000.0
    0.010  40500.0 0.015  44000.0 0.0183  46000.0 ENDT
TABLES1 604
    0.0    0.0    0.001  27900.0 0.002  39000.0 0.005  39300.0
    0.010  43500.0 0.015  50100.0 0.0183  52300.0 ENDT
TABLES1 606
    0.0    0.0    0.001  24500.0 0.002  29800.0 0.005  36300.0
    0.010  43000.0 0.015  49300.0 0.0183  52000.0 ENDT
TABLES1 608
    0.0    0.0    0.001  23800.0 0.002  25300.0 0.005  33400.0
    0.01   40000.0 0.015  43100.0 0.0183  45000.0 ENDT
TABLES1 610
    0.0    0.0    0.001  17400.0 0.002  24000.0 0.005  29600.0
    0.010  31200.0 0.015  33300.0 0.0183  34700.0 ENDT
TABLES1 612
    0.0    0.0    0.001  11200.0 0.002  14800.0 0.005  16700.0
    0.010  16900.0 0.015  17300.0 0.0183  17500.0 ENDT
CREEP  31    70.0   1.3e-32 CRLAW
    300    3.23e-26     2.7333      -0.667
NLPARM   909       10        0.0005
NLPARM   910       10        0.0005
NLPARM   911       10        0.0005
NLPARM   912       10        0.0005
NLPARM   913       10        0.0005
NLPARM   914       10        0.0005
NLPARM   915       10        0.0005
NLPARM   916       10        0.0005
NLPARM   917       10        0.0005
NLPARM   918       10        0.0005
```

```
NLPARM  919     10      0.0005
NLPARM  920     10      0.0005
NLPARM  921     10      0.0005
NLPARM  922     10      0.0005
NLPARM  923     10      0.0005
NLPARM  924     10      0.0005
NLPARM  925     10      0.0005
NLPARM  926     10      0.0005
NLPARM  927     10      0.0005
NLPARM  928     10      0.0005
NLPARM  929     10      0.0005
NLPARM  930     10      0.0005
NLPARM  931     10      0.0005
NLPARM  932     10  0.0005
$
$    ACTUAL MODEL - TEMPERATURE LOADS
$
TEMPP3 800   1   0.0375 90.41  0.1   90.356 0.1625 90.388 +1TEMP1
+1TEMP1                                     +1TEMP2
+1TEMP2                                     +1TEMP3
+1TEMP3 2    THRU  48
$
TEMPP3 802   1   0.0375 114.26 0.1   114.188 0.1625 114.17 +2TEMP1
+2TEMP1                                     +2TEMP2
+2TEMP2                                     +2TEMP3
+2TEMP3 2    THRU  48
$
TEMPP3 804   1   0.0375 146.26 0.1   146.282 0.1625 146.246 +3TEMP1
+3TEMP1                                     +3TEMP2
+3TEMP2                                     +3TEMP3
+3TEMP3 2    THRU  48
$
TEMPP3 806   1   0.0375 185.054 0.1  184.928 0.1625 184.874 +4TEMP1
+4TEMP1                                     +4TEMP2
+4TEMP2                                     +4TEMP3
+4TEMP3 2    THRU  48
$
TEMPP3 808   1   0.0375 229.118 0.1  228.956 0.1625 228.902 +5TEMP1
+5TEMP1                                     +5TEMP2
+5TEMP2                                     +5TEMP3
+5TEMP3 2    THRU  48
$
TEMPP3 810   1   0.0375 277.754 0.1  227.574 0.1625 277.502 +6TEMP1
+6TEMP1                                      +6TEMP2
+6TEMP2                                     +6TEMP3
+6TEMP3 2    THRU  48
$
TEMPP3 812   1   0.0375 327.902 0.1  327.722 0.1625 327.65 +7TEMP1
+7TEMP1                                     +7TEMP2
+7TEMP2                                     +7TEMP3
+7TEMP3 2    THRU  48
$
TEMPP3 814   1   0.0375 379.436 0.1  379.238 0.1625 379.148 +8TEMP1
+8TEMP1                                     +8TEMP2
+8TEMP2                                     +8TEMP3
+8TEMP3 2    THRU  48
$
TEMPP3 816   1   0.0375 431.474 0.1  431.348 0.1625 431.258 +9TEMP1
+9TEMP1                                     +9TEMP2
+9TEMP2                                     +9TEMP3
+9TEMP3 2    THRU  48
$
```

```
TEMPP3  818   1      0.0375  482.162 0.1      481.946 0.1625  481.838  +10TEM1
+10TEM1                                                 +10TEM2
+10TEM2                                                 +10TEM3
+10TEM3 2     THRU   48
$
TEMPP3  820   1      0.0375  530.582 0.1      530.348 0.1625  530.258  +11TEM1
+11TEM1                                                 +11TEM2
+11TEM2                                                 +11TEM3
+11TEM3 2     THRU   48
$
TEMPP3  822   1      0.0375  576.608 0.1      576.374 0.1625  576.266  +12TEM1
+12TEM1                                                 +12TEM2
+12TEM2                                                 +12TEM3
+12TEM3 2     THRU   48
$
TEMPP3  824   1      0.0375  621.122 0.1      620.888 0.1625  620.78   +13TEM1
+13TEM1                                                 +13TEM2
+13TEM2                                                 +13TEM3
+13TEM3 2     THRU   48
$
TEMPP3  826   1      0.0375  663.404 0.1      663.152 0.1625  663.044  +14TEM1
+14TEM1                                                 +14TEM2
+14TEM2                                                 +14TEM3
+14TEM3 2     THRU   48
$
TEMPP3  828   1      0.0375  703.418 0.1      703.184 0.1625  703.076  +15TEM1
+15TEM1                                                 +15TEM2
+15TEM2                                                 +15TEM3
+15TEM3 2     THRU   48
$
TEMPP3  830   1      0.0375  741.326 0.1      741.074 0.1625  740.966  +16TEM1
+16TEM1                                                 +16TEM2
+16TEM2                                                 +16TEM3
+16TEM3 2     THRU   48
$
TEMPP3  832   1      0.0375  777.074 0.1      776.84  0.1625  776.714  +17TEM1
+17TEM1                                                 +17TEM2
+17TEM2                                                 +17TEM3
+17TEM3 2     THRU   48
$
TEMPP3  834   1      0.0375  811.508 0.1      811.274 0.1625  811.148  +18TEM1
+18TEM1                                                 +18TEM2
+18TEM2                                                 +18TEM3
+18TEM3 2     THRU   48
$
TEMPP3  836   1      0.0375  844.682 0.1      844.43  0.1625  844.323  +19TEM1
+19TEM1                                                 +19TEM2
+19TEM2                                                 +19TEM3
+19TEM3 2     THRU   48
$
TEMPP3  838   1      0.0375  876.47  0.1      876.236 0.1625  876.11   +20TEM1
+20TEM1                                                 +20TEM2
+20TEM2                                                 +20TEM3
+20TEM3 2     THRU   48
$
TEMPP3  840   1      0.0375  906.746 0.1      906.494 0.1625  906.386  +21TEM1
+21TEM1                                                 +21TEM2
+21TEM2                                                 +21TEM3
+21TEM3 2     THRU   48
$
TEMPP3  842   1      0.0375  935.438 0.1      935.204 0.1625  935.078  +22TEM1
+22TEM1                                                 +22TEM2
+22TEM2                                                 +22TEM3
+22TEM3 2     THRU   48
$
TEMPP3  844   1      0.0375  963.464 0.1      963.23  0.1625  963.104  +23TEM1
+23TEM1                                                 +23TEM2
```

```
+23TEM2                                      +23TEM3
+23TEM3 2     THRU    48
$
TEMPP3  846    1      0.0375  989.708 0.1    989.474 0.1625  989.348 +24TEM1
+24TEM1                                      +24TEM2
+24TEM2                                      +24TEM3
+24TEM3 2     THRU    48
$&
$     AUTOMATIC CONSTRAINT OF SINGULAR  DOF = S
$
PARAM       AUTOSPC    YES
$
$       CONSTRAINTS
$
SPC         51      1        123
SPC         51      2        123
SPC         51      3        123
SPC         51      4        123
SPC         51      5        123
SPC         51      6        123
SPC         51      7        123
SPC         51      8        123
SPC         51      9        123
SPC         51      10       123
SPC         51      11       123
SPC         51      12       123
SPC         51      13       123
SPC         51      14       123
SPC         51      20       123
SPC         51      21       123
SPC         51      33       123
SPC         51      34       123
SPC         51      40       123
SPC         51      41       123
SPC         51      53       123
SPC         51      54       123
SPC         51      60       123
SPC         51      61       123
SPC         51      73       123
SPC         51      74       123
SPC         51      80       123
SPC         51      81       123
SPC         51      93       123
SPC         51      94       123
SPC         51      100      123
SPC         51      101      123
SPC         51      113      123
SPC         51      114      123
SPC         51      120      123
SPC         51      121      123
SPC         51      133      123
SPC         51      134      123
SPC         51      140      123
```

```
SPC      51      141     123
SPC      51      153     123
SPC      51      154     123
SPC      51      160     123
SPC      51      161     123
SPC      51      162     123
SPC      51      163     123
SPC      51      164     123
SPC      51      165     123
SPC      51      166     123
SPC      51      167     123
SPC      51      168     123
SPC      51      169     123
SPC      51      170     123
SPC      51      171     123
SPC      51      172     123
SPC      51      173     123
PSHELL   21      31      0.0625  31
$  LOAD - TYPE DATA
$FORCE    1       87      50.0    0.0     0.0     -1.0
ENDDATA
```

```
$$$$$$$$$$$$$$$$$$$$$$$$$$$$$$$$$$$$$$$$$$$$$$$$$$$$$$$$
$$                                                    $$
$$    Unix program controlling the loads for the      $$
$$          ANSYS buckling program on plate           $$
$$                                                    $$
$$$$$$$$$$$$$$$$$$$$$$$$$$$$$$$$$$$$$$$$$$$$$$$$$$$$$$$$
$$
$$
ansys.e < load1 > statout1
ansys.e < buckle > buckout1
rm  -f file* fort*
ansys.e < load2 > statout2
ansys.e < buckle > buckout2
rm -f file* fort*
ansys.e < load3 > statout3
ansys.e < buckle > buckout3
rm -f file* fort*
ansys.e < load4 > statout4
ansys.e < buckle > buckout4
rm -f file* fort*
ansys.e < load5 > statout5
ansys.e < buckle > buckout5
rm -f file* fort*
ansys.e < load6 > statout6
ansys.e < buckle > buckout6
rm -f file* fort*
ansys.e < load7 > statout7
ansys.e < buckle > buckout7
rm -f file* fort*
ansys.e < load8 > statout8
ansys.e < buckle > buckout8
rm -f file* fort*
ansys.e < load9 > statout9
ansys.e < buckle > buckout9
rm -f file* fort*
ansys.e < load10 > statout10
ansys.e < buckle > buckout10
rm -f file* fort*
ansys.e < load11 > statout11
ansys.e < buckle > buckout11
rm -f file* fort*
ansys.e < load12 > statout12
ansys.e < buckle >buckout12
rm -f file* fort*
$$$$$$$$$$$$$$$$$$$$$$$$$$$$$$$$$$$$$$$$$$$$$$$$$$$$$$$$$$$$
```

```
$$$$$$$$$$$$$$$$$$$$$$$$$$$$$$$$$$$$$$$$$$$$$$$$$$$$$$$$$$$$$$
$$                                                          $$
$$    Load Files for the ANSYS buckling prediction for      $$
$$    the plate.  They serve to increment the temperature   $$
$$    and time.  Note:  They are all merged                 $$
$$                                                          $$
$$$$$$$$$$$$$$$$$$$$$$$$$$$$$$$$$$$$$$$$$$$$$$$$$$$$$$$$$$$$$$
$$
$$ Load no. 1 $$
/prep7
/inp,geometry
tref,77.0 $tuni,80.0 $time,0.005
te,all,90.41,90.41,90.41,90.41,90.356,90.356
temo,90.356,90.356
lwri $afwr $fini
/inp,27 $fini
/eof
$$ Load no. 2 $$
/prep7
/inp,geometry
tref,77.0 $tuni,77.0 $time,0.01
te,all,114.26,114.26,114.26,114.26,114.17,114.17
temo,114.17,114.17
lwri $afwr $fini
/inp,27 $fini
/eof
$$ Load no. 3 $$
/prep7
/inp,geometry
tref,77.0 $tuni,77.0 $time,0.015
te,all,146.39,146.39,146.39,146.39,146.246,146.246
temo,146.246,146.246
lwri $afwr $fini
/inp,27 $fini
/eof
$$ Load no. 4 $$
/prep7
/inp,geometry
tref,77.0 $tuni,77.0 $time,0.02
te,all,185.054,185.054,185.054,185.054,184.874,184.874
temo,184.874,184.874
lwri $afwr $fini
/inp,27 $fini
/eof
$$ Load no. 5 $$
/prep7
/inp,geometry
tref,77.0 $tuni,77.0 $time,0.025
te,all,229.118,229.118,229.118,229.118,228.902,228.902
temo,228.902,228.902
lwri $afwr $fini
/inp,27 $fini
```

```
/eof
$$ Load no. 6 $$
/prep7
/inp,geometry
tref,77.0 $tuni,77.0 $time,0.03
te,all,277.54,277.54,277.54,277.54,277.502,277.502
temo,277.502,277.502
lwri $afwr $fini
/inp,27 $fini
/eof
$$ Load no. 7 $$
/prep7
/inp,geometry
tref,77.0 $tuni,77.0 $time,0.035
te,all,322.902,322.902,322.902,322.902,322.65,322.65
temo,322.65,322.65
lwri $afwr $fini
/inp,27 $fini
/eof
$$ Load no. 8 $$
/prep7
/inp,geometry
tref,77.0 $tuni,77.0 $time,0.04
te,all,379.436,379.436,379.436,379.436,379.148,379.148
temo,379.148,379.148
lwri $afwr $fini
/inp,27 $fini
/eof
$$ Load no. 9 $$
/prep7
/inp,geometry
tref,77.0 $tuni,77.0 $time,0.045
te,all,431.474,431.474,431.474,431.474,431.258,431.258
temo,431.258,431.258
lwri $afwr $fini
/inp,27 $fini
/eof
$$ Load no. 10 $$
/prep7
/inp,geometry
tref,77.0 $tuni,77.0 $time,0.05
te,all,482.162,482.162,482.162,482.162,481.838,481.838
temo,481.838,481.838
lwri $afwr $fini
/inp,27 $fini
/eof
$$ Load no. 11 $$
/prep7
/inp,geometry
tref,77.0 $tuni,77.0 $time,0.055
te,all,530.582,530.582,530.582,530.582,530.258,530.258
temo,530.258,530.258
```

```
lwri $afwr $fini
/inp,27 $fini
/eof
$$ Load no. 12 $$
/prep7
/inp,geometry
tref,77.0 $tuni,77.0 $time,0.06
te,all,576.608,576.608,576.608,576.608,576.266,576.266
temo,576.266,576.266
lwri $afwr $fini
/inp,27 $fini
/eof
$$$$$$$$$$$$$$$$$$$$$$$$$$$$$$$$$$$$$$$$$$$$$$$$$$$$$$$$$$$$$$
```

```
$$$$$$$$$$$$$$$$$$$$$$$$$$$$$$$$$$$$$$$$$$$$$$$$$$$$$$$$$$$$
$$                                                        $$
$$   Geometry and static load file for ANSYS plate        $$
$$                buckling analysis                       $$
$$                                                        $$
$$$$$$$$$$$$$$$$$$$$$$$$$$$$$$$$$$$$$$$$$$$$$$$$$$$$$$$$$$$$
$$
$$
n,1,0,0,0.1
n,13,24,0,0.1 $fill
n,14,0,4,0.1
n,20,24,4,0.1 $fill
ngen,7,20,1,20,1,0,8 $ndel,134,140
real,1,0.0625
et,1,93
type,1 $real,1 $mat,1
e,1,3,23,21,2,15,22,14
e,3,5,25,23,4,16,24,15
e,5,7,27,25,6,17,26,16
e,7,9,29,27,8,18,28,17
e,9,11,31,29,10,19,30,18
e,11,13,33,31,12,20,32,19
egen,6,20,1,6,1
knl,1
nlsi,48 $nlta,1,1
nl,1,1,2.495e-14,5.6415,-0.80082,62400,,0.0
nl,1,7,12.19e-17,6.5244,,62400,,1.0
nl,1,13,-2,0.00073,0.00145,0.01,0.04,0.12
nl,1,19,70.0,21535,42500,43070,54100,63500
nl,25,200,21097,40650,40900,50200,58200
nl,1,31,400,20367,39450,39688,62800,69400
nl,1,37,800,17374,24000,33500,48600,53100
nl,1,43,1300,5781.6,11200,14000,15000,15500
mpte,1,70,200,400,800,1300
mpda,ex,1,1,29.5e6,28.9e6,27.9e6,23.8e6,7.92e6
r,1,0.0625
nsel,x,0.0
d,all,uy $d,all,uz $d,all,ux $nall
nsel,y,0.0
d,all,uz $d,all,ux $d,all,uy $nall
krf,2
ktemp,-1
prst,1,1,13,1
iter,-200,200
f,20,fx,-1.0,,120,20
f,33,fx,-1.0,,133,20
f,122,fy,-1.0,,133,1
$$$$$$$$$$$$$$$$$$$$$$$$$$$$$$$$$$$$$$$$$$$$$$$$$$$$$$$$$$$$
```

```
$$$$$$$$$$$$$$$$$$$$$$$$$$$$$$$$$$$$$$$$$$$$$$$$$$$
$$                                               $$
$$    Buckle program called by ANSYS for         $$
$$                Plate Analysis                 $$
$$                                               $$
$$$$$$$$$$$$$$$$$$$$$$$$$$$$$$$$$$$$$$$$$$$$$$$$$$$
$$
$$
/buc,3,1,,,,1
iter,1,1,1
end
fini
/eof
$$$$$$$$$$$$$$$$$$$$$$$$$$$$$$$$$$$$$$$$$$$$$$$$$$$$
```

```
$$$$$$$$$$$$$$$$$$$$$$$$$$$$$$$$$$$$$$$$$$$$$$$$$$$$$$$$$$$$$
$$                                                          $$
$$      This is the NASTRAN input file for the post-        $$
$$      buckling of the plate                               $$
$$                                                          $$
$$$$$$$$$$$$$$$$$$$$$$$$$$$$$$$$$$$$$$$$$$$$$$$$$$$$$$$$$$$$$
$
$
$DBDIR
ID   MSC, D2460
$ID MSC, D2460 $ BASIC STATICS, MG 14 JUN 79
TIME 200
SOL 24
$SOL 101
$SOL 105
CEND
$
$        CASE
$
TITLE=DEMENSTRATION OF A FOUR ELEMENT PLATE
SUBTITLE=STATIC ANALYSIS WITH TWO LOADING CONDITIONS
     ECHO = NONE
     SPC =  51
     DISPLACEMENT = ALL
     ELFORCE = ALL
     STRESSES=ALL
SUBCASE 1
     LABEL = LOAD ONE
     TEMP(LOAD) = 800
     NLPARM = 909
SUBCASE 2
     LABEL = LOAD TWO
     TEMP(LOAD) = 802
     NLPARM = 910
SUBCASE 3
     LABEL = LOAD THREE, TIME AT 0.015
     TEMP(LOAD) = 804
     NLPARM = 911
SUBCASE 4
     LABEL = LOAD FOUR, TIME AT 0.02
     TEMP(LOAD) = 806
     NLPARM = 912
SUBCASE 5
     LABEL = LOAD FIVE, TIME AT 0.025
     TEMP(LOAD) = 808
     NLPARM = 913
SUBCASE 6
     LABEL = LOAD SIX, TIME AT 0.03
     TEMP(LOAD) = 810
     NLPARM = 914
SUBCASE 7
     LABEL = LOAD SEVEN, TIME AT 0.035
```

```
     TEMP(LOAD) = 812
     NLPARM = 915
SUBCASE 8
     LABEL = LOAD EIGHT, TIME AT 0.04
     NLPARM = 916
     TEMP(LOAD) = 814
SUBCASE 9
     LABEL = LOAD NINE, TIME AT 0.045
     TEMP(LOAD) = 816
     NLPARM = 917
SUBCASE 10
     LABEL = LOAD TEN, TIME AT 0.05
     TEMP(LOAD) = 818
     NLPARM = 918
SUBCASE 11
     LABEL = LOAD ELEVEN, TIME AT 0.055
     TEMP(LOAD) = 820
     NLPARM = 919
SUBCASE 12
     LABEL = LOAD TWELVE, TIME AT 0.06
     TEMP(LOAD) = 822
     NLPARM = 920
SUBCASE 13
     LABEL = LOAD THIRTEEN, TIME AT 0.065
     TEMP(LOAD) = 824
     NLPARM = 921
SUBCASE 14
     LABEL = LOAD FOURTEEN, TIME AT 0.07
     TEMP(LOAD) = 826
     NLPARM = 922
SUBCASE 15
     LABEL = LOAD FIFTEEN, TIME AT 0.075
     TEMP(LOAD) = 828
     NLPARM = 923
SUBCASE 16
     LABEL = LOAD SIXTEEN, TIME AT 0.08
     TEMP(LOAD) = 830
     NLPARM = 924
SUBCASE 17
     LABEL = LOAD SEVENTEEN, TIME AT 0.085
     TEMP(LOAD) = 832
     NLPARM = 925
SUBCASE 18
     LABEL = LOAD EIGHTEEN, TIME AT 0.09
     TEMP(LOAD) = 834
     NLPARM = 926
SUBCASE 19
     LABEL = LOAD NINETEEN, TIME AT 0.095
     TEMP(LOAD) = 836
     NLPARM = 927
SUBCASE 20
     LABEL = LOAD TWENTY, TIME AT 0.1
```

```
     TEMP(LOAD) = 838
     NLPARM = 928
SUBCASE 21
     LABEL = LOAD TWENTY-ONE, TIME AT 0.105
     TEMP(LOAD) = 840
     NLPARM = 929
SUBCASE 22
     LABEL = LOAD TWENTY TWO, TIME AT 0.11
     TEMP(LOAD) = 842
     NLPARM = 930
SUBCASE 23
     LABEL = LOAD TWENTY THREE, TIME AT 0.115
     TEMP(LOAD) = 844
     NLPARM = 931
SUBCASE 24
     LABEL = LOAD TWENTY FOUR, TIME AT 0.12
     TEMP(LOAD) = 846
     NLPARM = 932
BEGIN BULK
$
$    ACTUAL MODEL -- GRID POINTS
$
GRID    1       0       0.0     0.0     0.1
GRID    2       0       4.0     0.0     0.1
GRID    3       0       8.0     0.0     0.1
GRID    4       0       12.0    0.0     0.1
GRID    5       0       16.0    0.0     0.1
GRID    6       0       20.0    0.0     0.1
GRID    7       0       24.0    0.0     0.1
GRID    8       0       28.0    0.0     0.1
GRID    9       0       32.0    0.0     0.1
GRID    10      0       36.0    0.0     0.1
GRID    11      0       40.0    0.0     0.1
GRID    12      0       44.0    0.0     0.1
GRID    13      0       48.0    0.0     0.1
GRID    14      0       0.0     6.0     0.1
GRID    15      0       8.0     6.0     0.11368
GRID    16      0       16.0    6.0     0.12672
GRID    17      0       24.0    6.0     0.13948
GRID    18      0       32.0    6.0     0.12672
GRID    19      0       40.0    6.0     0.11368
GRID    20      0       48.0    6.0     0.1
GRID    21      0       0.0     12.0    0.1
GRID    22      0       4.0     12.0    0.11196
GRID    23      0       8.0     12.0    0.12380
GRID    24      0       12.0    12.0    0.13546
GRID    25      0       16.0    12.0    0.14696
GRID    26      0       20.0    12.0    0.15837
GRID    27      0       24.0    12.0    0.16986
GRID    28      0       28.0    12.0    0.15837
GRID    29      0       32.0    12.0    0.14696
GRID    30      0       36.0    12.0    0.13546
```

GRID	31	0	40.0	12.0	0.12380
GRID	32	0	44.0	12.0	0.11196
GRID	33	0	48.0	12.0	0.1
GRID	34	0	0.0	18.0	0.1
GRID	35	0	8.0	18.0	0.13078
GRID	36	0	16.0	18.0	0.16106
GRID	37	0	24.0	18.0	0.19114
GRID	38	0	32.0	18.0	0.16106
GRID	39	0	40.0	18.0	0.13078
GRID	40	0	48.0	18.0	0.1
GRID	41	0	0.0	24.0	0.1
GRID	42	0	4.0	24.0	0.11768
GRID	43	0	8.0	24.0	0.13530
GRID	44	0	12.0	24.0	0.15280
GRID	45	0	16.0	24.0	0.17021
GRID	46	0	20.0	24.0	0.18757
GRID	47	0	24.0	24.0	0.20498
GRID	48	0	28.0	24.0	0.18757
GRID	49	0	32.0	24.0	0.17021
GRID	50	0	36.0	24.0	0.15280
GRID	51	0	40.0	24.0	0.13530
GRID	52	0	44.0	24.0	0.11768
GRID	53	0	48.0	24.0	0.1
GRID	54	0	0.0	30.0	0.1
GRID	55	0	8.0	30.0	0.13794
GRID	56	0	16.0	30.0	0.17559
GRID	57	0	24.0	30.0	0.21311
GRID	58	0	32.0	30.0	0.17559
GRID	59	0	40.0	30.0	0.13794
GRID	60	0	48.0	30.0	0.1
GRID	61	0	0.0	36.0	0.1
GRID	62	0	4.0	36.0	0.11966
GRID	63	0	8.0	36.0	0.13929
GRID	64	0	12.0	36.0	0.15886
GRID	65	0	16.0	36.0	0.17837
GRID	66	0	20.0	36.0	0.19786
GRID	67	0	24.0	36.0	0.21736
GRID	68	0	28.0	36.0	0.19786
GRID	69	0	32.0	36.0	0.17837
GRID	70	0	36.0	36.0	0.15886
GRID	71	0	40.0	36.0	0.13929
GRID	72	0	44.0	36.0	0.11966
GRID	73	0	48.0	36.0	0.1
GRID	74	0	0.0	42.0	0.1
GRID	75	0	8.0	42.0	0.13990
GRID	76	0	16.0	42.0	0.17966
GRID	77	0	24.0	42.0	0.21932
GRID	78	0	32.0	42.0	0.17966
GRID	79	0	40.0	42.0	0.13990
GRID	80	0	48.0	42.0	0.1
GRID	81	0	0.0	48.0	0.1
GRID	82	0	4.0	48.0	0.12014

GRID	83	0	8.0	48.0	0.14024
GRID	84	0	12.0	48.0	0.16029
GRID	85	0	16.0	48.0	0.18029
GRID	86	0	20.0	48.0	0.20023
GRID	87	0	24.0	48.0	0.22014
GRID	88	0	28.0	48.0	0.20023
GRID	89	0	32.0	48.0	0.18029
GRID	90	0	36.0	48.0	0.16029
GRID	91	0	40.0	48.0	0.14024
GRID	92	0	44.0	48.0	0.12014
GRID	93	0	48.0	48.0	0.1
GRID	94	0	0.0	54.0	0.1
GRID	95	0	8.0	54.0	0.13990
GRID	96	0	16.0	54.0	0.17966
GRID	97	0	24.0	54.0	0.21931
GRID	98	0	32.0	54.0	0.17965
GRID	99	0	40.0	54.0	0.13990
GRID	100	0	48.0	54.0	0.1
GRID	101	0	0.0	60.0	0.1
GRID	102	0	4.0	60.0	0.11966
GRID	103	0	8.0	60.0	0.13929
GRID	104	0	12.0	60.0	0.15886
GRID	105	0	16.0	60.0	0.17837
GRID	106	0	20.0	60.0	0.19786
GRID	107	0	24.0	60.0	0.21736
GRID	108	0	28.0	60.0	0.19786
GRID	109	0	32.0	60.0	0.17837
GRID	110	0	36.0	60.0	0.15886
GRID	111	0	40.0	60.0	0.13929
GRID	112	0	44.0	60.0	0.11966
GRID	113	0	48.0	60.0	0.1
GRID	114	0	0.0	66.0	0.1
GRID	115	0	8.0	66.0	0.13794
GRID	116	0	16.0	66.0	0.17559
GRID	117	0	24.0	66.0	0.21311
GRID	118	0	32.0	66.0	0.17559
GRID	119	0	40.0	66.0	0.13794
GRID	120	0	48.0	66.0	0.1
GRID	121	0	0.0	72.0	0.1
GRID	122	0	4.0	72.0	0.11768
GRID	123	0	8.0	72.0	0.13530
GRID	124	0	12.0	72.0	0.15280
GRID	125	0	16.0	72.0	0.17021
GRID	126	0	20.0	72.0	0.18757
GRID	127	0	24.0	72.0	0.20498
GRID	128	0	28.0	72.0	0.18757
GRID	129	0	32.0	72.0	0.17021
GRID	130	0	36.0	72.0	0.15280
GRID	131	0	40.0	72.0	0.13530
GRID	132	0	44.0	72.0	0.11768
GRID	133	0	48.0	72.0	0.1
GRID	134	0	0.0	78.0	0.1

```
GRID    135     0       8.0     78.0    0.13078
GRID    136     0       16.0    78.0    0.16106
GRID    137     0       24.0    78.0    0.19114
GRID    138     0       32.0    78.0    0.16106
GRID    139     0       40.0    78.0    0.13078
GRID    140     0       48.0    78.0    0.1
GRID    141     0       0.0     84.0    0.1
GRID    142     0       4.0     84.0    0.11196
GRID    143     0       8.0     84.0    0.12380
GRID    144     0       12.0    84.0    0.13546
GRID    145     0       16.0    84.0    0.14696
GRID    146     0       20.0    84.0    0.15837
GRID    147     0       24.0    84.0    0.16986
GRID    148     0       28.0    84.0    0.15837
GRID    149     0       32.0    84.0    0.14696
GRID    150     0       36.0    84.0    0.13546
GRID    151     0       40.0    84.0    0.12380
GRID    152     0       44.0    84.0    0.11196
GRID    153     0       48.0    84.0    0.1
GRID    154     0       0.0     90.0    0.1
GRID    155     0       8.0     90.0    0.11368
GRID    156     0       16.0    90.0    0.12672
GRID    157     0       24.0    90.0    0.13948
GRID    158     0       32.0    90.0    0.12672
GRID    159     0       40.0    90.0    0.11368
GRID    160     0       48.0    90.0    0.1
GRID    161     0       0.0     96.0    0.1
GRID    162     0       4.0     96.0    0.1
GRID    163     0       8.0     96.0    0.1
GRID    164     0       12.0    96.0    0.1
GRID    165     0       16.0    96.0    0.1
GRID    166     0       20.0    96.0    0.1
GRID    167     0       24.0    96.0    0.1
GRID    168     0       28.0    96.0    0.1
GRID    169     0       32.0    96.0    0.1
GRID    170     0       36.0    96.0    0.1
GRID    171     0       40.0    96.0    0.1
GRID    172     0       44.0    96.0    0.1
GRID    173     0       48.0    96.0    0.1
$
$  ACTUAL MODEL -  -  ELEMENTS
$
CQUAD8 1   21  1   3   23  21  2   15  +CQUAD1
+CQUAD1 22 14
CQUAD8 2   21  3   5   25  23  4   16  +CQUAD2
+CQUAD2 24 15
CQUAD8 3   21  5   7   27  25  6   17  +CQUAD3
+CQUAD3 26 16
CQUAD8 4   21  7   9   29  27  8   18  +CQUAD4
+CQUAD4 28 17
CQUAD8 5   21  9   11  31  29  10  19  +CQUAD5
+CQUAD5 30 18
CQUAD8 6   21  11  13  33  31  12  20  +CQUAD6
+CQUAD6 32 19
CQUAD8 7   21  21  23  43  41  22  35  +CQUAD7
```

+CQUAD7 42	34							
CQUAD8 8	21	23	25	45	43	24	36	+CQUAD8
+CQUAD8 44	35							
CQUAD8 9	21	25	27	47	45	26	37	+CQUAD9
+CQUAD9 46	36							
CQUAD8 10	21	27	29	49	47	28	38	+CQUD10
+CQUD10 48	37							
CQUAD8 11	21	29	31	51	49	30	39	+CQUD11
+CQUD11 50	38							
CQUAD8 12	21	31	33	53	51	32	40	+CQUD12
+CQUD12 52	39							
CQUAD8 13	21	41	43	63	61	42	55	+CQUD13
+CQUD13 62	54							
CQUAD8 14	21	43	45	65	63	44	56	+CQUD14
+CQUD14 64	55							
CQUAD8 15	21	45	47	67	65	46	57	+CQUD15
+CQUD15 66	56							
CQUAD8 16	21	47	49	69	67	48	5	+CQUD16
+CQUD16 68	57							
CQUAD8 17	21	49	51	71	69	50	59	+CQUD17
+CQUD17 70	58							
CQUAD8 18	21	51	53	73	71	52	60	+CQUD18
+CQUD18 72	59							
CQUAD8 19	21	61	63	83	81	62	75	+CQUD19
+CQUD19 82	74							
CQUAD8 20	21	63	65	85	83	64	76	+CQUD20
+CQUD20 84	75							
CQUAD8 21	21	65	67	87	85	66	77	+CQUD21
+CQUD21 86	76							
CQUAD8 22	21	67	69	89	87	68	78	+CQUD22
+CQUD22 88	77							
CQUAD8 23	21	69	71	91	89	70	79	+CQUD23
+CQUD23 90	78							
CQUAD8 24	21	71	73	93	91	72	80	+CQUD24
+CQUD24 92	79							
CQUAD8 25	21	81	83	103	101	82	95	+CQUD25
+CQUD25 102	94							
CQUAD8 26	21	83	85	105	103	84	96	+CQUD26
+CQUD26 104	95							
CQUAD8 27	21	85	87	107	105	86	97	+CQUD27
+CQUD27 106	96							
CQUAD8 28	21	87	89	109	107	88	98	+CQUD28
+CQUD28 108	97							
CQUAD8 29	21	89	91	111	109	90	99	+CQUD29
+CQUD29 110	98							
CQUAD8 30	21	91	93	113	111	92	100	+CQUD30
+CQUD30 112	99							
CQUAD8 31	21	101	103	123	121	102	115	+CQUD31
+CQUD31 122	114							
CQUAD8 32	21	103	105	125	123	104	116	+CQUD32
+CQUD32 124	115							
CQUAD8 33	21	105	107	127	125	106	117	+CQUD33
+CQUD33 126	116							
CQUAD8 34	21	107	109	129	127	108	118	+CQUD34
+CQUD34 128	117							
CQUAD8 35	21	109	111	131	129	110	119	+CQUD35
+CQUD35 130	118							
CQUAD8 36	21	111	113	133	131	112	120	+CQUD36
+CQUD36 132	119							
CQUAD8 37	21	121	123	143	141	122	135	+CQUD37
+CQUD37 142	134							
CQUAD8 38	21	123	125	145	143	124	136	+CQUD38
+CQUD38 144	135							
CQUAD8 39	21	125	127	147	145	126	137	+CQUD39
+CQUD39 146	136							
CQUAD8 40	21	127	129	149	147	128	138	+CQUD40
+CQUD40 148	137							

```
CQUAD8 41    21    129   131   151   149   130   139   +CQUD41
+CQUD41 150  138
CQUAD8 42    21    131   133   153   151   132   140   +CQUD42
+CQUD42 152  139
CQUAD8 43    21    141   143   163   161   142   155   +CQUD43
+CQUD43 162  154
CQUAD8 44    21    143   145   165   163   144   156   +CQUD44
+CQUD44 164  155
CQUAD8 45    21    145   147   167   165   146   157   +CQUD45
+CQUD45 166  156
CQUAD8 46    21    147   149   169   167   148   158   +CQUD46
+CQUD46 168  157
CQUAD8 47    21    149   151   171   169   150   159   +CQUD47
+CQUD47 170  158
CQUAD8 48    21    151   153   173   171   152   160   +CQUD48
+CQUD48 172  159
$
$  MATERIAL PROPERTY DEFINITION
$
PARAM,TABS,459.69
MAT1   31    29.5E6     0.28   0.00025 6.5E-6  70.0
MATT1  31    66                 68
MATS1  31    79    NLELAST                                        2.0e7
TABLEM1 66
     70.0  29.5E6 200.0   28.9e6 400.0  27.9e6  600.0  24.5e6
     800.0  23.8E6 1000.0  17.4E6 1200.0  11.2E6  ENDT
TABLEM1 68
     70.0  6.5e-6 200.0   6.5e-6 400.0  6.9e-6  800.0  7.6e-6
     1300.0 8.6e-6 ENDT
TABLEST 79
     70.0  600    200.0  602    400.0  604     600.0  606
     800.0  608    1000.0  610    1200.0 612     ENDT
TABLES1 600
     0.0    0.0    0.001   29500.0 0.002  44000.0 0.005  42000.0
     0.010  42400.0 0.015   47500.0 0.0183  51500.0 ENDT
TABLES1 602
     0.0    0.0    0.001   28900.0 0.002  40600.0 0.005  40000.0
     0.010  40500.0 0.015   44000.0 0.0183  46000.0 ENDT
TABLES1 604
     0.0    0.0    0.001   27900.0 0.002  39000.0 0.005  39300.0
     0.010  43500.0 0.015   50100.0 0.0183  52300.0 ENDT
TABLES1 606
     0.0    0.0    0.001   24500.0 0.002  29800.0 0.005  36300.0
     0.010  43000.0 0.015   49300.0 0.0183  52000.0 ENDT
TABLES1 608
     0.0    0.0    0.001   23800.0 0.002  25300.0 0.005  33400.0
     0.01   40000.0 0.015   43100.0 0.0183  45000.0 ENDT
TABLES1 610
     0.0    0.0    0.001   17400.0 0.002  24000.0 0.005  29600.0
     0.010  31200.0 0.015   33300.0 0.0183  34700.0 ENDT
TABLES1 612
     0.0    0.0    0.001   11200.0 0.002  14800.0 0.005  16700.0
     0.010  16900.0 0.015   17300.0 0.0183  17500.0 ENDT
CREEP  31    70.0   1.3e-32 CRLAW
     300    3.2e-26 2.7333          -0.667
NLPARM   909        10        0.0005
NLPARM   910        10        0.0005
NLPARM   911        10        0.0005
NLPARM   912        10        0.0005
NLPARM   913        10        0.0005
NLPARM   914        10        0.0005
NLPARM   915        10        0.0005
NLPARM   916        10        0.0005
NLPARM   917        10        0.0005
```

```
NLPARM  918     10      0.0005
NLPARM  919     10      0.0005
NLPARM  920     10      0.0005
NLPARM  921     10      0.0005
NLPARM  922     10      0.0005
NLPARM  923     10      0.0005
NLPARM  924     10      0.0005
NLPARM  925     10      0.0005
NLPARM  926     10      0.0005
NLPARM  927     10      0.0005
NLPARM  928     10      0.0005
NLPARM  929     10      0.0005
NLPARM  930     10      0.0005
NLPARM  931     10      0.0005
NLPARM  932     10      0.0005
$
$    ACTUAL MODEL - TEMPERATURE LOADS
$
TEMPP3 800  1  0.0375 90.41   0.1  90.356 0.1625 90.388 +1TEMP1
+1TEMP1                                   +1TEMP2
+1TEMP2                                   +1TEMP3
+1TEMP3 2   THRU  48
TEMPP3 802  1  0.0375 114.26  0.1  114.188 0.1625 114.17 +2TEMP1
+2TEMP1                                   +2TEMP2
+2TEMP2                                   +2TEMP3
+2TEMP3 2   THRU  48
$
TEMPP3 804  1  0.0375 146.26  0.1  146.282 0.1625 146.246 +3TEMP1
+3TEMP1                                   +3TEMP2
+3TEMP2                                   +3TEMP3
+3TEMP3 2   THRU  48
$
TEMPP3 806  1  0.0375 185.054 0.1  184.928 0.1625 184.874 +4TEMP1
+4TEMP1                                   +4TEMP2
+4TEMP2                                   +4TEMP3
+4TEMP3 2   THRU  48
$
TEMPP3 808  1  0.0375 229.118 0.1  228.956 0.1625 228.902 +5TEMP1
+5TEMP1                                   +5TEMP2
+5TEMP2                                   +5TEMP3
+5TEMP3 2   THRU  48
$
TEMPP3 810  1  0.0375 277.754 0.1  227.574 0.1625 277.502 +6TEMP1
+6TEMP1                                   +6TEMP2
+6TEMP2                                   +6TEMP3
+6TEMP3 2   THRU  48
$
TEMPP3 812  1  0.0375 327.902 0.1  327.722 0.1625 327.65 +7TEMP1
+7TEMP1                                   +7TEMP2
+7TEMP2                                   +7TEMP3
+7TEMP3 2   THRU  48
$
TEMPP3 814  1  0.0375 379.436 0.1  379.238 0.1625 379.148 +8TEMP1
+8TEMP1                                   +8TEMP2
+8TEMP2                                   +8TEMP3
+8TEMP3 2   THRU  48
$
TEMPP3 816  1  0.0375 431.474 0.1  431.348 0.1625 431.258 +9TEMP1
+9TEMP1                                   +9TEMP2
+9TEMP2                                   +9TEMP3
+9TEMP3 2   THRU  48
$
```

```
TEMPP3  818    1    0.0375  482.162  0.1    481.946 0.1625  481.838  +10TEM1
+10TEM1                                                     +10TEM2
+10TEM2                                                     +10TEM3
+10TEM3 2      THRU   48
$
TEMPP3  820    1    0.0375  530.582  0.1    530.348 0.1625  530.258  +11TEM1
+11TEM1                                                     +11TEM2
+11TEM2                                                     +11TEM3
+11TEM3 2      THRU   48
$
TEMPP3  822    1    0.0375  576.608  0.1    576.374 0.1625  576.266  +12TEM1
+12TEM1                                                     +12TEM2
+12TEM2                                                     +12TEM3
+12TEM3 2      THRU   48
$
TEMPP3  824    1    0.0375  621.122  0.1    620.888 0.1625  620.78   +13TEM1
+13TEM1                                                     +13TEM2
+13TEM2                                                     +13TEM3
+13TEM3 2      THRU   48
$
TEMPP3  826    1    0.0375  663.404  0.1    663.152 0.1625  663.044  +14TEM1
+14TEM1                                                     +14TEM2
+14TEM2                                                     +14TEM3
+14TEM3 2      THRU   48
$
TEMPP3  828    1    0.0375  703.418  0.1    703.184 0.1625  703.076  +15TEM1
+15TEM1                                                     +15TEM2
+15TEM2                                                     +15TEM3
+15TEM3 2      THRU   48
$
TEMPP3  830    1    0.0375  741.326  0.1    741.074 0.1625  740.966  +16TEM1
+16TEM1                                                     +16TEM2
+16TEM2                                                     +16TEM3
+16TEM3 2      THRU   48
$
TEMPP3  832    1    0.0375  777.074  0.1    776.84  0.1625  776.714  +17TEM1
+17TEM1                                                     +17TEM2
+17TEM2                                                     +17TEM3
+17TEM3 2      THRU   48
$
TEMPP3  834    1    0.0375  811.508  0.1    811.274 0.1625  811.148  +18TEM1
+18TEM1                                                     +18TEM2
+18TEM2                                                     +18TEM3
+18TEM3 2      THRU   48
$
TEMPP3  836    1    0.0375  844.682  0.1    844.43  0.1625  844.323  +19TEM1
+19TEM1                                                     +19TEM2
+19TEM2                                                     +19TEM3
+19TEM3 2      THRU   48
$
TEMPP3  838    1    0.0375  876.47   0.1    876.236 0.1625  876.11   +20TEM1
+20TEM1                                                     +20TEM2
+20TEM2                                                     +20TEM3
+20TEM3 2      THRU   48
$
TEMPP3  840    1    0.0375  906.746  0.1    906.494 0.1625  906.386  +21TEM1
+21TEM1                                                     +21TEM2
+21TEM2                                                     +21TEM3
+21TEM3 2      THRU   48
$
TEMPP3  842    1    0.0375  935.438  0.1    935.204 0.1625  935.078  +22TEM1
+22TEM1                                                     +22TEM2
+22TEM2                                                     +22TEM3
+22TEM3 2      THRU   48
$
TEMPP3  844    1    0.0375  963.464  0.1    963.23  0.1625  963.104  +23TEM1
+23TEM1                                                     +23TEM2
```

```
+23TEM2                                        +23TEM3
+23TEM3 2    THRU   48
$
TEMPP3  846    1    0.0375  989.708  0.1    989.474  0.1625  989.348  +24TEM1
+24TEM1                                        +24TEM2
+24TEM2                                        +24TEM3
+24TEM3 2    THRU   48
$
$      AUTOMATIC CONSTRAINT OF SINGULAR  DOF = S
$
PARAM       AUTOSPC     YES
$
$      CONSTRAINTS
$
SPC       51        1         123
SPC       51        2         123
SPC       51        3         123
SPC       51        4         123
SPC       51        5         123
SPC       51        6         123
SPC       51        7         123
SPC       51        8         123
SPC       51        9         123
SPC       51        10        123
SPC       51        11        123
SPC       51        12        123
SPC       51        13        123
SPC       51        14        123
SPC       51        20        123
SPC       51        21        123
SPC       51        33        123
SPC       51        34        123
SPC       51        40        123
SPC       51        41        123
SPC       51        53        123
SPC       51        54        123
SPC       51        60        123
SPC       51        61        123
SPC       51        73        123
SPC       51        74        123
SPC       51        80        123
SPC       51        81        123
SPC       51        93        123
SPC       51        94        123
SPC       51        100       123
SPC       51        101       123
SPC       51        113       123
SPC       51        114       123
SPC       51        120       123
SPC       51        121       123
SPC       51        133       123
SPC       51        134       123
SPC       51        140       123
```

```
SPC     51      141     123
SPC     51      153     123
SPC     51      154     123
SPC     51      160     123
SPC     51      161     123
SPC     51      162     123
SPC     51      163     123
SPC     51      164     123
SPC     51      165     123
SPC     51      166     123
SPC     51      167     123
SPC     51      168     123
SPC     51      169     123
SPC     51      170     123
SPC     51      171     123
SPC     51      172     123
SPC     51      173     123
PSHELL  21      31      0.0625  31
$  LOAD - TYPE DATA
$FORCE   1       87       50.0  0.0     0.0     -1.0
ENDDATA
```